

# Regional climate mode impacts on the Wellington Region

*Full report consisting of Parts A to G*

*Prepared for Greater Wellington Regional Council*

# Regional climate mode impacts on the Wellington Region

*Part A: Introduction, Background, and Methodology*

*Prepared for Greater Wellington Regional Council*

Prepared by:  
Nicolas Fauchereau  
Nava Fedaeff  
Petra Pearce

For any information regarding this report please contact:

Nava Fedaeff  
Climate Scientist – Auckland  
Climate Application  
+64-9-375 6337  
Nava.Fedaeff@niwa.co.nz




National Institute of Water & Atmospheric Research Ltd  
Private Bag 99940  
Viaduct Harbour  
Auckland 1010

Phone +64 9 375 2050

NIWA CLIENT REPORT No: 2018259AK

Report date: July 2018

NIWA Project: WRC17106

Quality Assurance Statement		
	Reviewed by:	Dr Andrew Lorrey Principal Scientist – Climate NIWA Auckland
	Formatting checked by:	Petra Pearce
	Approved for release by:	Dr Sam Dean Chief Scientist for Climate

© All rights reserved. This publication may not be reproduced or copied in any form without the permission of the copyright owner(s). Such permission is only to be given in accordance with the terms of the client's contract with NIWA. This copyright extends to all forms of copying and any storage of material in any kind of information retrieval system.

Whilst NIWA has used all reasonable endeavours to ensure that the information contained in this document is accurate, NIWA does not give any express or implied warranty as to the completeness of the information contained herein, or that it will be suitable for any purpose(s) other than those specifically contemplated during the Project or agreed by NIWA and the Client.

# Contents

<b>Executive Summary</b> .....	<b>4</b>
<b>1 Introduction</b> .....	<b>6</b>
<b>2 Background on climate modes</b> .....	<b>7</b>
2.1 El Niño Southern Oscillation (ENSO) .....	7
2.2 The Southern Annular Mode (SAM) .....	9
2.3 The Indian Ocean Dipole (IOD).....	11
2.4 The South Pacific Subtropical Dipole (SPSD) .....	12
2.5 The Madden-Julian Oscillation (MJO) .....	13
2.6 The Interdecadal Pacific Oscillation (IPO) .....	14
<b>3 Methodology</b> .....	<b>17</b>
3.1 Spatial Analysis and Virtual Climate Station Network data.....	17
3.2 Station Analysis .....	17
3.3 Derivation of seasonal climate indices.....	19
3.4 Derivation of indices for the climate modes of variability .....	20
3.5 Statistical analyses.....	22
<b>Appendix A Station Metadata</b> .....	<b>24</b>
<b>Appendix B NIWA data quality control</b> .....	<b>27</b>
<b>4 References</b> .....	<b>28</b>

## Executive Summary

In this study we investigated the relationships between inter-annual, sub-seasonal, and decadal climate modes and different climate variables in the Wellington Region.

At the inter-annual timescale, the climate modes considered were El Niño Southern Oscillation (ENSO), the Southern Annular Mode (SAM), the Indian Ocean Dipole (IOD), and the South Pacific Subtropical Dipole (SPSD). A composite approach, which uncovered their potential non-linear impact over the regional climate of the Wellington Region, revealed that the signal associated with these inter-annual climate modes is, in general, neither strong nor symmetric. In particular:

- Both the positive and the negative ENSO phases (El Niño and La Niña respectively) are associated with decreased rainfall, an increase in the number of dry days (and conversely a decrease in the number of rain days) over parts of the Wellington Region.
- Temperature-derived indices (e.g. mean seasonal minimum and maximum temperatures, number of hot or frost days) are most significantly associated with the PSD, a mode which is associated with regional SST anomalies in the South Pacific, with a node or 'pole' located to the east of New Zealand.
- Wind-derived parameters (mean wind speed, number of days with wind gusts exceeding respectively 63 and 96 km/h) tend to respond more linearly to the above-mentioned climate modes, e.g. mean wind speed tends to increase during the positive phase of ENSO, and decrease during the negative phase.
- Soil moisture, which integrates signals from rainfall, temperatures and heat and moisture fluxes, tends to closely follow rainfall in terms of its relationship to inter-annual climate modes.

At the sub-seasonal timescale (i.e. 1 day to ~60 days), we considered the relationships between daily climate parameters over the Wellington Region and the Madden-Julian Oscillation (MJO), as well as the SAM (through a daily SAM index). Strong, statistically significant and relatively consistent signals are found at this timescale, much more so than at the inter-annual timescale. In particular:

- The MJO modulates daily rainfall significantly over the Wellington Region, irrespective of the season, but with a stronger signal during the winter (JJA). Given the propagative nature of the MJO and its relative predictability at the horizon of 2-3 weeks, this finding opens the possibility of deriving forecast guidance for forecast horizons exceeding the weather timescale (i.e. over ~10 days and up to ~1 month).
- The response of daytime and nighttime temperatures to the MJO can be contrasted, indicating that complex processes are involved, from changes in short wave and long wave radiation fluxes to changes in circulation modulating air mass origins and their interactions with the topography of the Wellington Region.
- In contrast to the inter-annual timescale, the signal associated with the SAM at the sub-seasonal timescale is strong, significant (in the western part of the Wellington Region) and mostly symmetric between the positive and negative phases of the SAM: the positive phase of the SAM is related to decreased rainfall over this area during spring and summer, while the reverse is true during the negative phase of the SAM. Mean maximum temperatures tend to increase during the positive phase of the SAM and decrease during the negative phase, while the response of minimum daily (i.e. night time) temperatures is less consistent.

At the decadal timescale, we stratified the long time series of climate parameters available in the Wellington Region according to the phase of the Interdecadal Pacific Oscillation (IPO). A compositing approach was used to investigate the potential differences in the distribution of these climate parameters between the two phases of the IPO. Bearing in mind the limitations due to the small number of stations presenting long records, we found:

- No significant differences in rainfall totals and the number of heavy rain days (rain > 90<sup>th</sup> climatological percentile) between the positive and negative phases of the IPO.
- Conversely, some stations show consistent differences in the number of rain days (rain > 0.5 mm) and dry days (no rain) between the positive and negative phases of the IPO.
- The temperature-derived indices do not show consistent and significant differences between the two phases of the IPO for the available stations.

Although an explicit seasonal outlook scheme for the Wellington Region is beyond the scope of this report, one obvious application is that some guidance can be gained for the purpose of predicting the seasons ahead. This can be done by monitoring the current phase and amplitude of the main inter-annual climate modes presented in this report, most of them being updated near real-time. The anomaly maps, and the SST correlation patterns, can then be jointly used in order to make an assessment of the likely seasonal behaviour just ahead of the start of a new season. There is an underlying assumption that the behaviour of modes like ENSO, IOD and SPSD can remain relatively constant on the seasonal scale. The latest global SST anomalies, and the evolution of the SSTs around New Zealand, can be used to evaluate the likely seasonal response over the correlation areas such as shown for rainfall on pages 75-77. Another aspect not covered in this report is the potential impacts of climate change on the climate modes. This is still a subject of significant international research and debate, with more research needed before this can be better understood (e.g. future frequency of El Niño events, etc.).

# 1 Introduction

The climate and weather of the Wellington Region is characterised by strong spatio-temporal variation, with influences from the Cook Strait and the rugged local topography. In general, the climate of the region reflects the general prevailing westerly flow, which includes west-to-east travelling low pressure systems interspersed with high pressure systems (anticyclones). The local impacts from variable weather is modified in specific places by the topography. The area to the west of the Tararua and Rimutaka Ranges experiences the most rainfall due to orographic effects. To the east of the Tararua and Rimutaka Ranges, the Wairarapa is sheltered from prevailing westerlies and experiences more temperature and rainfall extremes than the western part of the region. Wind conditions are the strongest around the southwestern tip of the Wellington region. The region as a whole is generally sunny and windy compared with other New Zealand locations. At sub-seasonal to decadal timescales, regional circulation is also significantly influenced by modes of variability such as the Madden Julian Oscillation (MJO; Fauchereau et al., 2016), El Niño-Southern Oscillation (ENSO; Mullan, 1995), the Southern Annular Mode (SAM; Ummenhofer and England, 2007), the Indian Ocean Dipole (IOD; Ashok et al., 2007), the South Pacific Subtropical Dipole (SPSD; Morioka et al., 2013), and the Interdecadal Pacific Oscillation (IPO; Salinger and Renwick, 2001).

The Greater Wellington Regional Council (GWRC) has identified weather and climate as having a far-reaching effect on the Council's operations in areas such as civil defence, flood protection, land management and water allocation. Climate patterns, as well as extreme events, have been linked to known climate cycles such as ENSO, the IOD and the SAM for New Zealand as a whole (e.g. Kidston et al., 2009, Ummenhofer and England, 2007), but only limited work has been carried out in the Wellington Region (e.g. Tait et al., 2002). In response to this knowledge gap, GWRC has commissioned NIWA to undertake a study to evaluate the relationships between climate modes and climate variables in the Wellington Region.

This report reviews six modes of climate variability (the MJO, ENSO, SAM, IOD, PSD and IPO), and provides analysis of how they impact the Wellington Region. The analysis is based on climate indices derived from *in situ* observations and the Virtual Climate Station Network (Tait et al., 2006) across the Wellington Region. Although climate change is cited as a potential mechanism that may alter these modes in the future, it is not analysed in depth in this report. For climate change projections for the Wellington Region as well as present-day climate in the region, the reader is referred to Pearce et al. (2017).

This report is divided into five parts. This part (Part A) includes the background information about climate modes that are considered in the study, as well as the methodology used for analysis of climate modes in the Wellington Region. The remaining parts of the report are divided by timescale. Part B, C, D, and E discuss the inter-annual climate modes (ENSO, SAM, IOD, and PSD) for each of the different climate variables (Part B: Rainfall, Part C: Temperature, Part D: Wind, Part E: Soil Moisture). Part F discusses the sub-seasonal MJO, a shorter timescale SAM index, and the multidecadal-scale IPO (for all climate variables) as the analyses undertaken and outputs derived for these climate modes were substantially different than for the inter-annual climate modes. Part G presents the limitations and conclusions of the study.

## 2 Background on climate modes

Variability in New Zealand's climate has been linked to a number of large-scale climate modes. This section provides background information about each of the climate modes that are considered in this study, as well as past research concerning the relationship between these climate modes and New Zealand's climate.

### 2.1 El Niño Southern Oscillation (ENSO)

El Niño Southern Oscillation (ENSO) is a natural fluctuation of the global climate and refers to the variation in sea surface temperatures across the equatorial Pacific Ocean and in surface atmospheric pressure in the tropical Pacific (Philander, 1990). El Niño and La Niña refer to opposite extremes of the ENSO cycle and occur every 2-7 years on average. When neither El Niño nor La Niña are present, (usually referred to as "neutral" or normal conditions), easterly trade winds blow across the Pacific, piling up warm surface water so that Indonesian sea levels are approximately 50 cm higher than those off the coast of Ecuador. Cool, nutrient-rich sea water upwelling off the South American west coast as part of the Humboldt current typically occurs under this situation, which is important for supporting eastern Pacific marine ecosystems and fisheries.

During El Niño, trade winds weaken which leads to a reduction in upwelling off South America and a rise in sea surface temperatures in the eastern equatorial Pacific. The opposite is true during La Niña events, when the trade winds strengthen, which is typified by enhanced upwelling of cool water off the South American west coast and westward propagation of cool SST anomalies.

Climatic differences arising from the ENSO cycle are seen most clearly in the tropics but New Zealand is also affected. In general, during El Niño, New Zealand experiences a stronger than normal southwesterly airflow leading to wetter than normal conditions in southern and western areas and drier than normal conditions in northern and eastern parts of the country (due to the rain shadow effect). Conversely, during La Niña, more frequent northerly and easterly quarter flows ensue leading to wetter than normal conditions in the north and east of the North Island and drier than normal conditions across the South Island. Individual ENSO events can differ substantially from this pattern and El Niño and La Niña effects are not exactly equal and opposite (Mullan, 1995).

El Niño or La Niña can occur at any time of the year but both usually peak during the Southern Hemisphere summer. For this reason, it is important to look at seasonal data when considering New Zealand climatic variability instead of only considering annual values (Mullan and Thompson, 2006). The recent development of computer models which simulate the coupled ocean-atmosphere dynamics of the central Pacific have been reasonably successful in forecasting the onset, development and breakdown of ENSO events (e.g. Barnston et al. (2011)). Research on past events shows that El Niño and La Niña events tend to follow similar patterns of development and decay. Therefore, once El Niño or La Niña events have commenced, their evolution (and impact) is partly predictable for the coming few months.

A common measure of the intensity and phase of ENSO is the Southern Oscillation Index (SOI). This index is derived by calculating the air pressure difference between Tahiti and Darwin (Troup, 1965). Persistence of the SOI below -1 coincides with El Niño events, and periods above +1 with La Niña events.

The SOI only measures the atmospheric component of ENSO; the Southern Oscillation. To consider the marine component of ENSO, sea surface temperature (SST) indices are used. The equatorial Pacific Ocean is divided into different SST regions, called NINO regions (Figure 2-1). The NINO3.4



region is the most commonly used as it encompasses the central Equatorial Pacific where both cold and warm anomalies arise. As such, it provides a good measure of important changes in SST that are used to identify El Niño or La Niña periods. The threshold generally used for identifying El Niño or La Niña periods is a departure from normal of more than or  $\pm 1$  standard deviation (positive SST for El Niño and negative for La Niña).

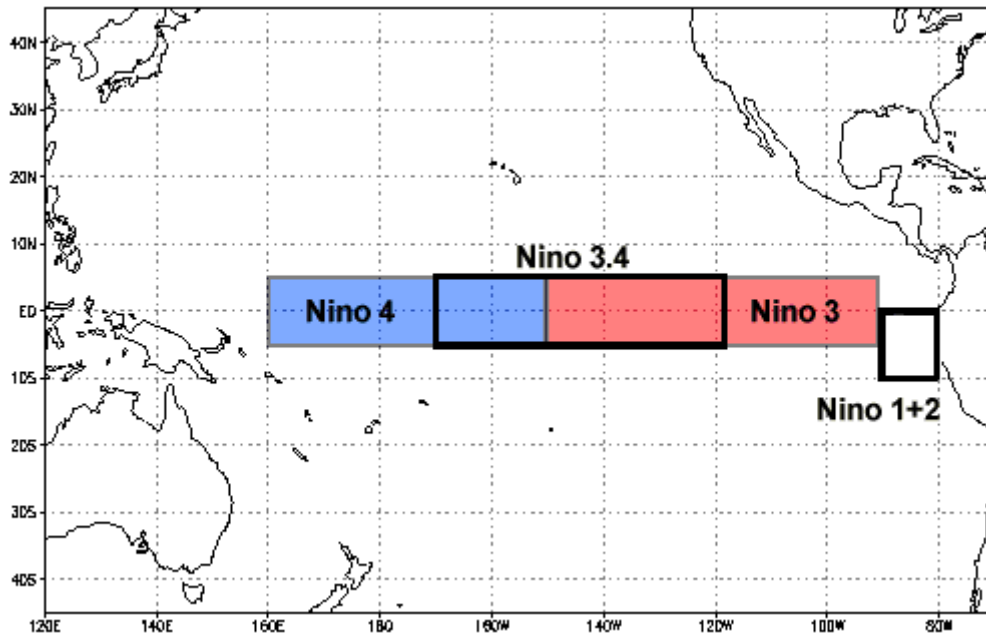


Figure 2-1: The NINO sea surface temperature regions in the tropical Pacific Ocean, used to measure the phase and intensity of ENSO. Source: <https://www.ncdc.noaa.gov/teleconnections/enso/indicators/sst.php>.

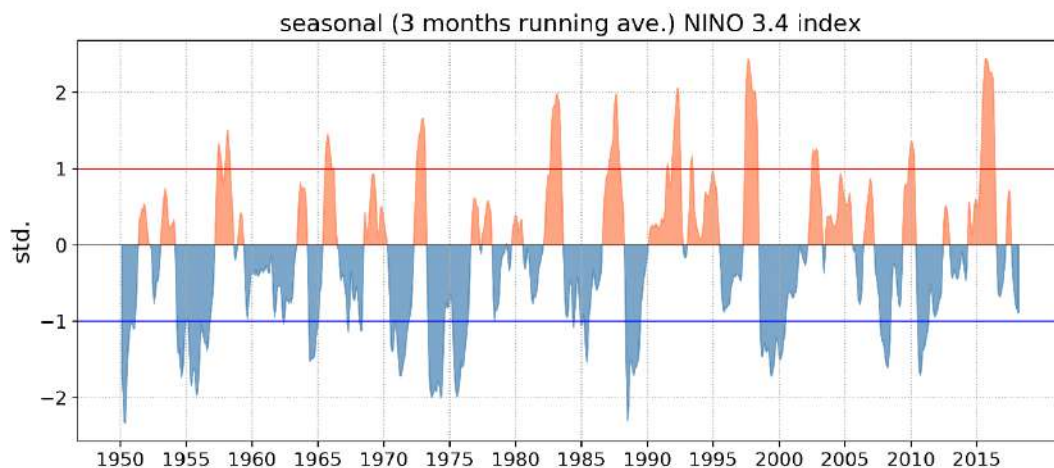


Figure 2-2: Time series of NINO3.4 sea surface temperature from 1950-2017. Data source: <http://www.cpc.ncep.noaa.gov/data/indices/ersst5.nino.mth.81-10.ascii>

According to the IPCC Fifth Assessment Report from Working Group I (IPCC, 2013), precipitation variability relating to ENSO will likely intensify due to increased moisture availability in the atmosphere. There is high confidence that ENSO will remain the dominant mode of natural climate

variability in the 21<sup>st</sup> century. However, variations in the amplitude and spatial pattern of ENSO are large and therefore any specific projected changes in ENSO remain uncertain at this stage.

Limited prior research has been carried out investigating the impact of ENSO in Wellington. Ummenhofer and England (2007) found that the entire North Island saw a decrease in rainfall during El Niño years. During La Niña years rainfall was below normal in southern and eastern parts of the Wellington Region and above normal for the Tararua Ranges and west of the Ranges, note however that their analysis only considered relationships to ENSO at the annual timescale.

In terms of regional SST anomalies, cooler than normal coastal waters around NZ are usually observed during El Niño years, while the reverse (warmer than normal regional ocean waters) is true during La Niña events (Figure 2-3). Note that the regional temperature anomalies are usually the opposite of the global average associated with El Niño (which is generally associated with higher temperatures) and La Niña (lower global temperatures).

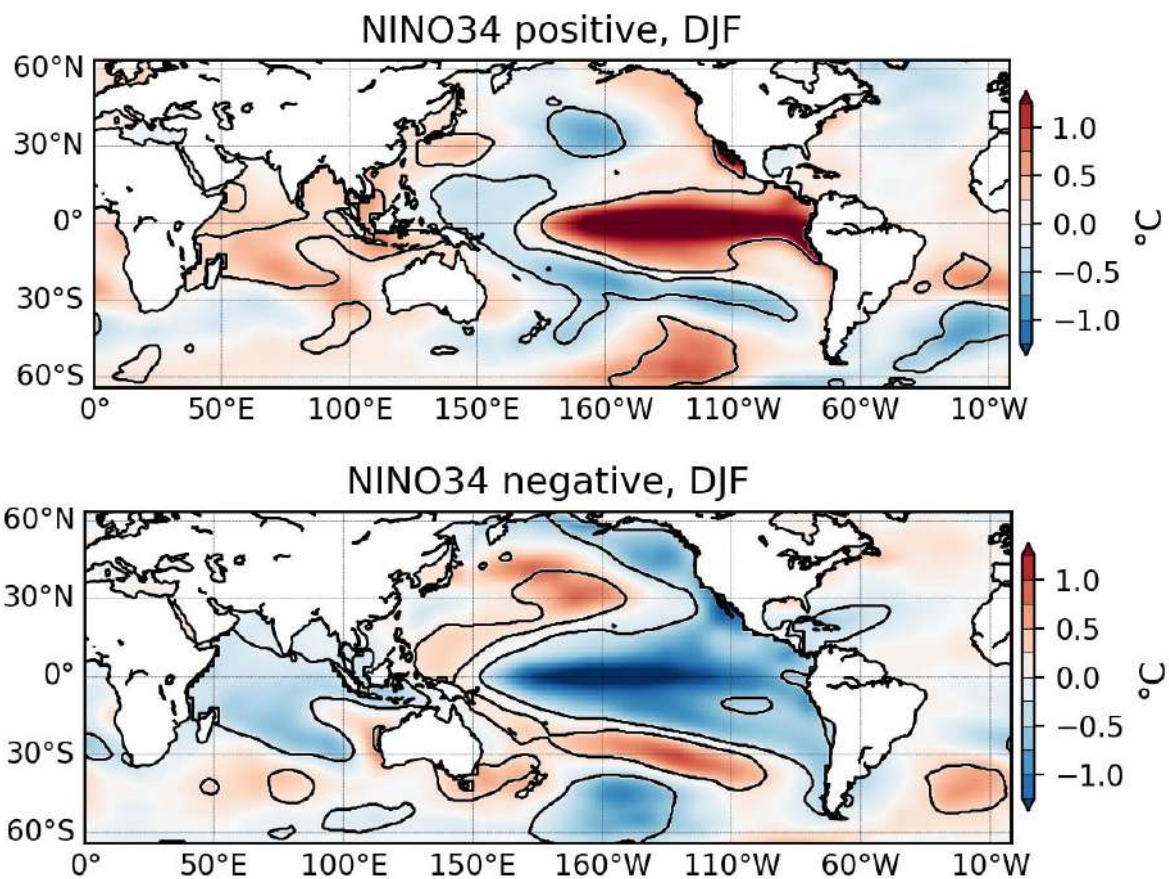


Figure 2-3: Composite SST anomalies associated with a) the positive (standardised anomalies > 1 std) and b) the negative (standardised anomalies < -1 std) phases of ENSO during the DJF season.

## 2.2 The Southern Annular Mode (SAM)

The Southern Annular Mode (SAM), also referred to as the Antarctic Oscillation (AAO), is a ring of climatic variability circling the South Pole and extending to the latitudes of New Zealand (Kidston et al., 2009, Ummenhofer and England, 2007). The SAM is an expression of the storm track and jet stream variability, and as such generally describes the position of the westerly surface winds, the

strength and position of cold fronts, windiness and storm activity between the middle latitudes, where New Zealand lies (40-50°S), and higher latitudes, over the southern oceans and Antarctic sea ice zone (50-70°S). New Zealand is positioned in a zone where the SAM displays the greatest seasonality, i.e. stronger westerlies in winter and weaker in summer, due to the influence of the southward-moving belt of sub-tropical anticyclones. The orography of the country also means that New Zealand's climate is strongly dependent upon wind speed and direction (Kidson, 2000). As the SAM is associated with pressure anomalies centred over Antarctica, the relative influence of the SAM is considered more dominant over the South Island than the North Island (Ummenhofer and England, 2007).

In its positive phase, the SAM is associated with relatively light winds and settled weather over New Zealand (Figure 2-4). Wind anomalies (differences from normal) over the summer are easterly and become northeasterly over the North Island and northwesterly over the southern South Island in winter (Kidston et al., 2009). Conversely, the negative phase of the SAM results in more unsettled conditions with more frequent and stronger westerly winds than normal.

Previous research suggests that in the Wellington Region on an annual scale, the positive SAM is associated with higher than normal daily maximum temperatures in central and western parts with the opposite true during the negative phase of SAM (Renwick and Thompson, 2006). During positive SAM years much of New Zealand (Wellington included) experiences drier than normal conditions. During negative SAM years much of the Wellington region is also slightly drier than normal with western areas slightly wetter than normal (Ummenhofer and England, 2007).

Seasonal relationships between the SAM and New Zealand rainfall are a reflection of the prevailing winds and orographic effects. Kidston et al. (2009) found that the positive phase of the SAM during summer induced wetter conditions than normal along the coastal region in the north and east of the North Island, Nelson and Marlborough and coastal north Canterbury with drier than normal conditions elsewhere. Likewise, the positive phase of the SAM in winter was found to bring wetter than normal conditions to the Bay of Plenty, Gisborne and parts of Hawke's Bay, Wellington, Nelson, Fiordland and Westland with drier than normal conditions elsewhere. Similarly, Ummenhofer et al. (2009) was also able to discern wetter than normal conditions along the east coast during positive SAM with the opposite true during negative SAM conditions.

On a week-to-week basis, the SAM can alternate between states, causing either windier or calmer weather over New Zealand. Although these changes in the SAM cannot be predicted more than few days in advance, once changed, the phases can persist for several weeks.

In contrast to the longer-lived oscillations of ENSO and the IPO, each phase of the SAM may only last for a number of weeks before switching to the opposite phase. Over the past two to three decades, there has been a trend in the SAM towards more periods of the positive phase. The trend appears to be related to the reduction of stratospheric ozone over Antarctica and, to a lesser amount, the increase in greenhouse gases in the troposphere (Arblaster and Meehl, 2006, Thompson et al., 2011) and is thus a manifestation of anthropogenic climate change. With the recovery of the ozone hole and reduction of ozone-depleting substances projected into the future, alongside increasing greenhouse gases, the trend of summertime SAM phases is expected to become less positive and stabilise slightly above zero (i.e., it is expected that there will be slightly more positive SAM phases than negative phases. Note that the phases of the SAM are defined relative to the historical climate). However, increasing concentration of greenhouse gases in the atmosphere will still cause an increasing positive trend in winter SAM phases, i.e. there will be more positive phases than negative phases into the future. The net result for SAM behaviour, as a consequence of both ozone recovery

and greenhouse gas increases, is therefore likely to be relatively little change from present by 2100. However, other drivers are likely to have an impact on SAM behaviour into the future, particularly changes to sea ice around Antarctica as well as changing temperature gradients between the equator and the high southern latitudes which could have an impact on zonal (westerly) wind strength in the mid-high latitudes.

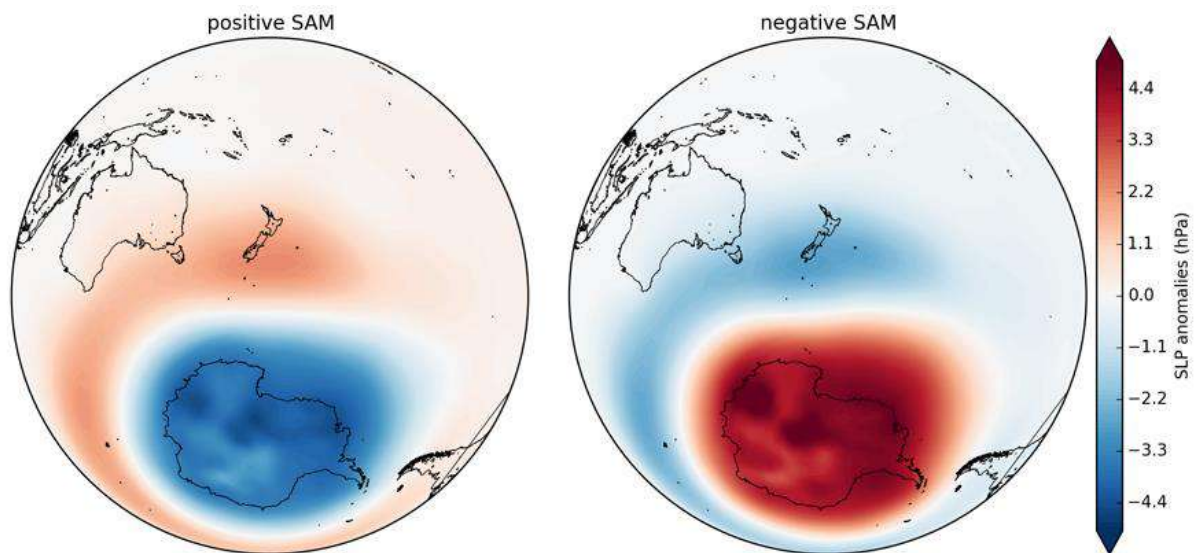


**Figure 2-4:** Pattern of the pressure variations associated with the positive (left) and negative (right) phases of the SAM. Blue shading indicates below-average pressures and red shading indicates above average pressures. Monthly composites were made using the PC associated with the first EOF of Southern Hemisphere monthly geopotential anomalies at 850 hPa from the NCEP / NCAR reanalysis (Section 2.3.3) using a threshold of +/- 1 std. Data source: <http://www.esrl.noaa.gov/psd/data/gridded/data.ncep.reanalysis.html>.

### 2.3 The Indian Ocean Dipole (IOD)

The Indian Ocean Dipole (IOD) is a coupled ocean-atmosphere phenomenon in the tropical Indian Ocean defined by the difference in sea surface temperature (SST) between two areas/poles – a western pole in the Arabian Sea (western Indian Ocean) and an eastern pole in the eastern Indian Ocean south of Indonesia. The SST difference usually develops and peaks between June and October, the IOD is thus strongly ‘phase-locked’ onto the seasonal cycle. A positive IOD is associated with above average sea surface temperatures and increased precipitation in the western Indian Ocean region with a corresponding cooling of water in the eastern Indian Ocean (Figure 2-5). The reverse effects prevail during negative IOD conditions. In addition, the IOD and ENSO are linked through the Walker Circulation, which is associated with Indonesian throughflow (the flow of warm ocean water from the Pacific into the Indian Ocean) (Behera et al., 2006). As such, positive IOD events are often (but not always) associated with El Niño and negative IOD events with La Niña.

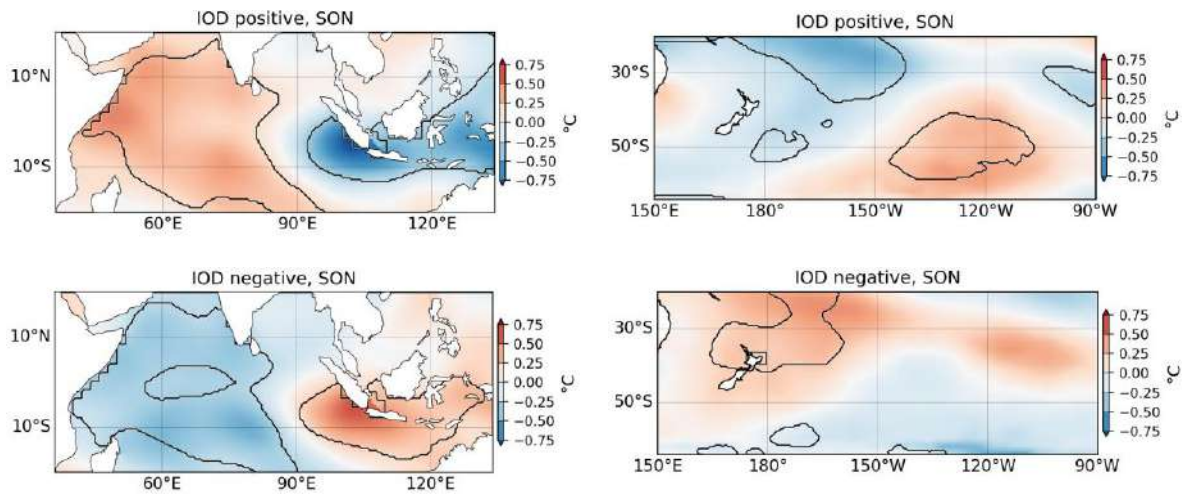


**Figure 2-5: The Indian Ocean Dipole (IOD) index for September-November, composite anomalies post-1950 using ERSST v5 detrended data, left panel presents the anomalies in the Indian Ocean (the domain of expression of the IOD), and the right panel the composite anomalies around New Zealand for the same season.**

Over the New Zealand region, positive phases of the IOD tend to be associated with cooler than normal SSTs, while the negative phase is related to the opposite pattern, particularly over the northern part of the country. In terms of circulation anomalies, and consistently with the SST anomalies presented above, Ashok et al. (2007) indicated that the positive phase of the IOD is related to weakened storm track activity with a corresponding reduction in rainfall from June–November over northern parts of the country. In the negative IOD phase, storm related precipitation tends to be significantly enhanced over the northern parts of New Zealand.

Indian Ocean sea surface temperature patterns are also known to modulate winter circulation patterns about New Zealand. Warmer tropical Indian Ocean water in autumn is generally followed by more rainfall in western South Island and drier conditions in areas exposed to the north and east (Mullan, 1998).

## 2.4 The South Pacific Subtropical Dipole (SPSD)

The South Pacific Subtropical Dipole (SPSD) is a mode of SST variability recently described by Morioka et al. (2013) and Guan et al. (2014). Statistically, the SPSP appears as the first empirical orthogonal function (EOF) mode of the SST anomalies in the South Pacific (20°S – 65°S, 150°E – 85°W) and is associated with a northwest–southeast-oriented dipole of positive and negative SST anomalies in the central basin (Morioka et al., 2013) (Figure 2-6). It is partly related to ENSO, and is also partly predictable at timescales of a few months to seasons (Guan et al., 2014).

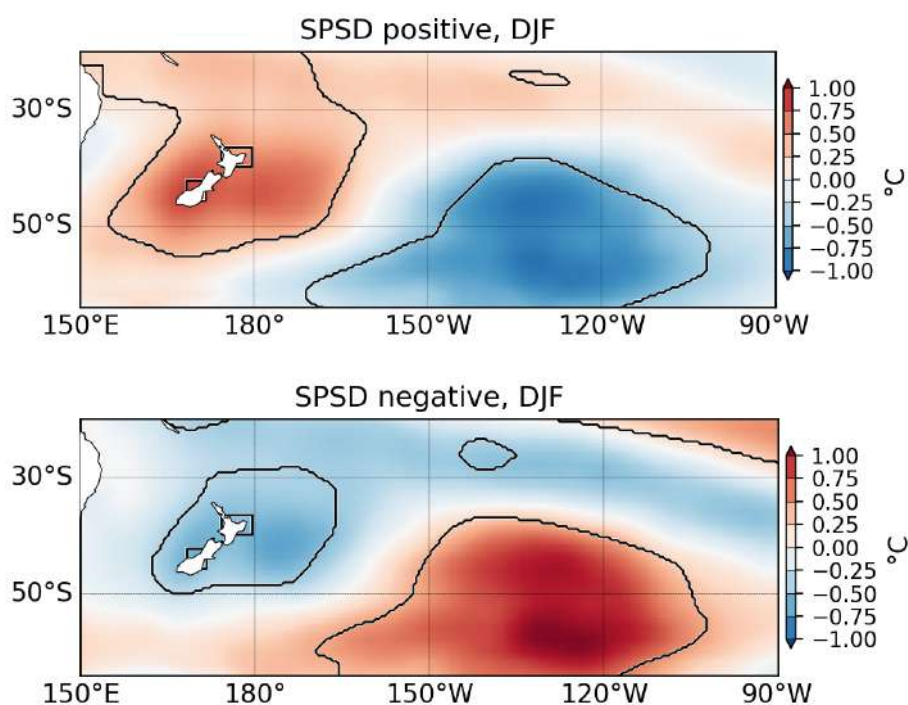


**Figure 2-6: Pattern of the SST anomalies associated with the positive and negative phases of the SPSD during the DJF season.**

The SPSD has recently been used to understand climate variability in the Hawke’s Bay Region (Fedaeff and Fauchereau, 2015). They found that up to 15% of the variation in seasonal rainfall and up to 41% of the variation in seasonal temperature was explained by the SPSD. As such, the SPSD may also be an important climate mode for the Wellington Region.

## 2.5 The Madden-Julian Oscillation (MJO)

The Madden-Julian Oscillation (MJO; Madden and Julian, 1972) is the dominant mode of atmospheric variability at the intra-seasonal time scale in the tropics, with a periodicity typically comprised between 30 to 60 days. Its core signal is associated with a west-to-east propagation of large-scale convective clusters (~10,000 km). These convective events are initiated in the western Indian Ocean basin, they migrate across the Maritime Continent and then they terminate in the tropical western Pacific basin along the Equator (Figure 2-7).

Large-scale impacts of the MJO are found in the tropics (Zhang, 2005, Zhang, 2013) as well as outside the tropics (Hoskins and Karoly, 1981) and in the Southern Hemisphere (Matthews and Meredith, 2004, Pohl et al., 2010). For the New Zealand region, the most comprehensive study of the MJO signal is, to our knowledge, the one of Fauchereau et al. (2016), which demonstrated that the MJO has significant impacts on New Zealand rainfall, and linked this impact partly to the modulation by the MJO of the probability of occurrence of regional circulation regimes known as the Kidson Types (Kidson, 2000). Their study was however limited to the austral summer season (November – March) and considered only daily rainfall anomalies.

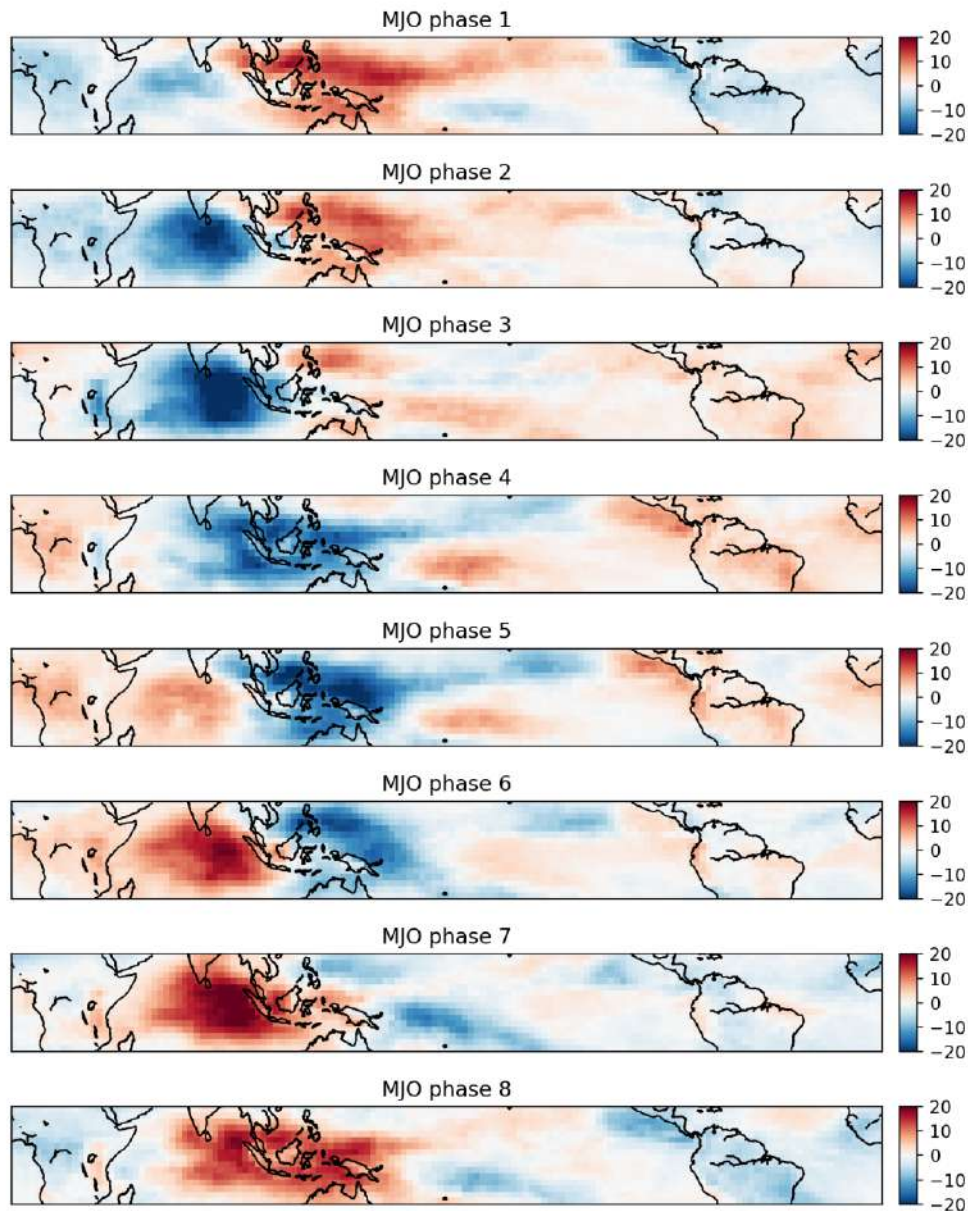


**Figure 2-7: OLR (Outgoing Longwave Radiation) anomalies associated with each phase of the MJO (amplitude > 1 std.) over the 1979-2013 period, all seasons considered, between 20°N and 20°S. The OLR dataset is taken from the NOAA at ([https://www.esrl.noaa.gov/psd/data/gridded/data.interp\\_OLR.html](https://www.esrl.noaa.gov/psd/data/gridded/data.interp_OLR.html)), the climatological period with respect to which the daily anomalies are calculated is 1981-2010. Negative OLR values (in blue) indicate increased convection, and positive values (red) decreased convection.**

## 2.6 The Interdecadal Pacific Oscillation (IPO)

The Interdecadal Pacific Oscillation (IPO) is a natural fluctuation in the climate over the Pacific Ocean and is considered to be a Pacific-wide and low-frequency manifestation of the Pacific Decadal Oscillation (PDO), originally described by Mantua et al. (1997) over the north Pacific (north of 20°N). Schematically, the positive phase of the IPO is characterised by warmer SSTs in the northeast Pacific and to a lesser extent the eastern Equatorial Pacific, while cooler than normal ocean temperatures dominate the northwest Pacific and the southwest Pacific (Figure 2-8). The negative phase is associated with the reversed pattern.

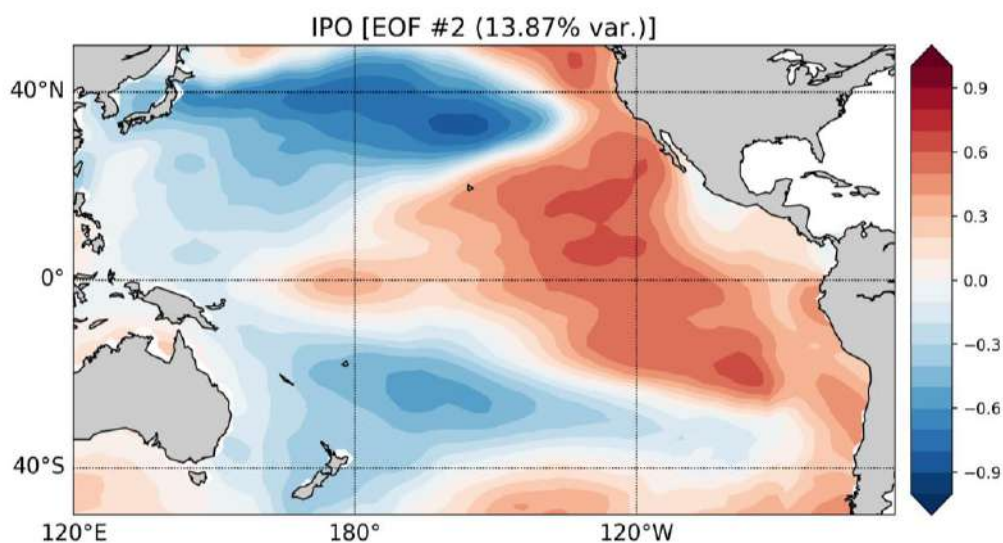


**Figure 2-8: SST anomaly spatial pattern (Empirical Orthogonal Function, or EOF) associated with the positive phase of the Interdecadal Pacific Oscillation. Data source: ERSST version 5 dataset.**

Three major phases of the IPO occurred during the 20<sup>th</sup> Century – a positive phase (~1922–1945), a mostly negative phase (1947–1977), and another positive phase (1978–1999). The start of the 21<sup>st</sup> Century saw the IPO turn negative with a return to positive conditions observed over the last few years (Figure 2-9).

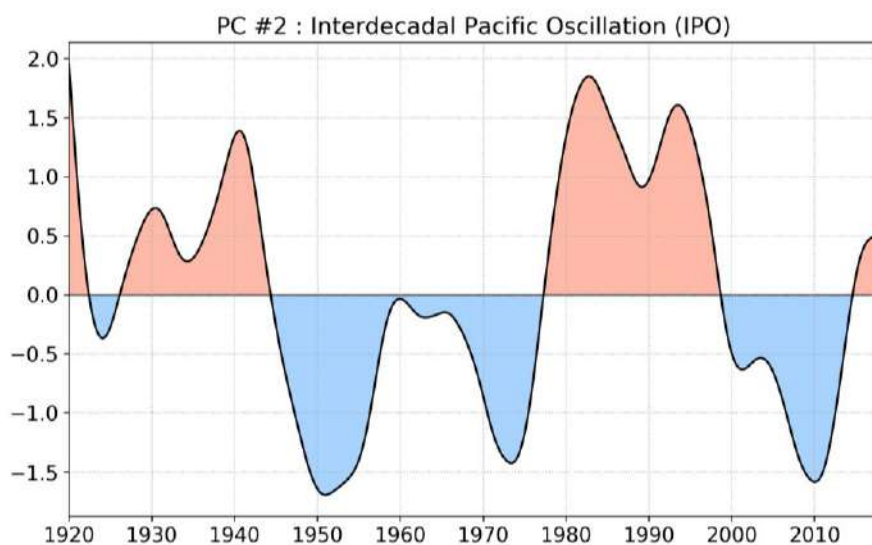


**Figure 2-9: The Interdecadal Pacific Oscillation (IPO) index. Positive values indicate periods when stronger-than-normal westerlies occur over New Zealand, with more anticyclones than usual over northern New Zealand. Negative values indicate periods with more northeasterlies than normal over northern regions of the country. Vertical axis is the IPO index, and horizontal axis is the year. The IPO index used in this report is calculated as the 2nd Principal Component (PC) of time-filtered (low-pass filter, keeping only low frequency oscillations over 11 years) monthly sea surface temperature anomalies in the Pacific domain (50°S- 50°N, 120°E- 295°E) over the January 1920 – February 2017 period. The Dataset used is the Extended Reconstructed SST (ERSST) Dataset (Version 4) developed by the US National Oceanic and Atmospheric Administration (NOAA) and made available by the US National Climate Data Centre (NCDC).**



Long term fluctuations in New Zealand's climate show an association with changes in the IPO. Typically, SSTs around New Zealand tend to be cooler and westerly winds stronger than normal during the positive IPO phase (Salinger et al., 2001). This circulation leads to drier conditions along the eastern coasts of New Zealand and higher than normal rainfall along the west coast of the South Island. The opposite is true for the negative phase of the IPO. SSTs in the western Pacific cool and more easterly and northeasterly flows over New Zealand are favoured, compared with normal, which in turn bring enhanced precipitation to northeastern regions.

These patterns are the "average" response and do not mean that every year of a particular IPO phase will behave in the same way. Although the IPO and ENSO operate on different time scales, they are similar in their expression in Tropical Pacific SSTs, suggesting that the IPO exerts a modulating effect on ENSO (Salinger et al., 2001, Power et al., 1999). Based on the correlations between the IPO and SST, on average the IPO is positively associated with enhanced and more frequent El Niño events.

### 3 Methodology

#### 3.1 Spatial Analysis and Virtual Climate Station Network data

Spatial analysis carried out in this report utilised the Virtual Climate Station Network (VCSN) dataset (Tait et al., 2006). The VCSN consists of an interpolated grid of 11,491 virtual climate stations covering the New Zealand area. Each of these virtual climate stations has daily interpolated values of rainfall, wind speed, maximum and minimum temperature, relative humidity, mean sea level pressure, vapour pressure, potential evapotranspiration, soil moisture, 10 cm earth temperature and global solar radiation. The virtual stations start with rain values only in 1960, from 1972 all the above parameters except wind, and from 1997 onward it includes wind. The grid point separation is 0.05 degrees latitude and longitude which is approximately 5 km. Data from 1972 was used in this study.

VCSN data are calculated using ANUSplin: a software tool that takes data values from irregularly-spaced observing sites and provides interpolated values at regularly spaced grid point locations. Specifically, the data are calculated by the ANUSplin trivariate (three independent variables: easting, northing and a third variable, e.g. elevation) thin-plate smoothing spline interpolation methodology, described by Tait et al. (2006).

#### 3.2 Station Analysis

In addition to the spatial analysis carried out using VCSN data, site specific station data was also analysed. In order to get a longer record for analysis, station records were combined in some cases and data gaps were infilled using either nearby station data if available or VCSN data. A map of stations used for analysis can be seen in Figure 3-1 and metadata is available in Appendix A.

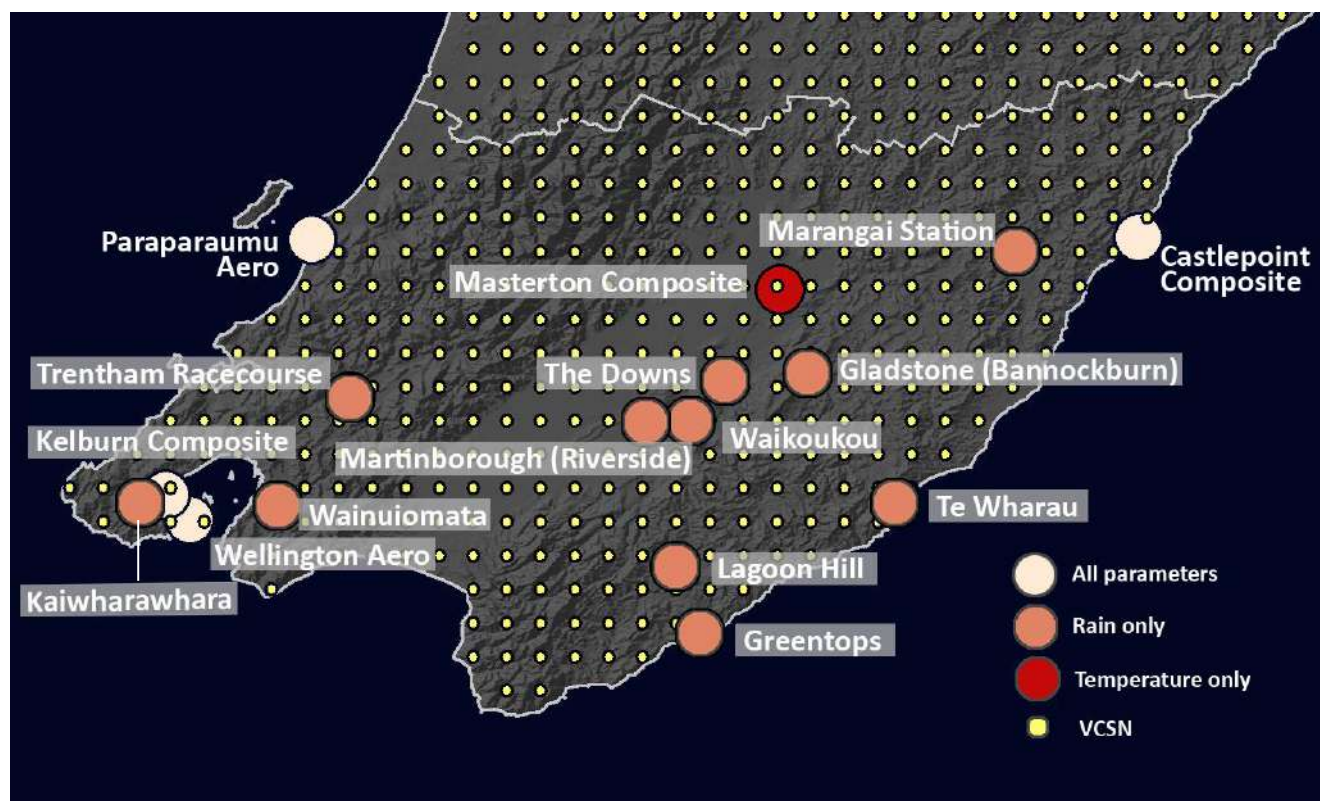


Figure 3-1: Rainfall, temperature and wind sites used for analysis as well as the location of VCSN points.

### 3.2.1 Data availability and quality

Most station data used for analysis in this report were derived from raw data values extracted from NIWA's National Climate Database (CliDB). These raw data are accessible from <http://cliflo.niwa.co.nz>. While no guarantee is made regarding the accuracy of the data, all reasonable skill and care has been applied so that the data in the database are as reliable as possible. For further information on NIWA's quality control procedures see Appendix B.

There are certain aspects of climate data which can compromise quality but are not taken into account in this study as it was outside the scope for this work. For example, the accuracy of data is affected by the instrument accuracy. It is well known that rain gauges underestimate rainfall during windy conditions. In addition, as the earlier records are all manual records, their quality is largely dictated by the diligence of the observer. In some instances, notes in the station history files state that there is concern over the observer not checking rain gauges every day but only on days when it rains. This means that days where they may have been a light overnight shower could have been missed. Although such detail would have minimal effect on seasonal rainfall totals, it may impact how many dry days (days with 0 mm of rain) are counted. Despite this limitation, the records selected for analysis are considered to be good quality for the purpose of this study.

Other station rainfall data from Greater Wellington Regional Council's network (and not available through CliDB) was provided by the hydrology team within GWRC's Environmental Science department.

### 3.2.2 Data infilling procedure

A search for long duration, high quality daily and monthly records of temperature, rainfall and wind in the Wellington Region was carried out using CliDB. Stations were selected to maximise geographical coverage throughout the Wellington Region. Additional site records were provided by GWRC to augment the NIWA-held dataset. As long-term climate analysis is the principal focus of this report, the primary requirements for data were:

- High data quality (i.e. relatively few missing records); and
- Extended record with minimal site changes and preferably still operative today.

After identifying several potential stations, it was evaluated if station records from nearby stations could be combined to extend the modern record and provide more data for analysis. A long record is especially important for analysis of longer period climate cycles such as the IPO.

For each of the locations selected (see Appendix A), the following infilling process was used on the daily data:

1. Select an open climate station and download daily climate for temperature, rainfall, mean wind and wind gusts (or all available variables. Identify missing daily values;
2. Extract daily VCSN data from the nearest grid point to this station for the period 1 January 1972 to 31 December 2017;
3. See if there are any older (mostly closed) climate stations nearby that could be used to extend the time series. Download this data if available;

4. Produce regression plots using the overlapping data of the open and closed climate stations, then estimate the open station values based on the closed station data, according to the regression equation;
5. Merge the two-time series to create an extended time series, using open station data where available;
6. If there are still data gaps and there is no nearby station to fill them with, produce a regression plot between the open station and VCSN data, then estimate the climate station values based on the VCSN data, according to the regression equation;
7. Substitute missing daily station data with adjusted VCSN data.

The VCSN could not be used for infilling wind gust values as there is no wind gust variable in the VCSN dataset.

After extending and infilling daily data records, the data was combined into monthly data as both types were used for analysis. In some cases, monthly data was able to be extended further back in time than daily data due to monthly data being digitised in CliDB over a longer period than daily data. Details of daily and monthly record length can be seen in Appendix A.

In addition to the methodology above, a composite monthly temperature time-series for Masterton and Kelburn was used which has undergone a different homogenisation process. These stations are part of NIWA's 7-station series and a full peer-reviewed report on the temperature data homogenisation methodology and adjustments for each of the seven climate stations and the combined 7SS has been produced and is available from:

<https://www.niwa.co.nz/climate/information-and-resources/nz-temperature-record>.

### 3.3 Derivation of seasonal climate indices

Data analysed in this report was aggregated at a seasonal timescale based on the four meteorological seasons: December-February (DJF; summer), March-May (MAM; autumn), July-August (JJA; winter) and September-November (SON; spring). Seasonal anomalies were, when possible, calculated relative to the more recent climatological 'normal' base period of 1981–2010.

The following climate indices were analysed:

- Total rainfall (mm)
- Rain days (days with >0.5mm of rainfall, count)
- Dry days (days with 0mm of rainfall, count)
- Heavy rainfall days (days with rainfall above 90<sup>th</sup> percentile, count)
- Extreme daily rainfall (Rx1day, mm)
- Extreme 3-day rainfall (Rx3day, mm)
- Mean maximum temperature (°C)
- Mean minimum temperature (°C)
- Frost days (days with Tmin < 0°C, count)

- Hot days (days with  $T_{max} > 25^{\circ}\text{C}$ , count)
- Mean wind speed (km/h)
- Windy days (days with gusts  $> 63$  km/h and  $> 96$  km/h, count)
- Soil moisture (mm)

### 3.4 Derivation of indices for the climate modes of variability

The variability over time of large-scale climate phenomena such as El Niño-Southern Oscillation (ENSO) and the Interdecadal Pacific Oscillation (IPO) is usually encapsulated by an index: i.e. a single time-series summarizing the changes in phase and amplitude of the climate modes. In this section we describe how the indices for the climate modes considered in this study have been calculated. With the exception of the NINO sea surface temperature indices, obtained directly from the US National Climate Data Centre (NCDC), the Madden Julian Oscillation (MJO) index, obtained from the Australian Bureau of Meteorology, and the daily SAM index, obtained from the NOAA Climate Prediction Centre, all the other indices are calculated from the recently released ERSSTv5 dataset (Huang et al., 2017).

#### 3.4.1 El Niño Southern Oscillation

ENSO phases (Section 2.1) are identified in this study using an index of tropical Pacific sea surface temperature (SST) anomaly for the NINO3.4 region ( $5^{\circ}\text{N}$ - $5^{\circ}\text{S}$ ,  $120^{\circ}\text{W}$ - $170^{\circ}\text{W}$ ). Figure 2-1 shows the NINO3.4 region. Positive ENSO phases, i.e. when SSTs are greater than 1 standard deviation above the climatological normal (1981-2010) signify El Niño events. Conversely, negative ENSO phases occur when SSTs are less than 1 standard deviation below the climatological normal, and signify La Niña events. Neutral ENSO phases occur when NINO3.4 SSTs are within 1 standard deviation of the climatological normal.

#### 3.4.2 Southern Annular Mode

Indices used for quantifying the SAM (Section 2.2) are based on very limited observations prior to the satellite era (preceding 1979) as there were only a handful of climate stations over the high latitudes of the Southern Hemisphere and no continuous data records over Antarctica prior to 1958. This study calculates the SAM index as the Principal Component (PC) associated with the first Empirical Orthogonal Function (EOF), coming from an EOF analysis of monthly 850 hPa geopotential anomalies for the Southern Hemisphere ( $90^{\circ}\text{S}$  –  $20^{\circ}\text{S}$ ), using the NCEP / NCAR (NCEP 1) reanalysis (Kalnay et al., 1996). When considering the impact of the SAM over the Wellington Region at sub-seasonal timescales, we used the daily SAM (or AAO) index made available by the US NOAA via the Climate Prediction Center, at:

<ftp://ftp.cpc.ncep.noaa.gov/cwlinks/norm.daily.aao.index.b790101.current.ascii>, which was derived using a similar approach and therefore consistent with the index used for the seasonal timescale.

Supplementary analyses have been conducted, testing the impact of different definitions of the SAM on the robustness of the results: for comparison we also used the Marshall SAM index, which is derived exclusively from mean sea level pressure data and calculated as the difference between zonal pressure difference between the latitudes of  $40^{\circ}\text{S}$  and  $65^{\circ}\text{S}$  (see Marshall, 2003) as well as the monthly aggregated (averaged) daily AAO index (from the CPC). The results indicate that the response of the Wellington region to the SAM at inter-annual timescale is rather insensitive to the definition used to characterise the SAM variability (not shown). It appears however important to note here again that, *e.g.* contrary to the ENSO, which is a mode resulting from the coupling

between the Ocean and the Atmosphere and has a clear inter-annual signature – the SAM is an *internal mode of atmospheric variability*, and its preferred timescale of variability can be argued to be at the sub-seasonal timescale (with an *e*-folding timescale of ~ 10 – 20 days). Some differences between the patterns (amplitude and statistical significance) could therefore arise between the analyses conducted at the inter-annual timescale and intra-seasonal timescale.

### 3.4.3 Indian Ocean Dipole

The Indian Ocean Dipole (IOD, Section 2.3) index is calculated as the difference between monthly SST anomalies in the western (10°S – Equator, 50°W – 70°W) and eastern (10°S – Equator, 90°W – 110°W) tropical Indian Ocean. As for the IPO (below), we used the ERSST (V5) dataset over the 1920–2017 period. The IOD index is thus positive when the western (eastern) Indian Ocean is warmer (cooler) than normal. Seasonal anomalies (DJF, MAM, etc.) were calculated from the monthly anomalies.

### 3.4.4 South Pacific Subtropical Dipole

Using the ERSST (V5) dataset, we derived a South Pacific Subtropical Dipole Index (hereafter SPSD) as the difference between the monthly SST anomalies in the northwest subtropical Pacific (50°S – 30°S, 170°E – 10°W) and the southeast extra-tropical Pacific (57.5°S – 45°S, 140°E – 120°W). Seasonal anomalies (DJF, MAM, JJA and SON) were then calculated from the monthly anomalies.

### 3.4.5 Madden Julian Oscillation

The MJO signal is captured by the real-time multivariate MJO indices developed by Wheeler and Hendon (2004) and available online in real-time at <http://www.bom.gov.au/climate/mjo/graphics/rmm.74toRealtime.txt>.

The indices are the principal component (PC) time series of the two leading EOFs of combined daily mean tropical (averaged 15°N– 15°S) 850- and 200-hPa zonal wind and outgoing longwave radiation (OLR) anomalies. These so-called RMM1 and RMM2 time-series are approximately in quadrature and describe the average large-scale, west-to-east propagation of convective and circulation anomalies associated with the MJO. WH04 divide the MJO pseudocycle into eight distinct phases. Figure 2-7 illustrates the large scale convective anomalies along the tropics (20°N – 20°S) typically associated with each phase. For all analyses, MJO phases are restricted to days for which the amplitude of the MJO signals exceeds one standard deviation (1 std.).

### 3.4.6 Interdecadal Pacific Oscillation

An updated index of the Interdecadal Pacific Oscillation (IPO, Section 2.6) is not readily available elsewhere (the most up to date one is available from the UK Met-Office and stops in 2008), therefore we derived an original IPO index following the methodology in Folland et al. (1999). In brief, the IPO index used in this report is calculated as the 2<sup>nd</sup> Principal Component (PC) of time-filtered (low-pass filter, keeping only low frequency oscillations over 11 years) monthly sea surface temperature anomalies in the Pacific domain (50°S- 50°N, 120°E- 295°E) over the January 1920 – December 2017 period. The dataset used is the Extended Reconstructed SST (ERSST) Dataset (Version 5) developed by the US National Oceanic and Atmospheric Administration (NOAA) and made available by the US National Climate Data Centre (NCDC).

### 3.4.7 Sea Surface Temperatures

The ocean constitutes the slow varying component of the climate system, and therefore hold the potential for predictability of some aspects of atmospheric variability over the region. To identify

potential predictability arising from SST anomalies, we also calculated the correlation and composite fields between the GWRC climate variables and the global SSTs, also taken from the ERSSTv5 dataset for consistency.

### 3.5 Statistical analyses

The relationships between the seasonal climate indices in the Wellington Region and the climate modes of variability (summarized by time-series of indices, see above) are investigated in two ways:

- i) Calculation of the (linear) correlation coefficient between the time-series of seasonal climate indices and climate mode indices or global SST fields; and
- ii) Calculation of 'composite' anomalies.

#### 3.5.1 Correlation

The correlation coefficient used is the Pearson's correlation coefficient (Pearson's R): it is a measure of the linear correlation (dependence) between two variables X and Y, giving a value between +1 and -1 inclusive, where +1 is total positive correlation (peaks and lows are aligned; an in-phase relationship), 0 is no correlation, and -1 is total negative correlation (the peaks of one time-series are systematically related to the lows in the other; an out-of-phase relationship). It is widely used in the sciences as a measure of the degree of **linear dependence** between two variables.

The statistical significance of the correlation calculated between e.g. time-series of seasonal climate indices in the Wellington Region and the global SST field is tested using a standard two-tailed test and we highlighted areas where correlations are significant at the 95% confidence level ( $p$ -value < 0.05). As we are investigating time-series of seasonal values, the rank-1 autocorrelation is assumed to be negligible (e.g. the value of DJF total rainfall for the year 2014 is assumed to be uncorrelated to the value for DJF 2013): this assumption would be violated only in the case of a strong trend or strong cyclical component in the time-series.

#### 3.5.2 Composite analysis

The goal of composite analysis is to determine how deviations in one climate signal may be associated with deviations in another climate signal. For example, if we want to determine the typical precipitation anomalies at one station associated with El Niño events during the DJF season: the first step is to select DJF seasons when the NINO3.4 index was strongly positive (corresponding to strong El Niño events). The second step is to select (sample) from the time-series of seasonal precipitation values for the same seasons. The average for this sample is then compared to either the long-term DJF average (climatology) or all the remaining DJF seasons. An advantage of composite analysis over the Pearson's correlation coefficient is that it can uncover potential non-linear and asymmetric relationships.

In comparing the means of two samples (e.g. the El Niño sample and either the climatological normal or all the remaining seasons), one can test whether the calculated differences are statistically significant at a given risk of error using the standard Student's T-test (see [http://en.wikipedia.org/wiki/Student%27s\\_t-test](http://en.wikipedia.org/wiki/Student%27s_t-test)). The assumptions made are that the two samples are approximately normally distributed and have similar variances, both relatively reasonable assumptions when dealing with seasonally-aggregated values such as those investigated here. Note that in the cases where the seasonally aggregated variables are non-normally distributed (when we consider for example the number of days above or below a given threshold, such as hot days or frost days) we also compared the results with a non-parametric Mann-Whitney 'U' test and they were

qualitatively similar. One also needs to stress that statistical significance per-se is not equivalent to physical meaning and that attention needs to be given in interpreting the results to the spatial coherency and the consistency of the results across different related climate variables (*e.g.* soil moisture and rainfall).



## Appendix A Station Metadata

Stations used for daily station analysis				Temperature		Rainfall		Wind Gust		Mean Winds	
	Agent No.	Latitude	Longitude	Start Date	End Date	Start Date	End Date	Start Date	End Date	Start Date	End Date
Kelburn	3385	-41.286	174.767	3/12/1927	27/10/2005	4/12/1927	1/10/2005	1/01/1972	31/12/2008	4/12/1927	10/09/1998
Kelburn AWS	25354	-41.285	174.768	1/01/1972	present	1/01/1960	present	13/07/2004	present	14/07/2004	present
<b>Kelburn Composite</b>				3/12/1927	present	4/12/1927	present	1/01/1972	present	4/12/1927	present
<b>Wellington Aero</b>	3445	-41.322	174.804	1/01/1972	present	2/01/1960	present	1/01/1972	present	1/08/1994	present
Castlepoint Lighthouse	2591	-40.903	176.225	1/01/1972	31/12/1993	2/05/1907	1/01/1994	1/02/1972	28/04/1990	1/01/1962	6/09/1999
Castlepoint AWS	2592	-40.90417	176.2118	15/03/1985	present	18/03/1985	present	4/10/1993	present	5/10/1993	present
<b>Castelpoint composite</b>				1/01/1972	present	2/05/1907	present	1/02/1972	present	1/01/1962	present
<b>Paraparaumu Aero</b>	3145	-40.907	174.984	1/01/1972	present	2/01/1951	present	1/02/1972	present	1/12/1961	present
<b>Trentham Racecourse</b>	3476	-41.14	175.041	-	-	2/08/1930	present	-	-	-	-
<b>Lagoon Hill</b>	2672	-41.3904	175.52414	-	-	2/04/1923	present	-	-	-	-
<b>Martinborough (Riverside)</b>	2629	-41.179	175.482	-	-	2/01/1924	present	-	-	-	-
<b>Gladstone (Bannockburn)</b>	2633	-41.1094	175.6364			1/10/1936	present				
<b>Greentops</b>	2684	-41.481	175.576			1/07/1923	present				

<b>Marangai Station</b>	2587	-40.9057	176.00429			1/09/1914	present				
<b>Te Wharau</b>	2675	-41.3271	175.84032			1/02/1923	present				
<b>The Downs</b>	2631	-41.106	175.56			1/04/1946	present				
<b>Waikoukou</b>	2657	-41.201	175.607			1/01/1947	present				
<b>Kaiwharawhara Resrvoir</b>	GWRC site	-41.2980	174.74477			03/01/1879	30/06/2017				
<b>Wainuiomata Reservoir</b>	GWRC site	-41.2688	174.98991			02/01/1890	30/06/2017				

Stations used for monthly station analysis				Temperature		Rainfall		Wind Gust		Mean Winds	
	Agent No.	Latitude	Longitude	Start Date	End Date	Start Date	End Date	Start Date	End Date	Start Date	End Date
Kelburn	3385	-41.286	174.767	1/12/1927	31/08/2005	1/01/1928	31/10/2005	1/01/1972	31/12/2008	1/12/1927	31/08/1998
Kelburn AWS	25354	-41.285	174.768	1/05/2004	present	1/05/2004	present	1/08/2004	present	1/08/2004	present
<b>Kelburn Composite</b>				1/12/1927	present	1/01/1928	present	1/01/1972	present	1/12/1927	present
<b>Wellington Aero</b>	3445	-41.322	174.804	1/01/1962	present	1/01/1960	present	1/01/1972	present	1/08/1994	present
Castlepoint Lighthouse	2591	-40.903	176.225	1/01/1972	31/12/1993	1/01/1902	31/12/1993	1/02/1972	27/03/1990	1/01/1962	31/08/1999
Castlepoint AWS	2592	-40.9041	176.2118	1/04/1985	present	1/01/1986	present	4/10/1993	present	1/11/1993	present
<b>Castelpoint composite</b>				1/01/1972	present	1/01/1902	present	1/02/1972	present	1/01/1962	present
<b>Parapraumu Aero</b>	3145	-40.907	174.984	1/01/1953	present	1/01/1945	present	1/02/1972	present	1/12/1961	present
<b>Trentham Racecourse</b>	3476	-41.14	175.041	-	-	2/08/1930	present	-	-	-	-

<b>Lagoon Hill</b>	2672	-41.3904	175.52414	-	-	2/04/1923	present	-	-	-	-
<b>Martinborough (Riverside)</b>	2629	-41.179	175.482	-	-	2/01/1924	present	-	-	-	-
<b>Masterton composite</b>				1/02/1912	present	-	-	-	-	-	-
<b>Gladstone (Bannockburn)</b>	2633	-41.1094	175.6364			1/10/1936	present				
<b>Greentops</b>	2684	-41.481	175.576			1/07/1923	present				
<b>Marangai Station</b>	2587	-40.9057	176.00429			1/09/1914	present				
<b>Te Wharau</b>	2675	-41.3271	175.84032			1/02/1923	present				
<b>The Downs</b>	2631	-41.106	175.56			1/04/1946	present				
<b>Waikoukou</b>	2657	-41.201	175.607			1/01/1947	present				
<b>Kaiwharawhara Reservoir</b>	GWRC site	-41.2980	174.74477			03/01/1879	30/06/2017				
<b>Wainuiomata Reservoir</b>	GWRC site	-41.2688	174.98991			02/01/1890	30/06/2017				

## Appendix B NIWA data quality control

The following quality control procedure is undertaken for all data in CLIDB at the time of print. As observed values are transferred into permanent data tables in the database (e.g. MAX\_MIN\_TEMP, RAIN etc.) from temporary input tables (e.g. RMS\_AWS, RMS\_DLYCLI etc.) they are automatically inspected for errors. These are either gross errors when values fall outside very wide universal limits so that an error flag is given the value “E” and the observation is not transferred into CLIDB, or they are potential errors as they lie sufficiently outside of the 1 or 99 percentile for that place/time so that an error flag is given the value “W” and the observation is transferred into CLIDB.

Most data originating from the various data streams entering CLIDB (i.e. of different origins or message types) do so as frequently as possible (e.g. RMS\_AWS is hourly but the suite of UPPER\_AIR messages are every 6 hours). These frequent transfers do not report errors and warnings but daily collectives are also run and the errors and warnings are reported with these runs. The daily collective runs also log any errors or warnings into the ERRLOG and WARNLOG tables except for AWS data which do not have a daily collective but a daily reporting/logging process runs just after midnight. Time series plots centred on the observation with a “W” warning are generated and the 1 and 99 percentiles are also used to standardise observations and facilitate manual checking of the data.

After manual inspection and depending upon the inspection outcome, the data are either unchanged or corrected (with associated quality flags) or deleted from CLIDB. Data remaining in the database are deemed sufficiently high quality for inclusion in the station data record, and for subsequent data analysis. Should users of the climate data query its validity, then additional user-initiated manual data checks are also made.

## 4 References

- ARBLASTER, J. M. & MEEHL, G. A. 2006. Contributions of external forcings to Southern Annular Mode Trends. *Journal of Climate*, 19, 2896-2905.
- BARNSTON, A. G., TIPPETT, M. K., L'HEUREUX, M. L., LI, S. & DEWITT, D. G. 2011. Skill of real-time seasonal ENSO model predictions during 2002–2011: Is our capability increasing? *Bulletin of the American Meteorological Society*, 93, 631-351.
- BEHERA, S. K., LUO, J. J., MASSON, S., RAO, S. A., SAKUMA, H. & YAMAGATA, T. 2006. A CGCM Study on the Interaction between IOD and ENSO. *Journal of Climate*, 19, 1688-1705.
- FAUCHEREAU, N., POHL, B. & LORREY, A. 2016. Extratropical Impacts of the Madden–Julian Oscillation over New Zealand from a Weather Regime Perspective. *Journal of Climate*, 29, 2161-2175.
- FEDAEFF, N. & FAUCHEREAU, N. 2015. Relationship between climate modes and Hawke's Bay seasonal rainfall and temperature. NIWA Client Report prepared for Hawke's Bay Regional Council, Report Number AKL2015-016, 50pp.
- FOLLAND, C. K., PARKER, D. E., COLMAN, A. W. & WASHINGTON, R. 1999. Large Scale Modes of Ocean Surface Temperature Since the Late Nineteenth Century. In: NAVARRA, A. (ed.) *Beyond El Niño SE - 4*. Springer Berlin Heidelberg.
- GUAN, Y., ZHU, J., HUANG, B., HU, Z.-Z. & III, J. L. K. 2014. South Pacific Ocean Dipole: A Predictable Mode on Multiseasonal Time Scales. *Journal of Climate*, 27, 1648-1658.
- HOSKINS, B. J. & KAROLY, D. J. 1981. The steady linear response of a spherical atmosphere to thermal and orographic forcing. *Journal of Atmospheric Sciences*, 38, 1179-1196.
- HUANG, B., THORNE, P. W., BANZON, V. F., BOYER, T., CHEPURIN, G., LAWRIK, J. H., MENNE, M. J., SMITH, T. M., VOSE, R. S. & ZHANG, H.-M. 2017. Extended Reconstructed Sea Surface Temperature, Version 5 (ERSSTv5): Upgrades, Validations, and Intercomparisons. *Journal of Climate*, 30, 8179-8205.
- IPCC (ed.) 2013. *Climate Change 2013: The Physical Science Basis. Contribution of Working Group I to the Fifth Assessment Report of the Intergovernmental Panel on Climate Change*, Cambridge, United Kingdom and New York, NY, USA: Cambridge University Press.
- KALNAY, E., KANAMITSU, M., KISTLER, R., COLLINS, W., DEAVEN, D., GANDIN, L., IREDELL, M., SAHA, S., WHITE, G., WOOLLEN, J., ZHU, Y., CHELLIAH, M., EBISUZAKI, W., HIGGINS, W., JANOWIAK, J., MO, K. C., ROPELEWSKI, C., WANG, J., LEETMAA, A., REYNOLDS, R., JENNE, R. & JOSEPH, D. 1996. The NCEP/NCAR 40-Year Reanalysis Project. *Bulletin of the American Meteorological Society*, 77, 437-472.
- KIDSON, J. W. 2000. An analysis of New Zealand synoptic types and their use in defining weather regimes. *International Journal of Climatology*, 20, 299-316.
- KIDSTON, J., RENWICK, J. & MCGREGOR, J. 2009. Hemispheric-Scale Seasonality of the Southern Annular Mode and Impacts on the Climate of New Zealand. *Journal of Climate*, 22, 4759-4770.
- MADDEN, R. A. & JULIAN, P. R. 1972. Description of Global-Scale Circulation Cells in the Tropics with a 40–50 Day Period. *Journal of the Atmospheric Sciences*, 29, 1109-1123.
- MANTUA, N. J., HARE, S. R., ZHANG, Y., WALLACE, J. M. & FRANCIS, R. C. 1997. A Pacific Interdecadal Climate Oscillation with Impacts on Salmon Production. *Bulletin of the American Meteorological Society*, 78, 1069-1079.
- MATTHEWS, A. & MEREDITH, M. 2004. Variability of Antarctic circumpolar transport and the Southern Annular Mode associated with the Madden-Julian Oscillation. *Geophysical Research Letters*, 31, 1-5.
- MORIOKA, Y., RATNAM, J. V., SASAKI, W. & MASUMOTO, Y. 2013. Generation Mechanism of the South Pacific Subtropical Dipole. *Journal of Climate*, 26, 6033-6045.
- MULLAN, A. B. 1995. On the inearity and stability of the Southern Oscillation climate relationships for New Zealand. *International Journal of Climatology*, 15, 1365-1386.
- MULLAN, A. B. 1998. Southern hemisphere sea-surface temperatures and their contemporary and lag association with New Zealand temperature and precipitation. *International Journal of Climatology*, 18, 817-840.

- MULLAN, A. B. & THOMPSON, C. 2006. Analogue forecasting of New Zealand Climate Anomalies. *International Journal of Climatology*, 26, 485-504.
- PEARCE, P. R., FEDAEFF, N., MULLAN, A. B., SOOD, A., BELL, R. G., TAIT, A., COLLINS, D. & ZAMMIT, C. 2017. Climate change and variability - Wellington Region. NIWA Client Report prepared for Greater Wellington Regional Council, Client Report Number 2017066AK, 192 pp.
- PHILANDER, S. G. H. 1990. *El Niño, La Niña, and the Southern Oscillation*, International Geophysics Series, Academic Press.
- POHL, B., FAUCHEREAU, N., REASON, C. J. C. & ROUAULT, M. 2010. Relationships between the Antarctic Oscillation, the Madden–Julian Oscillation, and ENSO, and Consequences for Rainfall Analysis. *Journal of Climate*, 23, 238-254.
- POWER, S., CASEY, T., FOLLAND, C. K., COLMAN, A. W. & MEHTA, V. 1999. Inter-decadal modulation of the impact of ENSO on Australia. *Climate Dynamics*, 15, 319-324.
- RENWICK, J. A. & THOMPSON, D. 2006. The Southern Annular Mode and New Zealand climate. *Water & Atmosphere*, 14, 24-25.
- SALINGER, M. J., RENWICK, J. A. & MULLAN, A. B. 2001. Interdecadal Pacific Oscillation and South Pacific climate. *International Journal of Climatology*, 21, 1705-1721.
- TAIT, A., BELL, R. G., BURGESS, S., GORMAN, R. G., GRAY, W., LARSEN, H., MULLAN, A. B., REID, S., SANSOM, J., THOMPSON, C. & WRATT, D. 2002. Meteorological hazards and the potential impacts of climate change in Wellington Region. NIWA Client Report WLG2002/19, 155 pp.
- TAIT, A., HENDERSON, R., TURNER, R. & ZHENG, X. G. 2006. Thin plate smoothing spline interpolation of daily rainfall for New Zealand using a climatological rainfall surface. *International Journal of Climatology*, 26, 2097-2115.
- THOMPSON, D. W. J., SOLOMON, S., KUSHNER, P. J., ENGLAND, M. H., GRISE, K. M. & KAROLY, D. J. 2011. Signatures of the Antarctic ozone hole in Southern Hemisphere surface climate change. *Nature Geoscience*, 4, 741-749.
- TROUP, A. J. 1965. The Southern Oscillation. *Quarterly Journal of the Royal Meteorological Society*, 91, 490-506.
- UMMENHOFER, C. C. & ENGLAND, M. H. 2007. Interannual extremes in New Zealand precipitation linked to modes of Southern Hemisphere climate variability. *Journal of Climate*, 20, 5418-5440.
- UMMENHOFER, C. C., SEN GUPTA, A. & ENGLAND, M. H. 2009. Causes of late twentieth-century trends in New Zealand precipitation. *Journal of Climate*, 22, 3-19.
- WHEELER, M. C. & HENDON, H. H. 2004. An All-Season Real-Time Multivariate MJO Index: Development of an Index for Monitoring and Prediction. *Monthly Weather Review*, 132, 1917-1932.
- ZHANG, C. 2005. Madden-Julian Oscillation. *Reviews of Geophysics*, 43.
- ZHANG, C. 2013. Madden-Julian Oscillation: Bridging weather and climate. *Bulletin of the American Meteorological Society*, 94, 1849-1870.

# Regional climate mode impacts on the Wellington Region

*Part B: Relationships between inter-annual climate modes and rainfall*

## Contents

<b>1</b>	<b>Total Rainfall</b> .....	<b>33</b>
1.1	ENSO .....	33
1.2	SAM .....	37
1.3	IOD .....	40
1.4	SPSD .....	43
<b>2</b>	<b>Total rain days</b> .....	<b>46</b>
2.1	ENSO .....	46
2.2	SAM .....	49
2.3	IOD .....	52
2.4	SPSD .....	55
<b>3</b>	<b>Heavy rain days</b> .....	<b>58</b>
3.1	ENSO .....	58
3.2	SAM .....	61
3.3	IOD .....	64
3.4	SPSD .....	67
<b>4</b>	<b>Dry days</b> .....	<b>70</b>
4.1	ENSO .....	70
4.2	SAM .....	71
4.3	IOD .....	72
4.4	SPSD .....	73
<b>5</b>	<b>Relationship to Sea Surface Temperature (SST) anomalies</b> .....	<b>74</b>
<b>6</b>	<b>References</b> .....	<b>77</b>



This is Part B of the 'Regional climate mode impacts on the Wellington Region' report. Refer to Part A: Introduction, Methodology and Background for a thorough introduction to this study.

In this section, the relationships between seasonally (DJF, MAM, JJA, SON) aggregated rainfall parameters (total rainfall, number of rain days, number of days exceeding the climatological 90<sup>th</sup> percentile of daily rainfall, referred to as 'heavy rainfall', and number of dry days) and the inter-annual climate modes (El Niño Southern Oscillation (ENSO), Southern Annular Mode (SAM), Indian Ocean Dipole (IOD) and South Pacific Subtropical Dipole (SPSD)) are presented, first using the Virtual Climate Station Network (VCSN) and by means of composite analyses, then using the available station data.

For the VCSN, composite anomalies are calculated for the extreme phases of each mode: *i.e.* when standardized seasonal values exceed + 1 standard deviation (referred to as the positive phase of the mode) and are below -1 standard deviation (negative phase of the mode). For consistency, the 1981-2010 climatological normal is used for both the VCSN dataset (to define the 'normal' rainfall) and for the climate mode index (to define the mean and standard deviation for the seasonally stratified standardisation).

For the station data, the composites are expressed in the original unit (e.g. mm for total rainfall, days for the number of rain days), and shown for each season and for each phase of the mode (positive, negative, and neutral). For each extreme phases of the climate mode, the mean as well as inter-quartile range (25 to 75<sup>th</sup> percentile) are displayed for each season, as well as the mean of the 'Neutral' phase (standard deviation between -1 and 1 standard deviation). This representation thus gives a summary of the distribution of the values included in the three samples, and illustrates the variability in the corresponding rainfall parameter observed during each phase of the mode. Because of the large number of rainfall stations analysed, we generally only present figures for some of the stations displaying a significant ( $p < 0.05$  according to a Student t-test) association for the mode during at least one season. The figures not included are all available as supplementary electronic material to this report.

# 1 Total Rainfall

Total (cumulative rainfall) anomalies derived from the VCSN are presented in percentage of normal (1981-2010 climatology), with the anomalies expressed in mm available in the electronic supplementary material to this report: note that they present the same patterns and – by construction – the same areas of statistical significance.

## 1.1 ENSO

### 1.1.1 VCSN

The VCSN composite anomalies suggest that the relationship between seasonal rainfall amount and ENSO is highly non-linear, notably during DJF (the usual peak of ENSO events) where a general decrease in rainfall amounts is observed during both the positive (El Niño) (Figure 1-1) and negative (La Niña) (Figure 1-2) phases of ENSO.

During both phases and in DJF, the largest – and statistically significant – anomalies (rainfall deficits reaching to ~70% of the normal rainfall for this season) are observed in the western part of the Wellington Region. During MAM, usually corresponding increases in rainfall amounts are experienced during both positive and negative phases of ENSO, particularly in the western part of the Wellington Region. During JJA and SON and the positive phases of ENSO, statistically significant decreases in rainfall are also experienced over large parts of the Wellington Region. In summary, El Niño is therefore generally associated with rainfall deficits over the Wellington Region from spring to winter. The anomalies composites for the negative phase of ENSO (La Niña) indicate that the relationship of rainfall to ENSO is not symmetric: rainfall deficits are also observed during La Niña especially in DJF and to some extent in SON: i.e. in summer, the Wellington Region is prone to observe rainfall deficits during both phases of ENSO.

**Figure 1-1: Rainfall anomalies during the positive phase (El Niño) of ENSO (VCSN anomalies).** Red lines outline areas of statistical significance at  $p \leq 0.05$ . The years indicated on each figure are those of the last month in the season (e.g. DJF 1973 refers to December 1972 – February 1973).

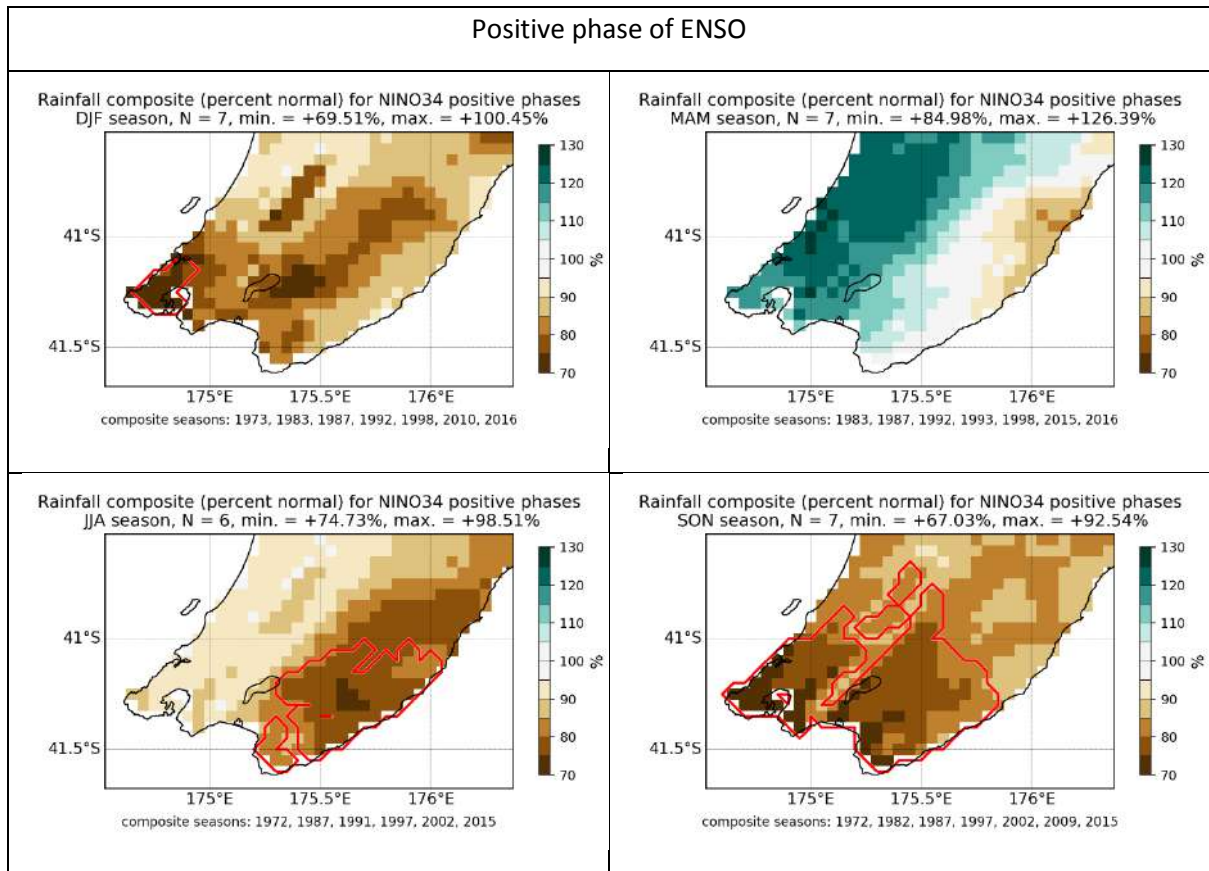
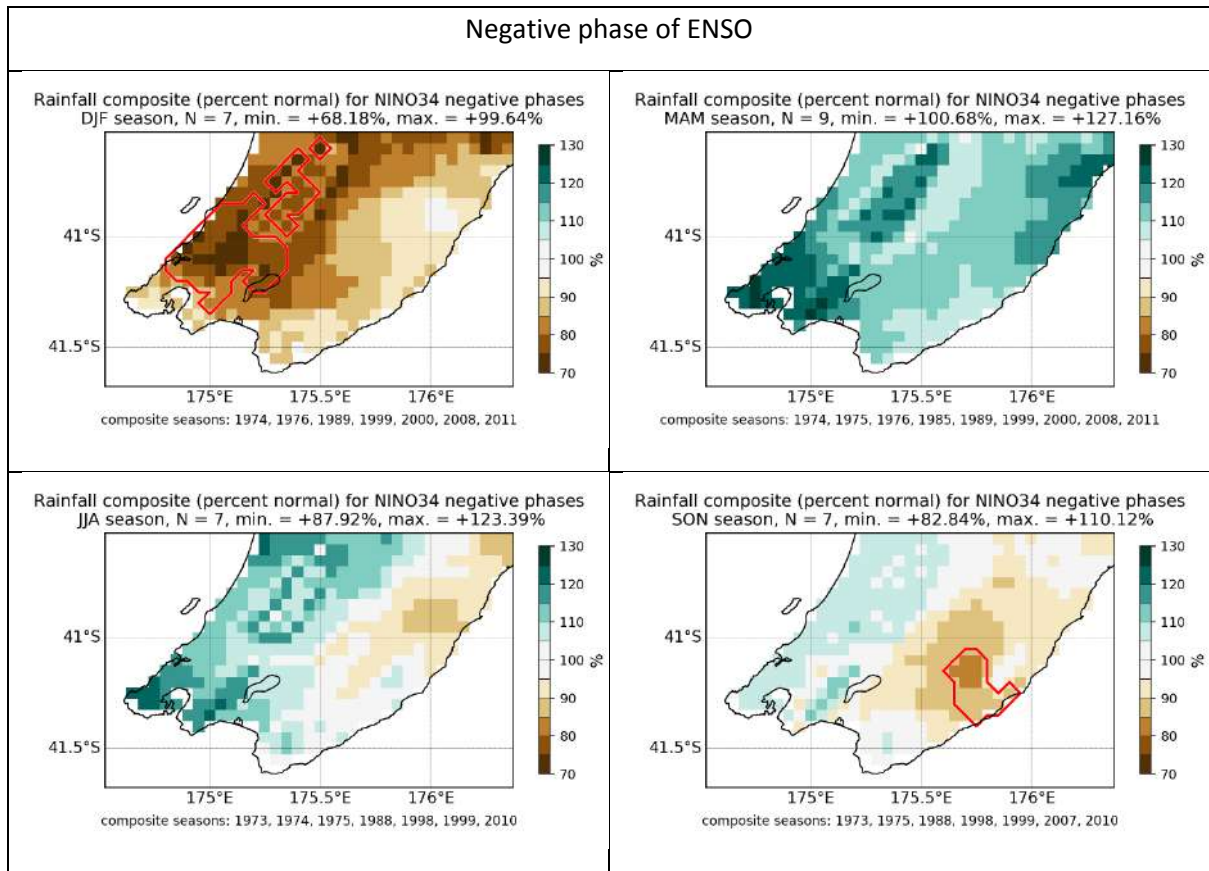


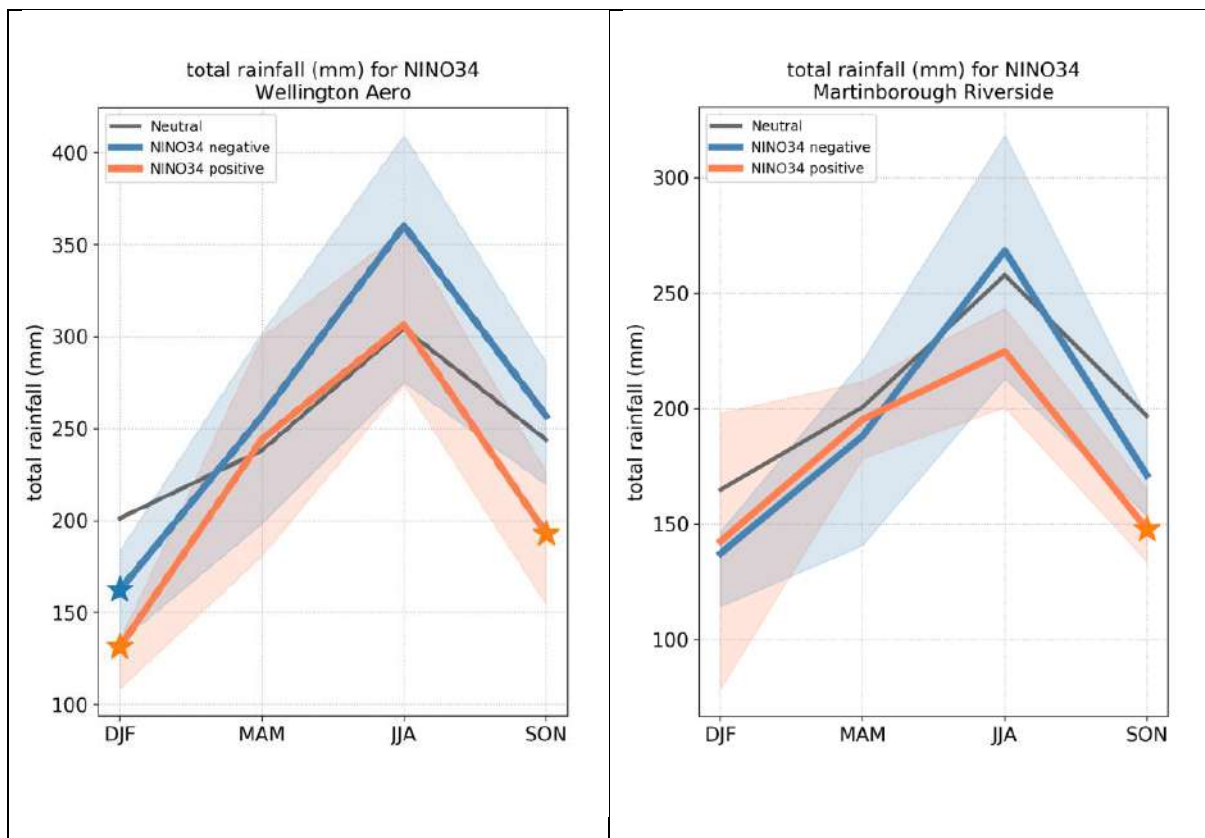
**Figure 1-2: Rainfall anomalies during the negative phase (La Niña) of ENSO (VCSN anomalies).** Red lines outline areas of statistical significance at  $p \leq 0.05$ .



### 1.1.2 Station data

The composite analyses for the station data are generally consistent with the patterns displayed by the VCSN. The relationships are in many cases non-linear, with decreased total rainfall observed during both phases of ENSO, and the most significant anomalies are generally found in SON and / or DJF: this is illustrated by Figure 1-3, which presents the mean seasonal rainfall for the positive, negative and neutral phases of ENSO (NINO3.4) for the Wellington Aero station, as well as for the Martinborough (riverside) station in the Wairarapa: significantly lower than normal rainfall amounts are recorded in DJF for both phases of ENSO, with decreased rainfall being significant as well for the negative phase of ENSO during SON in Wellington. For the Martinborough (riverside) station – as is the case of most station in the Wairarapa, significantly lower than normal total rainfall are recorded during the positive phase of ENSO in SON.

**Figure 1-3: Total rainfall and ENSO phase at Wellington (Aero) and Martinborough (riverside) station.** The stars indicate statistical significance at  $p \leq 0.05$ , and the shaded area indicates the interquartile range (25<sup>th</sup> to 75<sup>th</sup> percentile) of the corresponding composite sample.



## 1.2 SAM

### 1.2.1 VCSN

The clearest relationship between seasonal rainfall amounts and the SAM is during DJF (Figure 1-4), for large parts of the Wellington Region, where rainfall tends to be lower than normal during the positive phase of the SAM (i.e. when the westerly wind belt is shifted poleward). Anomalies during the negative phase of the SAM are much less prominent (Figure 1-5), although rainfall tends to be lower than normal during MAM for the northeast of the region (Masterton District) as well as around Wellington City and the Hutt Valley in SON. As was the case for ENSO, the relationship of the Wellington Region's rainfall total to the SAM is therefore neither symmetric nor linear.

**Figure 1-4: Rainfall anomalies during the positive phase of SAM (VCSN anomalies).** Red lines outline areas of statistical significance at  $p \leq 0.05$ .

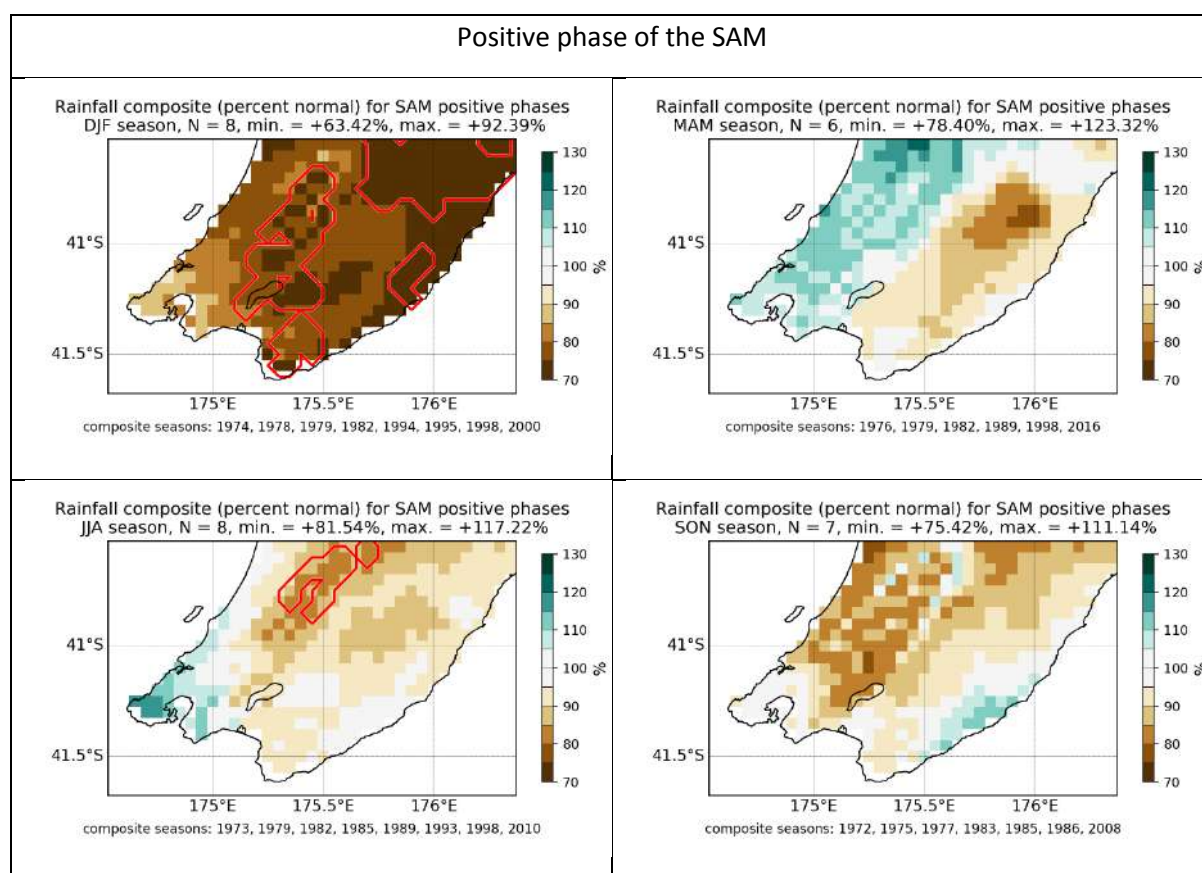
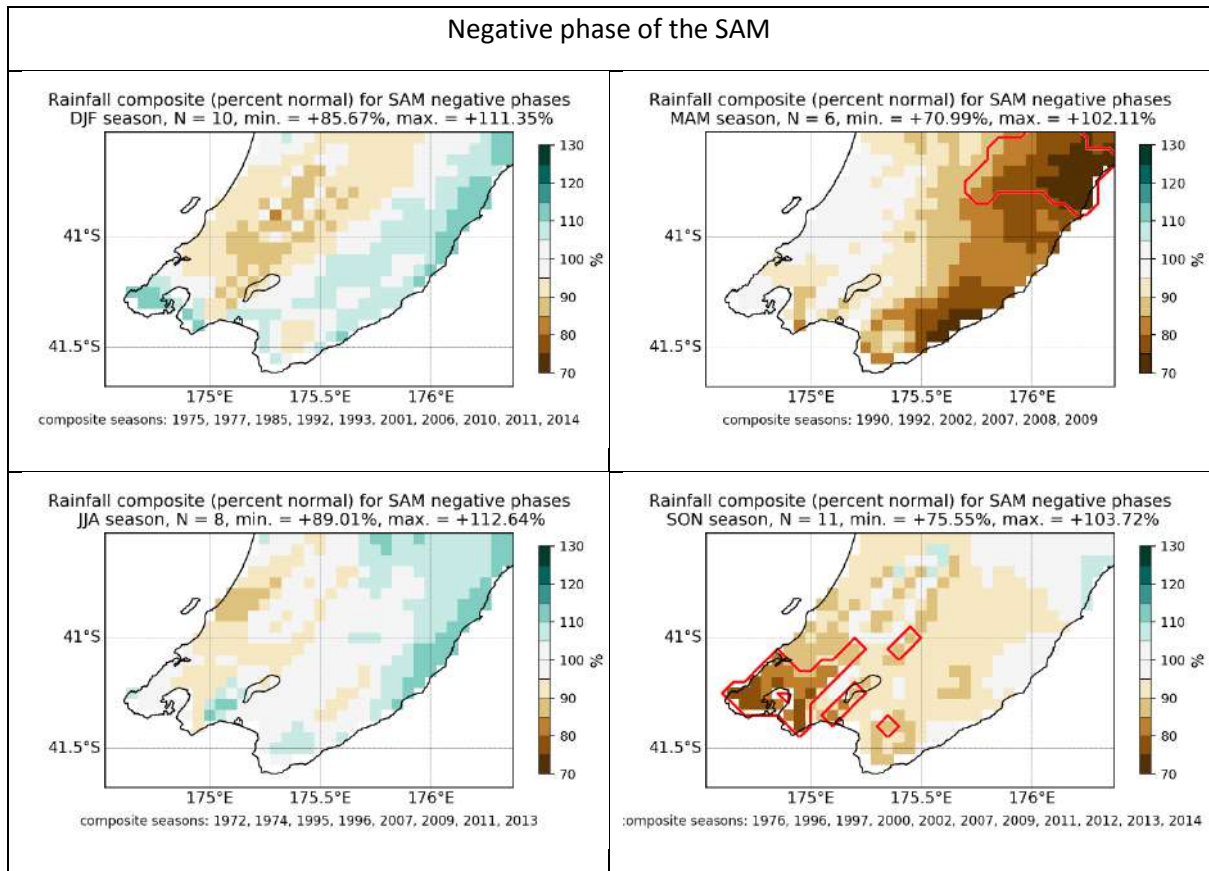


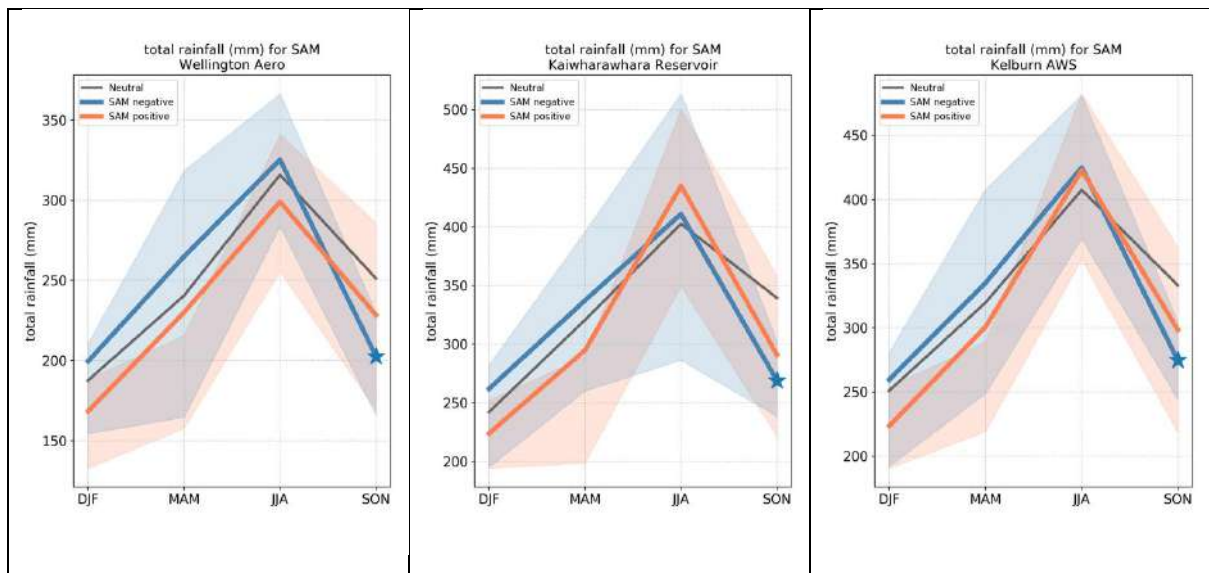
**Figure 1-5: Rainfall anomalies during the negative phase of SAM (VCSN anomalies).** Red lines outline areas of statistical significance at  $p \leq 0.05$ .



### 1.2.2 Station data

The only clear and significant ( $p=0.01$ ) relationships between total (cumulative) seasonal rainfall and the SAM is found for the Wellington Aero, Kaiwharawhara Reservoir and Kelburn stations during SON (Figure 1-6). In all cases the SON seasonal rainfall amounts tend to be lower than normal during the negative phase of the SAM.

**Figure 1-6: Total rainfall and SAM phase at Wellington Aero, Kaiwharawhara Reservoir and Kelburn.** The stars indicate statistical significance at  $p \leq 0.05$ , and the shaded area indicates the interquartile range (25<sup>th</sup> to 75<sup>th</sup> percentile) of the corresponding composite sample.





## 1.3 IOD

### 1.3.1 VCSN

The most significant relationships between the IOD and seasonal rainfall are found during MAM, where large parts of the western and southern Wellington Region experience lower rainfall than usual during the positive phase of the IOD (Figure 1-7). Note however that while statistically significant, the anomalies are modest (minimum of ~77% of normal). Moreover, the IOD is a mode of variability which is strongly phase-locked onto the seasonal cycle, with its expression resulting from ocean – atmosphere interaction peaking during the Southern Hemisphere spring (SON and OND), it is therefore likely that the rainfall anomalies shown during the MAM season are reflecting an indirect relationship to large scale SST gradients in the tropical Indian Ocean which are not a manifestation of the IOD *per-se*. This caveat needs to be kept in mind throughout the report when interpreting anomalies related to extreme phases of the IOD index outside of the SON season.

**Figure 1-7: Rainfall anomalies during the positive phase of IOD (VCSN anomalies).** Red lines outline areas of statistical significance at  $p \leq 0.05$ .

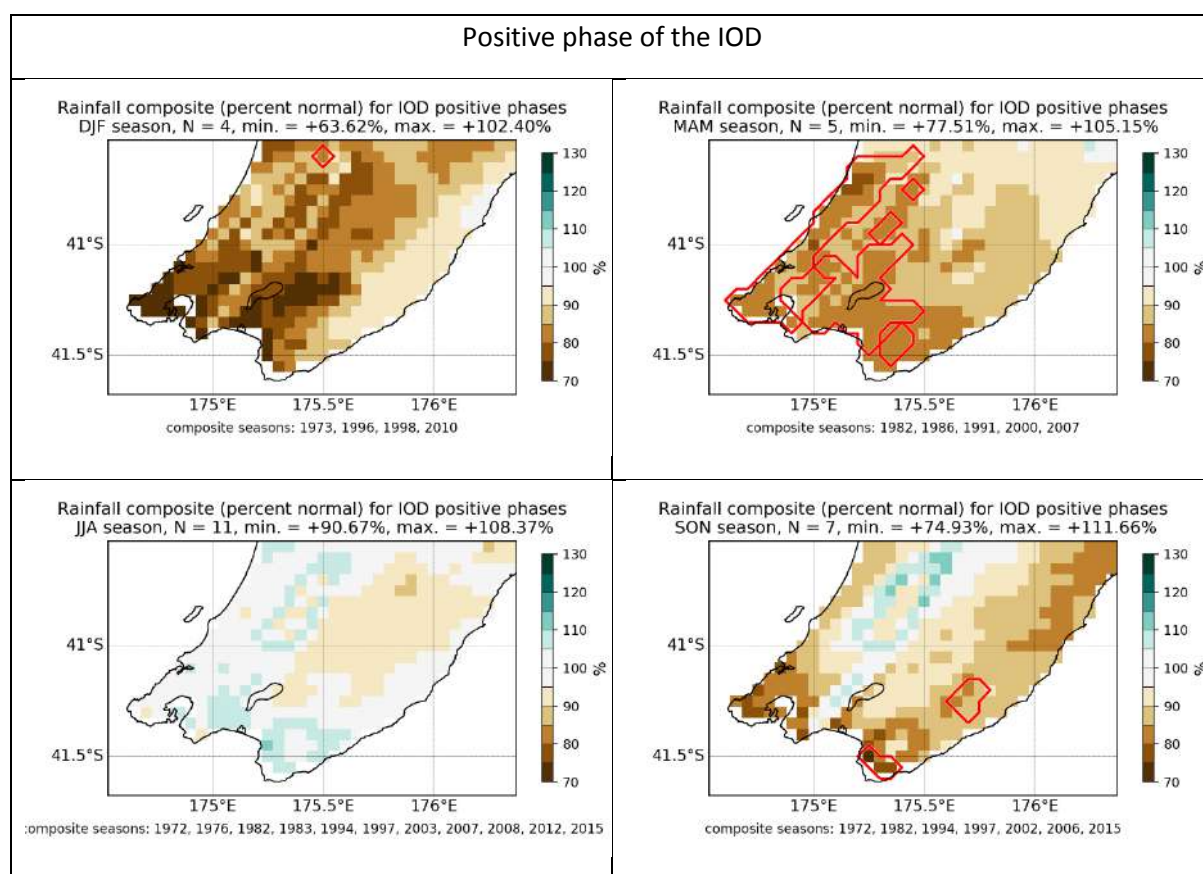
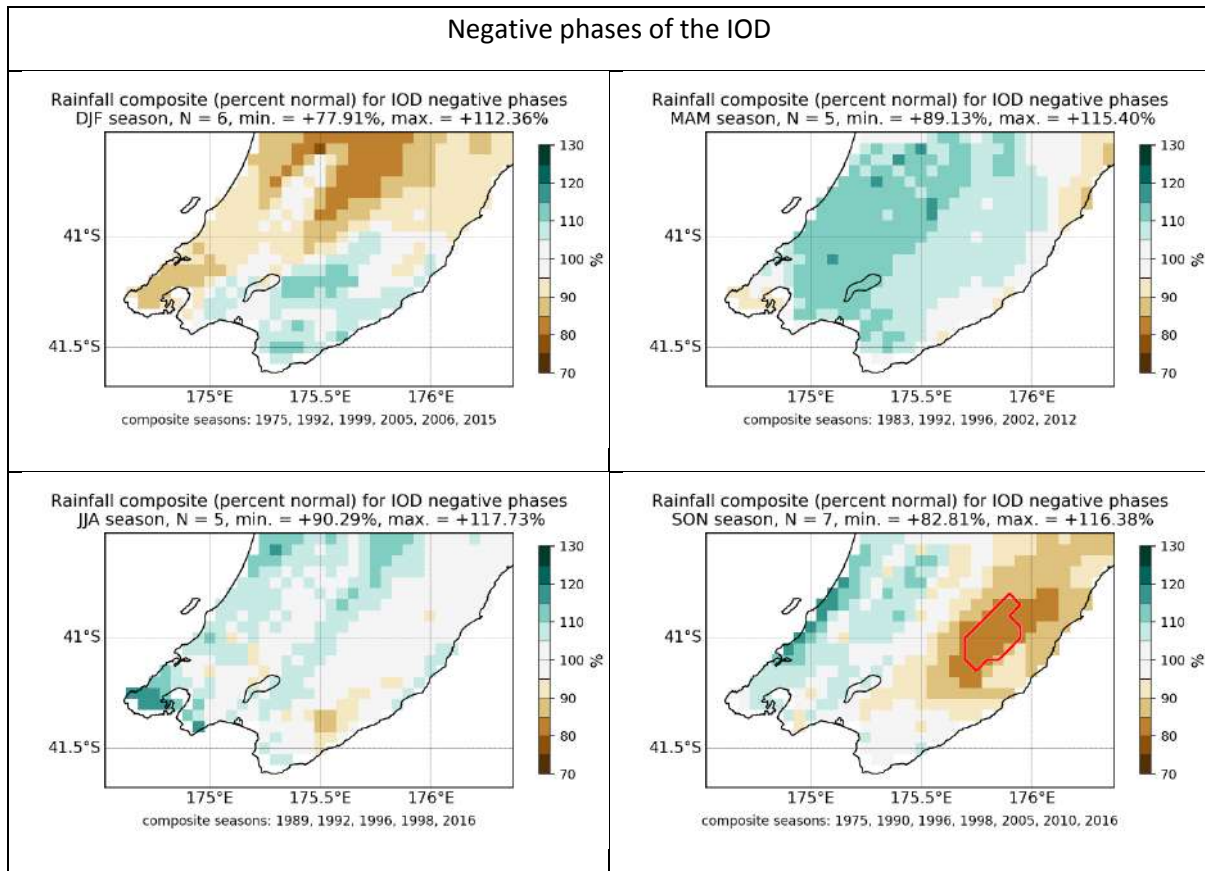


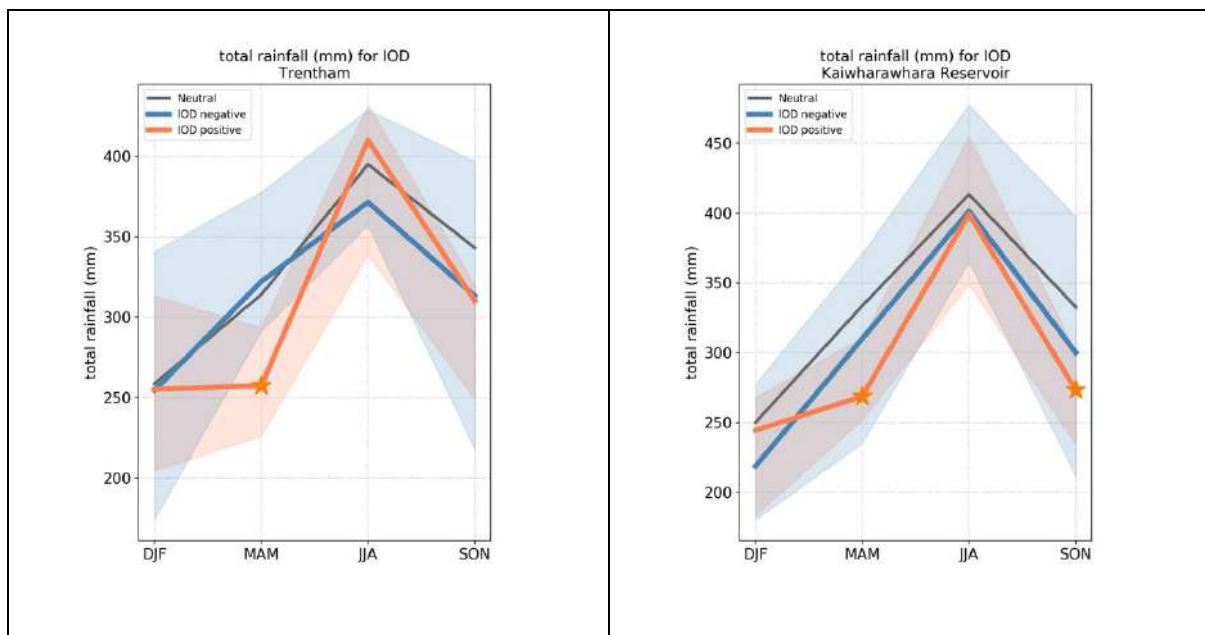
**Figure 1-8: Rainfall anomalies during the negative phase of IOD (VCSN anomalies).** Red lines outline areas of statistical significance at  $p \leq 0.05$ .



### 1.3.2 Station data

Confirming the general pattern displayed by the VCSN composites, significant cumulative rainfall anomalies are found for the following stations during the MAM season: Trentham, Paraparaumu Aero, Kelburn, Wellington Aero, Kaiwharawhara Reservoir and Greentops. For these stations, total rainfall tends to be lower than normal during the positive phase of the IOD. At Kaiwharawhara Reservoir, the positive phase of the IOD is also associated with significantly lower than normal rainfall in OND. For the sake of space, only the plots for Trentham and Kaiwharawhara Reservoir are shown on Figure 1-9.

**Figure 1-9: Total rainfall and IOD phase at Trentham and Kaiwharawhara Reservoir.** The stars indicate statistical significance at  $p \leq 0.05$ , and the shaded area indicates the interquartile range (25<sup>th</sup> to 75<sup>th</sup> percentile) of the corresponding composite sample.



## 1.4 SPSD

### 1.4.1 VCSN

Significant anomalies are only observed for JJA in the western part of the Wellington Region during the positive phase of the SPSD, where below normal rainfall tends to occur (Figure 1-10). Note however that again the anomalies are very modest (minimum of ~86 % of normal rainfall). In general rainfall anomalies are similar for the positive and negative phases of the SPSD.

**Figure 1-10: Rainfall anomalies during the positive phase of SPSD (VCSN anomalies).** Red lines outline areas of statistical significance at  $p \leq 0.05$ .

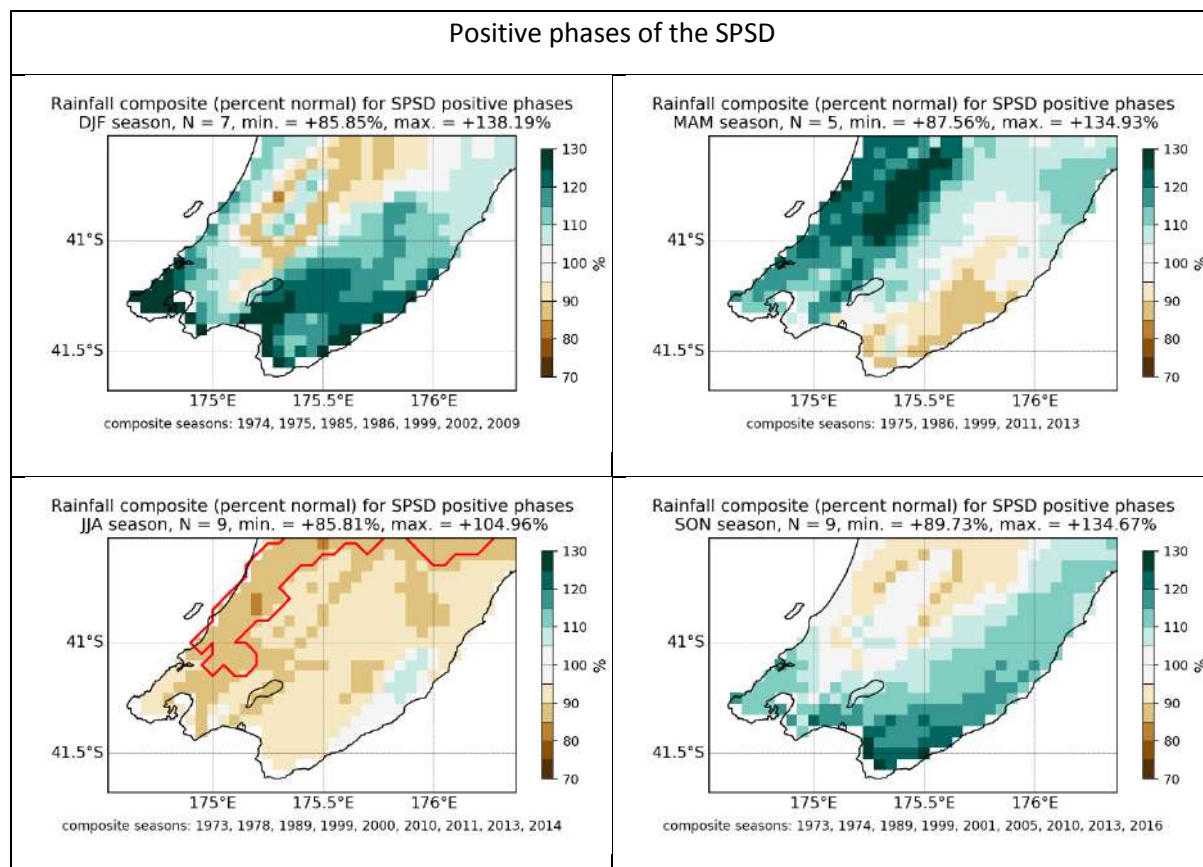
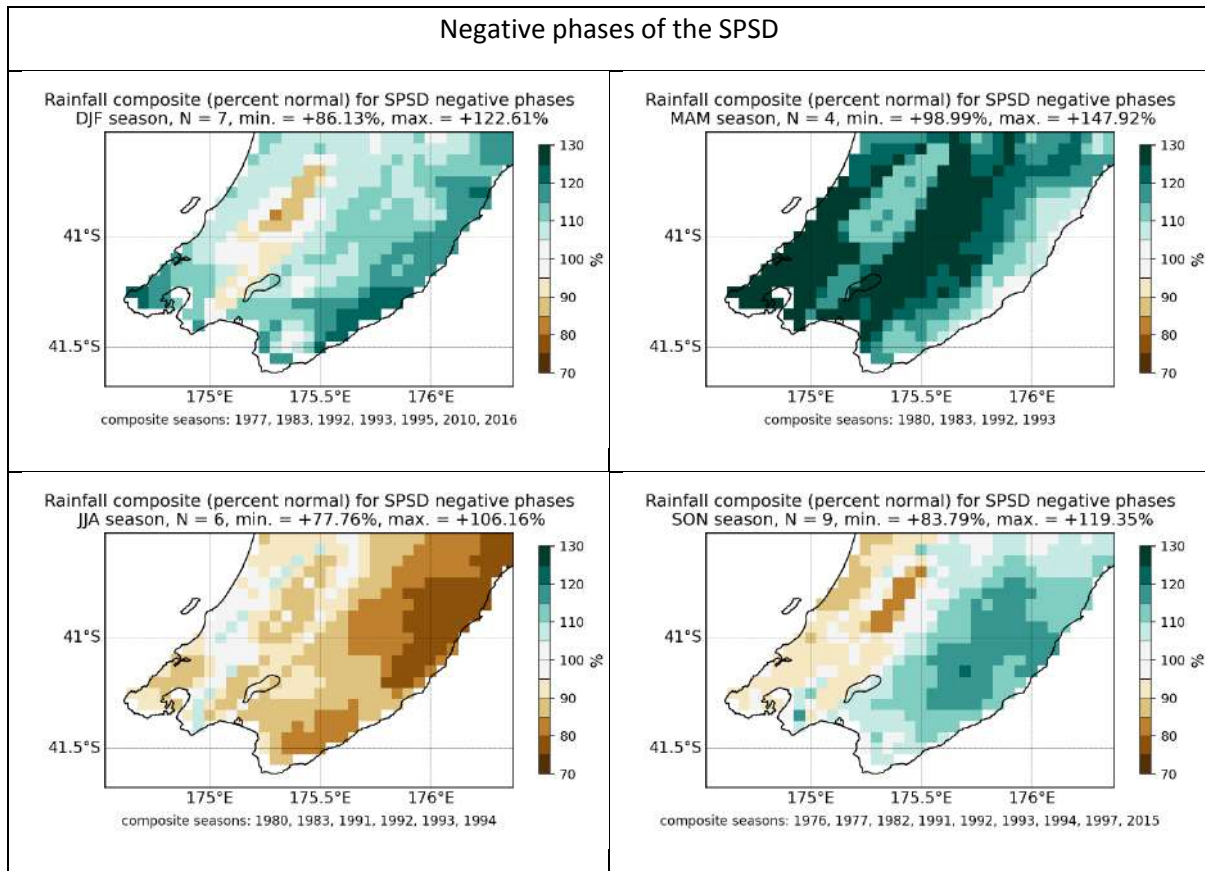


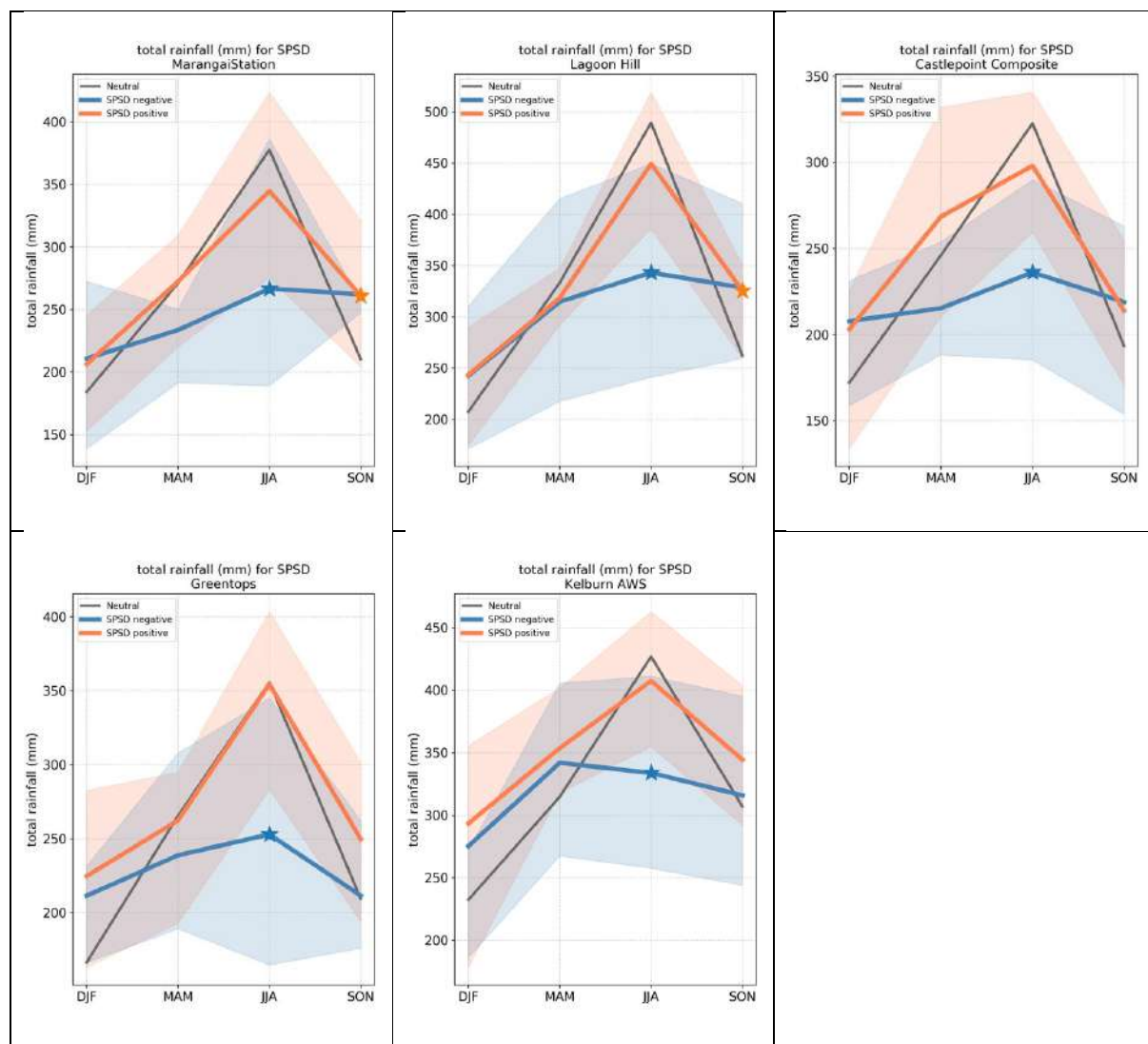
**Figure 1-11: Rainfall anomalies during the negative phase of SPSP (VCSN anomalies).** Red lines outline areas of statistical significance at  $p \leq 0.05$ .



### 1.4.2 Station data

Confirming the VCSN composite anomalies, all the significant ( $p \leq 0.05$ ) relationships with the SPSP are found during the winter season (JJA) for the following stations (Figure 1-12): Marangai Station, Lagoon Hill, Castlepoint (composite), Greentops and Kelburn AWS. For all these stations, the total JJA seasonal rainfall tends to be lower than normal during the negative phase of the SPSP. Note that reduced rainfall during the negative phase of the SPSP is consistent with the cooler than normal SSTs usually observed around NZ during this phase of the mode.

**Figure 1-12: Total rainfall and SPSP phase at Marangai Station, Lagoon Hill, Castlepoint (composite), Greentops, and Kelburn AWS.** The stars indicate statistical significance at  $p \leq 0.05$ , and the shaded area indicates the interquartile range (25<sup>th</sup> to 75<sup>th</sup> percentile) of the corresponding composite sample.



## 2 Total rain days

Rain day anomalies derived from the VCSN are presented in the departure from normal in days (1981-2010 climatology). A rain day is counted when rainfall exceeds 0.5 mm.

### 2.1 ENSO

#### 2.1.1 VCSN

The clearest relationship between the number of rain days (days with rain >0.5 mm) and ENSO is found again during SON and DJF, but here again the relationship is found to be highly non-linear: a decrease in the number of rain days is found during these seasons during both the positive and negative phases of ENSO. During DJF, the number of rain days tend to decrease mainly in the eastern half of the Wellington Region during El Niño (Figure 2-1), while during La Niña the largest decrease is observed in the western half (Figure 2-2). In SON, the largest anomalies are found in the eastern areas of the Wellington Region for both phases of ENSO.

**Figure 2-1: Rain day anomalies during the positive phase of ENSO (VCSN anomalies).** Red lines outline areas of statistical significance at  $p \leq 0.05$ .

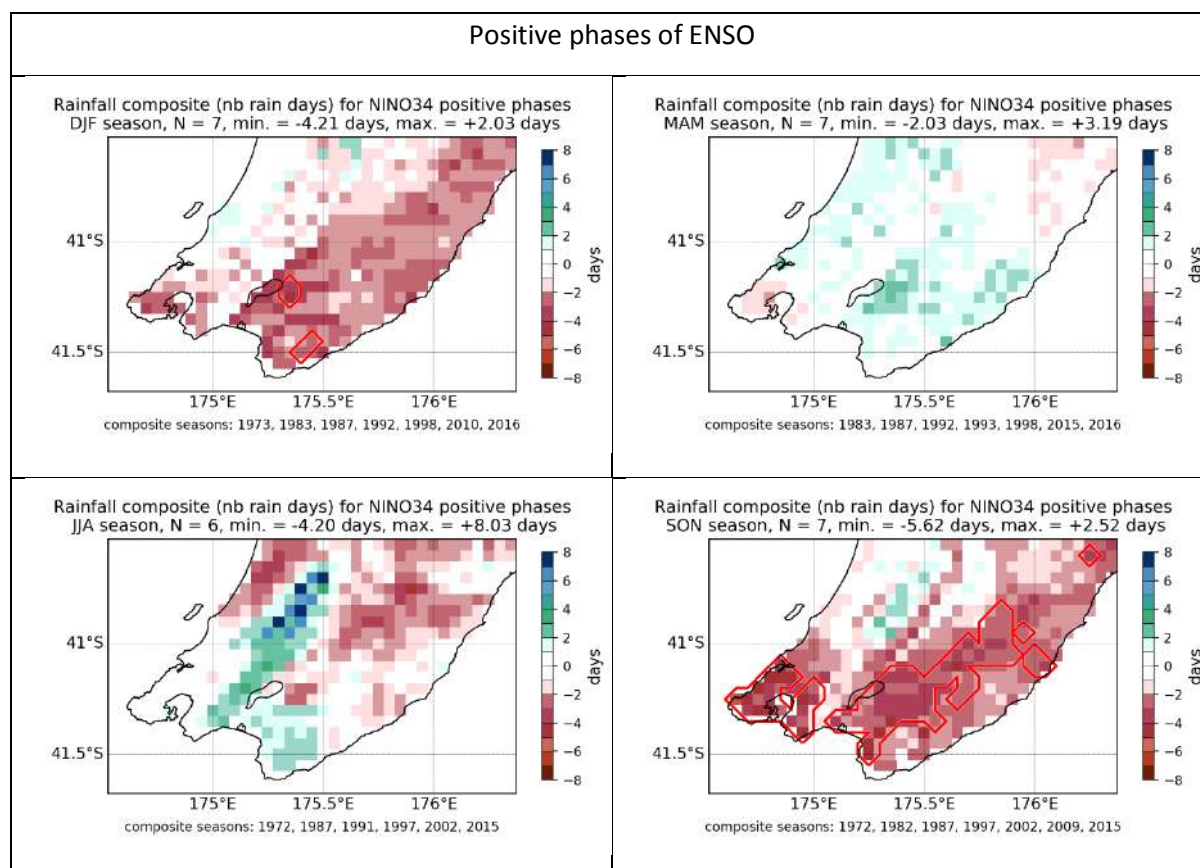
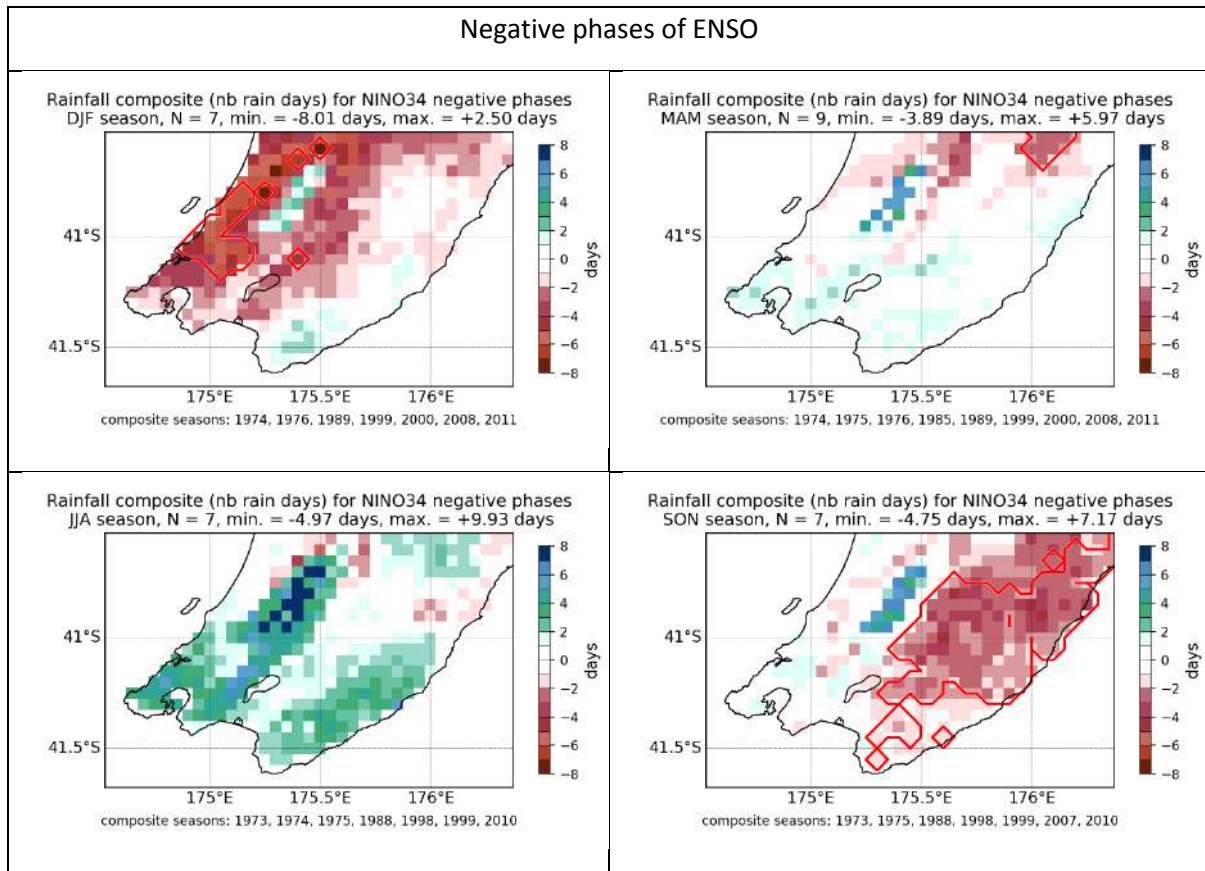


**Figure 2-2: Rain day anomalies during the negative phase of ENSO (VCSN anomalies).** Red lines outline areas of statistical significance at  $p \leq 0.05$ .

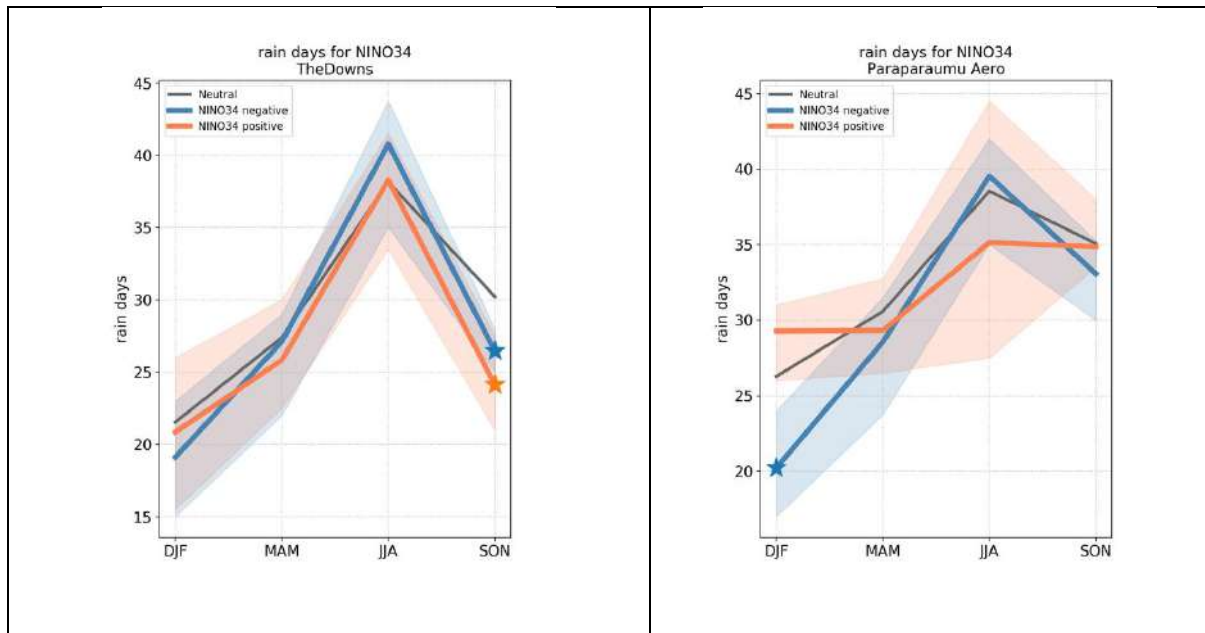




### 2.1.2 Station data

The relationships between the ENSO index and the number of rain days at the selected stations tend to confirm the patterns shown by the VCSN composites. A decrease in the number of rain days is observed at most stations during both phases of ENSO, and mostly during the SON and/or the DJF season, this is illustrated by the stations of The Downs and Paraparaumu (Figure 2-3).

**Figure 2-3: Total rain days and ENSO phase at The Downs and Paraparaumu (Aero) stations.** The stars indicate statistical significance at  $p \leq 0.05$ , and the shaded area indicates the interquartile range (25<sup>th</sup> to 75<sup>th</sup> percentile) of the corresponding composite sample.



## 2.2 SAM

### 2.2.1 VCSN

The positive phase of the SAM is associated with fewer rain days than usual in DJF, particularly in the northeastern part of the Wellington Region, including most of the Masterton District (Figure 2-4). The negative phase of the SAM is not related to widespread and consistent anomalies in the number of rain days, with the exception of a limited area in the Tararua Ranges where less rain days than normal are observed in MAM (Figure 2-5).

**Figure 2-4: Rain day anomalies during the positive phase of SAM (VCSN anomalies).** Red lines outline areas of statistical significance at  $p \leq 0.05$ .

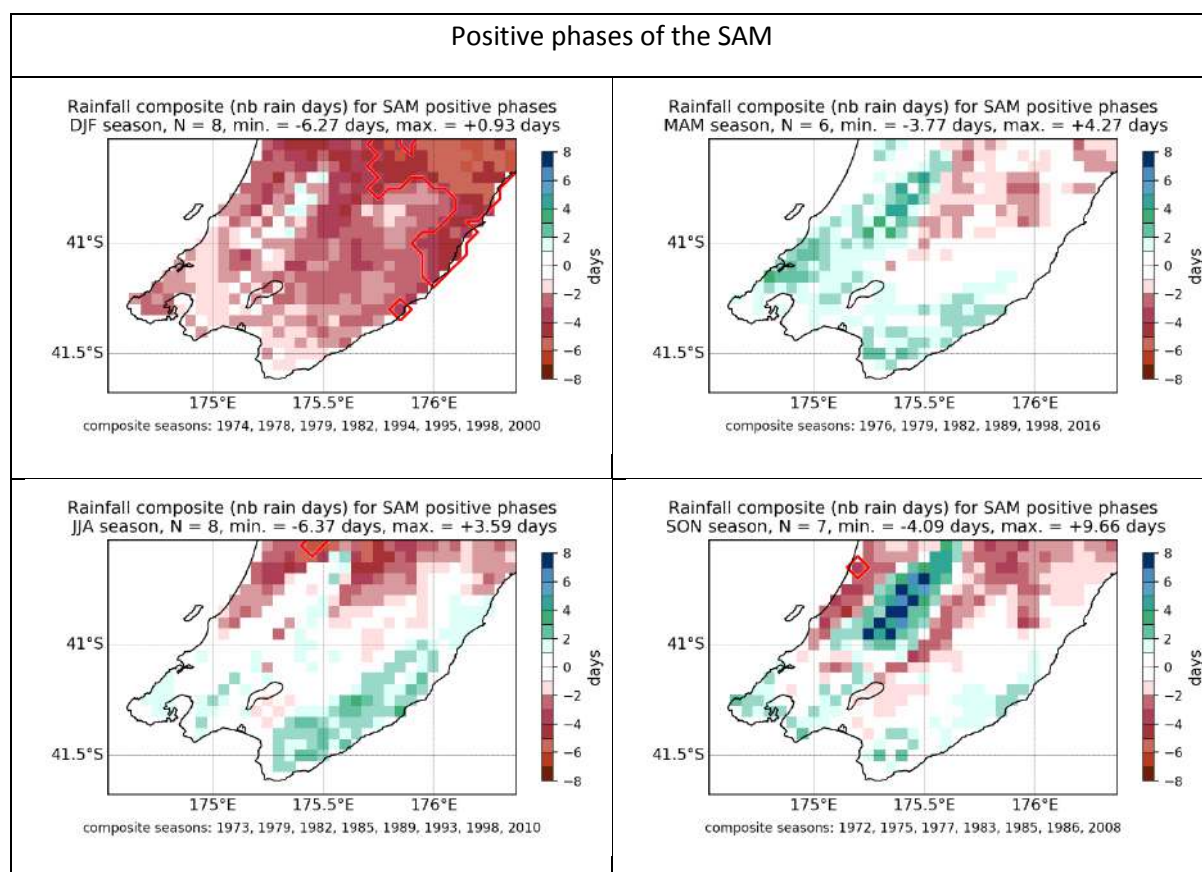
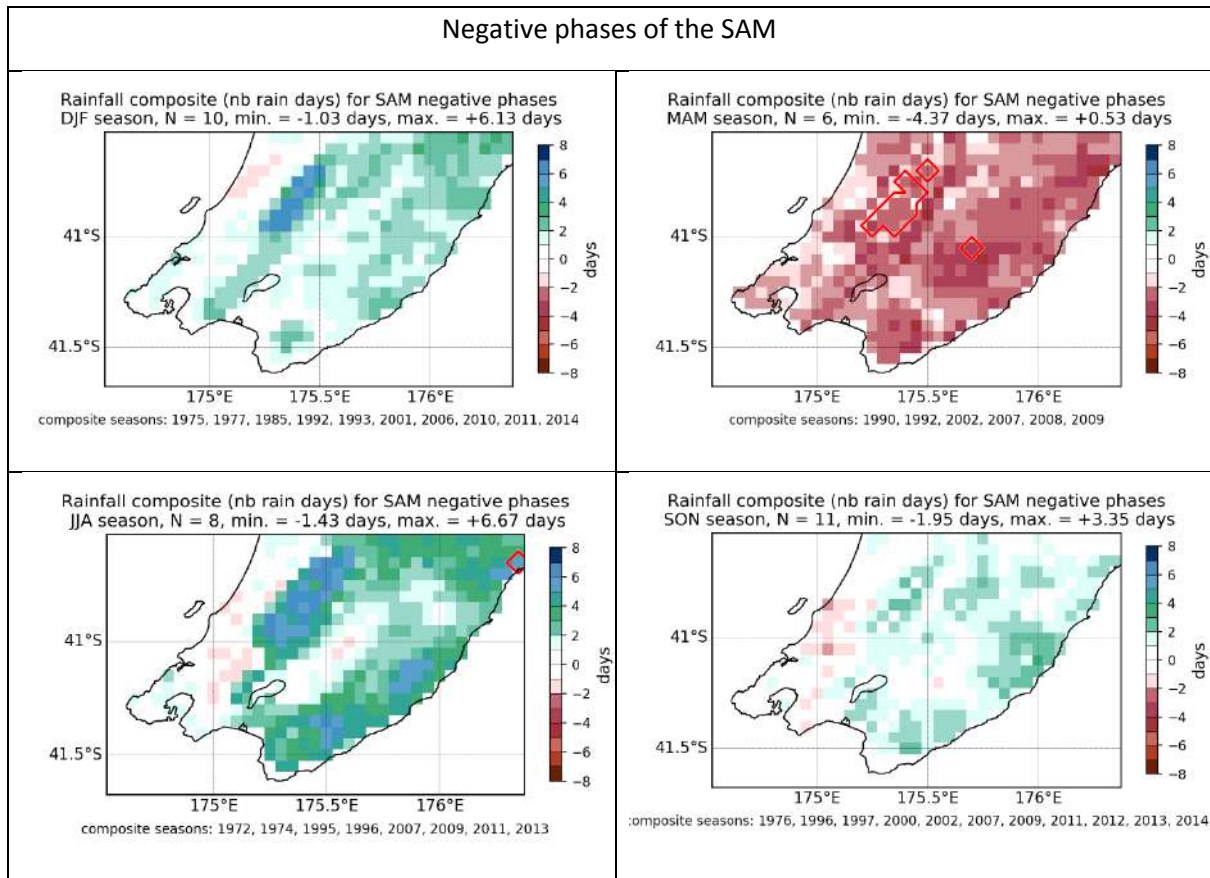


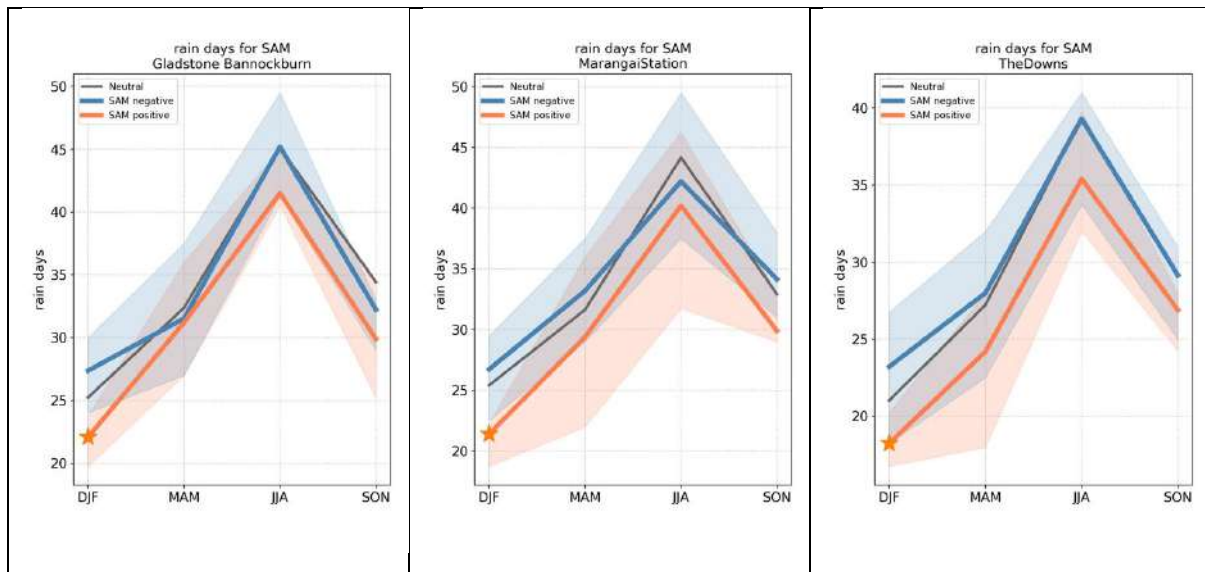
**Figure 2-5: Rain day anomalies during the negative phase of SAM (VCSN anomalies).** Red lines outline areas of statistical significance at  $p \leq 0.05$ .



## 2.2.2 Station data

In general agreement with the VCSN composites, the station data shows significant anomalies in the number of rain days mostly during the DJF season and the positive phase of the SAM, this is the case for Gladstone Bannockburn, Marangai Station and The Downs. Note that this is consistent with expected atmospheric anomalies associated with a positive SAM (decreased westerlies = decrease in the number of days of rain) and consistent with the VCSN composites (Section 2.2.1).

**Figure 2-6: Total rain days and SAM phase at Gladstone Bannockburn, Marangai station and the Downs.** The stars indicate statistical significance at  $p \leq 0.05$ , and the shaded area indicates the interquartile range (25<sup>th</sup> to 75<sup>th</sup> percentile) of the corresponding composite sample.



## 2.3 IOD

### 2.3.1 VCSN

The Wairarapa experiences fewer rain days than normal for SON during positive phases of the IOD (Figure 2-7). This season has the clearest relationship due to the phase locking of the IOD to the austral spring (SON) season. Reductions in rain days are also quite widespread across the region in DJF and MAM for positive phases of the IOD. The relationship between SON rain days the negative phase of the IOD is less clear. Increases in the number of rain days are seen across the Wellington Region for JJA during negative phases of the IOD, although the anomalies are not significant (Figure 2-8).

**Figure 2-7: Rain day anomalies during the positive phase of IOD (VCSN anomalies).** Red lines outline areas of statistical significance at  $p \leq 0.05$ .

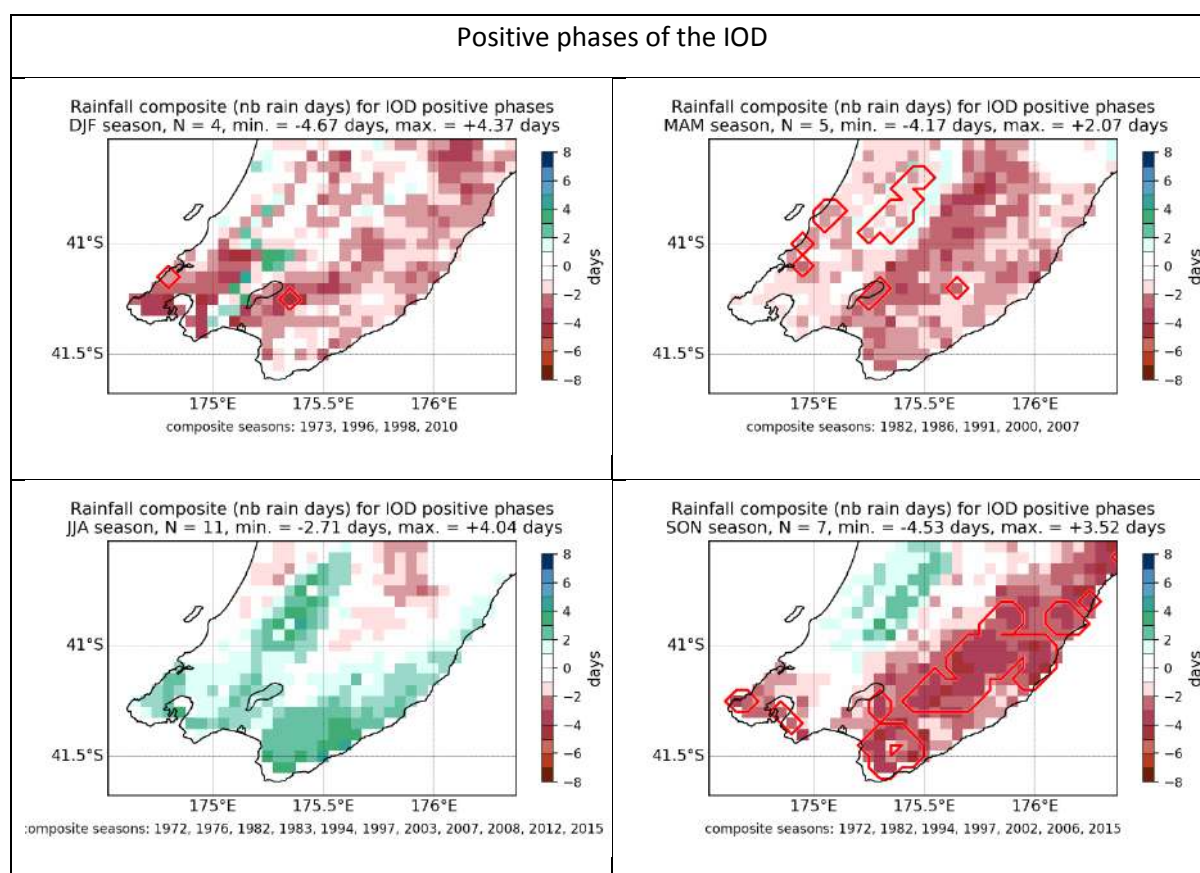
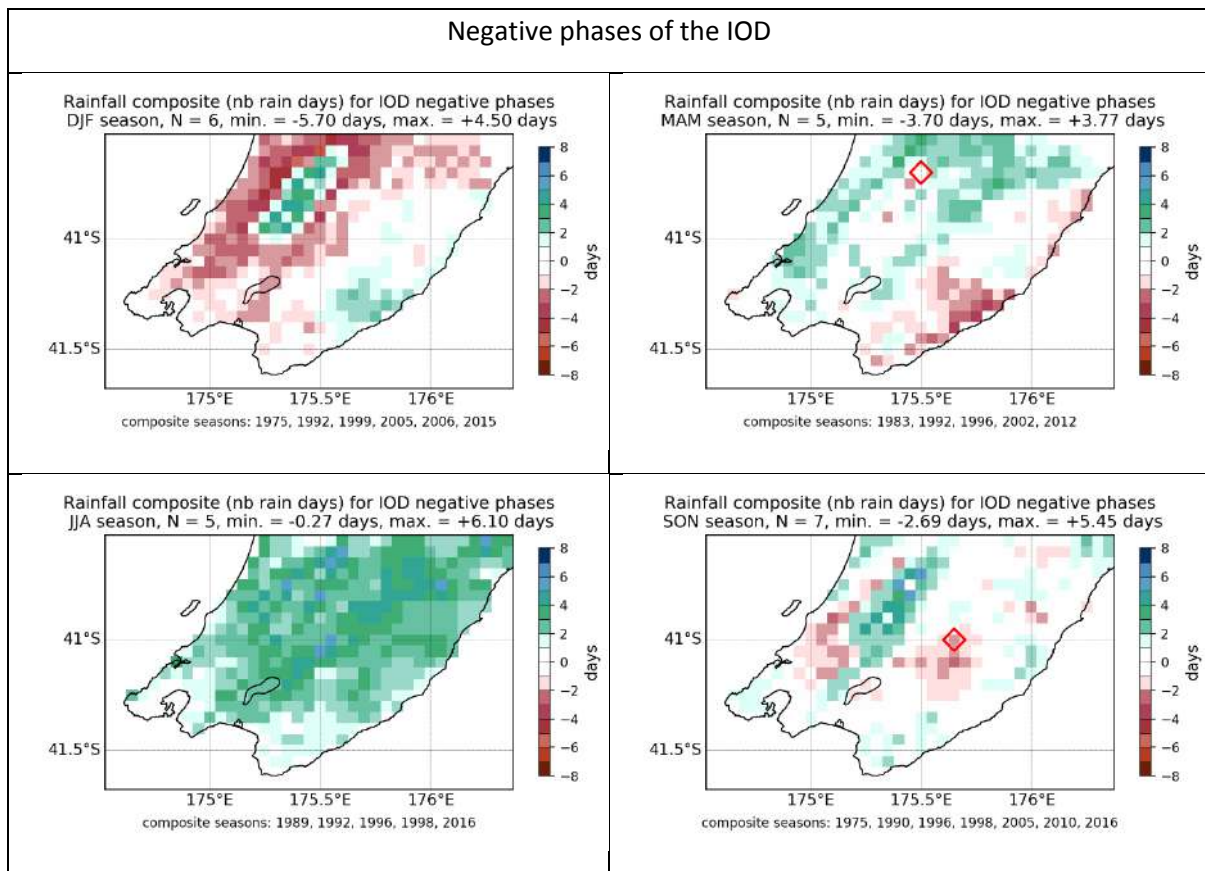


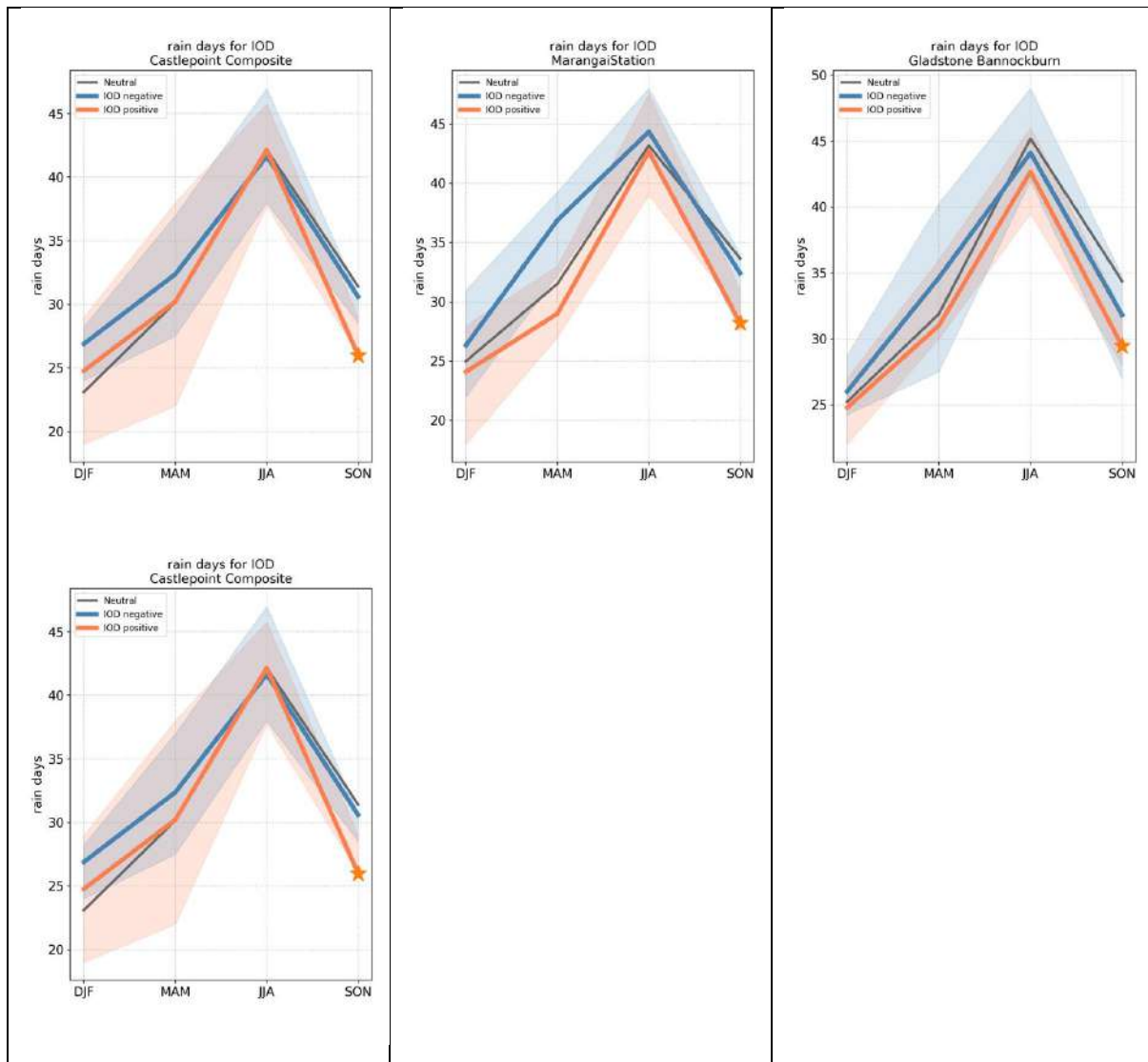
**Figure 2-8: Rain day anomalies during the negative phase of IOD (VCSN anomalies).** Red lines outline areas of statistical significance at  $p \leq 0.05$ .



### 2.3.2 Station data

Consistent with the VCSN composite anomalies, most station level significant relationships are found during the SON season, for the following stations: The Downs, Castlepoint (composite), Marangai Station, Gladstone Bannockburn, Martinborough Riverside and Waikoukou (Figure 2-9). Note that the relationships are non-linear: a reduction in the number of rain days can also be observed during the negative phase of the IOD, as for Paraparaumu Aero and Te Wharau during the same season.

**Figure 2-9: Total rain days and IOD phase at Castlepoint (composite), Marangai station and Gladstone Bannockburn.** The stars indicate statistical significance at  $p \leq 0.05$ , and the shaded area indicates the interquartile range (25<sup>th</sup> to 75<sup>th</sup> percentile) of the corresponding composite sample.



## 2.4 SPSD

### 2.4.1 VCSN

The relationships between rain days and the SPSD are weak and generally non-significant. Patches of significant decreases in rain days are observed in the northwest of the Wellington Region during JJA in the positive phase of the SPSD (Figure 2-10), and some areas of increases in rain days are observed during SON in the negative phase of the SPSD (Figure 2-11).

**Figure 2-10: Rain day anomalies during the positive phase of SPSD (VCSN anomalies).** Red lines outline areas of statistical significance at  $p \leq 0.05$ .

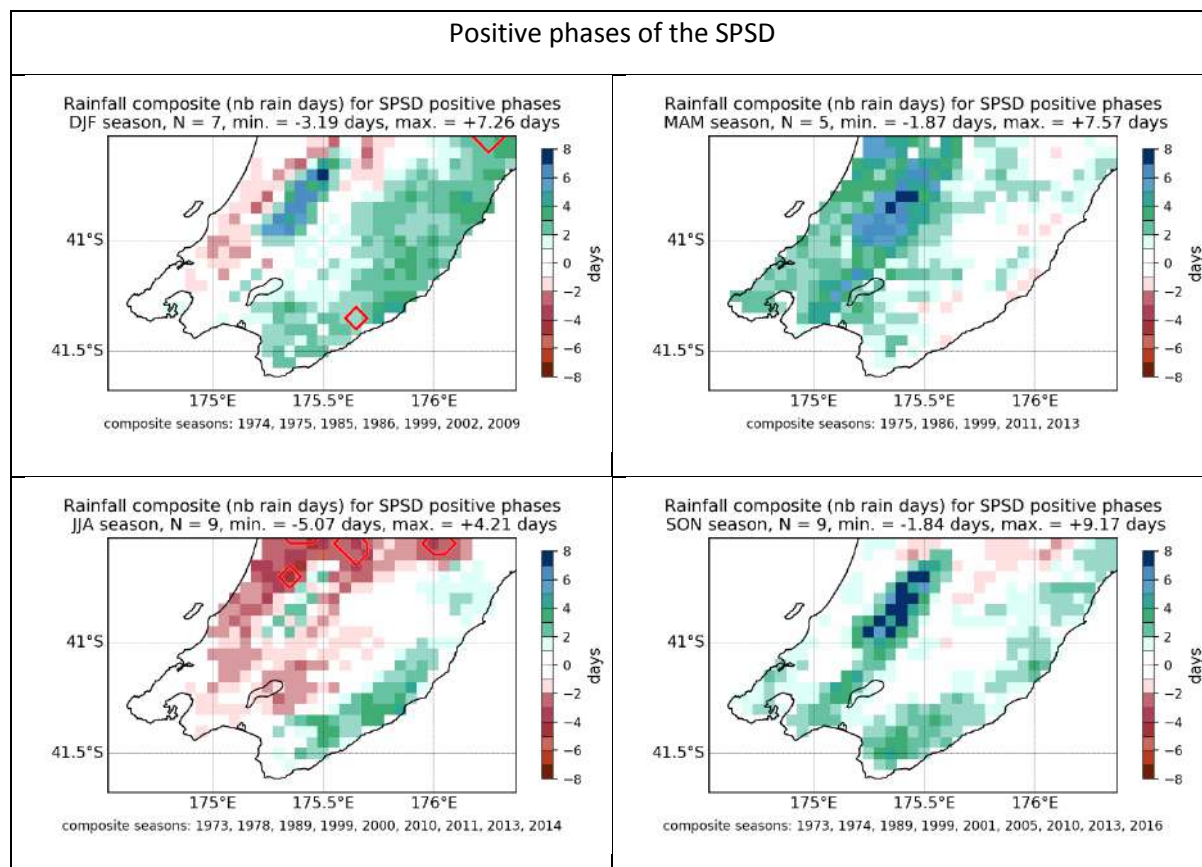
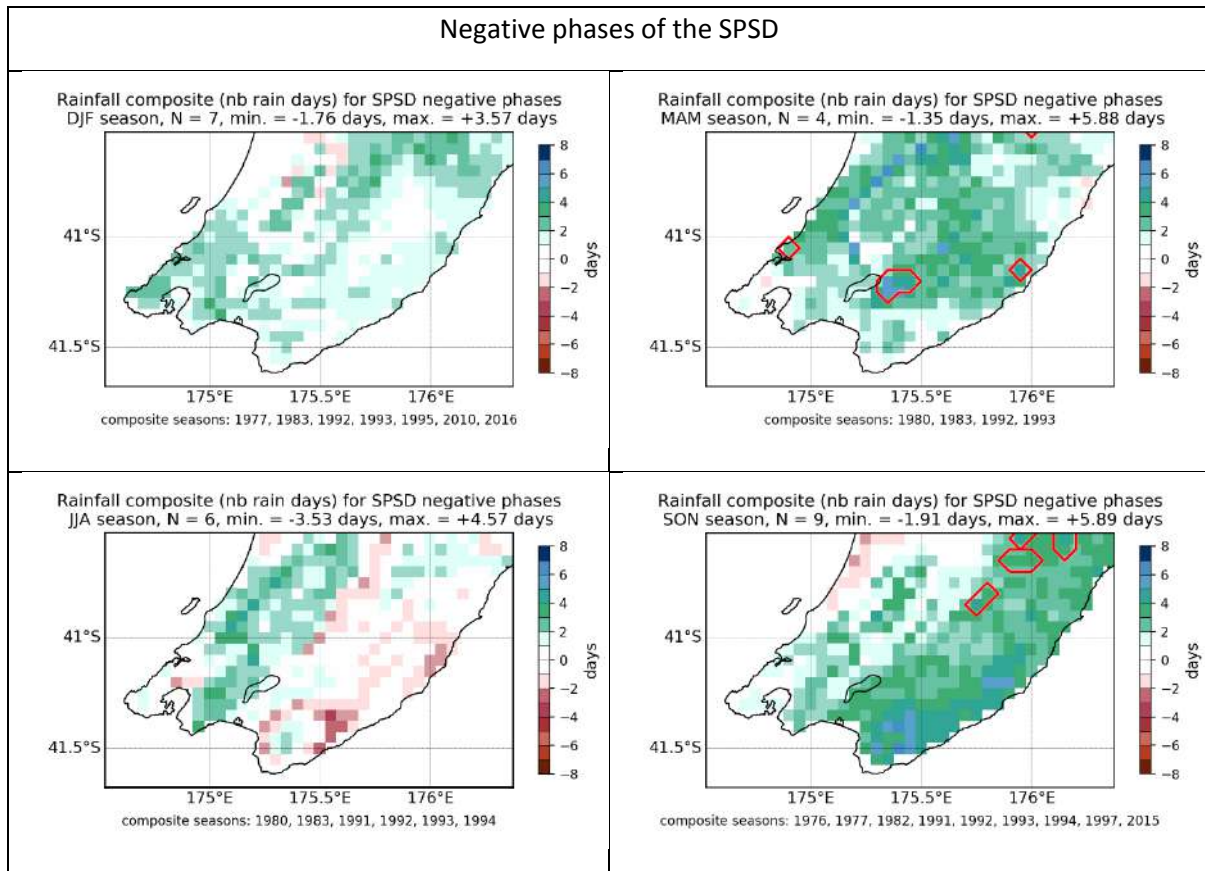




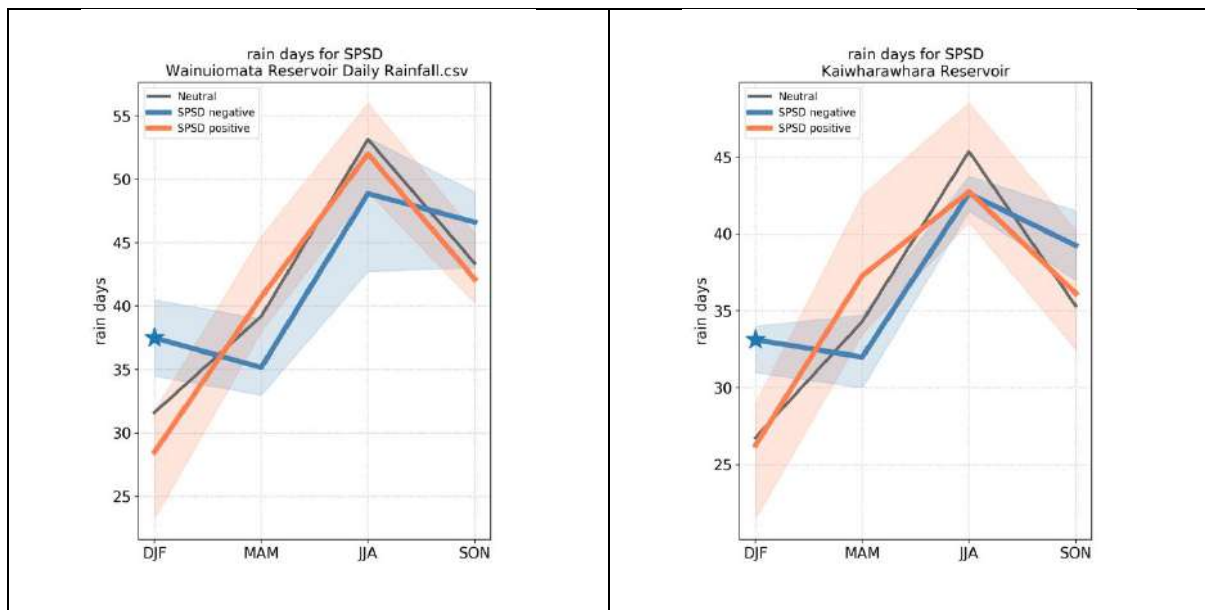
**Figure 2-11: Rain day anomalies during the negative phase of SPSP (VCSN anomalies).** Red lines outline areas of statistical significance at  $p \leq 0.05$ .



## 2.4.2 Station data

The only significant relationships are found for the negative phase of the SPSD in DJF, which is consistent with a relative phase locking of the SPSD mode over the summer period. The stations with significant relationships are for Wainuiomata Reservoir and Kaiwharawhara Reservoir. Notably, the number of DJF rain days tend to increase during the negative phase of the SPSD.

**Figure 2-12: Total rain days and SPSD phase at Wainuiomata Reservoir and Kaiwharawhara Reservoir.** The stars indicate statistical significance at  $p \leq 0.05$ , and the shaded area indicates the interquartile range (25<sup>th</sup> to 75<sup>th</sup> percentile) of the corresponding composite sample.



### 3 Heavy rain days

Heavy rain day anomalies derived from the VCSN are presented in the departure from normal in days (1981-2010 climatology). A heavy rain day is counted when daily rainfall exceeds the climatological 90<sup>th</sup> percentile (i.e. the top 10% of rain days).

#### 3.1 ENSO

##### 3.1.1 VCSN

There are clearer relationships between heavy rainfall and ENSO during the positive phase (El Niño) than the negative phase (La Niña). During the positive phase (Figure 3-1), there is notably a decrease in heavy rain days during JJA and SON over large parts of Wellington Region. The anomalies related to the negative phase of ENSO are not significant.

**Figure 3-1: Heavy rain day anomalies during the positive phase of ENSO (VCSN anomalies).** Red lines outline areas of statistical significance at  $p \leq 0.05$ .

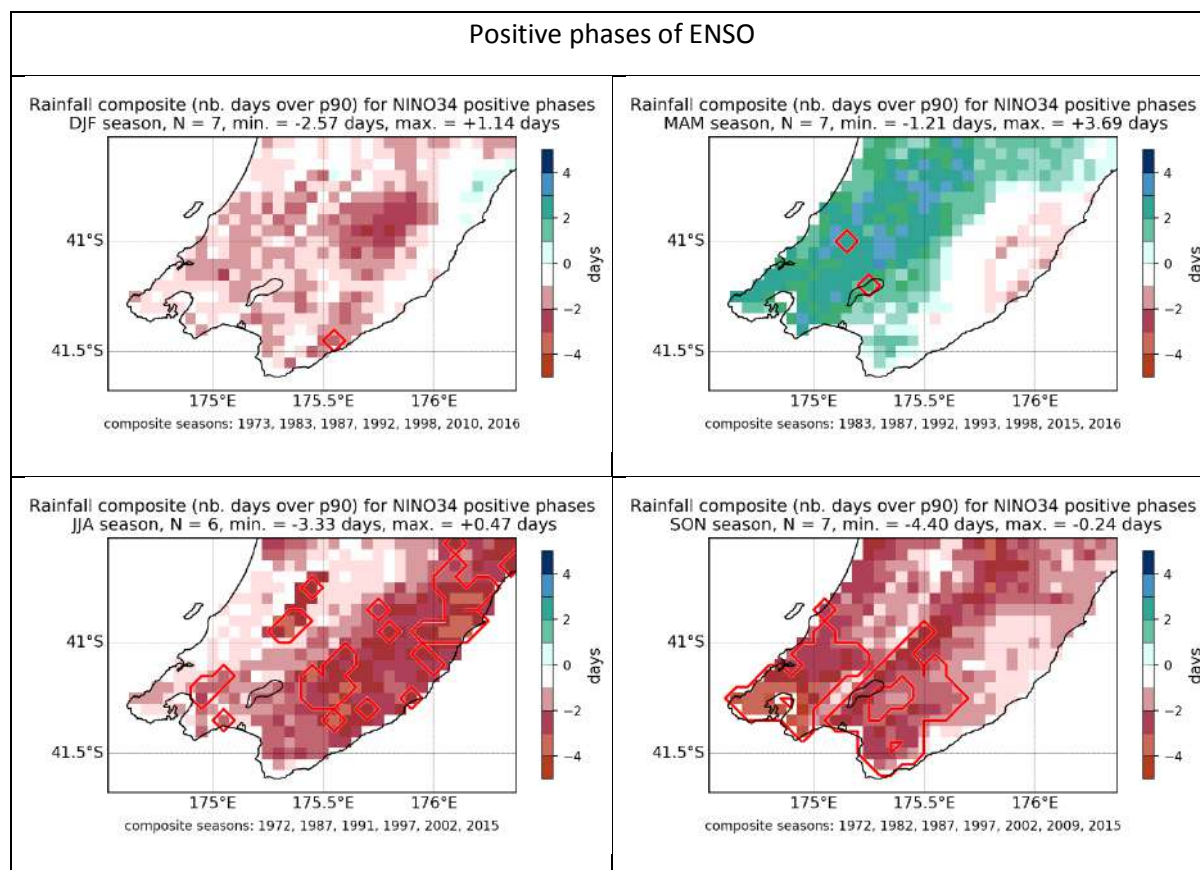
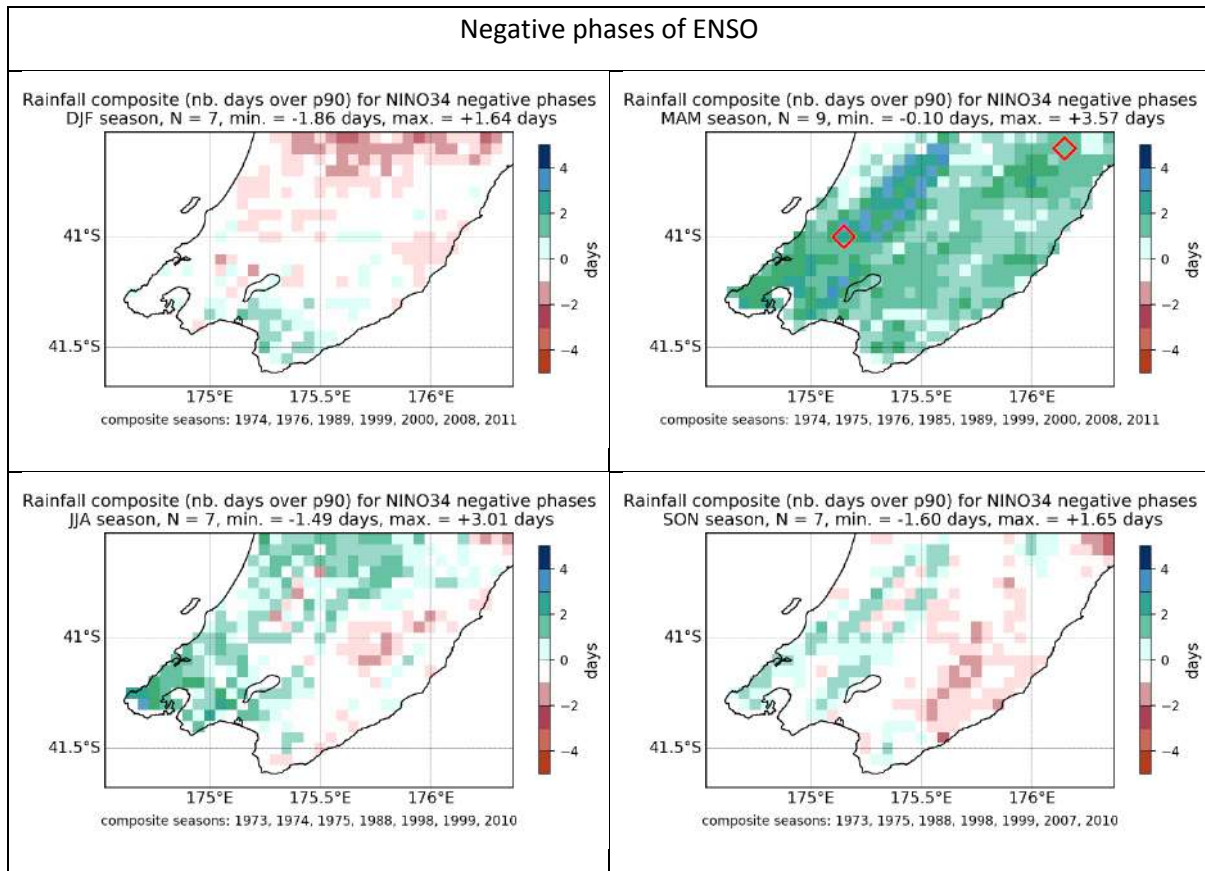


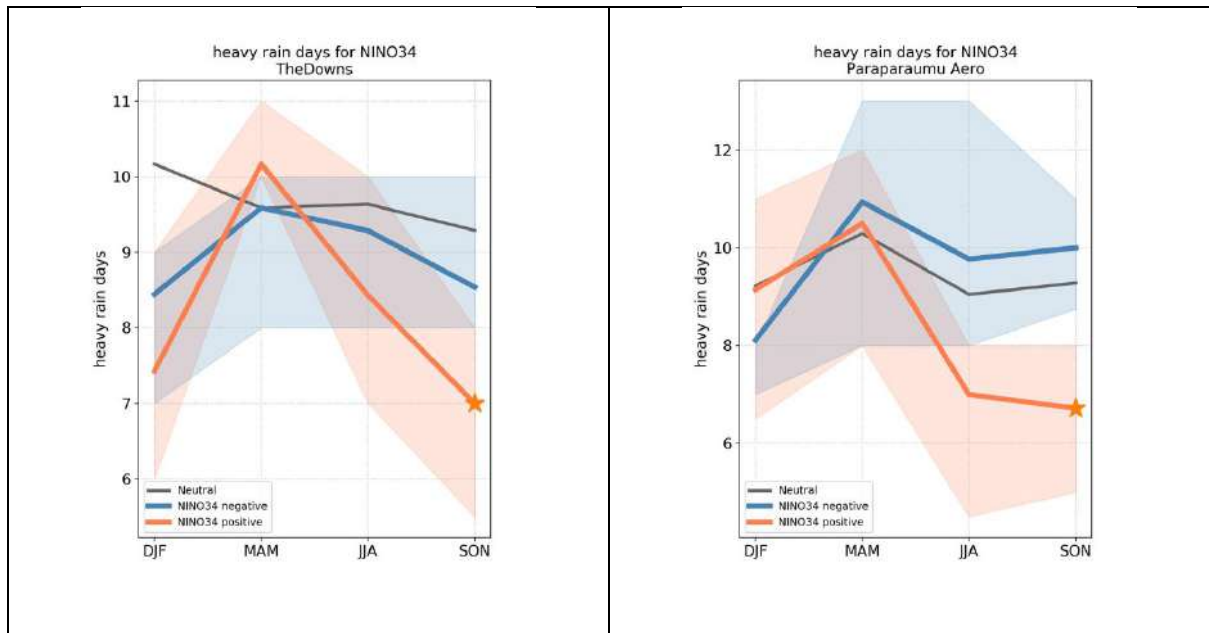
**Figure 3-2: Heavy rain day anomalies during the negative phase of ENSO (VCSN anomalies).** Red lines outline areas of statistical significance at  $p \leq 0.05$ .



### 3.1.2 Station data

The station level anomalies are in general accordance with the overall patterns shown by the VCSN. The positive phase of ENSO is generally related to a decrease in the number of heavy rain days, notably in SON (see Figure 3-3 for the Paraparaumu Aero and The Downs stations). The anomalies associated with the negative phase of ENSO are generally weak and non-significant.

**Figure 3-3: Heavy rain days and ENSO phase at The Downs and Paraparaumu Aero.** The stars indicate statistical significance at  $p \leq 0.05$ , and the shaded area indicates the interquartile range (25<sup>th</sup> to 75<sup>th</sup> percentile) of the corresponding composite sample.



## 3.2 SAM

### 3.2.1 VCSN

During the positive phase of the SAM, the number of heavy rain days decreases in DJF and increases for the western part of the region in MAM (Figure 3-4). For the negative phase of the SAM, the clearest relationships are for DJF where increased numbers of heavy rain days are observed in the southern part of the region (Figure 3-5).

**Figure 3-4: Heavy rain day anomalies during the positive phase of SAM (VCSN anomalies).** Red lines outline areas of statistical significance at  $p \leq 0.05$ .

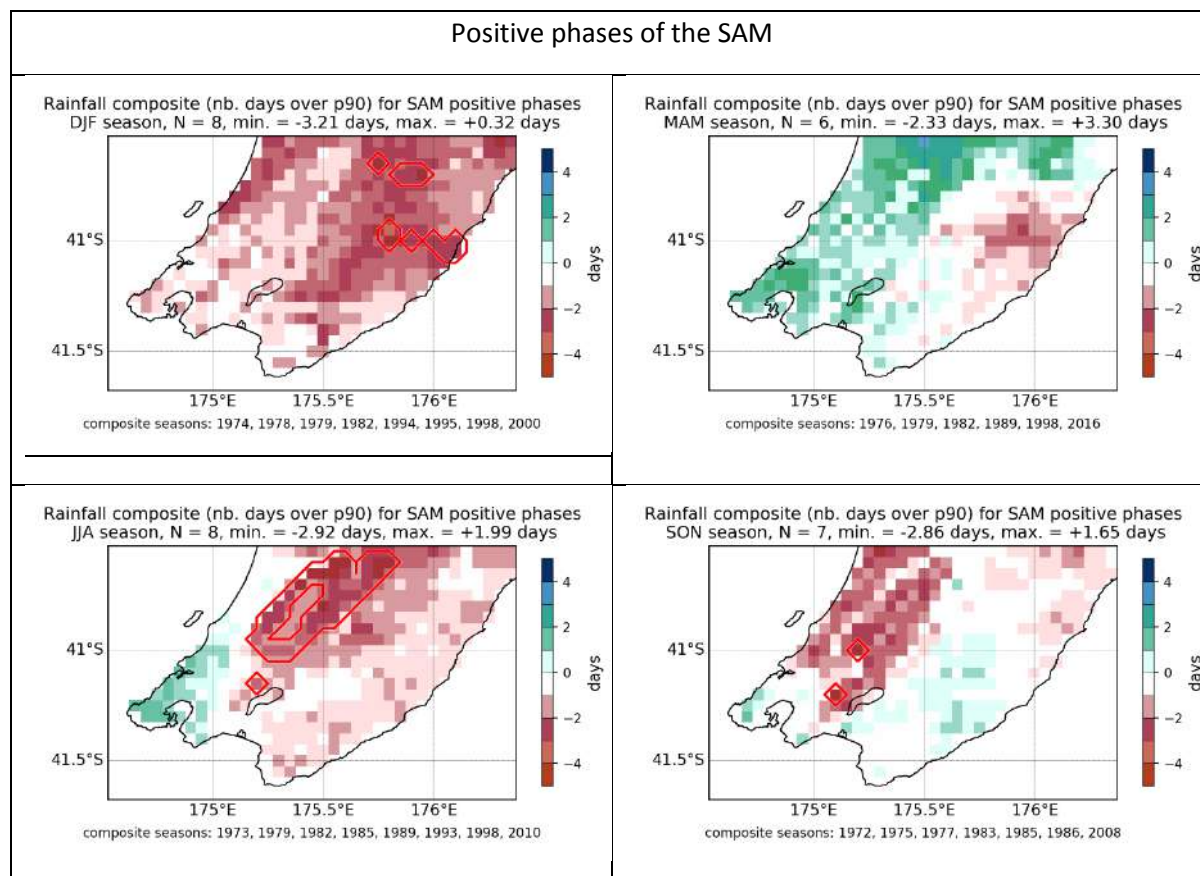
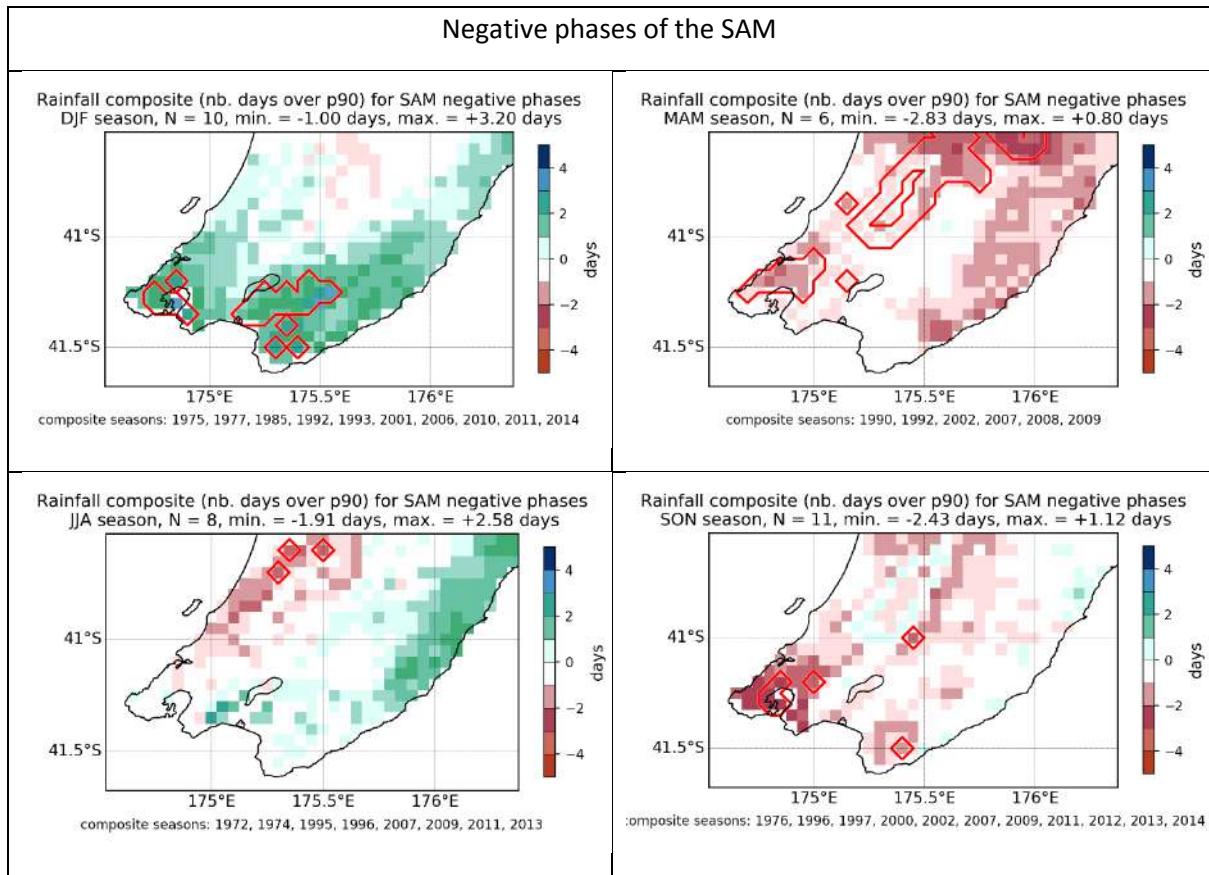


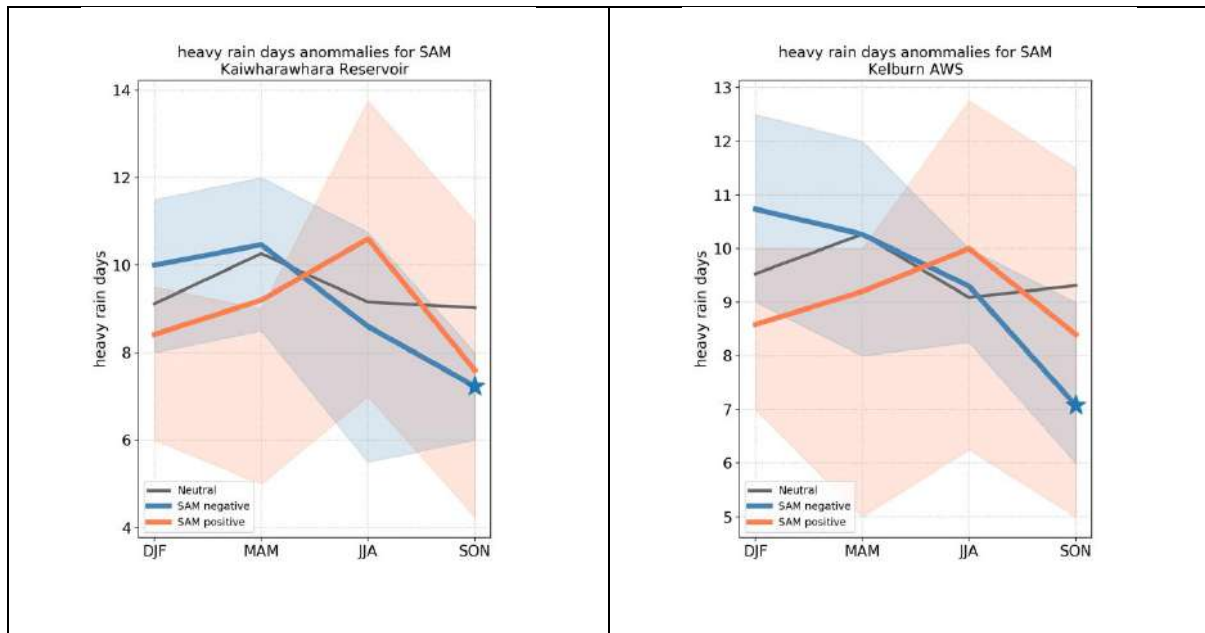
**Figure 3-5: Heavy rain day anomalies during the negative phase of SAM (VCSN anomalies).** Red lines outline areas of statistical significance at  $p \leq 0.05$ .



### 3.2.2 Station data

The only significant relationships at the station level with the SAM are found for the stations of Kelburn AWS and Kaiwharawhara Reservoir, for which a significant decrease in the number of rain days are registered during the negative phase of the SAM in SON (Figure 3-6).

**Figure 3-6: Heavy rain days and SAM phase at Kaiwharawhara Reservoir and Kelburn AWS.** The stars indicate statistical significance at  $p \leq 0.05$ , and the shaded area indicates the interquartile range (25<sup>th</sup> to 75<sup>th</sup> percentile) of the corresponding composite sample.





### 3.3 IOD

#### 3.3.1 VCSN

Relationships between the IOD and heavy rain days are generally quite weak. The clearest relationships are observed for MAM during the positive phase, when fewer heavy rain days than usual are observed across the region (Figure 3-7). During the negative phase of the IOD, there are weak (and non-significant) signals indicating a decrease in the number of heavy rain days during DJF and an increase in the numbers of heavy rain days for MAM in the west of the region (Figure 3-8).

**Figure 3-7: Heavy rain day anomalies during the positive phase of IOD (VCSN anomalies).** Red lines outline areas of statistical significance at  $p \leq 0.05$ .

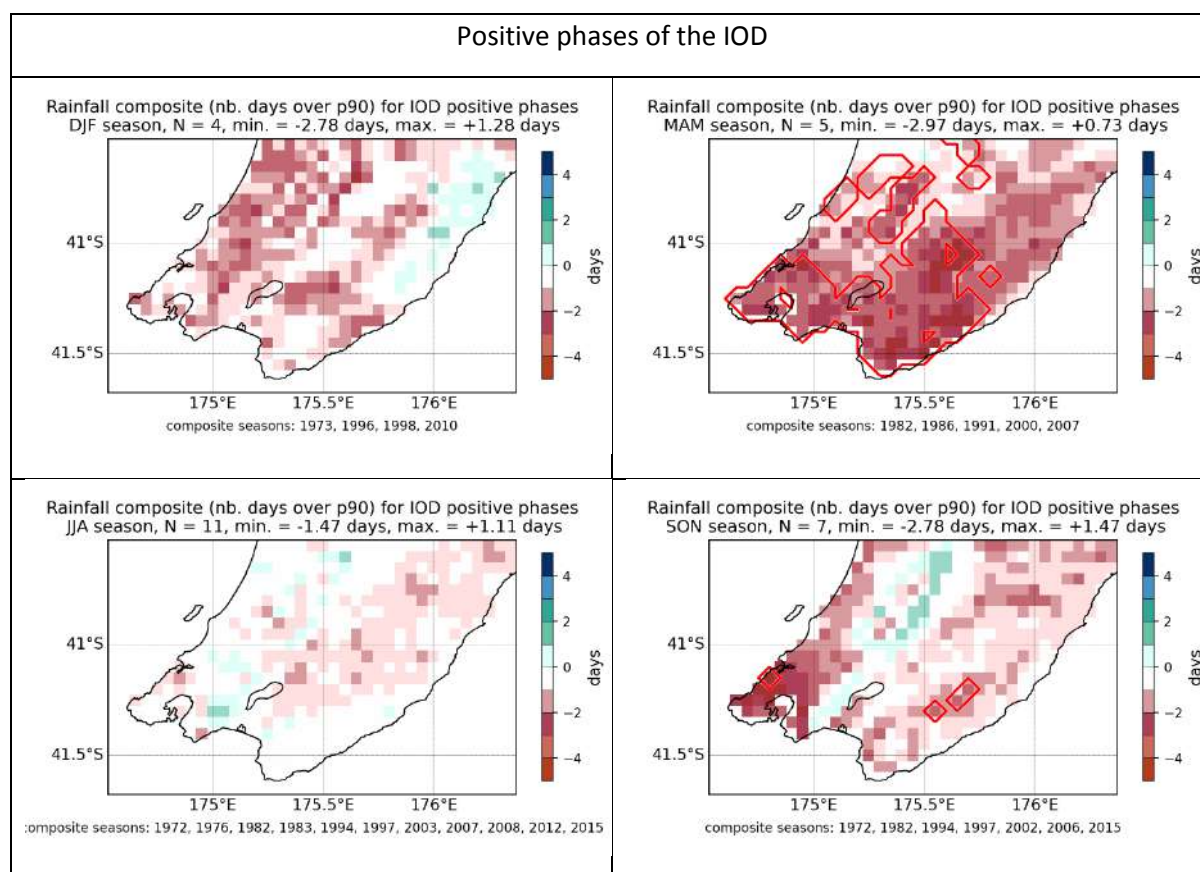
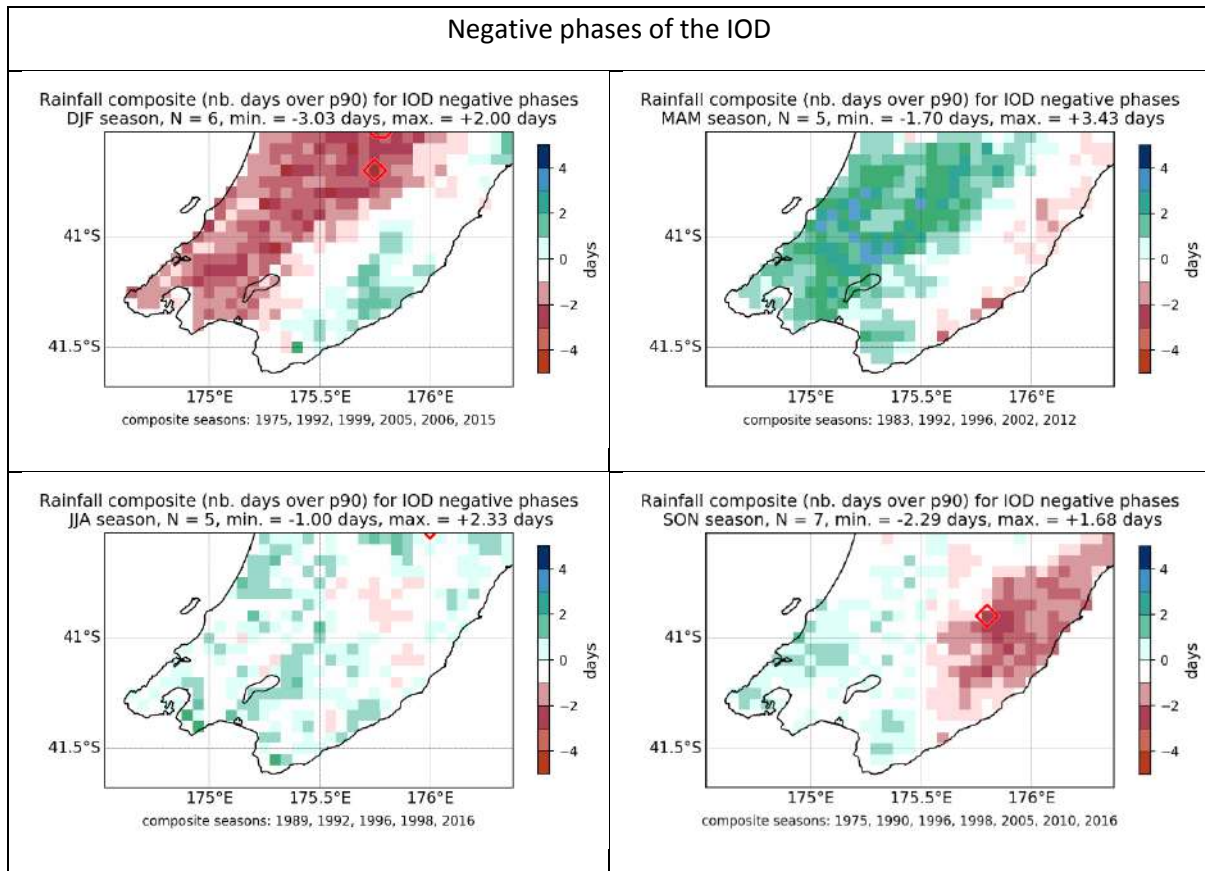


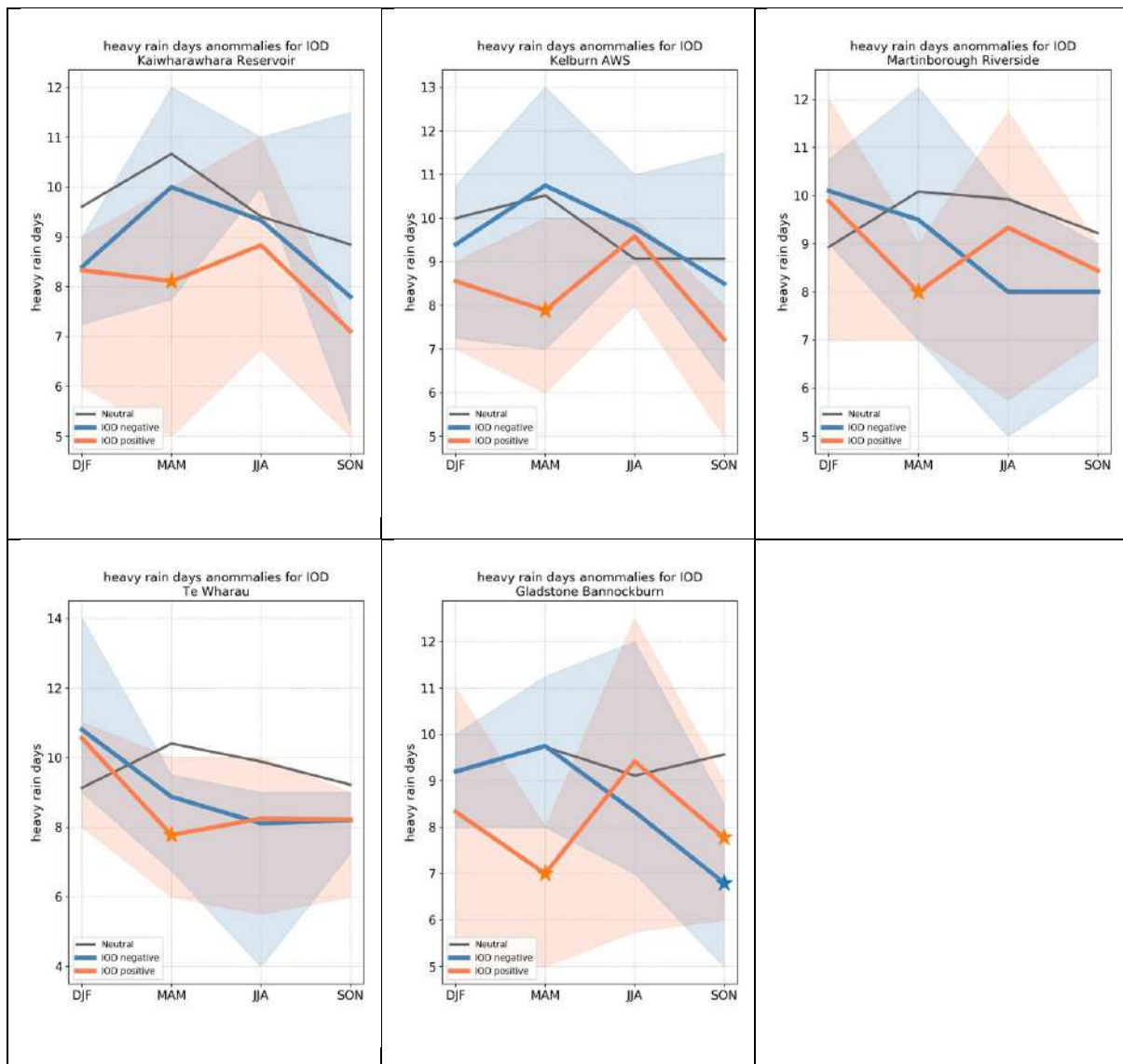
**Figure 3-8: Heavy rain day anomalies during the negative phase of IOD (VCSN anomalies).** Red lines outline areas of statistical significance at  $p \leq 0.05$ .



### 3.3.2 Station data

The main signal identified using the VCSN (decrease in the number of heavy rain days during the positive phase of the IOD in MAM) is reflected at the station level. The stations Kaiwharawhara Reservoir, Kelburn AWS, Martinborough Riverside, Te Wharau and Gladstone Bannockburn all show a significant decrease in the number of heavy rain days in MAM (Figure 3-9).

**Figure 3-9: Heavy rain days and IOD phase at Gladstone Bannockburn and Paraparaumu Aero.** The stars indicate statistical significance at  $p \leq 0.05$ , and the shaded area indicates the interquartile range (25<sup>th</sup> to 75<sup>th</sup> percentile) of the corresponding composite sample.



### 3.4 SPSD

#### 3.4.1 VCSN

The clearest relationship between the SPSP and the number of heavy rain days is observed during the negative phase of the SPSP, notably in JJA, where a generalized decrease in the number of heavy rain days is observed across the region, and during MAM, where the reverse (increase in the number of heavy rain days) tend to occur (Figure 3-11). During other seasons and during the positive phase of the SPSP, the anomalies are less spatially coherent and the areas of significance less extent (Figure 3-10).

**Figure 3-10: Heavy rain day anomalies during the positive phase of SPSP (VCSN anomalies).** Red lines outline areas of statistical significance at  $p \leq 0.05$ .

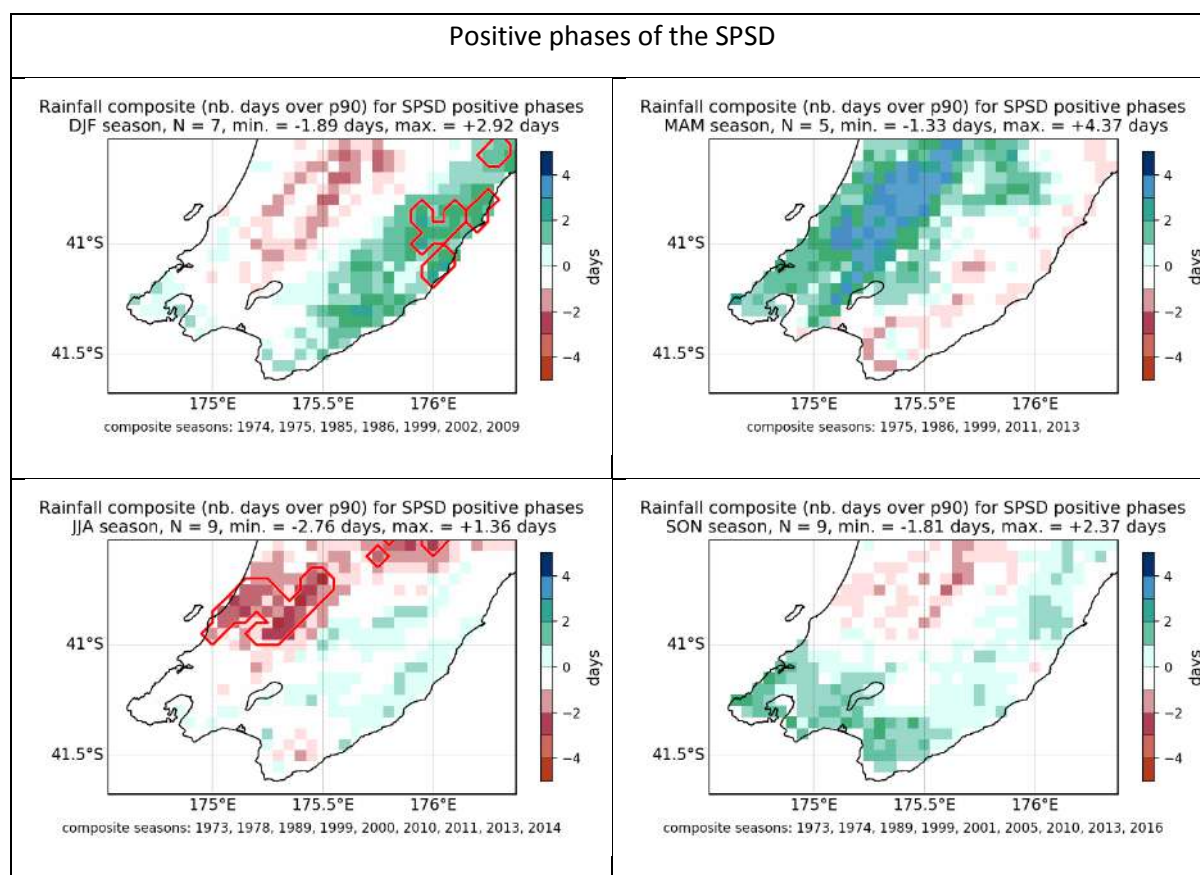
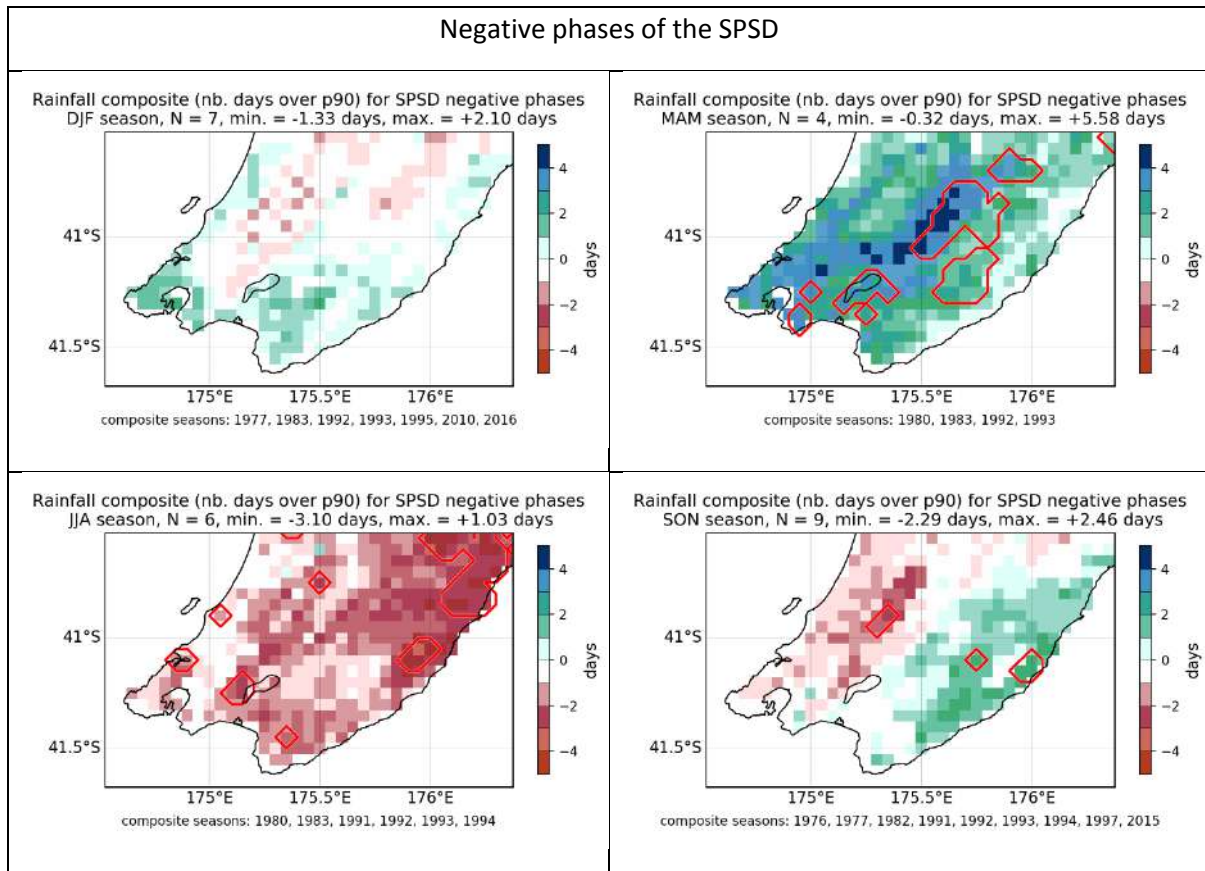


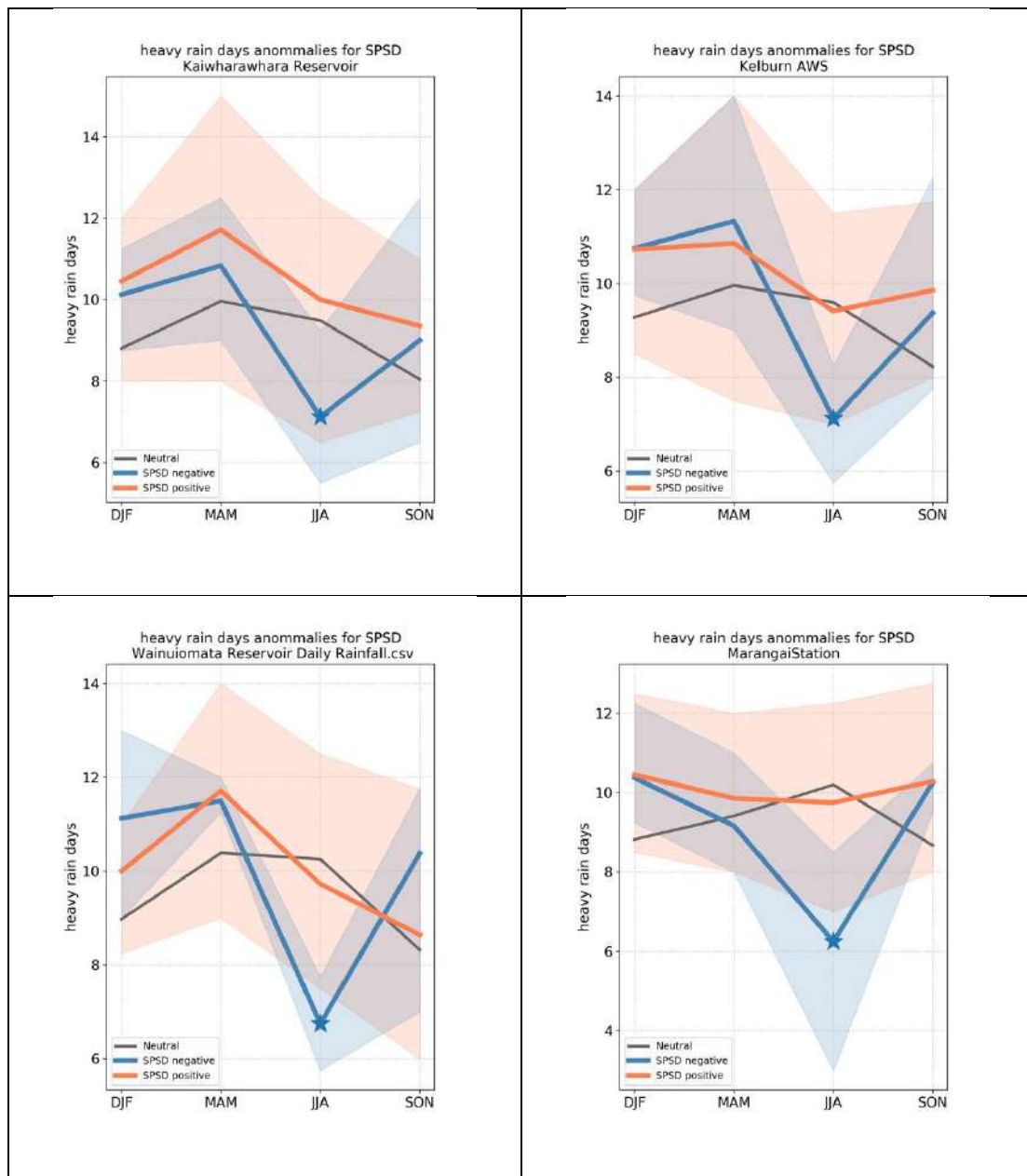
**Figure 3-11: Heavy rain day anomalies during the negative phase of SPSP (VCSN anomalies).** Red lines outline areas of statistical significance at  $p \leq 0.05$ .



### 3.4.2 Station data

The SPSD in its negative phase is significantly associated with a decrease in the number of heavy rain days during the JJA season for the following stations: Kaiwharawhara Reservoir, Kelburn AWS, Marangai Station and Wainuiomata Reservoir (Figure 3-12), confirming the pattern shown by the VCSN composite anomalies and .

**Figure 3-12: Heavy rain days and SPSD phase at Kaiwharawhara Reservoir, Kelburn AWS, Marangai Station and Wainuiomata Reservoir.** The stars indicate statistical significance at  $p \leq 0.05$ , and the shaded area indicates the interquartile range (25<sup>th</sup> to 75<sup>th</sup> percentile) of the corresponding composite sample.



## 4 Dry days

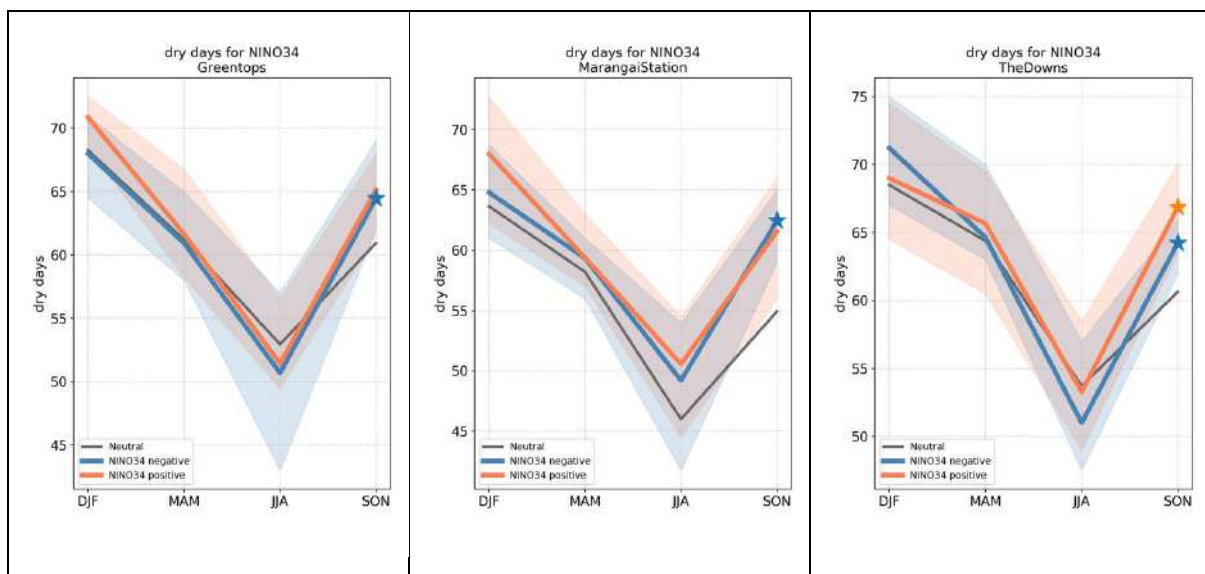
Dry days are defined as days when accumulated rainfall was equal to 0 mm. The results are hereby only presented for the station derived number of dry days, as the VCSN composite anomalies show patterns exactly complementary to the one shown for the number of wet days.

### 4.1 ENSO

#### 4.1.1 Station data

A significant increase in the number of dry days is observed in SON during La Niña (negative ENSO) for Greentops, Marangai Station and The Downs (Figure 4-1).

**Figure 4-1: Dry days and ENSO phase at Marangai Station, Paraparamu Aero and Lagoon Hill.** The stars indicate statistical significance at  $p \leq 0.05$ , and the shaded area indicates the interquartile range (25<sup>th</sup> to 75<sup>th</sup> percentile) of the corresponding composite sample.

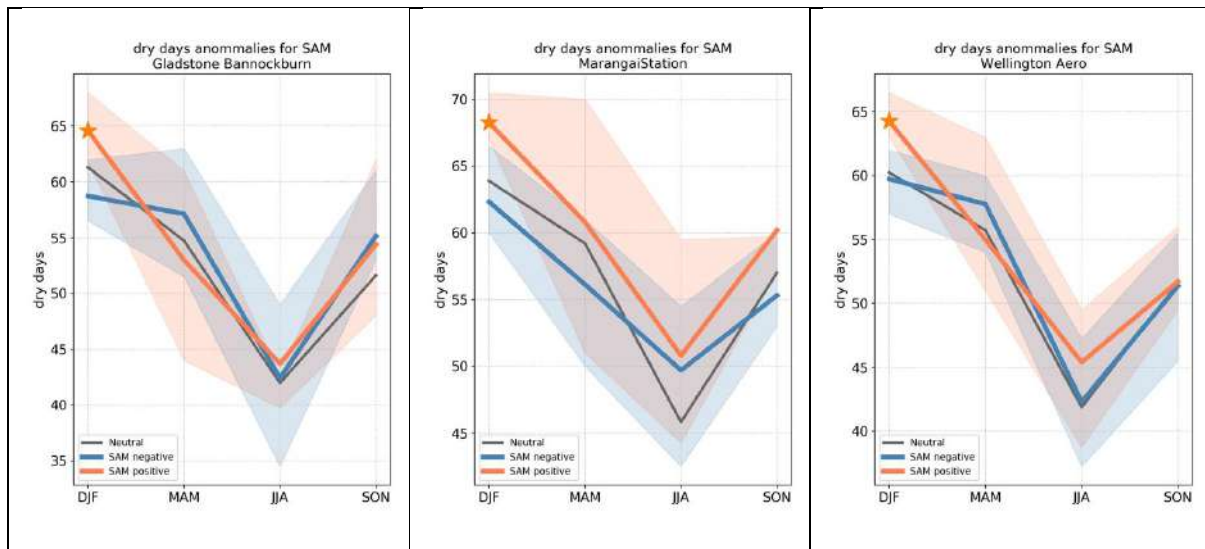


## 4.2 SAM

### 4.2.1 Station data

The number of dry days is significantly associated with the SAM during the DJF season for the following stations: Gladstone Bannockburn, Marangai Station and Wellington Aero (Figure 4-2). Consistently across the stations, the number of dry days tends to be higher than normal during the positive phase of the SAM.

**Figure 4-2: Dry days and SAM phase at Gladstone Bannockburn, Marangai Station, and Wellington Aero.** The stars indicate statistical significance at  $p \leq 0.05$ , and the shaded area indicates the interquartile range (25<sup>th</sup> to 75<sup>th</sup> percentile) of the corresponding composite sample.



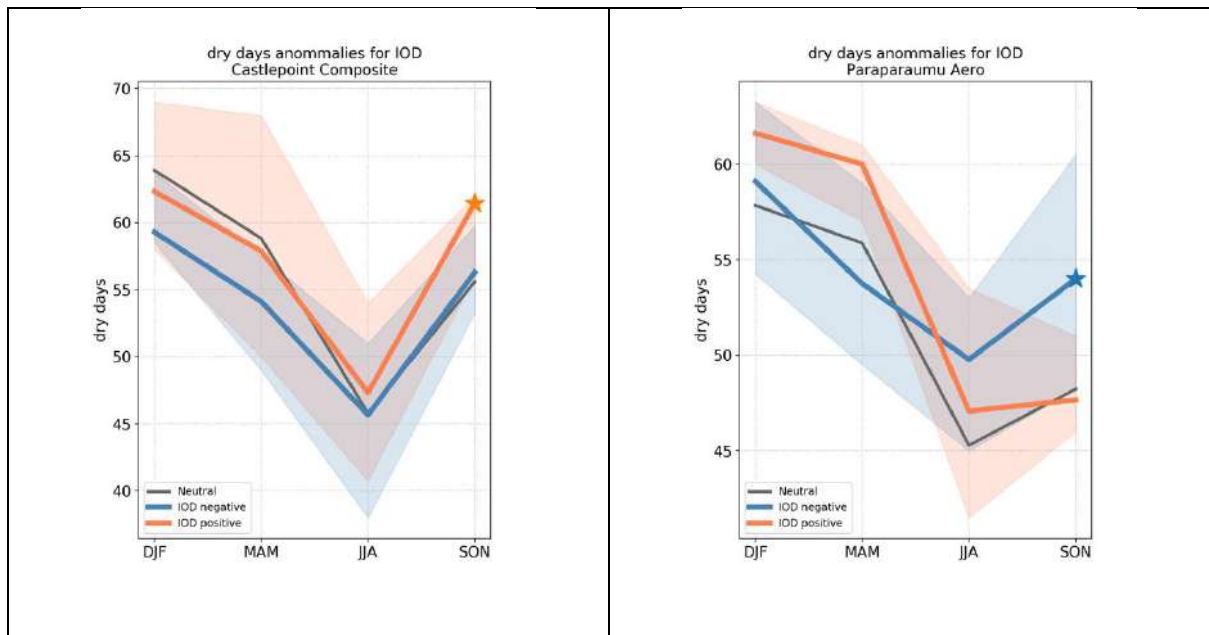


## 4.3 IOD

### 4.3.1 Station data

A significant increase in the number of dry days during SON for the positive phase of the IOD is observed for several stations: Castlepoint Composite, Gladstone Bannockburn, Marangai Station, The Downs and Waikoukou (see Figure 4-3). A significant increase in the number of dry days in SON is also observed for Kaiwharawhara Reservoir, Te Wharau and Paraparaumu Aero.

**Figure 4-3: Dry days and IOD phase at Castlepoint (composite) and Paraparaumu Aero.** The stars indicate statistical significance at  $p \leq 0.05$ , and the shaded area indicates the interquartile range (25<sup>th</sup> to 75<sup>th</sup> percentile) of the corresponding composite sample.

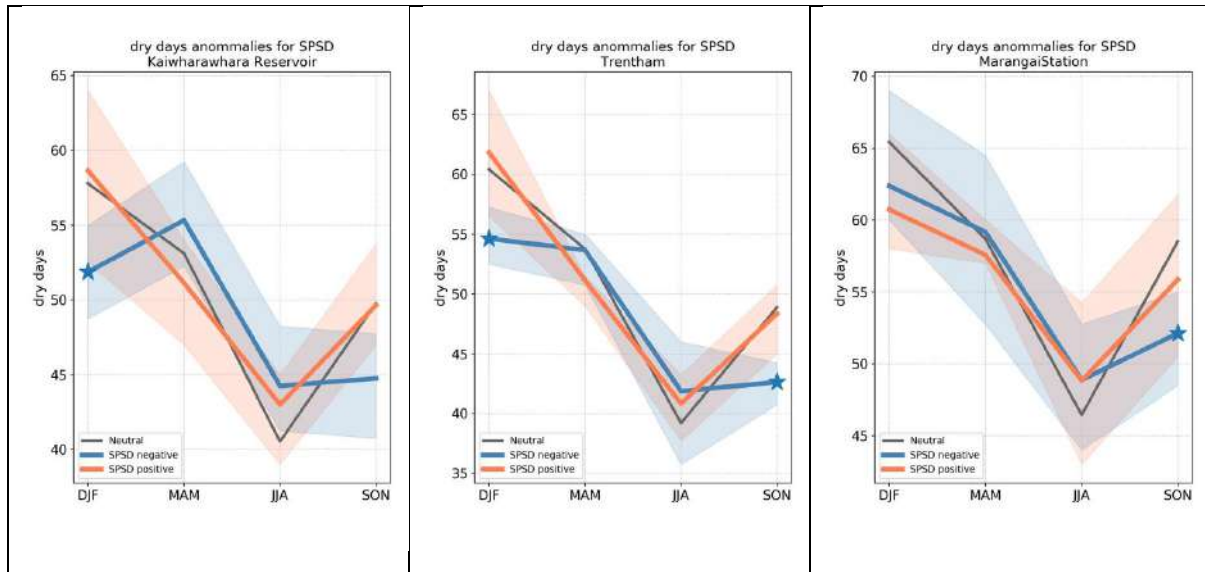


## 4.4 SPSD

### 4.4.1 Station data

Most significant anomalies found at the station level are related to a decrease in the number of dry days, mostly during the negative phase of the SPSD, and during SON and / or DJF, as illustrated for Kaiwharawhara Reservoir, Trentham and Marangai Station (Figure 4-4).

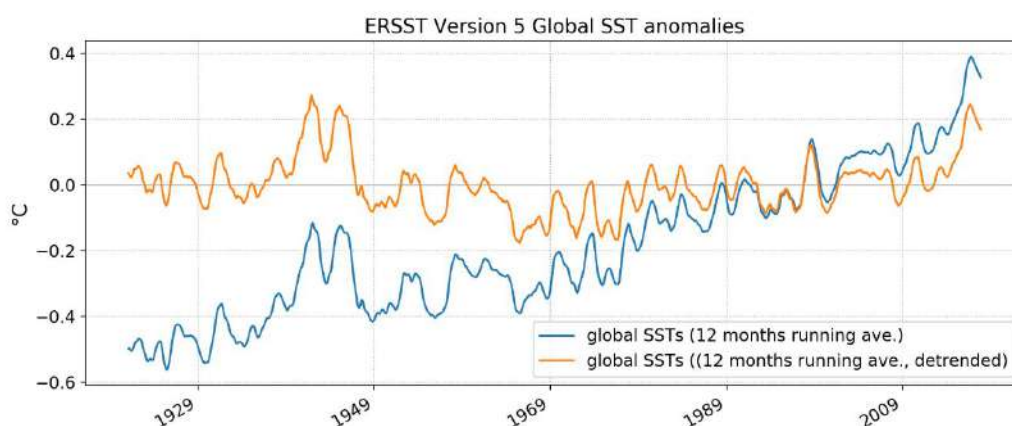
**Figure 4-4: Dry days and SPSD phase at Kaiwharawhara Reservoir, Trentham, and Marangai Station.** The stars indicate statistical significance at  $p \leq 0.05$ , and the shaded area indicates the interquartile range (25<sup>th</sup> to 75<sup>th</sup> percentile) of the corresponding composite sample.



## 5 Relationship to Sea Surface Temperature (SST) anomalies

In this section, the relationships between station data and global sea surface temperatures (SSTs, ERSST version 5 dataset) are explored. The correlation fields between seasonal rainfall variables (cumulative rainfall, number of rain days, number of dry days, number of days with heavy rainfall) and seasonal SST anomalies are first calculated independently for each season and station. Because of the presence of a large trend in the SSTs (see Figure 5-1), the seasonal SST anomalies are linearly detrended prior to analysis.

**Figure 5-1: Global SST raw and detrended time series from early 20th century to present. Data source: ERSST v5 dataset.**



The correlations were calculated successively for the whole period of overlap between the ERSSTv5 dataset (1920 – present) and the rainfall station time series, as well as over the more recent period (post-1950). The results were found to be qualitatively similar. Because of the large number of figures generated (4 rainfall variables x 13 stations x 4 seasons), we present here only a selection of results, highlighting the main conclusions that can be derived from the analyses.

The only station which shows a clear relationship with consistent ENSO-like patterns in the tropical central and eastern Pacific Ocean is the station of Paraparaumu Aero. An increase (decrease) in the number of dry days during the DJF season in Paraparaumu is related to a clear La Niña (El Niño) like pattern in the tropical eastern Pacific (Figure 5-2 and Figure 5-3)

**Figure 5-2: Correlation field between respectively the total rainfall (top panel) and the number of dry days (bottom panel) in Paraparaumu and seasonal SST anomalies. Black lines indicate areas of statistical significance at  $p \leq 0.05$ .**

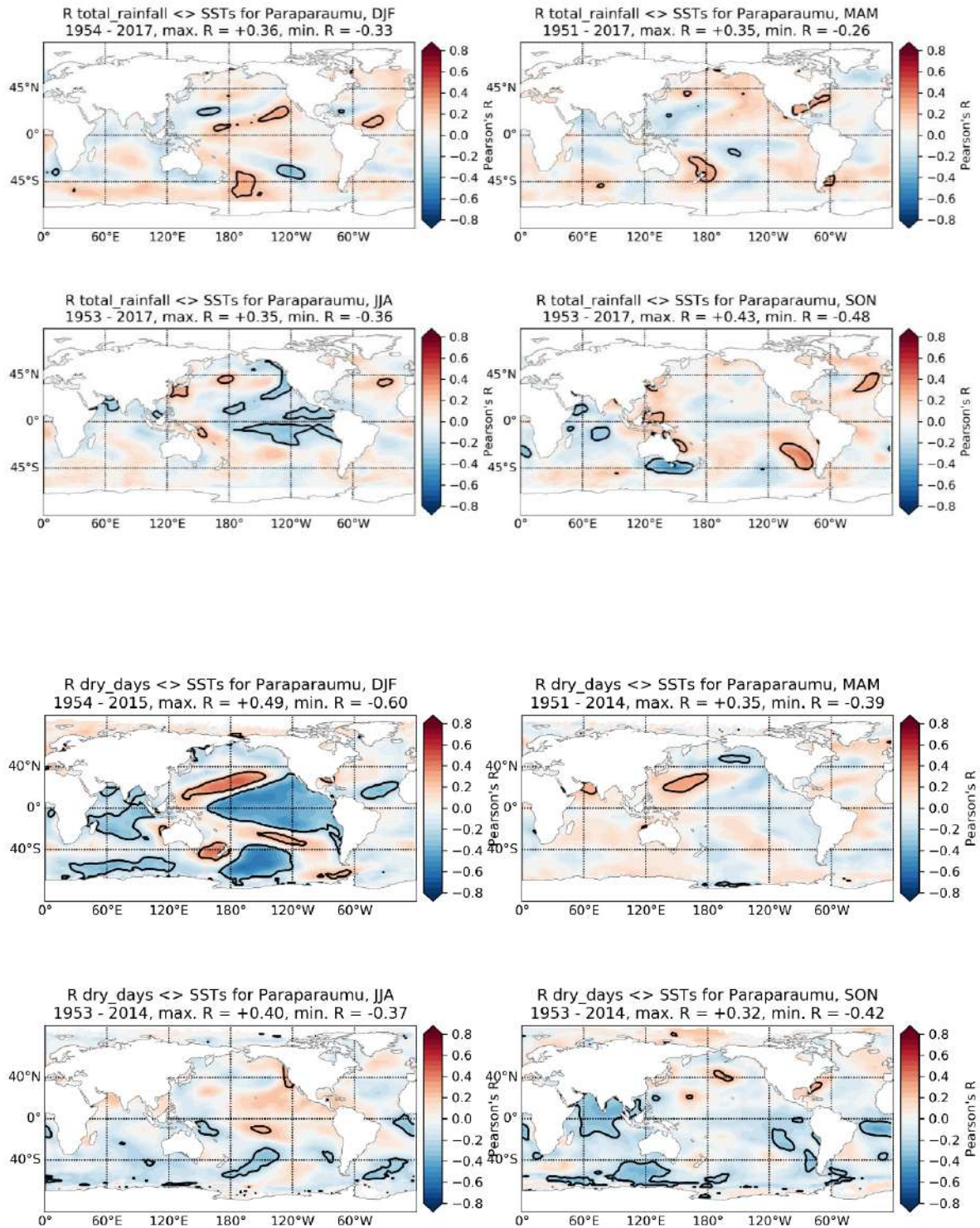
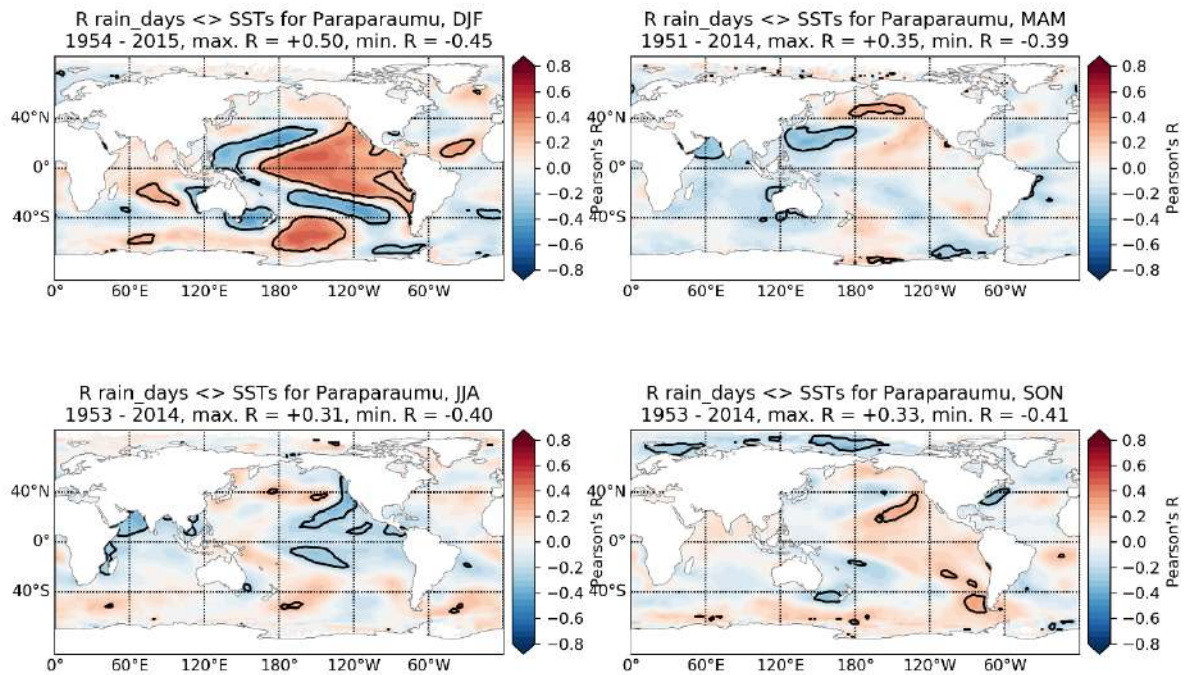
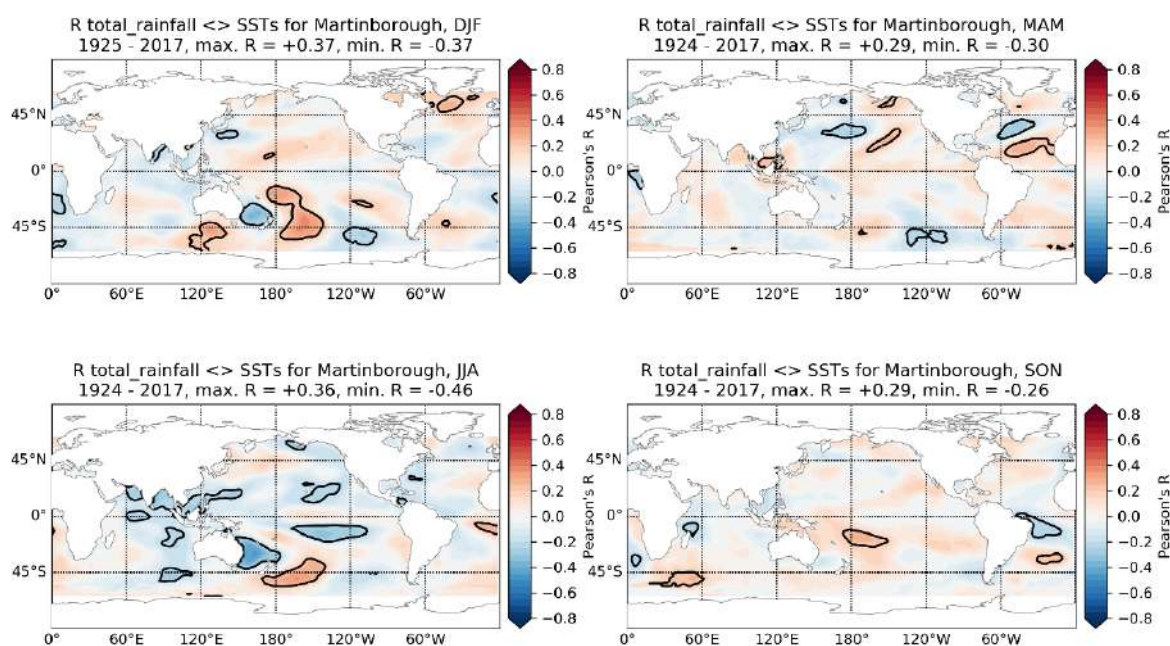


**Figure 5-3: Correlation field between the number of rain days in Paraparaumu and seasonal SST anomalies.** Black lines indicate areas of statistical significance at  $p \leq 0.05$ .



With the exception of Paraparaumu, the strongest and most consistent correlations between the various rainfall parameters and the global SSTs are mostly found at the regional scale, i.e. for ocean waters around New Zealand. More specifically, a rather consistent pattern implicates SSTs anomalies respectively in the Tasman Sea, and to the east and southeast of New Zealand. Generally speaking, the correlations are slightly stronger during the peak summer (DJF) and winter (JJA) seasons, and less so during the transition seasons (MAM and SON). This behaviour, replicated to some extent for all stations, is illustrated by Figure 5-4 for the Martinborough station: cumulative seasonal rainfall in Martinborough is negatively correlated to SSTs in the Tasman Sea, and positively correlated to SSTs east and southeast of New Zealand during DJF and JJA. The relationship with other seasonal rainfall variables is consistent with this pattern: e.g. the number of dry days tends to be positively correlated to SSTs in the Tasman sea, and negatively correlated to SSTs east of New Zealand, while the opposite is true for the number of rain days.

**Figure 5-4: Correlation field between total rainfall at Martinborough and seasonal SST anomalies.**



In conclusion, there are rarely consistent and strong *linear* relationships between rainfall parameters in the Wellington Region, and large-scale SST patterns that can be attributed to large scale climate modes. If one focuses on linear relationships, the main influence on rainfall regionally seems to be the SST gradient between the Tasman Sea and the oceanic region east and southeast of New Zealand. These regional SST anomalies seem instrumental in modulating the inter-annual variability of seasonal rainfall variables.

Note that the pattern does not correspond to the canonical signature of the South Pacific Subtropical Dipole Mode: the core anomalies of the SPSD (as defined by Guan et al. (2014) and Morioka et al. (2013)) are located respectively to the southeast of NZ and at the mid-latitudes of the South Pacific Ocean (see Figure 6 in Part A).

## 6 References

- GUAN, Y., ZHU, J., HUANG, B., HU, Z.-Z. & III, J. L. K. 2014. South Pacific Ocean Dipole: A Predictable Mode on Multiscale Time Scales. *Journal of Climate*, 27, 1648-1658.
- MORIOKA, Y., RATNAM, J. V., SASAKI, W. & MASUMOTO, Y. 2013. Generation Mechanism of the South Pacific Subtropical Dipole. *Journal of Climate*, 26, 6033-6045.

# Regional climate mode impacts on the Wellington Region

*Part C: Relationship between climate modes and temperature*

## Contents

<b>1</b>	<b>Mean maximum temperature .....</b>	<b>81</b>
1.1	ENSO .....	81
1.2	SAM .....	84
1.3	IOD.....	87
1.4	SPSD.....	90
<b>2</b>	<b>Mean minimum temperature .....</b>	<b>93</b>
2.1	ENSO .....	93
2.2	SAM .....	96
2.3	IOD.....	99
2.4	SPSD.....	102
<b>3</b>	<b>Hot days.....</b>	<b>105</b>
3.1	ENSO .....	105
3.2	SAM .....	108
3.3	IOD.....	110
3.4	SPSD.....	113
<b>4</b>	<b>Frost days.....</b>	<b>116</b>
4.1	ENSO .....	116
4.2	SAM .....	118
4.3	IOD.....	121
4.4	SPSD.....	124
<b>5</b>	<b>Relationship to Sea Surface Temperature (SST) anomalies .....</b>	<b>127</b>



This is Part C of the 'Regional climate mode impacts on the Wellington Region' report. Refer to Part A: Introduction, Methodology and Background for a thorough introduction to this study.

In this section, the relationships between seasonally (DJF, MAM, JJA, SON) aggregated temperature parameters (mean maximum temperature, mean minimum temperature, hot days, and frost days) and the inter-annual climate modes (El Niño Southern Oscillation (ENSO), Southern Annular Mode (SAM), Indian Ocean Dipole (IOD) and South Pacific Subtropical Dipole (SPSD)) are presented, first using the Virtual Climate Station Network (VCSN) and by means of composite analyses, then using the available station data.

For the VCSN, composite anomalies are calculated for the extreme phases of each mode: i.e. when standardized seasonal values exceed + 1 standard deviation (referred to as the positive phase of the mode) and are below -1 standard deviation (negative phase of the mode). For consistency, the 1981-2010 climatological normal is used for both the VCSN dataset (to define the 'normal' temperature) and for the climate mode index (to define the mean and standard deviation for the seasonally stratified standardisation).

For the station data, the composite anomalies are expressed in the original unit (e.g. degrees Celsius for mean maximum and mean minimum temperature, days for the number of hot days and frost days), and shown for each season and for each phase of the mode (positive, negative neutral) and displayed as a line plot. This representation thus gives a summary of the distribution of the values included in the three samples, and illustrates the variability in the corresponding temperature parameter observed during each phase of the mode. Because of the large number of stations, we only present the figures for the stations displaying a significant ( $p \leq 0.05$  according to a Student t-test) association for the mode during at least one season. The figures not included are available as supplementary electronic material to this report.

# 1 Mean maximum temperature

Mean maximum temperature is considered to reflect 'daytime' temperature, as the highest temperature during the diurnal cycle is usually recorded during daytime hours. Anomalies in mean maximum temperature derived from the VCSN are presented as a departure from the 1981-2010 climatology and expressed in degrees Celsius.

## 1.1 ENSO

### 1.1.1 VCSN

The VCSN composites indicate the largest cool anomalies of mean maximum temperature tend to be over the western half of the Wellington Region during El Niño events (Figure 1-1), notably in DJF (the usual peak of ENSO events), with above average maximum temperatures in the Wairarapa during DJF and MAM. During negative ENSO phases (La Niña), warm anomalies in maximum temperature are generally present across most of the region (Figure 1-2). Note however that the anomalies are weak, rarely exceed +/- 0.5°C, and are not statistically significant.

**Figure 1-1: Mean maximum temperature anomalies during the positive phase (El Niño) of ENSO (VCSN anomalies).** Red lines outline areas of statistical significance at  $p \leq 0.05$ .

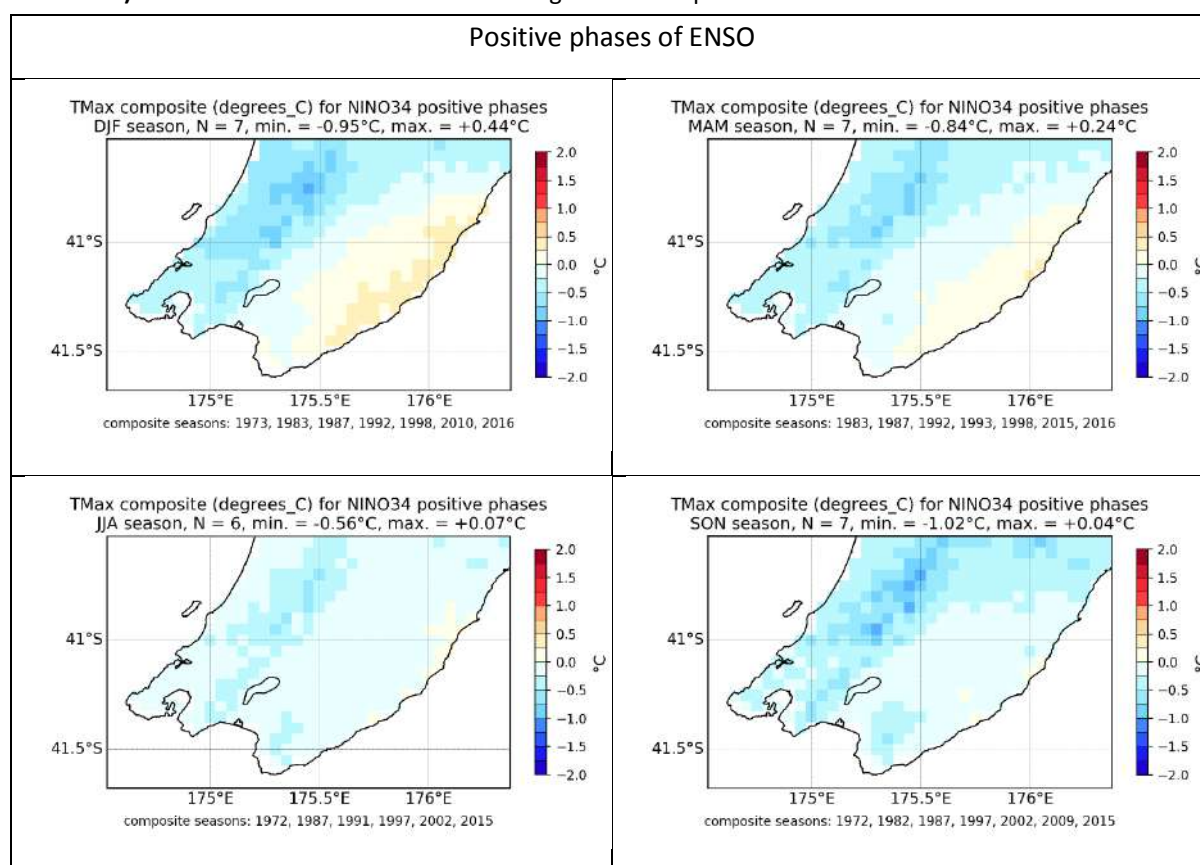
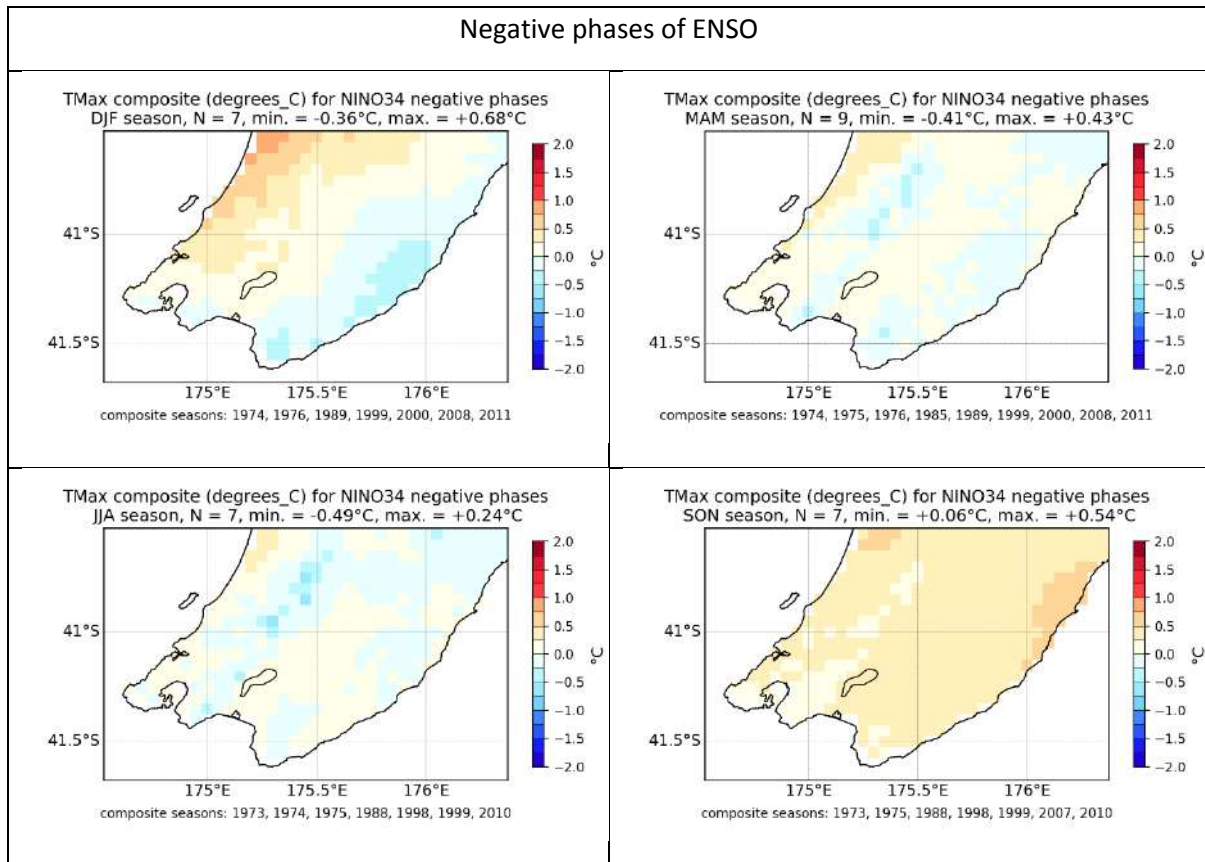


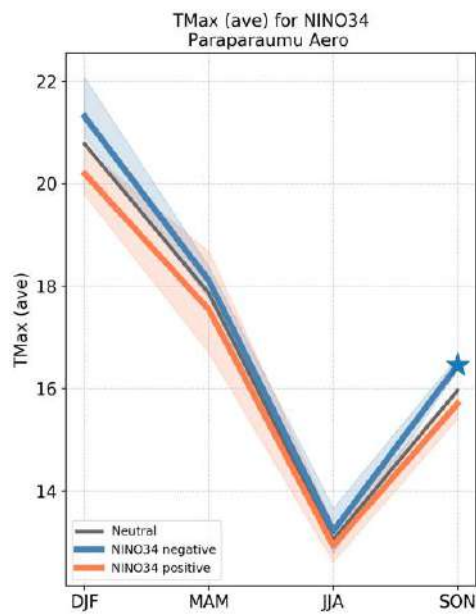
**Figure 1-2: Mean maximum temperature anomalies during the negative phase (La Niña) of ENSO (VCSN anomalies).** Red lines outline areas of statistical significance at  $p \leq 0.05$ .



### 1.1.2 Station data

The only statistically significant anomalies are found for the Paraparaumu Aero station, for which slightly higher than normal seasonally averaged daytime temperatures are found during the negative phase of ENSO in SON (Figure 1-3).

**Figure 1-3: Mean maximum temperature and ENSO phase at Paraparaumu Aero.** The stars indicate statistical significance at  $p \leq 0.05$ , and the shaded area indicates the interquartile range (25<sup>th</sup> to 75<sup>th</sup> percentile) of the corresponding composite sample.



## 1.2 SAM

### 1.2.1 VCSN

The clearest relationships between mean maximum temperature and SAM phase occur during the negative SAM phase (Figure 1-5) in JJA and SON, where mean maximum temperatures are lower than usual in south and east of the Wellington Region. In other seasons, the VCSN composites do not show a clear and consistent response of mean maximum temperatures to the SAM over the Wellington Region.

**Figure 1-4: Mean maximum temperature anomalies during the positive phase of SAM (VCSN anomalies).** Red lines outline areas of statistical significance at  $p \leq 0.05$ .

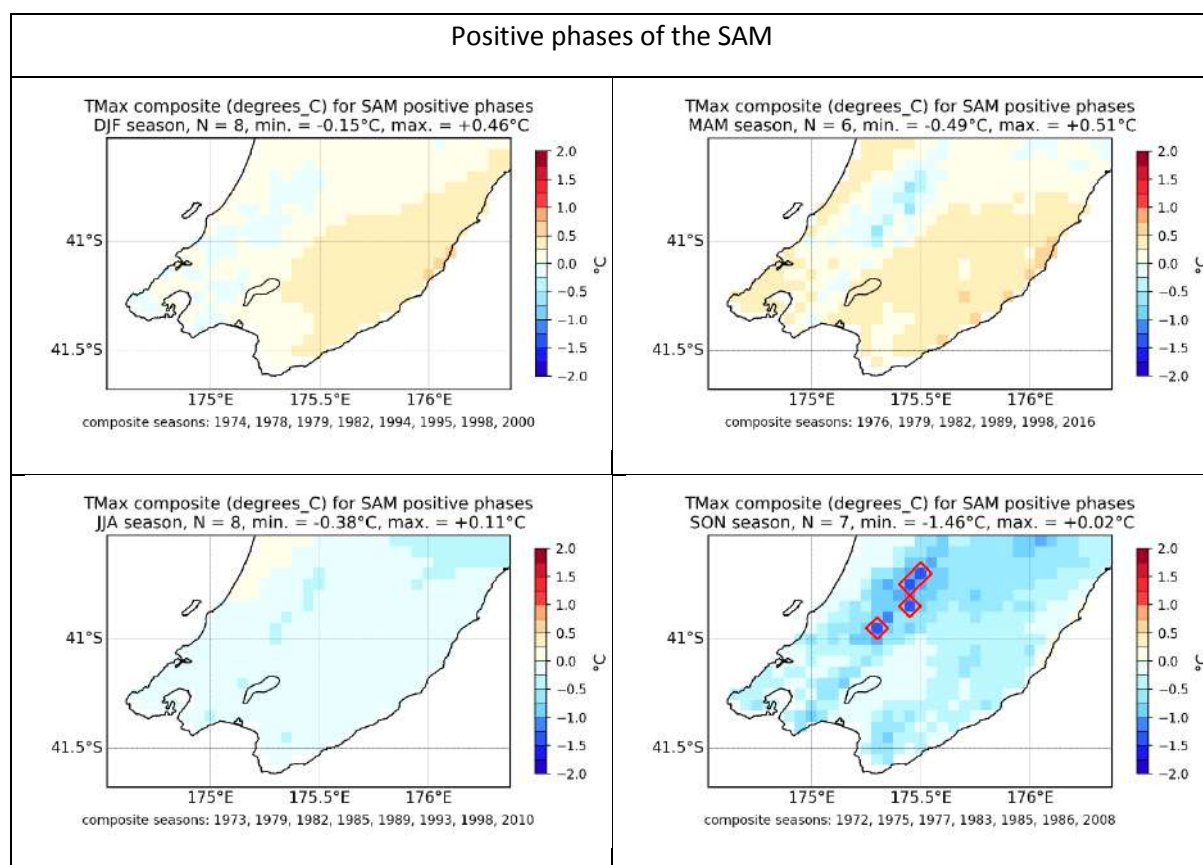
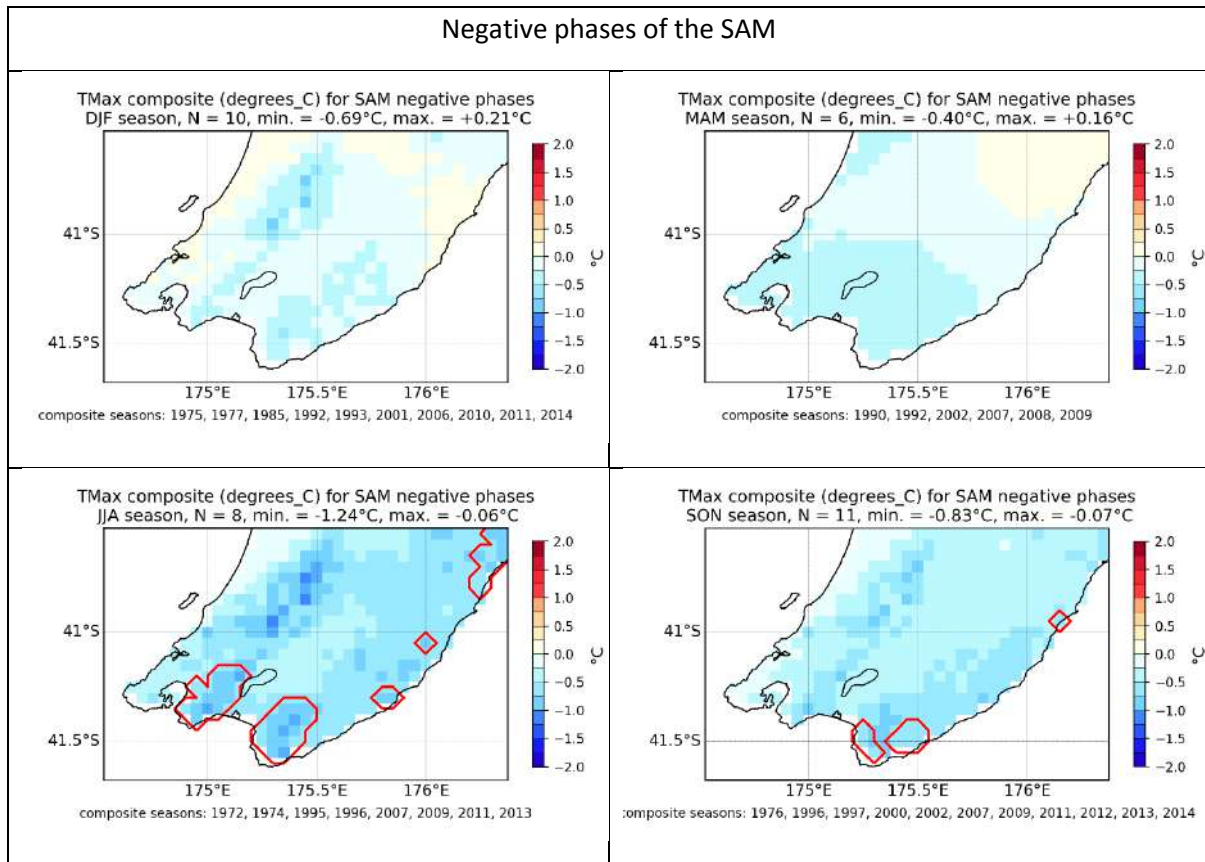


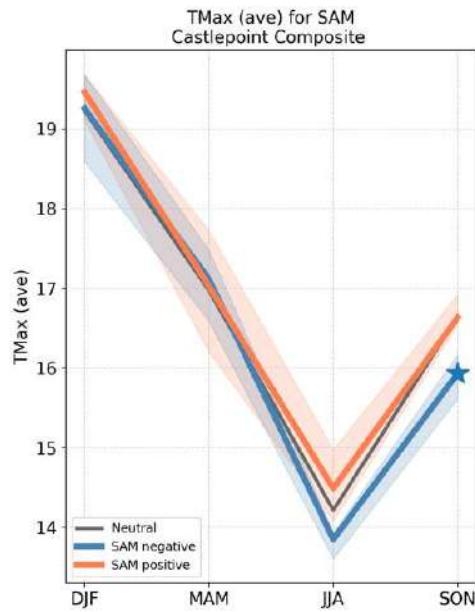
**Figure 1-5: Mean maximum temperature anomalies during the negative phase of SAM (VCSN anomalies).**  
 Red lines outline areas of statistical significance at  $p \leq 0.05$ .



### 1.2.2 Station data

The only significant relationship between mean maximum temperature and the SAM is found at Castlepoint (composite) during SON and for the negative phases of the SAM, during which mean maximum temperatures tend to be lower than normal (Figure 1-6).

**Figure 1-6: Mean maximum temperature and SAM phase at Castlepoint (composite).** The stars indicate statistical significance at  $p \leq 0.05$ , and the shaded area indicates the interquartile range (25<sup>th</sup> to 75<sup>th</sup> percentile) of the corresponding composite sample.



## 1.3 IOD

### 1.3.1 VCSN

The VCSN composite patterns do not show a strong and consistent relationship between the IOD and mean maximum temperatures. During SON (season during which the IOD is generally expressed), mean maximum temperatures tend to be lower than normal during the positive phase (Figure 1-7), and higher than normal during the negative phase (Figure 1-8), but the anomalies again are weak ( $< \pm 1^\circ\text{C}$ ).

**Figure 1-7: Mean maximum temperature anomalies during the positive phase of IOD (VCSN anomalies).** Red lines outline areas of statistical significance at  $p \leq 0.05$ .

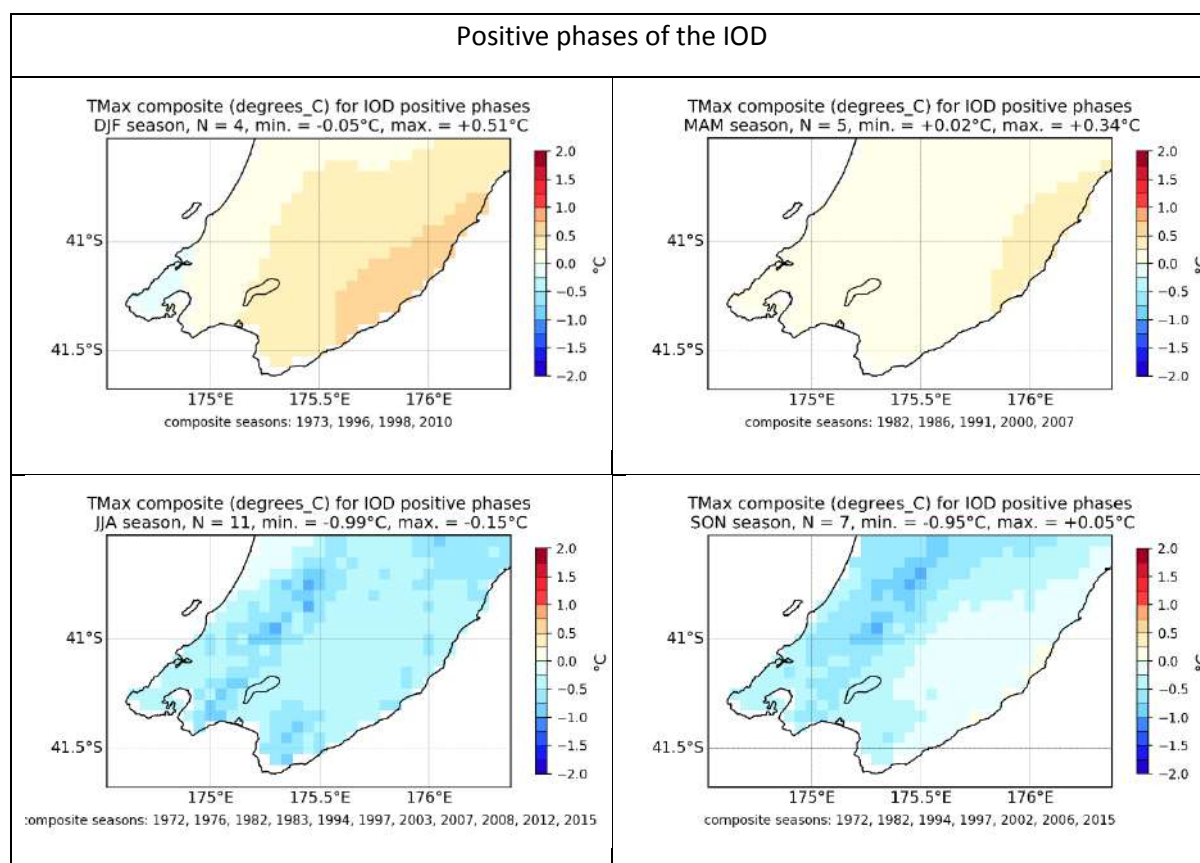
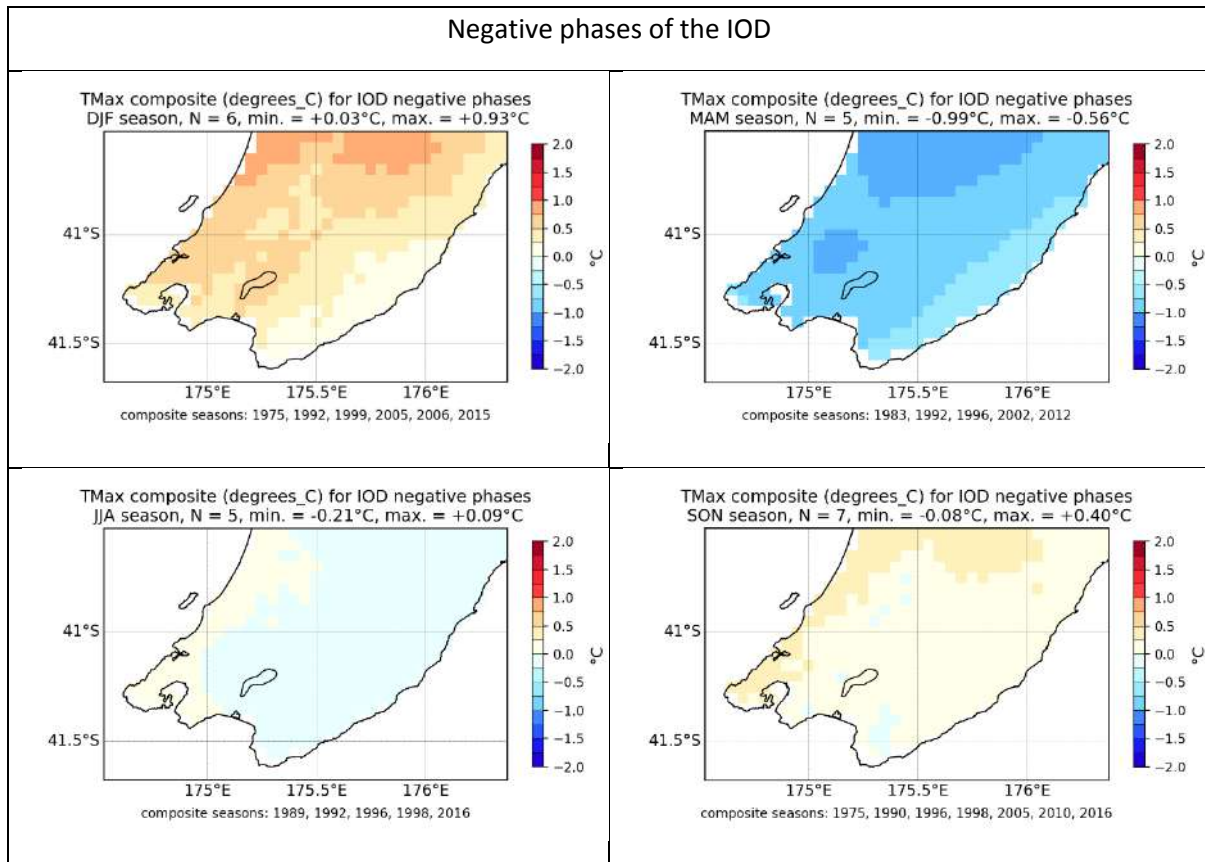




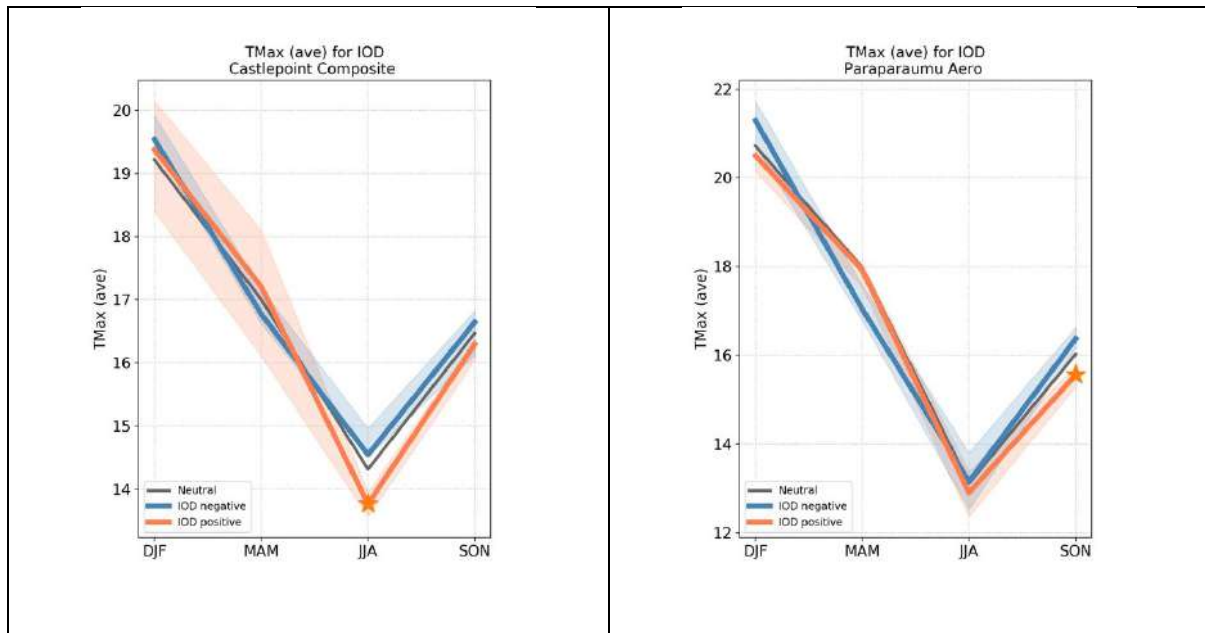
**Figure 1-8: Mean maximum temperature anomalies during the negative phase of IOD (VCSN anomalies).**  
 Red lines outline areas of statistical significance at  $p \leq 0.05$ .



### 1.3.2 Station data

The only significant ( $p \leq 0.05$ ) relationships are found for Castlepoint (Composite) in JJA, and for Paraparaumu Aero in SON, for the positive phase of the IOD (Figure 1-9), during which mean maximum temperatures tend to be lower than normal. It is generally consistent with the composite anomalies derived from the VCSN.

**Figure 1-9: Mean maximum temperature and IOD phase at Castlepoint (Composite) and Paraparaumu Aero.** The stars indicate statistical significance at  $p \leq 0.05$ , and the shaded area indicates the interquartile range (25<sup>th</sup> to 75<sup>th</sup> percentile) of the corresponding composite sample.



## 1.4 SPSD

### 1.4.1 VCSN

The VCSN composites show a relatively consistent relationship between mean maximum temperatures over the Wellington Region and the SPSD: mean maximum temperatures tend to be higher than normal during the positive phase of the SPSD (Figure 1-10), notably from spring (SON) to autumn (MAM) and conversely lower than normal during the negative phase of the SPSD (Figure 1-11). Note that it is fully consistent with the sign of the SST anomalies surrounding New Zealand associated with the corresponding phases of the SPSD.

**Figure 1-10: Mean maximum temperature anomalies during the positive phase of SPSD (VCSN anomalies).** Red lines outline areas of statistical significance at  $p \leq 0.05$ .

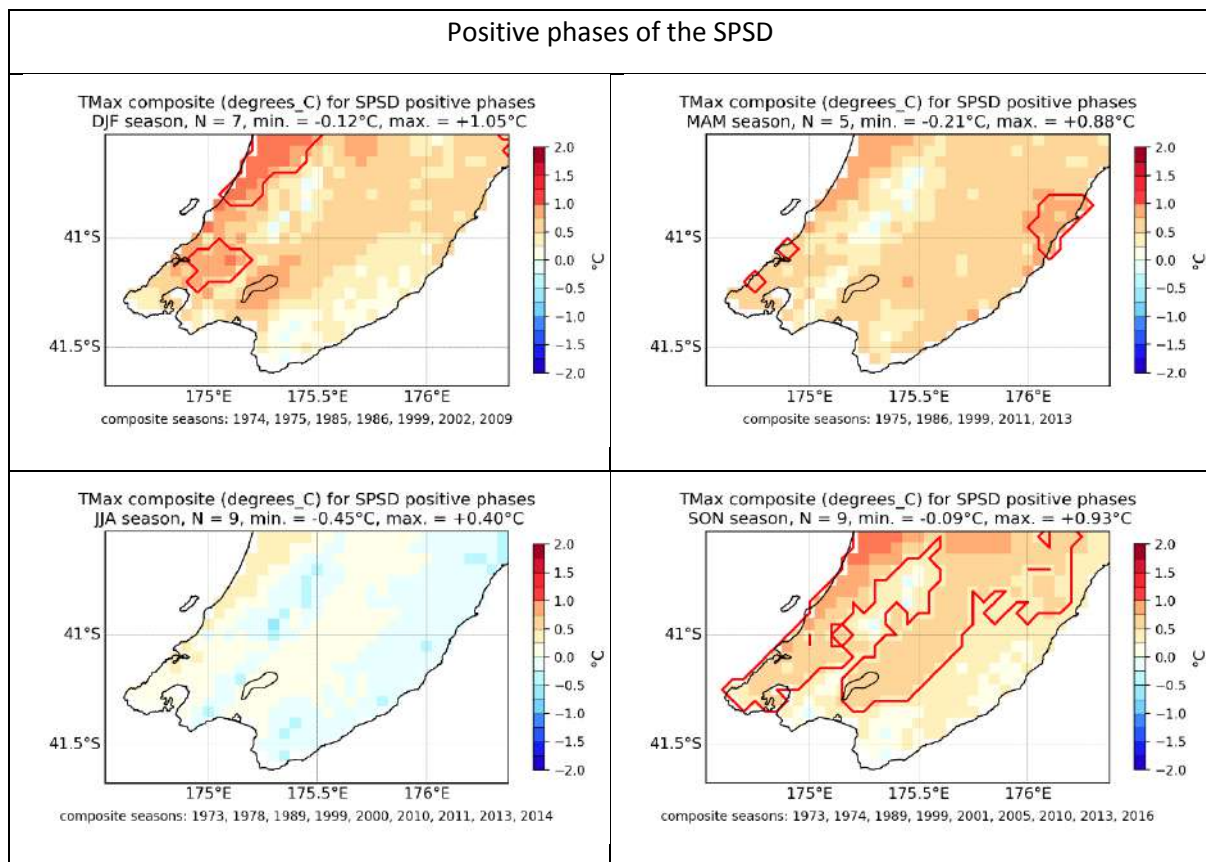
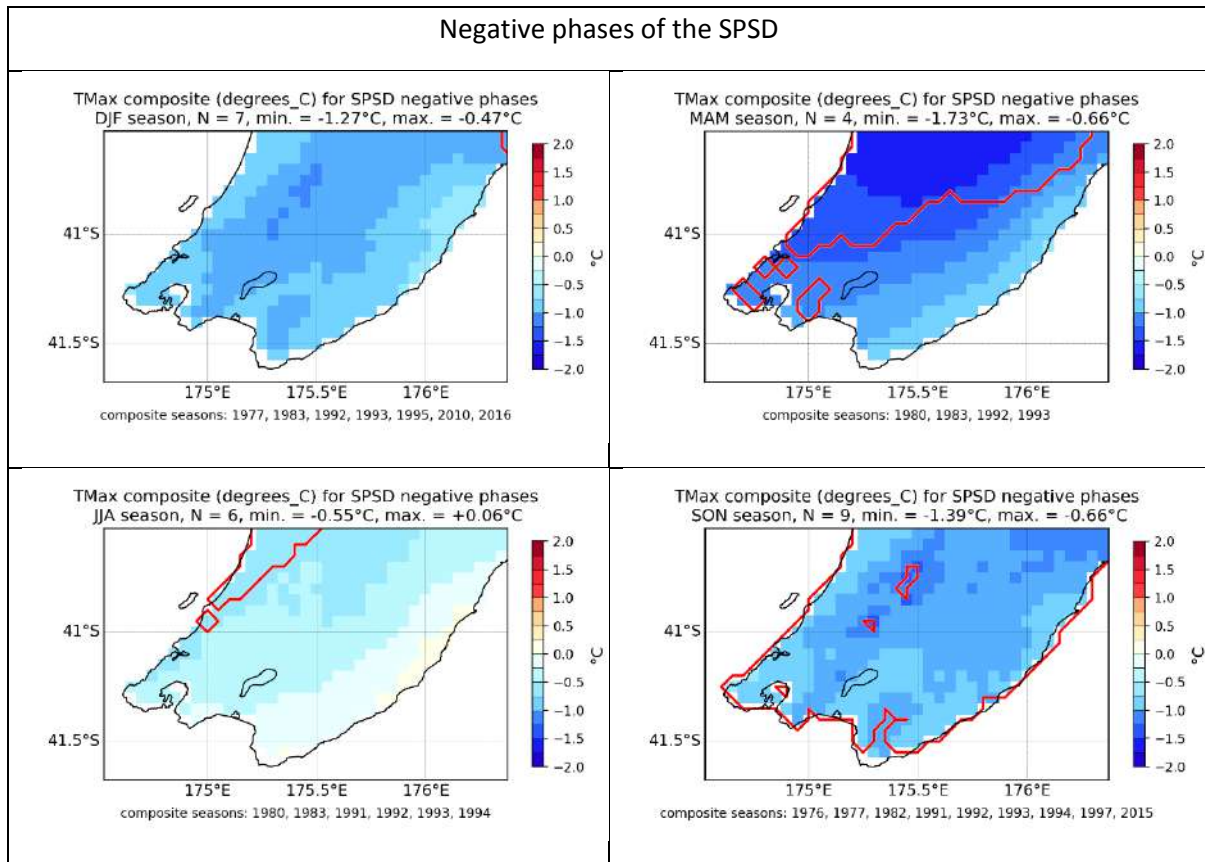


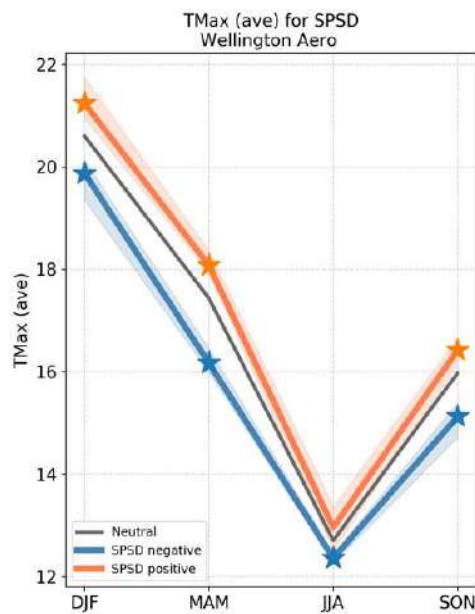
**Figure 1-11: Mean maximum temperature anomalies during the negative phase of SPSP (VCSN anomalies).**  
 Red lines outline areas of statistical significance at  $p \leq 0.05$ .



### 1.4.2 Station data

Again, the general pattern derived from the station level data confirms the conclusions derived from the VCSN composite anomalies. Higher than normal mean maximum temperature tends to be observed during the positive phase of the SPSD, while the reverse is true for the negative phase of this mode. This is best illustrated for the Wellington Aero station in Figure 1-12. Note that this is fully consistent with the regional SST anomalies associated with the SPSD: during the positive phase of the SPSD, warmer than normal coastal waters are usually observed, especially around the North Island, while the reverse is true during the negative phase of the SPSD.

**Figure 1-12: Mean maximum temperature and SPSD phase at Wellington Aero.** The stars indicate statistical significance at  $p \leq 0.05$ , and the shaded area indicates the interquartile range (25<sup>th</sup> to 75<sup>th</sup> percentile) of the corresponding composite sample.



## 2 Mean minimum temperature

Mean minimum temperature is considered to be the 'night time' temperature, as the lowest temperature during the diurnal cycle is usually recorded during night time hours. Anomalies in mean minimum temperature derived from the VCSN are presented as a departure from the 1981-2010 climatology in degrees Celsius.

### 2.1 ENSO

#### 2.1.1 VCSN

The VCSN composites for mean minimum temperatures show a very weak relationship to the positive and negative phases of ENSO, with most anomalies weaker than +/- 0.5°C (i.e. technically in the normal range). Generally cooler than usual mean minimum temperatures are experienced during the positive phase and warmer than usual mean minimum temperatures are experienced during the negative phase of ENSO (Figure 2-1). This is therefore consistent with the sign of the mean maximum temperature anomalies associated with both phases of ENSO (see Figure 1-1, Figure 1-2).

**Figure 2-1: Mean minimum temperature anomalies during the positive phase of ENSO (VCSN anomalies).** Red lines outline areas of statistical significance at  $p \leq 0.05$ .

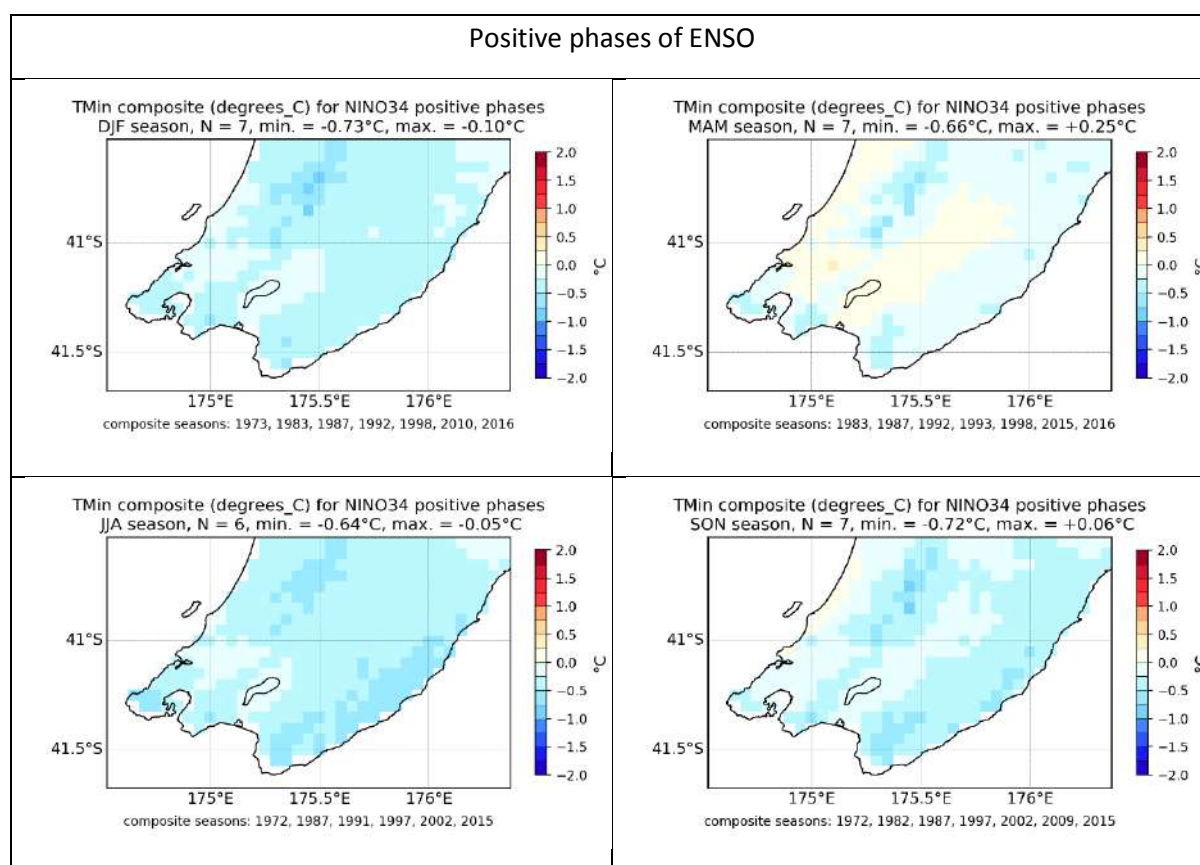
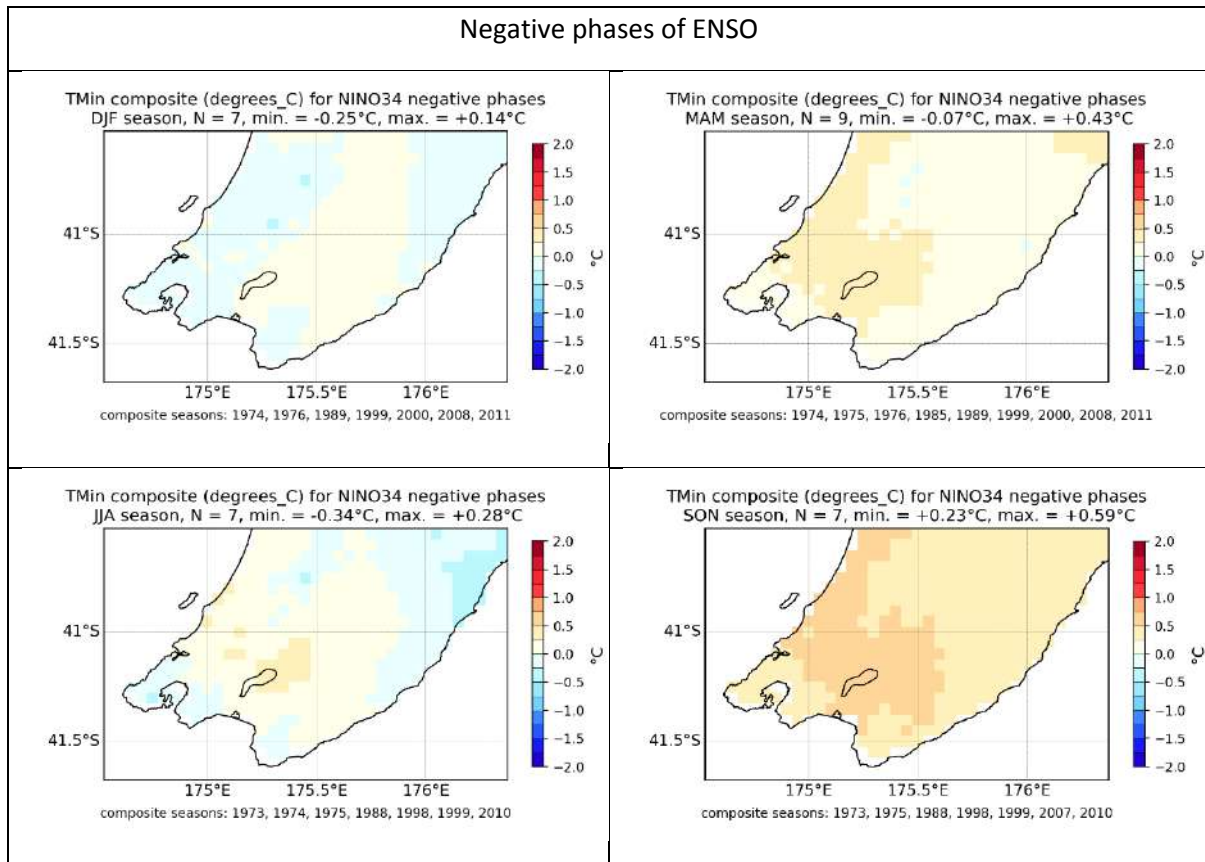


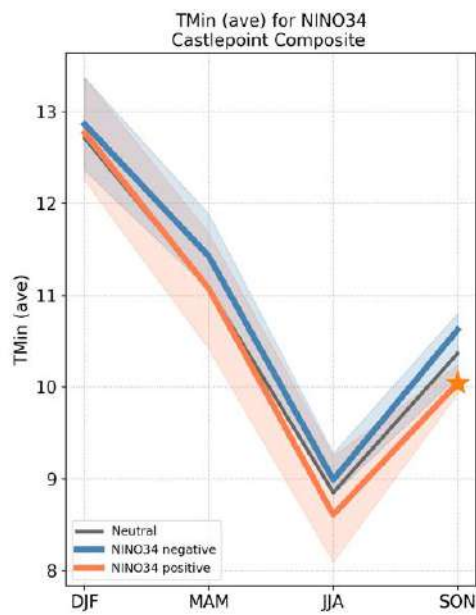
**Figure 2-2: Mean minimum temperature anomalies during the negative phase of ENSO (VCSN anomalies).**  
 Red lines outline areas of statistical significance at  $p \leq 0.05$ .



### 2.1.2 Station data

The only statistically significant anomalies are found for the Castlepoint (Composite) station, for which lower than normal minimum temperatures are found during the positive phase of ENSO (Figure 2-3).

**Figure 2-3: Mean minimum temperature and ENSO phase at Castlepoint (composite).** The stars indicate statistical significance at  $p \leq 0.05$ , and the shaded area indicates the interquartile range (25<sup>th</sup> to 75<sup>th</sup> percentile) of the corresponding composite sample.





## 2.2 SAM

### 2.2.1 VCSN

The clearest relationships between mean minimum temperatures and the SAM phase are observed during SON in the negative phase of the SAM (Figure 2-5), where cooler than normal temperatures are observed (statistically significant). In the positive phase (Figure 2-4), the strongest anomalies are experienced in MAM, with warmer than usual mean minimum temperatures – however these anomalies are not statistically significant.

**Figure 2-4: Mean minimum temperature anomalies during the positive phase of SAM (VCSN anomalies).** Red lines outline areas of statistical significance at  $p \leq 0.05$ .

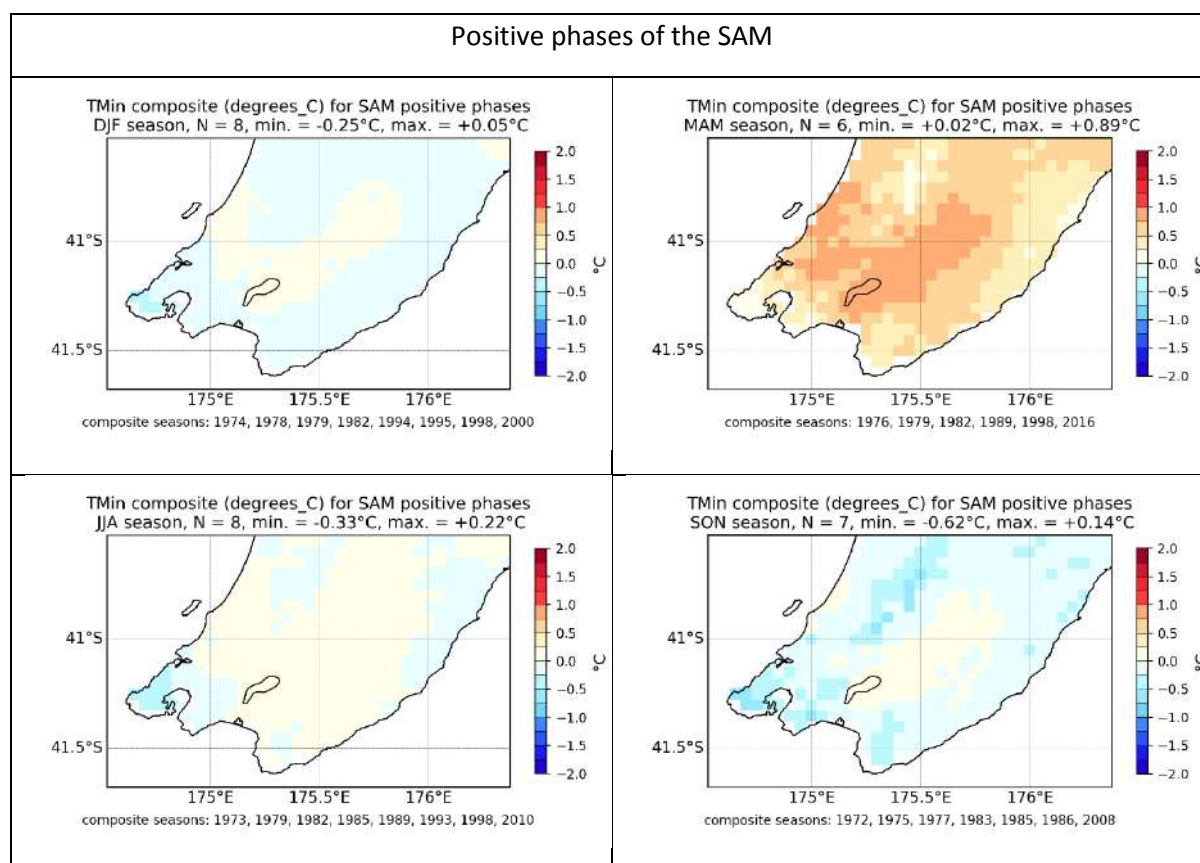
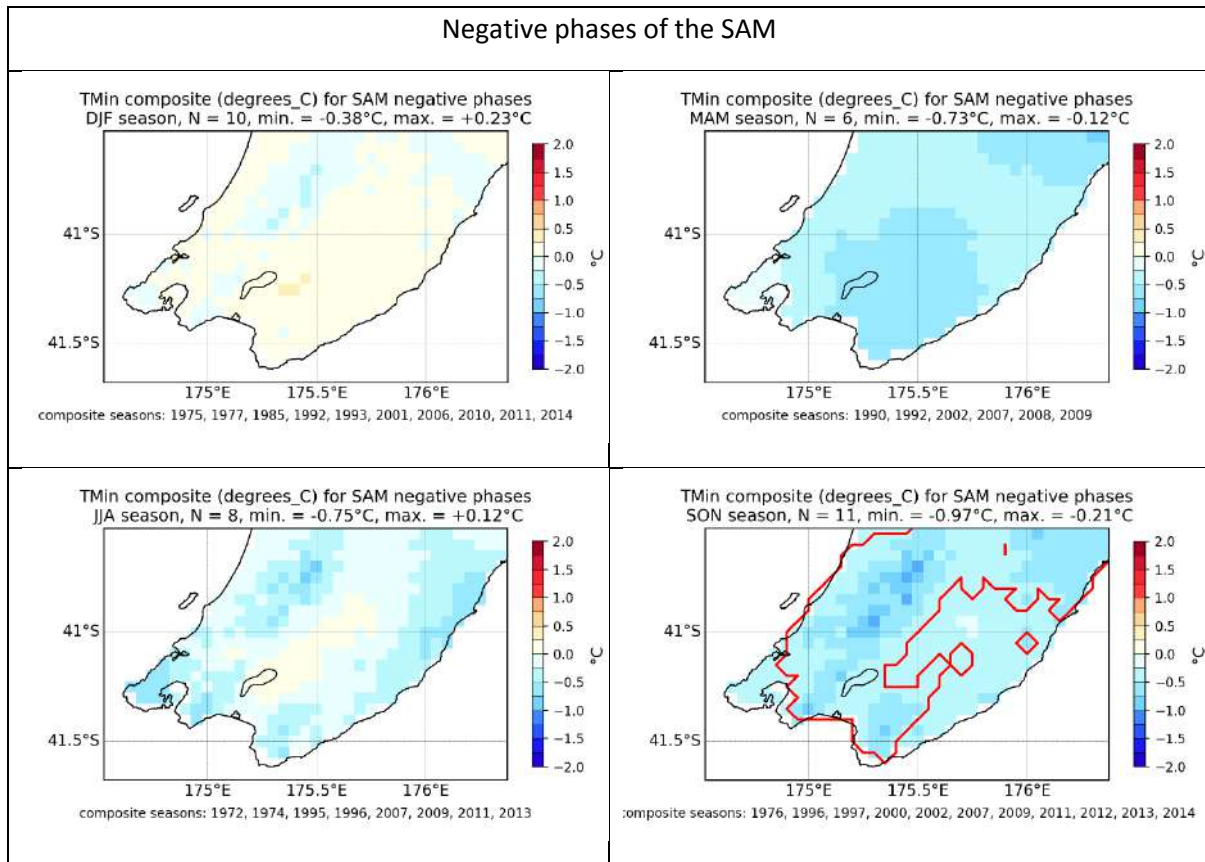


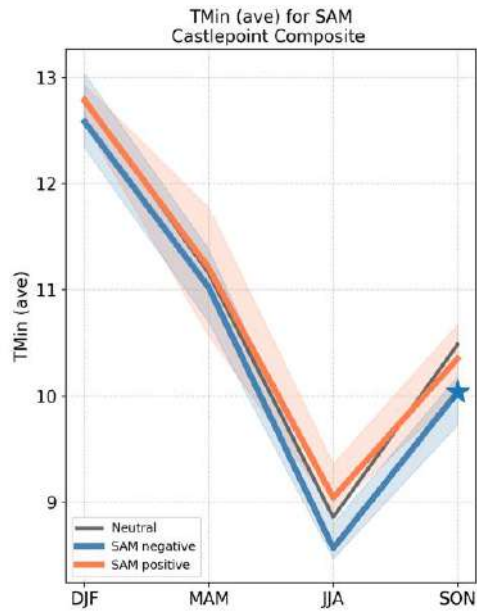
**Figure 2-5: Mean minimum temperature anomalies during the negative phase of SAM (VCSN anomalies).**  
 Red lines outline areas of statistical significance at  $p \leq 0.05$ .



### 2.2.2 Station data

The only statistically significant anomalies are found for the Castlepoint (Composite) station, for which lower than normal minimum temperatures are found during the negative phase of the SAM (Figure 2-6).

**Figure 2-6: Mean minimum temperature and SAM phase at Castlepoint (composite).** The stars indicate statistical significance at  $p \leq 0.05$ , and the shaded area indicates the interquartile range (25<sup>th</sup> to 75<sup>th</sup> percentile) of the corresponding composite sample.



## 2.3 IOD

### 2.3.1 VCSN

The strongest relationships between mean minimum temperature and the IOD phase are observed in JJA during the positive phase, when statistically significant cool anomalies are observed in the Wairarapa (Figure 2-7). Other seasons show weak mean minimum temperature anomalies.

**Figure 2-7: Mean minimum temperature anomalies during the positive phase of IOD (VCSN anomalies).** Red lines outline areas of statistical significance at  $p \leq 0.05$ .

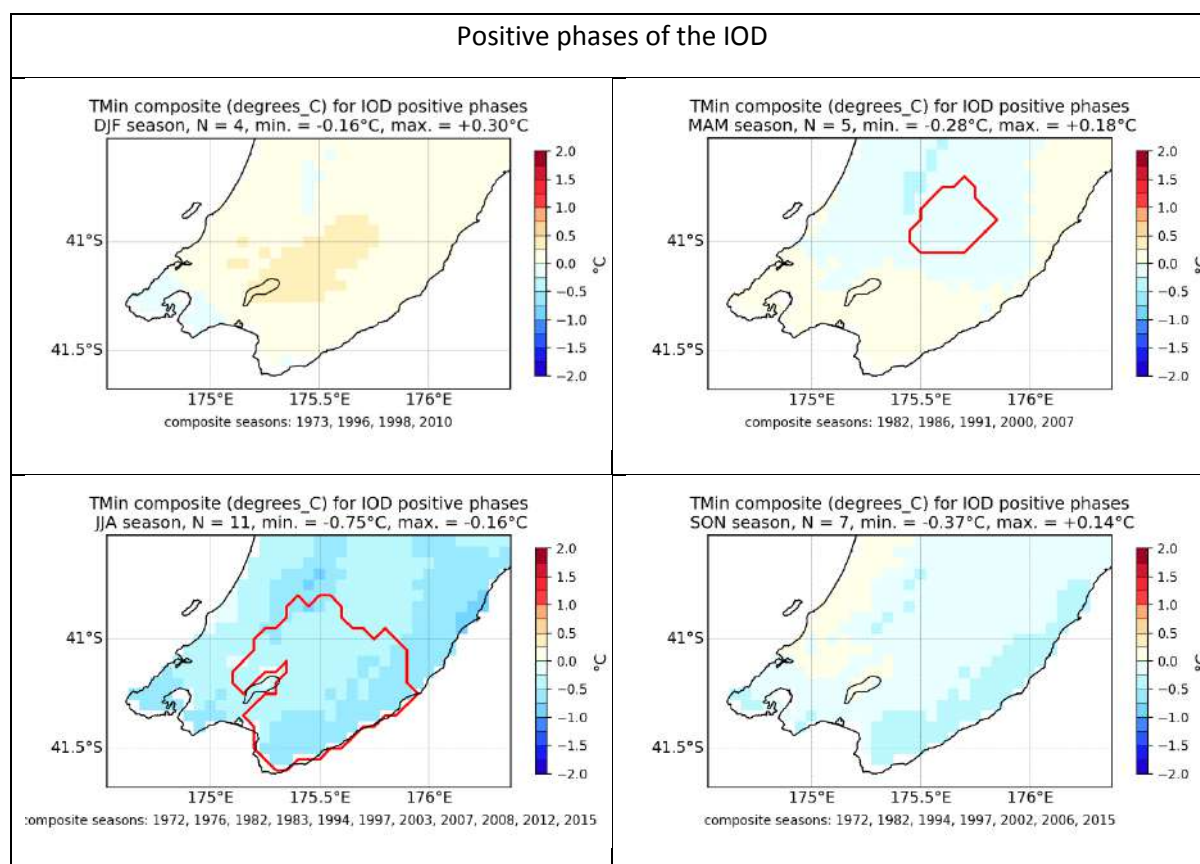
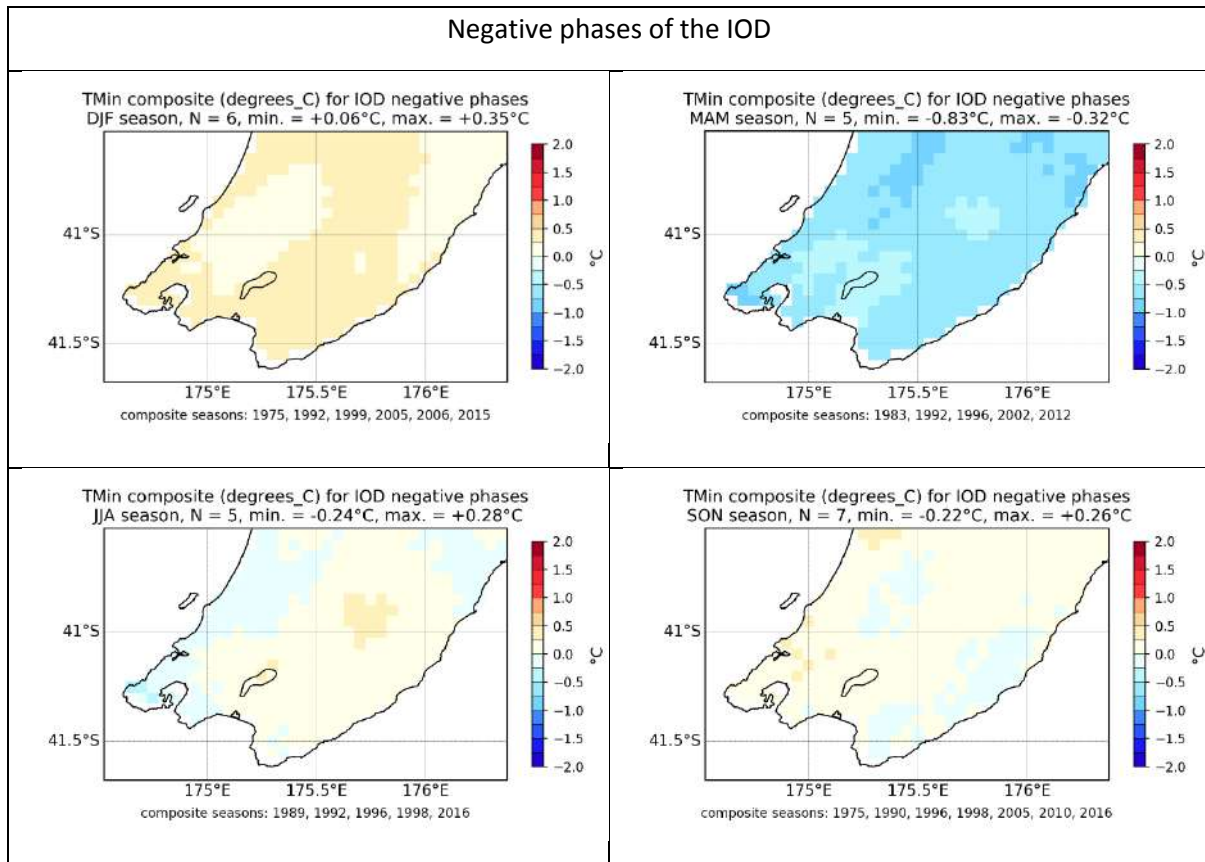


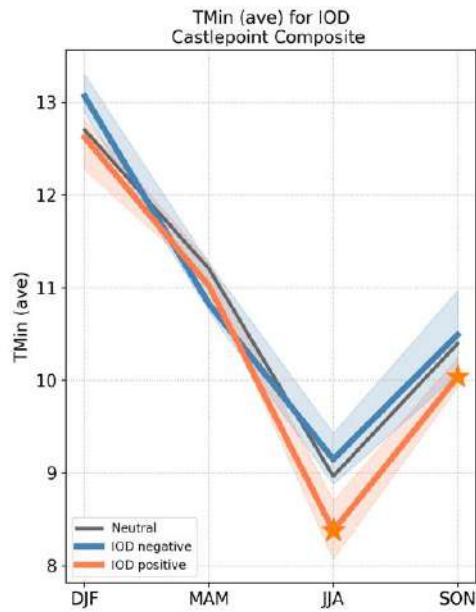
**Figure 2-8: Mean minimum temperature anomalies during the negative phase of IOD (VCSN anomalies).**  
 Red lines outline areas of statistical significance at  $p \leq 0.05$ .



### 2.3.2 Station data

The only statistically significant anomalies are found for the Castlepoint (Composite) station, for which lower than normal minimum temperatures are found during the positive phase of the IOD in JJA and SON (Figure 2-9).

**Figure 2-9: Mean minimum temperature and IOD phase at Castlepoint (composite).** The stars indicate statistical significance at  $p \leq 0.05$ , and the shaded area indicates the interquartile range (25<sup>th</sup> to 75<sup>th</sup> percentile) of the corresponding composite sample.



## 2.4 SPSD

### 2.4.1 VCSN

As with the mean maximum temperatures, the VCSN composites show a consistent relationship between mean minimum temperatures over the Wellington Region and the SPSD: mean minimum temperatures tend to be higher than normal during the positive phase of the SPSD (Figure 2-10), notably from spring (SON) to autumn (MAM) and conversely lower than normal during the negative phase of the SPSD (Figure 2-11). Again, this is fully consistent with the sign of the SST anomalies around NZ during the respective phases of this mode.

**Figure 2-10: Mean minimum temperature anomalies during the positive phase of SPSD (VCSN anomalies).** Red lines outline areas of statistical significance at  $p \leq 0.05$ .

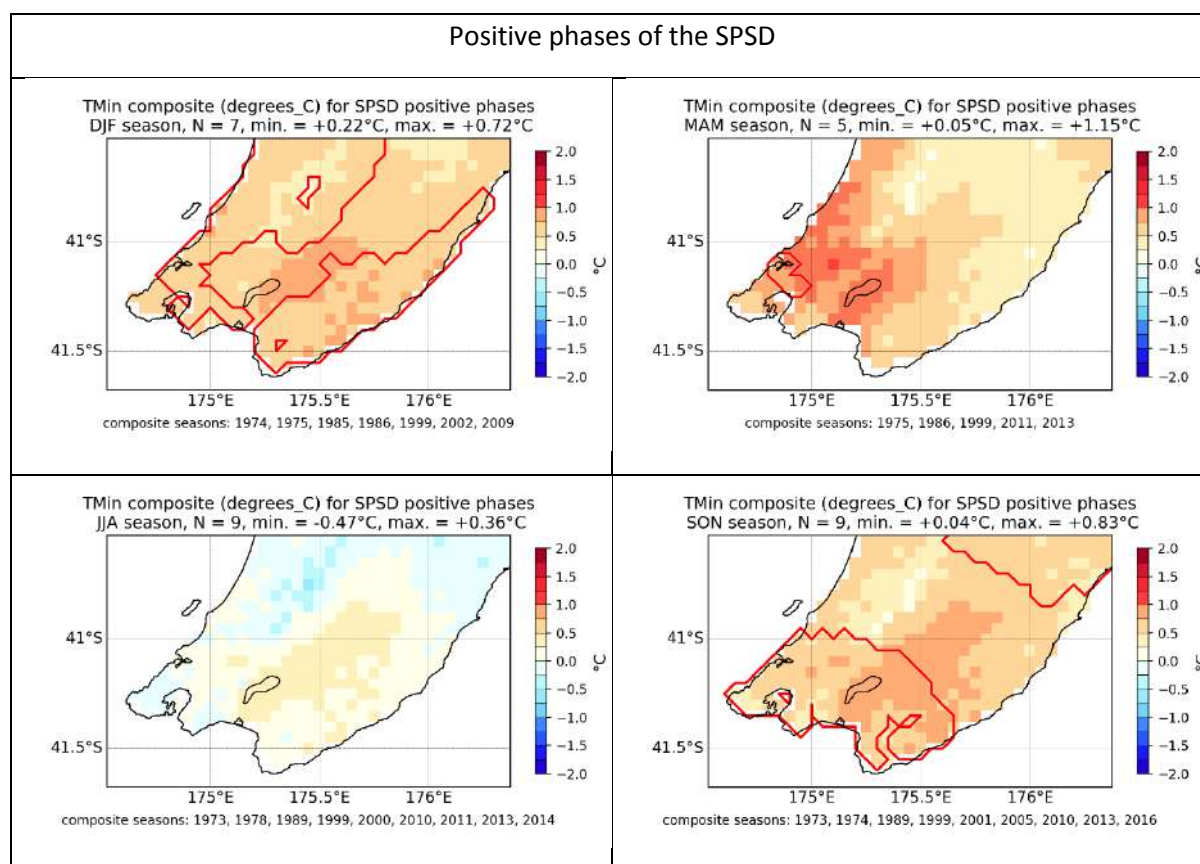
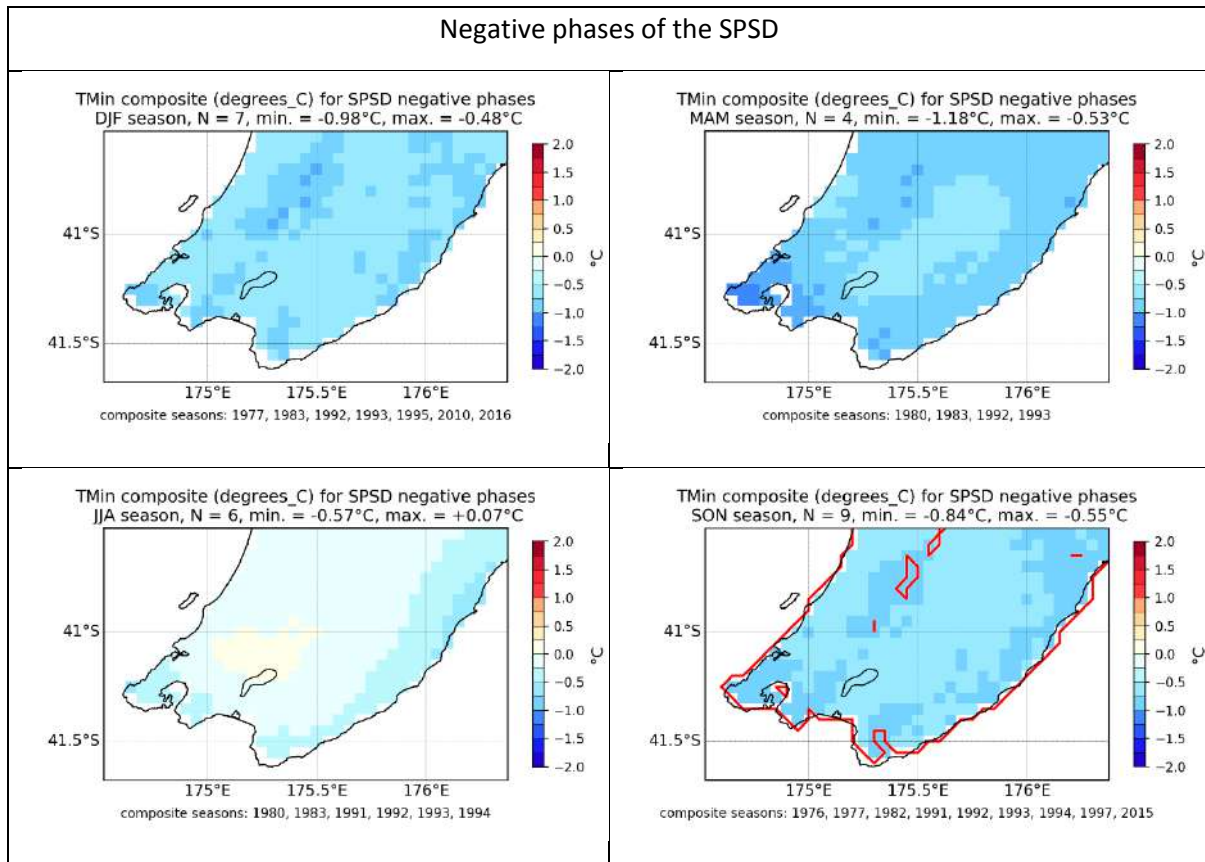


**Figure 2-11: Mean minimum temperature anomalies during the negative phase of SPSP (VCSN anomalies).**  
 Red lines outline areas of statistical significance at  $p \leq 0.05$ .

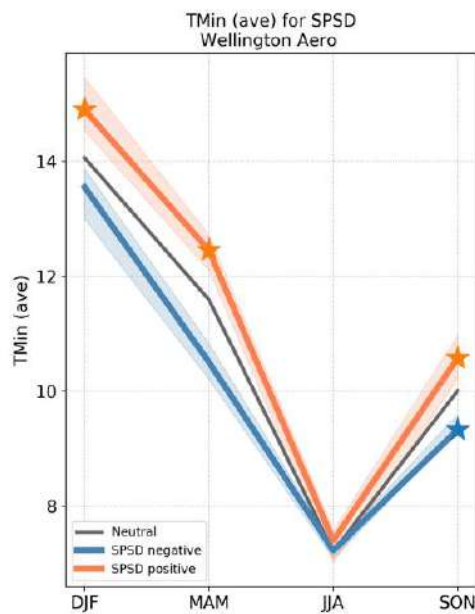




## 2.4.2 Station data

Again, the SPSP presents the most consistent relationships with station-level mean minimum temperatures, and the station data broadly confirms the relationships shown in the VCSN dataset: positive SPSP phases, especially during the SON to MAM seasons, tend to be related to increased minimum temperatures, while negative SPSP phases tend to be related to decreased minimum temperatures, notably during SON, this is best illustrated by the Wellington Aero station (Figure 2-12).

**Figure 2-12: Mean minimum temperature and SPSP phase at Wellington Aero.** The stars indicate statistical significance at  $p \leq 0.05$ , and the shaded area indicates the interquartile range (25<sup>th</sup> to 75<sup>th</sup> percentile) of the corresponding composite sample.



### 3 Hot days

Hot day anomalies derived from the VCSN are presented in the departure from normal in days (1981-2010 climatology). A hot day is counted when the maximum daily temperature exceeds 25°C.

#### 3.1 ENSO

##### 3.1.1 VCSN

While the VCSN composites anomalies for the number of hot days during the extreme ENSO phases are rarely significant, they show a relatively consistent pattern: consistently with the mean maximum temperatures (Figure 1-1 and Figure 1-2); the number of hot days tends to decrease over the western half of the Wellington Region and increase over the Wairarapa during the peak of the positive ENSO phase (El Niño) in DJF (Figure 3-1), while the reverse is broadly true during the negative phases of ENSO (La Niña) (Figure 3-2).

**Figure 3-1: Hot day anomalies during the positive phase of ENSO (VCSN anomalies).** Red lines outline areas of statistical significance at  $p \leq 0.05$ .

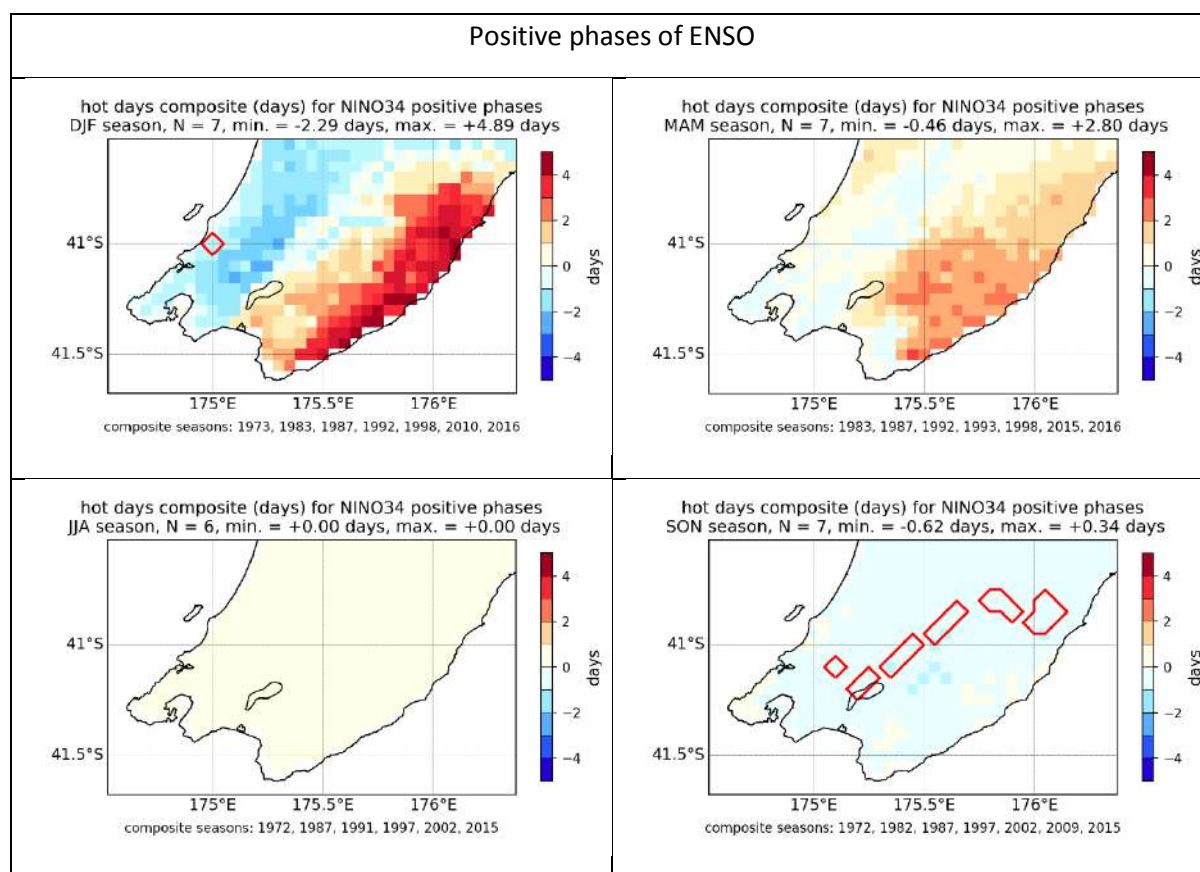
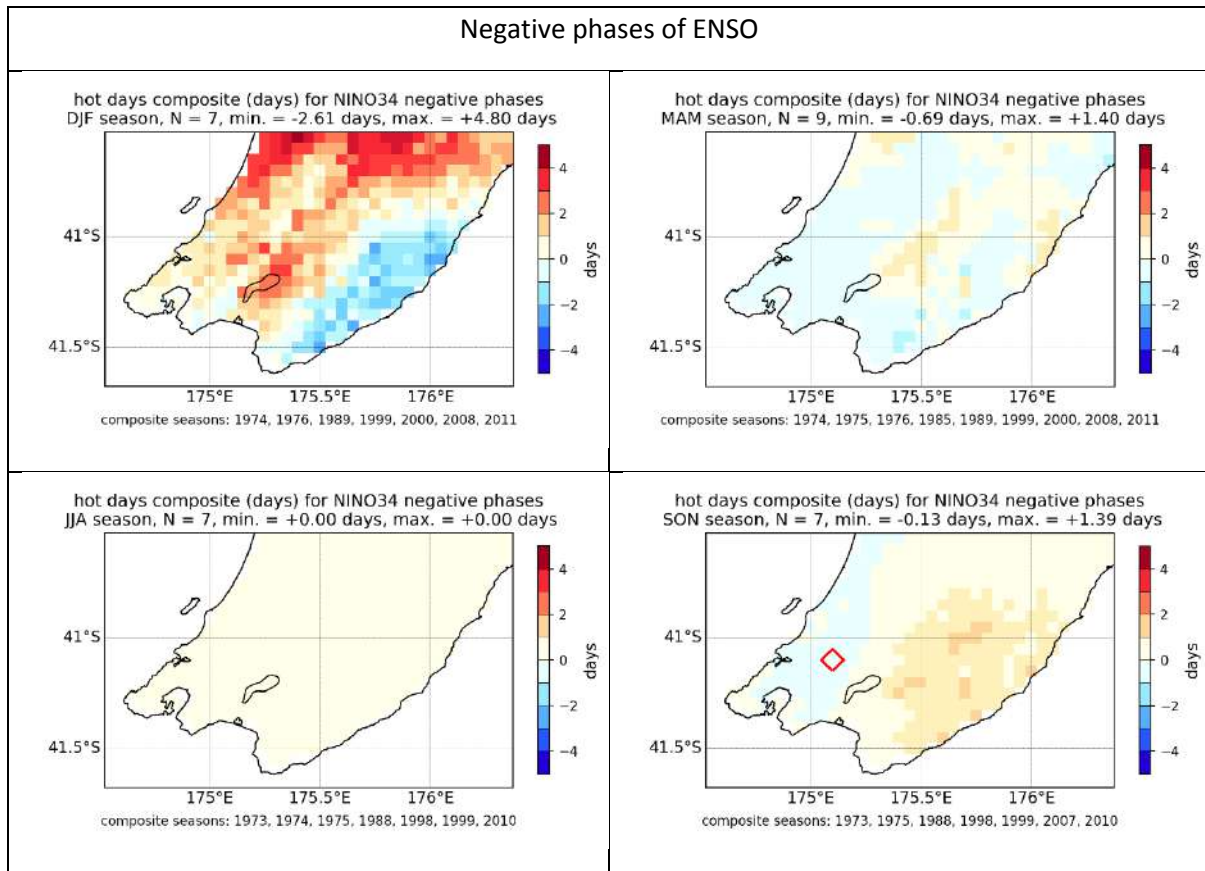


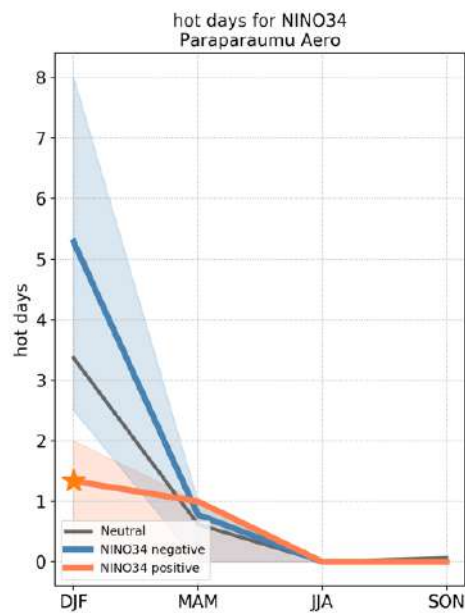
**Figure 3-2: Hot day anomalies during the negative phase of ENSO (VCSN anomalies).** Red lines outline areas of statistical significance at  $p \leq 0.05$ .



### 3.1.2 Station data

The only statistically significant relationship between ENSO and the number of hot days at the station level are found for Paraparaumu Aero station, for which a decrease in the number of hot days is observed in DJF during the positive phase of ENSO (Figure 3-3).

**Figure 3-3: Hot days and ENSO phase at Paraparaumu Aero.** The stars indicate statistical significance at  $p \leq 0.05$ , and the shaded area indicates the interquartile range (25<sup>th</sup> to 75<sup>th</sup> percentile) of the corresponding composite sample.



## 3.2 SAM

### 3.2.1 VCSN

During the positive phase of the SAM, the number of hot days increases for the Wairarapa in both DJF and MAM, but decreases for the Kapiti Coast in DJF (Figure 3-4). For the negative phase of the SAM, the number of hot days decreases across the region in DJF but slightly increases for the northern Wairarapa in MAM (Figure 3-5), but the anomalies are not significant.

**Figure 3-4: Hot day anomalies during the positive phase of SAM (VCSN anomalies).** Red lines outline areas of statistical significance at  $p \leq 0.05$ .

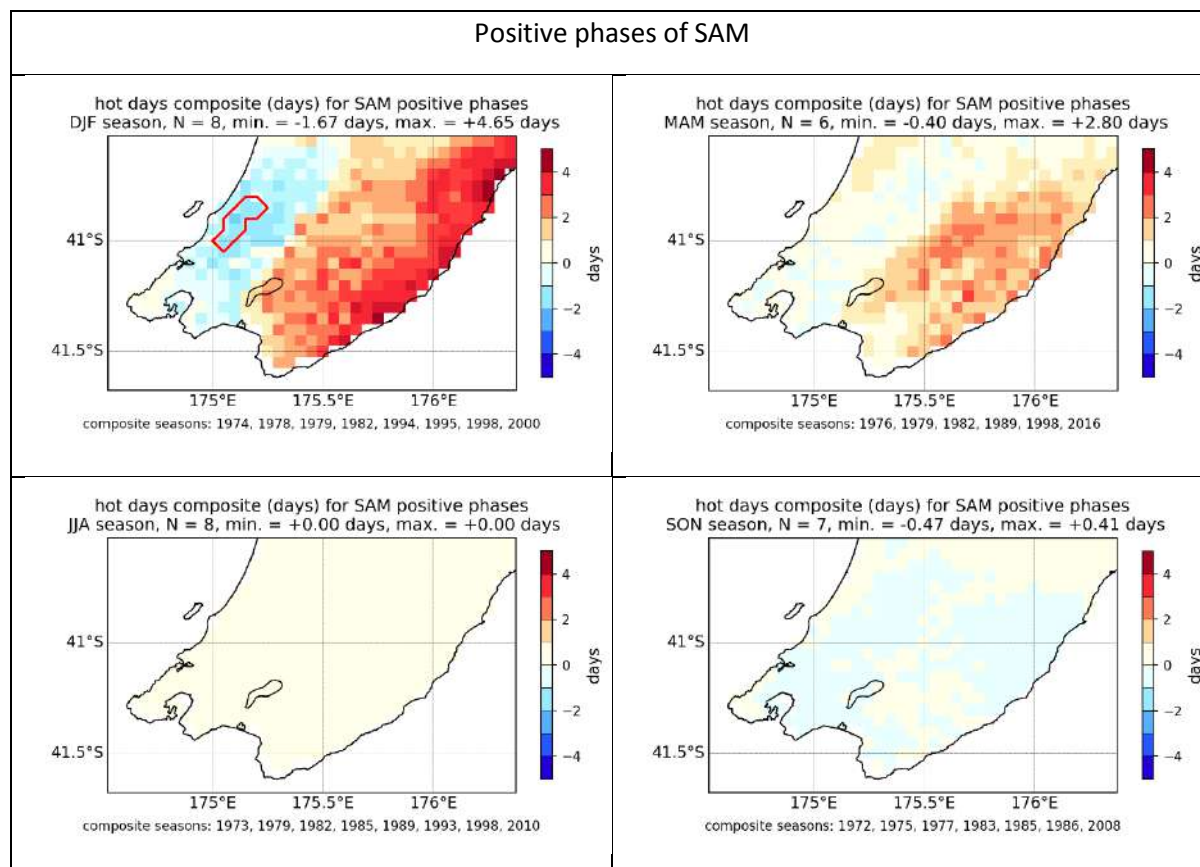
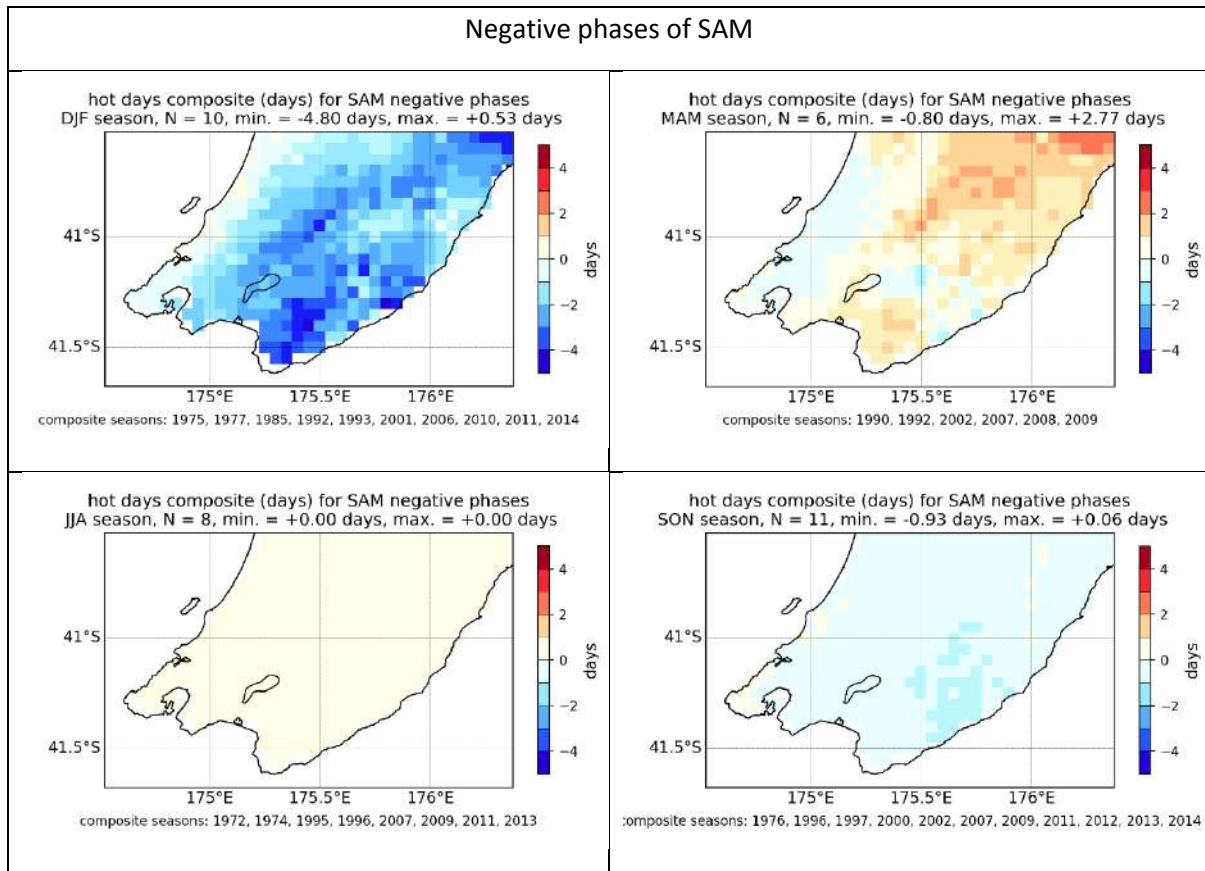


**Figure 3-5: Hot day anomalies during the negative phase of SAM (VCSN anomalies).** Red lines outline areas of statistical significance at  $p \leq 0.05$ .



### 3.2.2 Station data

There is no consistent pattern of significant relationship between hot days at stations and the SAM phase.

### 3.3 IOD

#### 3.3.1 VCSN

The VCSN composites indicate that the relationship between the number of hot days and the IOD are weak, with – to some extent – the exception of the MAM, during which a decrease in the number of hot days is observed over large parts of the Wellington Region during the negative phase (Figure 3-7) of the IOD. Note that the large hot day anomalies during DJF in both the positive and negative phases are not statistically significant and are likely the result of one year in the ensemble having extreme values and thereby pulling up the average result.

**Figure 3-6: Hot day anomalies during the positive phase of IOD (VCSN anomalies).** Red lines outline areas of statistical significance at  $p \leq 0.05$ .

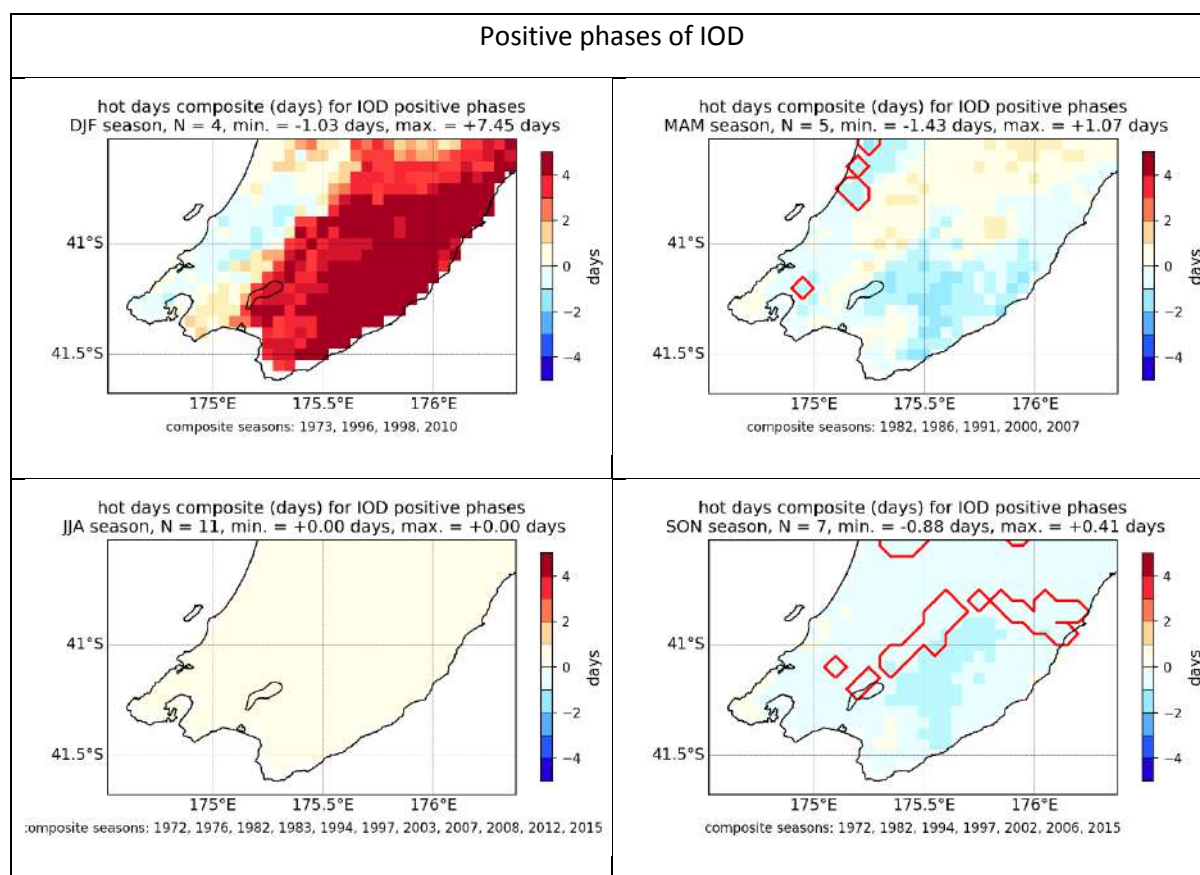
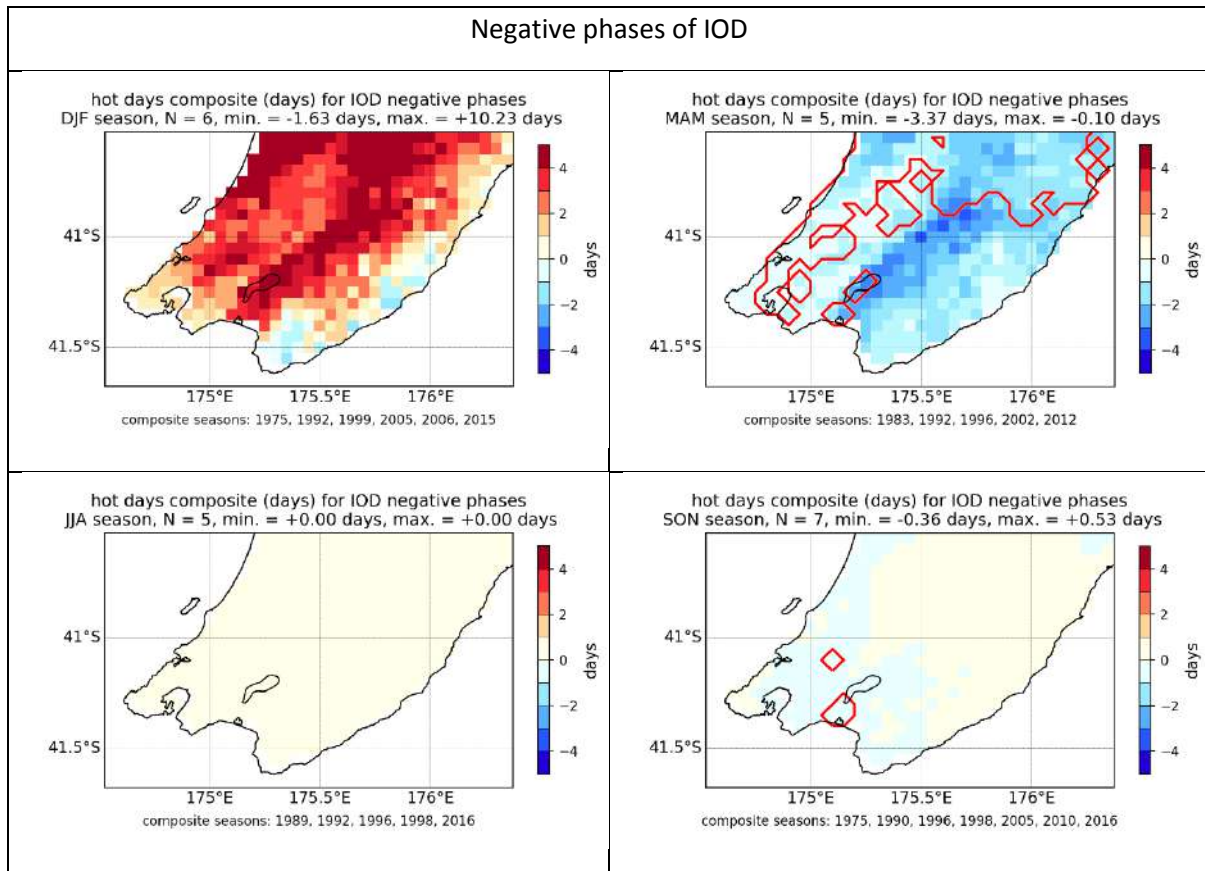


**Figure 3-7: Hot day anomalies during the negative phase of IOD (VCSN anomalies).** Red lines outline areas of statistical significance at  $p \leq 0.05$ .

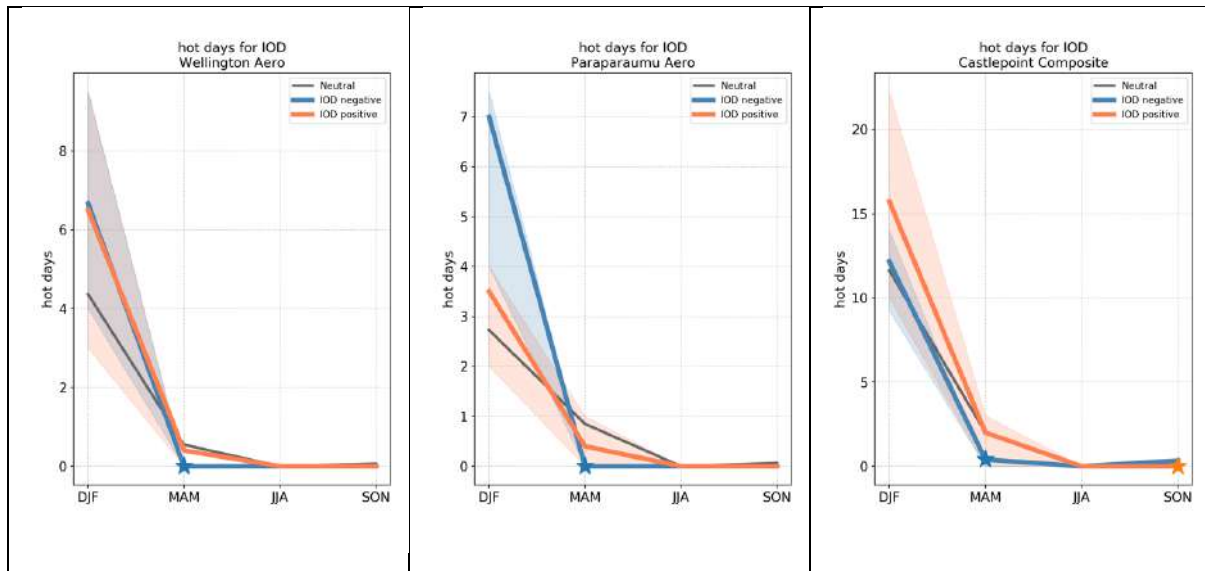




### 3.3.2 Station data

Confirming the VCSN composite anomalies significant decreases in the number of hot days are found for the following stations: Wellington Aero, Paraparaumu Aero, Castlepoint (Composite) and Kelburn, for which a decrease in the number of hot days is found in MAM during the negative phase of the IOD (Figure 3-8).

**Figure 3-8: Hot days and IOD phase at Wellington Aero, Paraparaumu Aero, and Castlepoint (composite).** The stars indicate statistical significance at  $p \leq 0.05$ , and the shaded area indicates the interquartile range (25<sup>th</sup> to 75<sup>th</sup> percentile) of the corresponding composite sample.



### 3.4 SPSP

#### 3.4.1 VCSN

The strongest relationships are found in DJF and to a lesser extent in SON and MAM: during the negative phase of the SPSP, the number of hot days tends to decrease over a large part of the Wellington Region (Figure 3-10). During the positive phase (Figure 3-9), some weak (but statistically significant) decrease in the number of hot days is observed in the western and southern areas of the Wellington Region in MAM. Note that this pattern is broadly consistent with the composite mean maximum temperature anomalies presented above (Figure 1-10 and Figure 1-11).

**Figure 3-9: Hot day anomalies during the positive phase of SPSP (VCSN anomalies).** Red lines outline areas of statistical significance at  $p \leq 0.05$ .

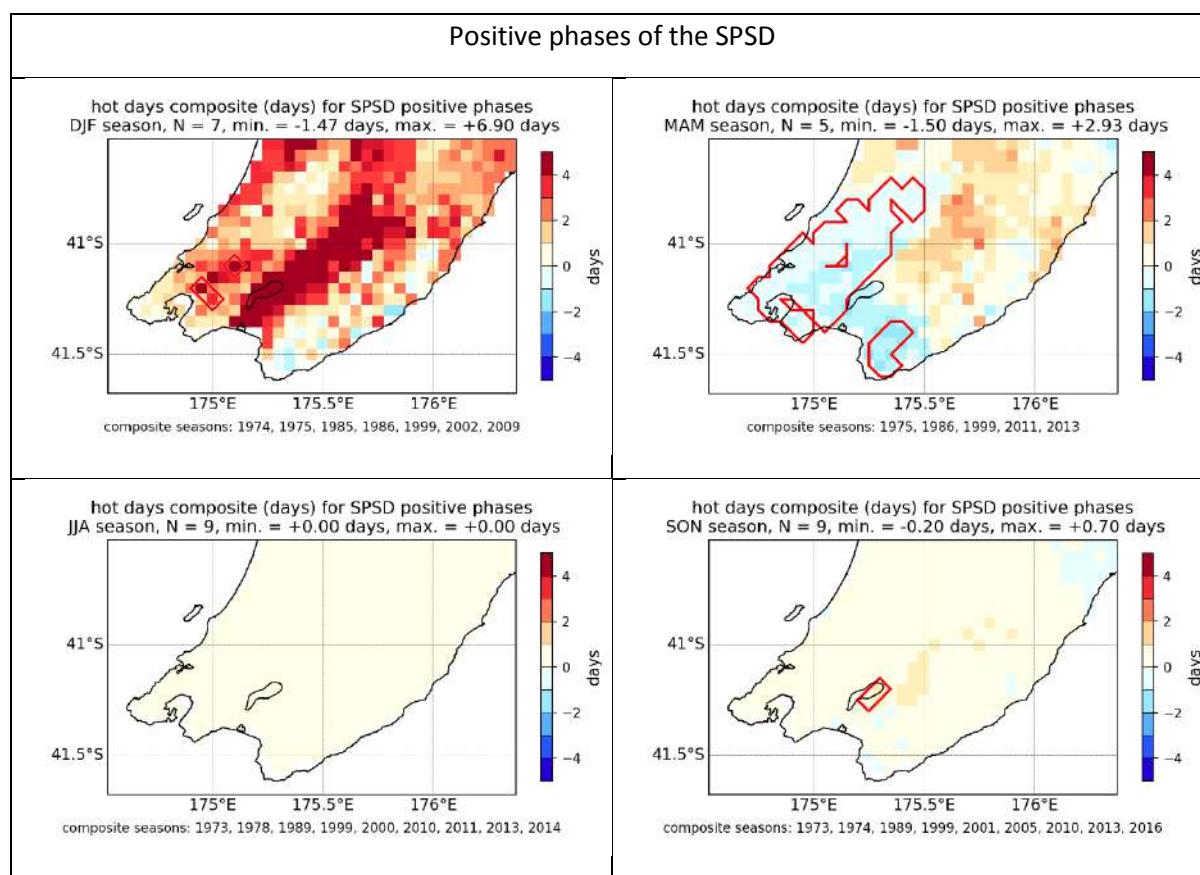
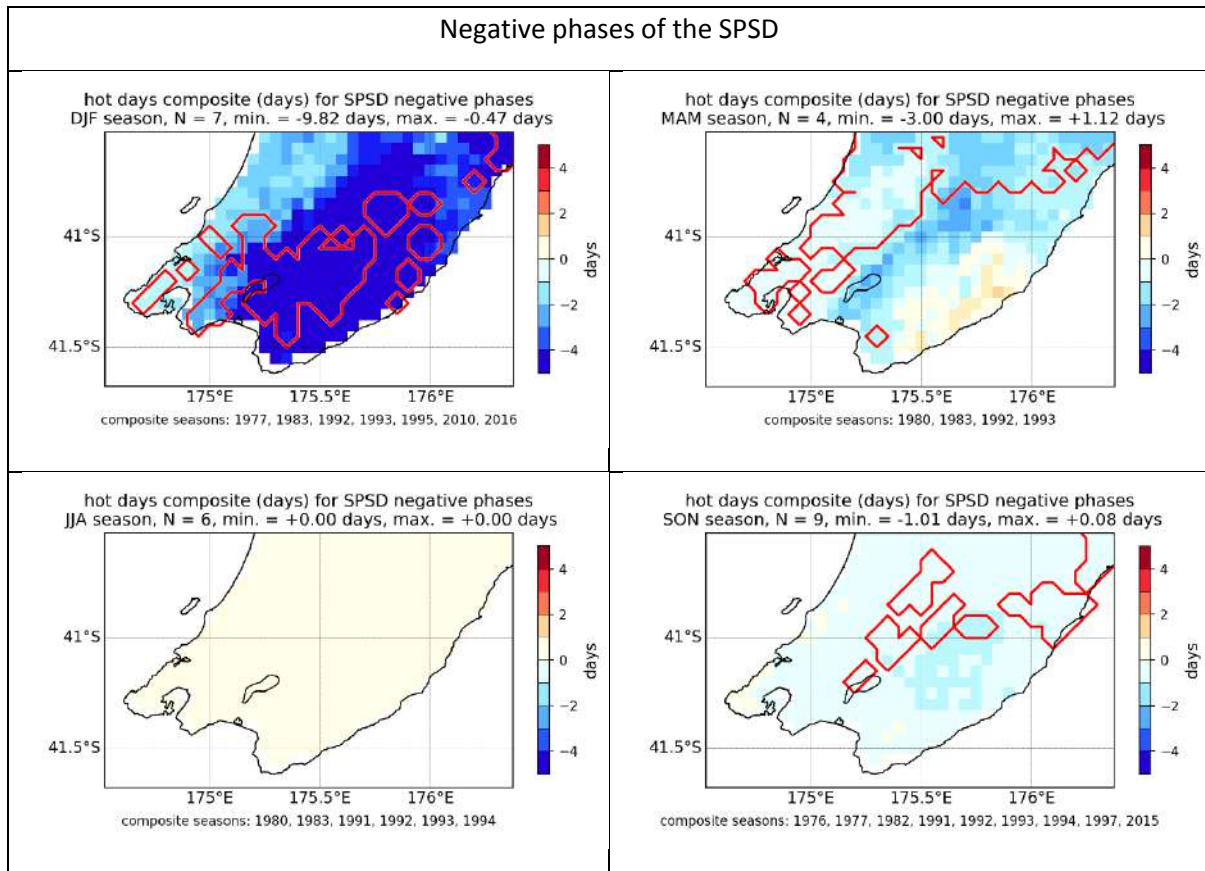


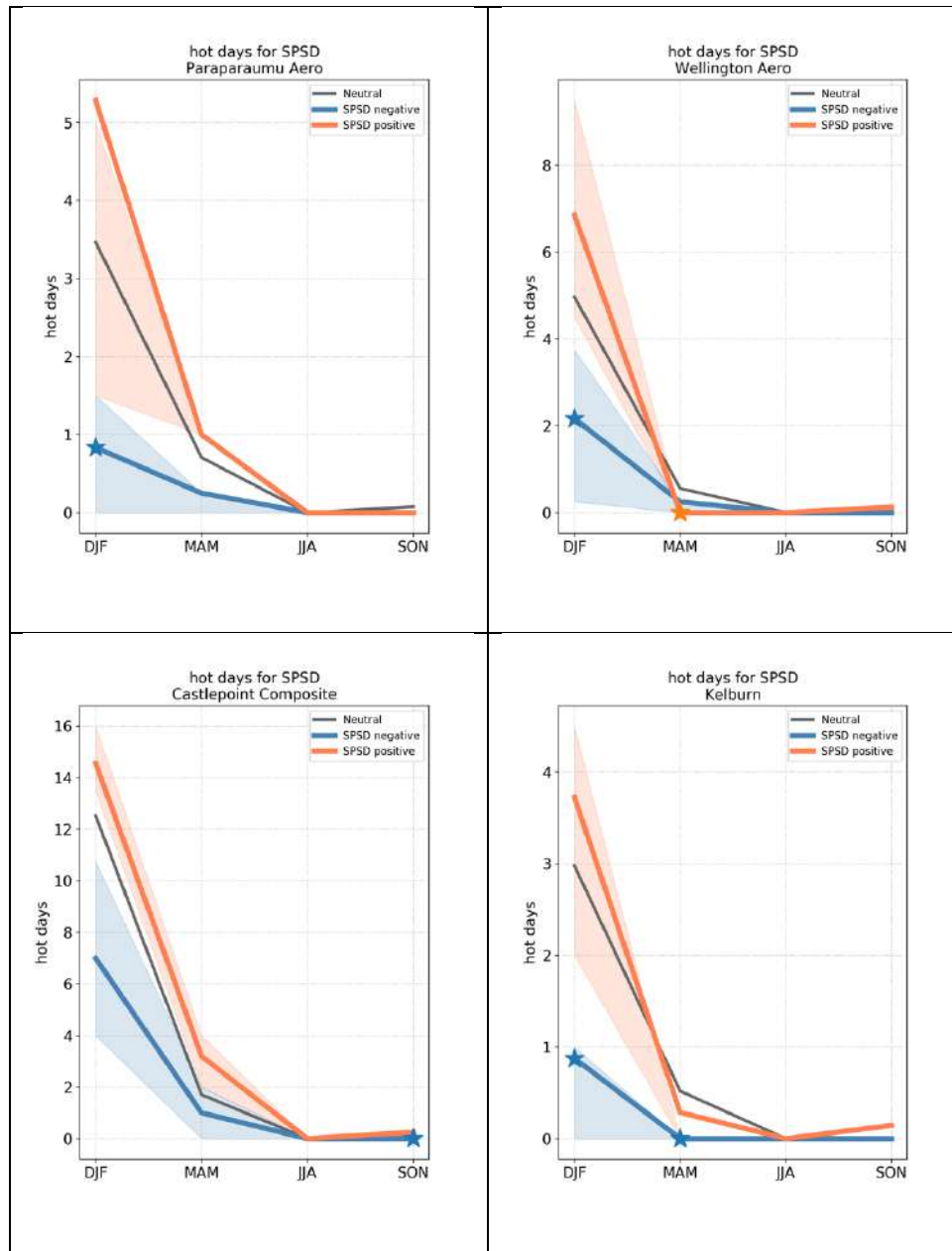
**Figure 3-10: Hot day anomalies during the negative phase of SPSD (VCSN anomalies).** Red lines outline areas of statistical significance at  $p \leq 0.05$ .



### 3.4.2 Station data

Station-based composite anomalies are consistent with the VCSN composites, as illustrated for the Paraparaumu Aero, Wellington Aero, Castelpoint (Composite) and Kelburn stations: in DJF notably, the number of hot days tends to be lower for the negative phase of the SPSP (Figure 3-11).

**Figure 3-11: Hot days and SPSP phase at Paraparaumu Aero, Wellington Aero, Castlepoint (composite) and Kelburn.** The stars indicate statistical significance at  $p \leq 0.05$ , and the shaded area indicates the interquartile range (25<sup>th</sup> to 75<sup>th</sup> percentile) of the corresponding composite sample.



## 4 Frost days

Frost day anomalies derived from the VCSN are presented in the departure from normal in days (1981-2010 climatology). A frost day is counted when the minimum daily temperature falls below 0°C.

### 4.1 ENSO

#### 4.1.1 VCSN

The VCSN composites show a relative increase in the number of frost days in JJA during the positive phase of ENSO, notably over the ranges and the Wairarapa (Figure 4-1), and a slight decrease during the negative phase (Figure 4-2), however the relationship is not perfectly symmetric, and the anomalies do not reach statistical significance.

**Figure 4-1: Frost day anomalies during the positive phase of ENSO (VCSN anomalies).** Red lines outline areas of statistical significance at  $p \leq 0.05$ .

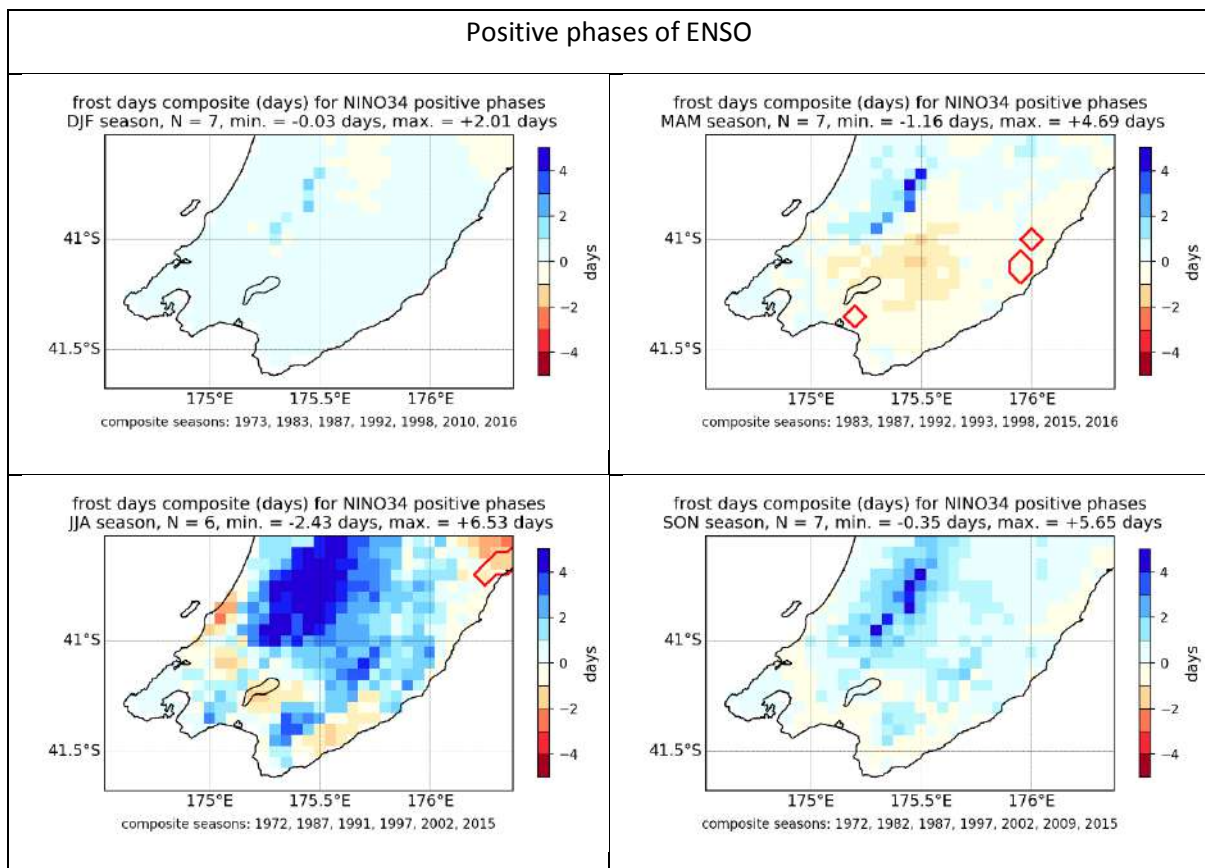
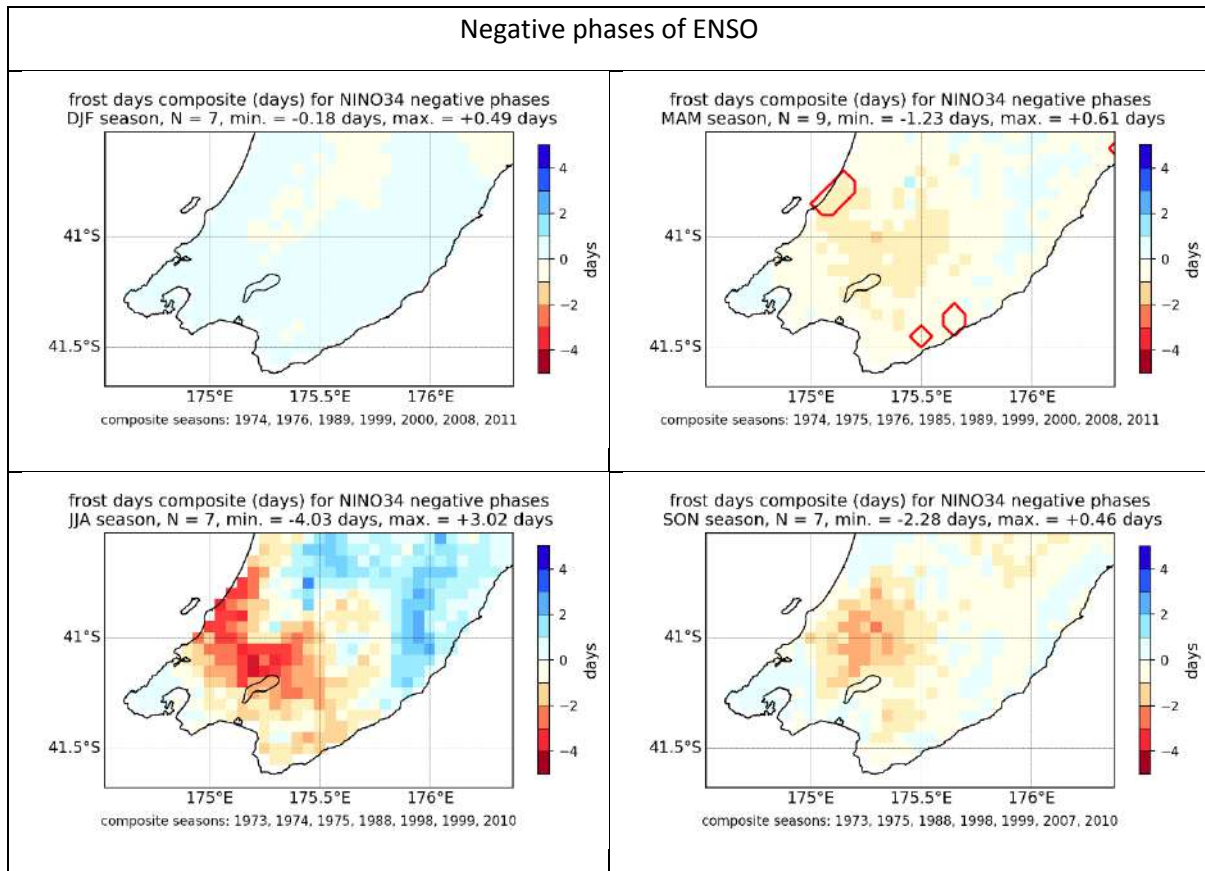


**Figure 4-2: Frost day anomalies during the negative phase of ENSO (VCSN anomalies).** Red lines outline areas of statistical significance at  $p \leq 0.05$ .



#### 4.1.2 Station data

No significant relationships are found between station-based frost days and ENSO, confirming the weak and non-significant anomalies derived from the VCSN.

## 4.2 SAM

### 4.2.1 VCSN

The VCSN composite anomalies for the number of frost days indicate that the positive phase of the SAM (Figure 4-3) tends to be associated with a decrease in the number of frost days during MAM, notably over the centre of the Wellington Region. The reverse (increase in frost days) is observed during SON in the negative phases of the SAM (Figure 4-4).

**Figure 4-3: Frost day anomalies during the positive phase of SAM (VCSN anomalies).** Red lines outline areas of statistical significance at  $p \leq 0.05$ .

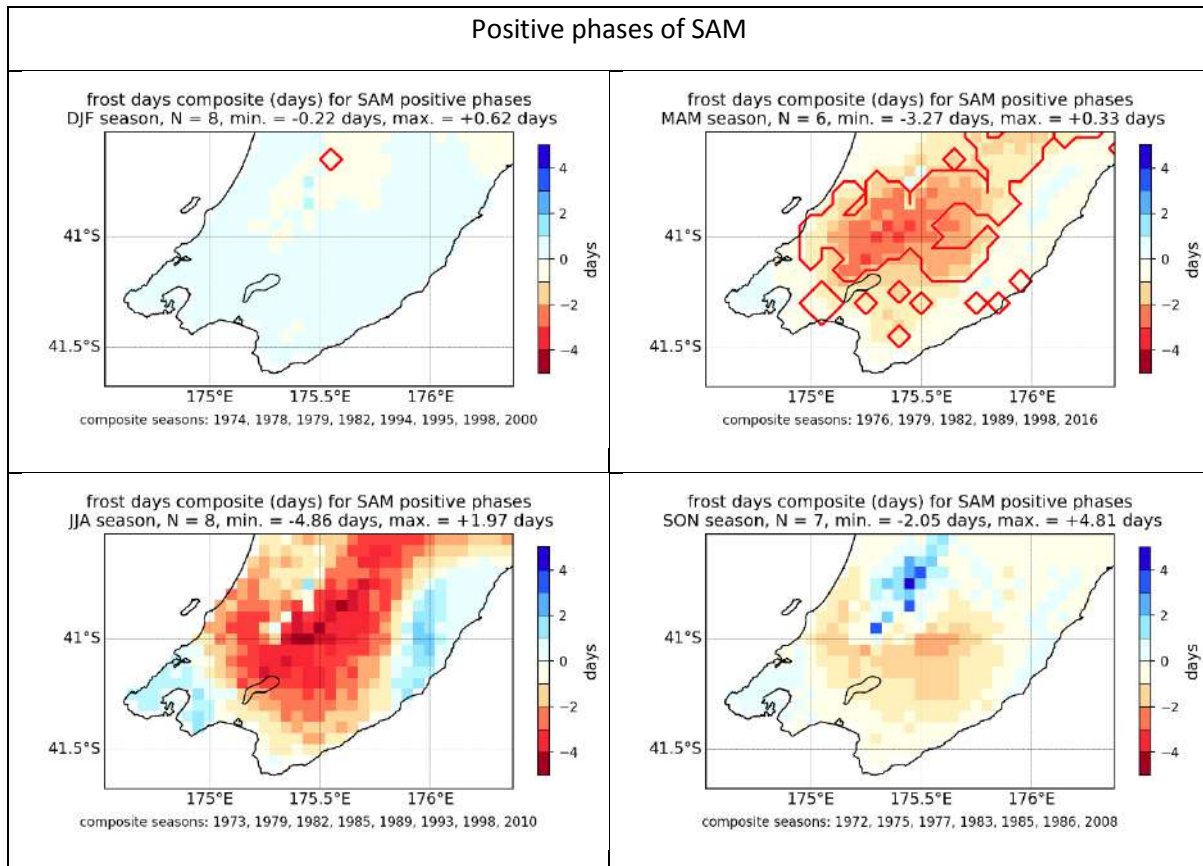
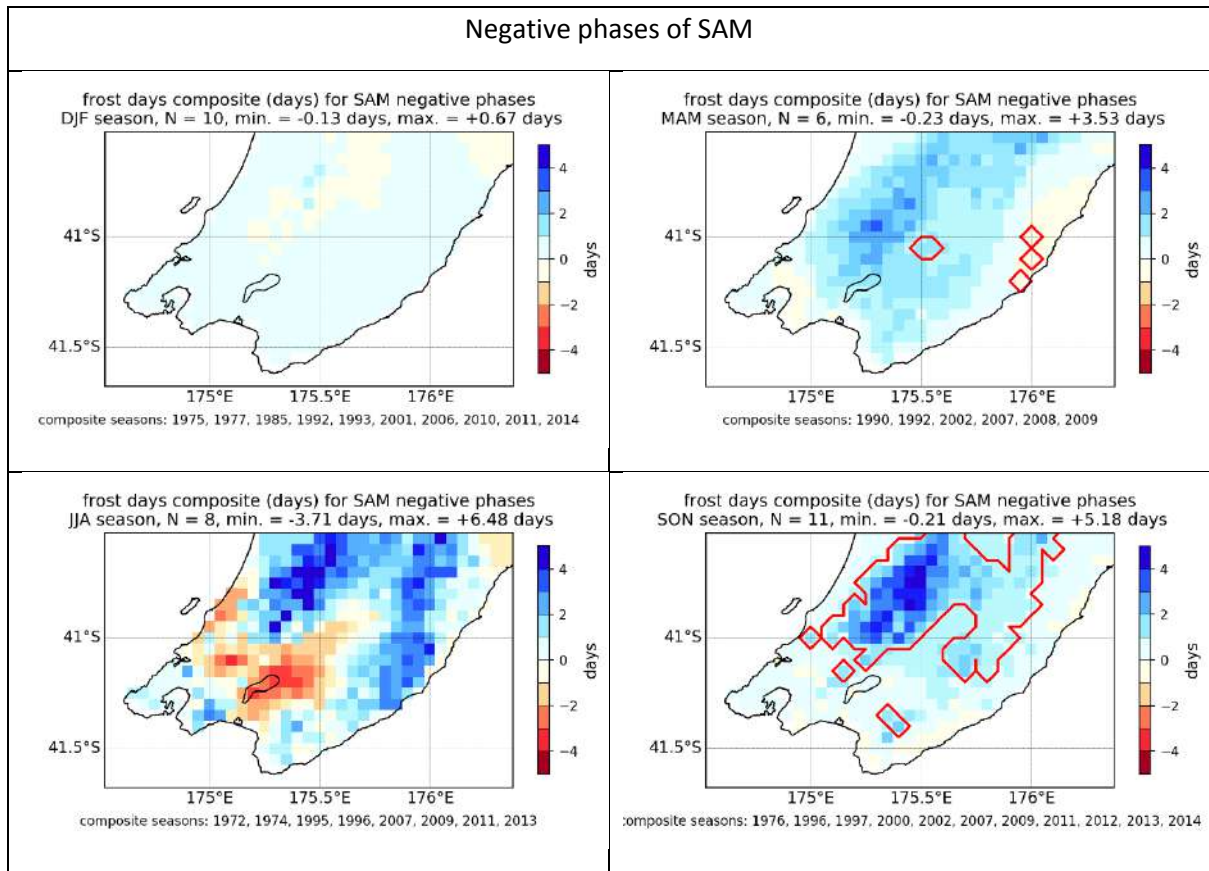


**Figure 4-4: Frost day anomalies during the negative phase of SAM (VCSN anomalies).** Red lines outline areas of statistical significance at  $p \leq 0.05$ .

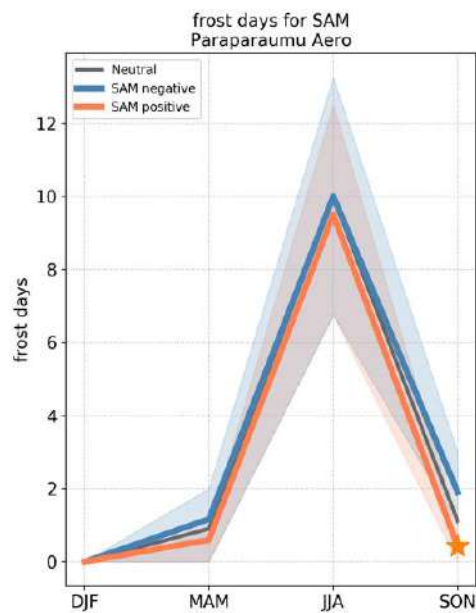




#### 4.2.2 Station data

The only station showing statistically significant anomalies is Paraparaumu Aero, where (consistent with sign of the anomalies shown in the VCSN), a decrease in the number of frost days is observed during the positive phase of the SAM in SON (Figure 4-5).

**Figure 4-5: Frost days and SAM phase at Paraparaumu Aero.** The stars indicate statistical significance at  $p \leq 0.05$ , and the shaded area indicates the interquartile range (25<sup>th</sup> to 75<sup>th</sup> percentile) of the corresponding composite sample.



## 4.3 IOD

### 4.3.1 VCSN

The VCSN composites show a slight increase in the number of frost days during the JJA season during the positive phases of the IOD (Figure 4-6), and decreases in the number of frost days during MAM during the positive phases of the IOD and SON during the negative phases (Figure 4-7).

**Figure 4-6: Frost day anomalies during the positive phase of IOD (VCSN anomalies).** Red lines outline areas of statistical significance at  $p \leq 0.05$ .

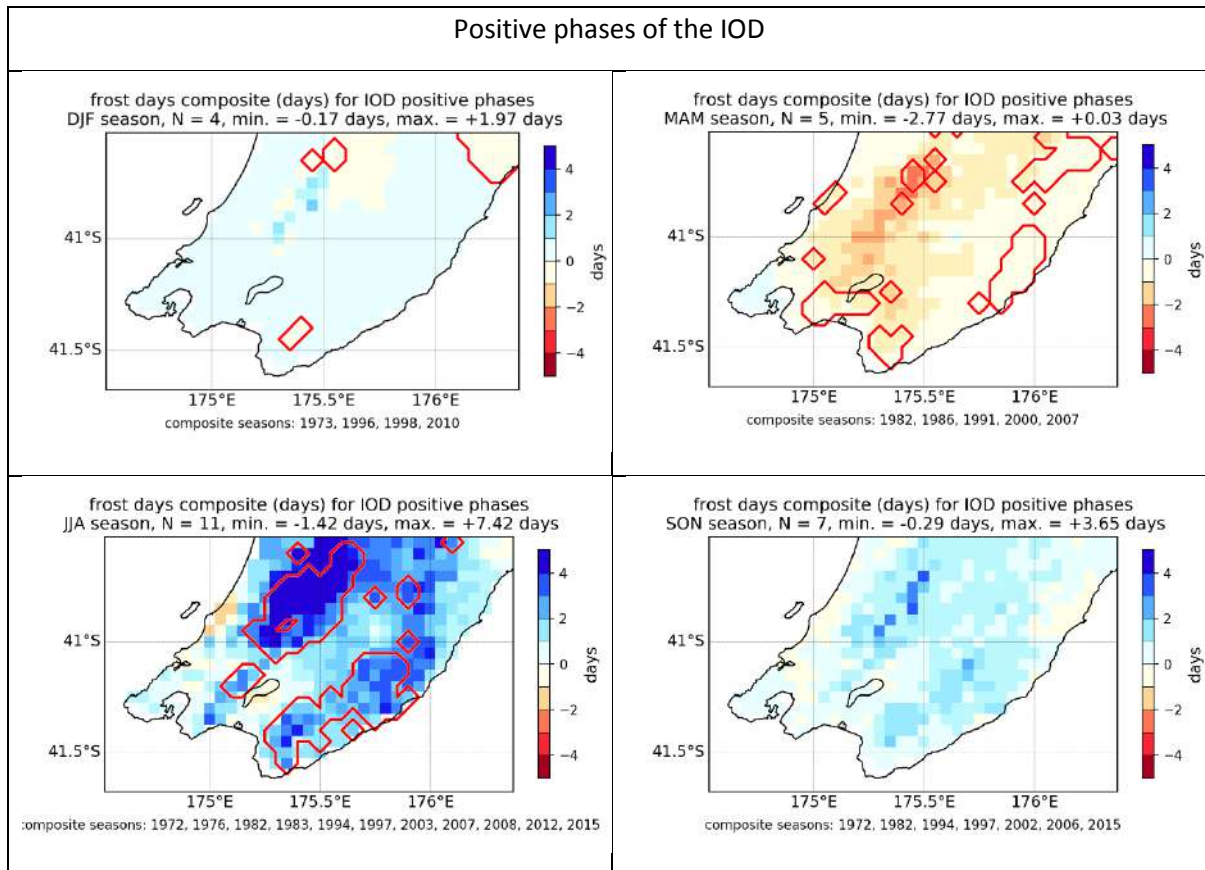
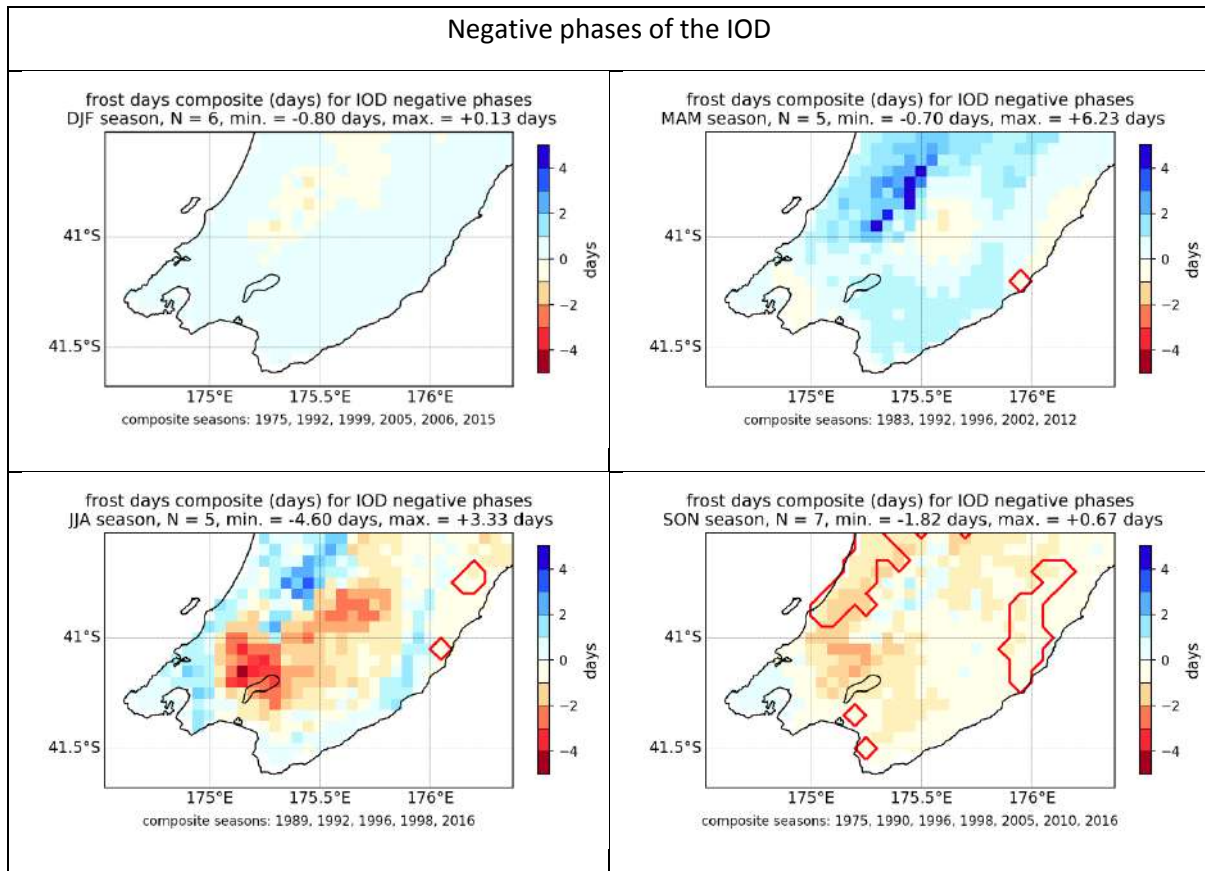


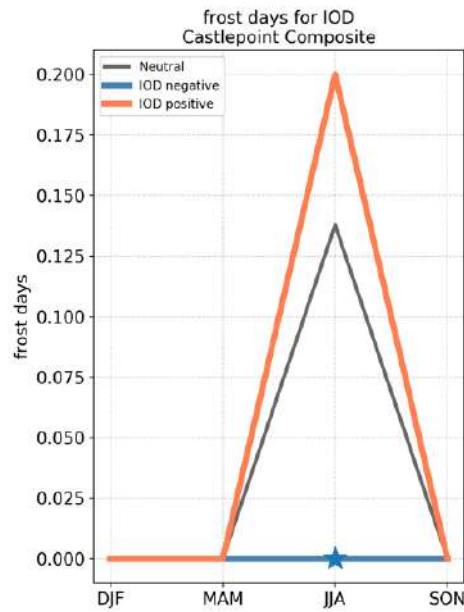
**Figure 4-7: Frost day anomalies during the negative phase of IOD (VCSN anomalies).** Red lines outline areas of statistical significance at  $p \leq 0.05$ .



### 4.3.2 Station data

The only statistically significant anomaly is found for the Castlepoint (Composite) station, for which the number of frost days falls to 0 during the negative phase of the IOD in JJA, but this is to be compared to a very modest average (~0.13 days during the neutral phase of the IOD) (Figure 4-8).

**Figure 4-8: Frost days and IOD phase at Castlepoint (composite).** The stars indicate statistical significance at  $p \leq 0.05$ , and the shaded area indicates the interquartile range (25<sup>th</sup> to 75<sup>th</sup> percentile) of the corresponding composite sample.



## 4.4 SPSD

### 4.4.1 VCSN

The VCSN composites show that during the positive phase of the SPSD and during MAM and SON, the number of frost days tend to decrease in parts of the region (Figure 4-9). However, the anomalies are generally not statistically significant during the negative phase of the SPSD (Figure 4-10).

**Figure 4-9: Frost day anomalies during the positive phase of SPSD (VCSN anomalies).** Red lines outline areas of statistical significance at  $p \leq 0.05$ .

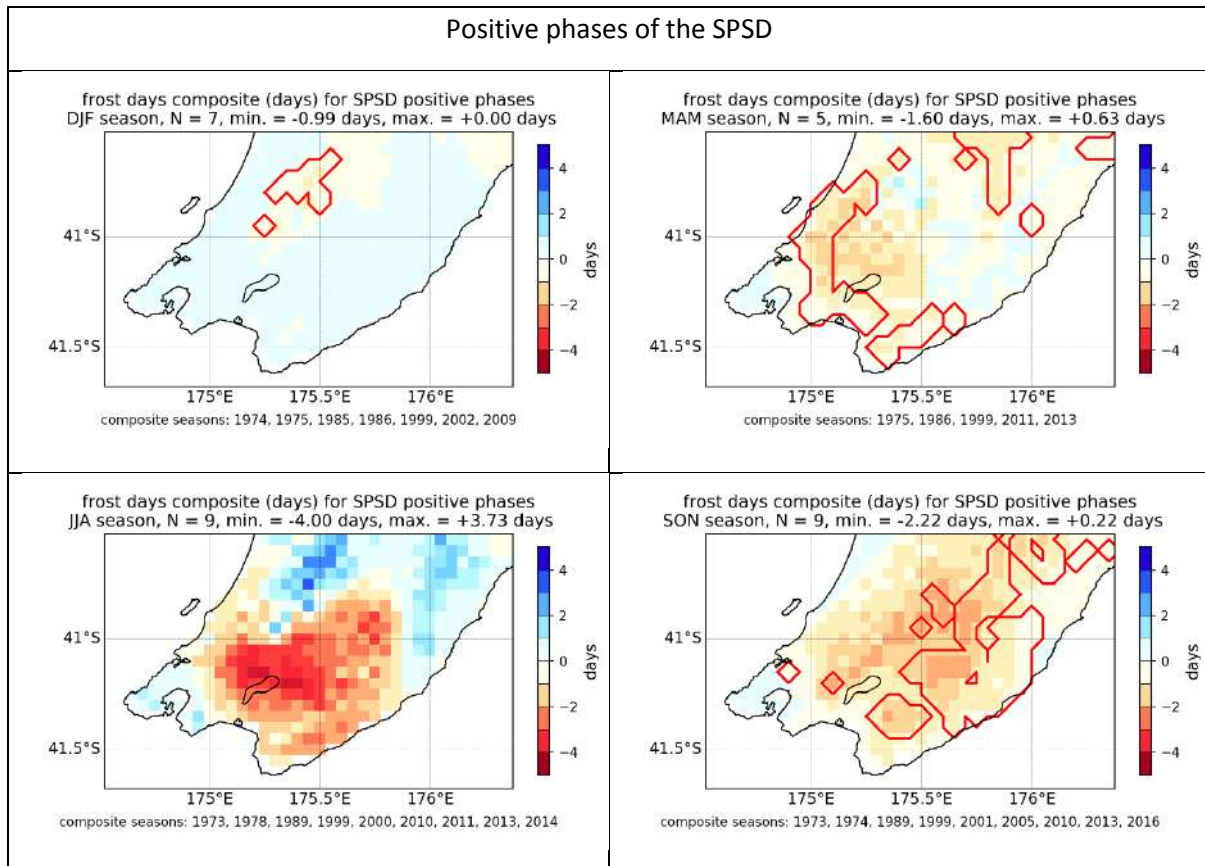
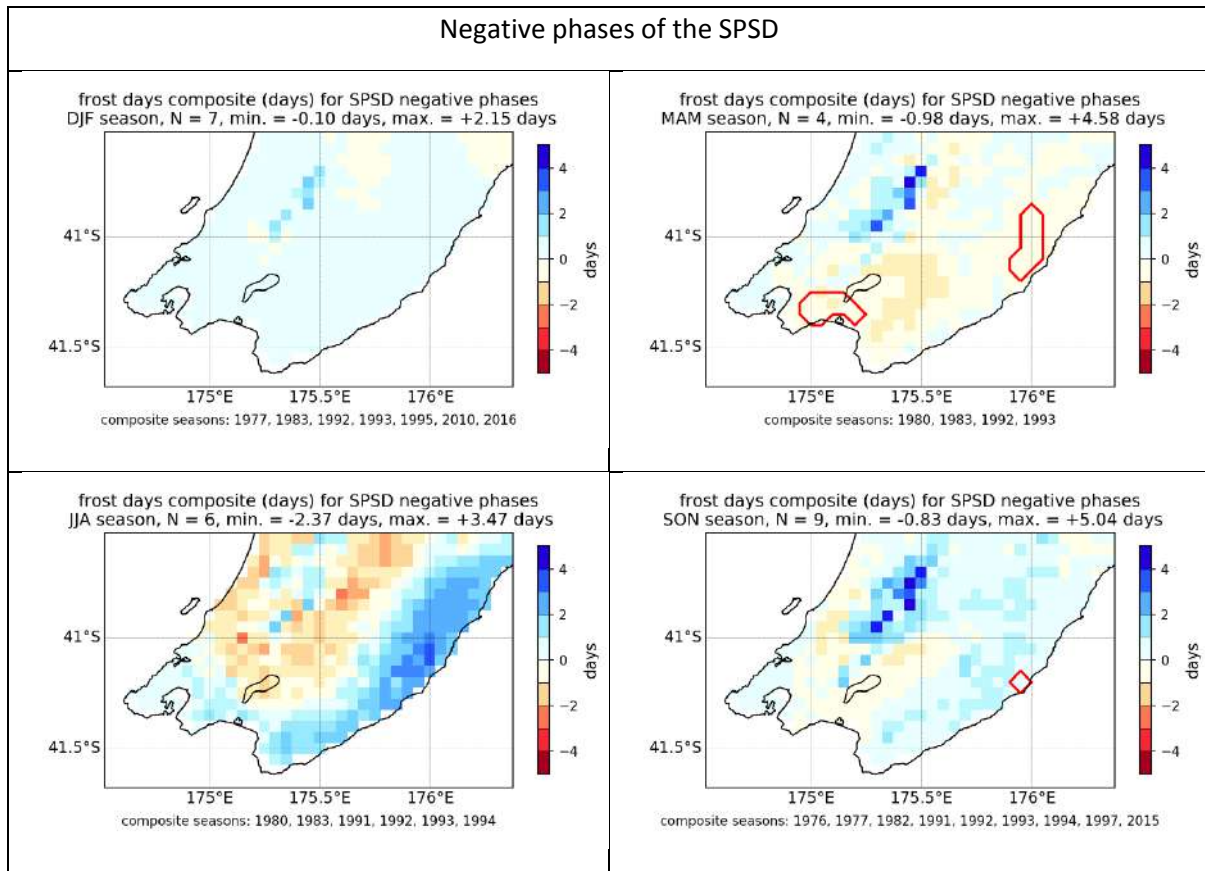


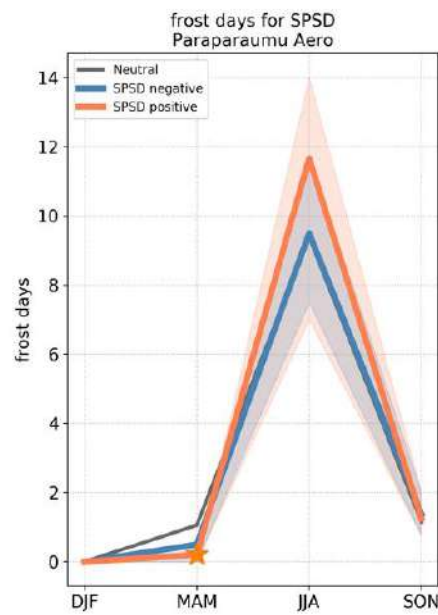
**Figure 4-10: Frost day anomalies during the negative phase of SPSP (VCSN anomalies).** Red lines outline areas of statistical significance at  $p \leq 0.05$ .



#### 4.4.2 Station data

The only statistically significant relationship is found for Paraparaumu Aero for which a slight decrease in the number of frost days is observed in MAM during the positive phase of the SPSD (Figure 4-11).

**Figure 4-11: Frost days and SPSD phase at Paraparaumu Aero.** The stars indicate statistical significance at  $p \leq 0.05$ , and the shaded area indicates the interquartile range (25<sup>th</sup> to 75<sup>th</sup> percentile) of the corresponding composite sample.



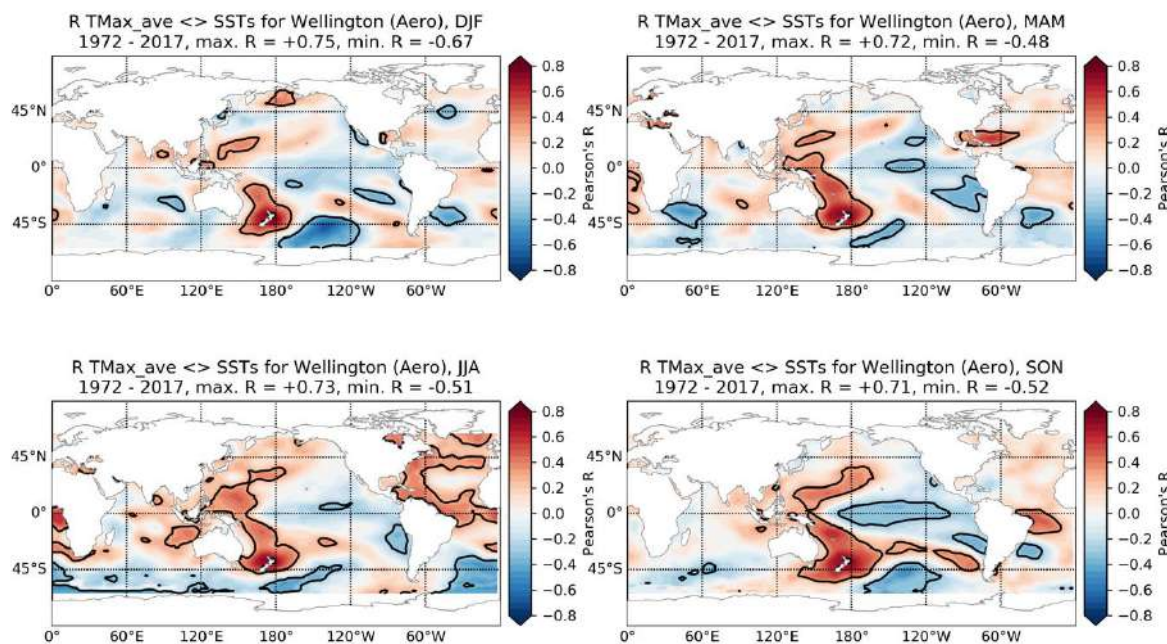
## 5 Relationship to Sea Surface Temperature (SST) anomalies

Similar to the analyses conducted for the rainfall parameters, time-series of seasonally aggregated temperature variables (mean maximum and minimum temperatures, number of hot days and number of frost days) are correlated to the global SST field (detrended seasonal SST anomalies from the ERSSTv5 dataset). Only a selection of figures is presented below, with the remaining ones being available in the electronic supplement to this report.

In general, and as expected, the strongest correlations between temperature parameters in the Wellington Region and SSTs are found with regional SSTs: i.e. sea surface temperatures around New Zealand are an important driver of surface air temperatures in the region, with warmer than normal ocean waters around the country being related to an increase in both minimum and maximum temperatures, an increase in the number of hot days and a decrease in the number of frost days. The strong correlations indicate that this relationship is to a large extent symmetric and linear: cooler than normal regional SSTs are related to colder surface air temperature anomalies.

This is illustrated in Figure 5-1, which presents the correlation field between seasonal maximum temperature at Wellington Aero and SSTs. This correlation is very strongly positive with SSTs around New Zealand, extending in the Tasman Sea and towards the Coral Sea. Of interest, strong negative correlations are found (see e.g. a good example in DJF) with a large area in the mid-latitudes of the central South Pacific (between 170 and 120°W). The resulting 'dipole' pattern is reminiscent of the signature of the South Pacific Subtropical Dipole mode, indirectly confirming that this configuration of SST anomalies seem to constitute a relatively coherent mode of inter-annual variability, and the mostly symmetric patterns displayed (in the sections above) by e.g. the VCSN mean maximum or minimum temperature anomalies associated with the extreme phases of the SPSPD.

**Figure 5-1: Correlation field between mean maximum temperature at Wellington Aero and seasonal SST anomalies.** The black lines highlight the areas of statistical significance at  $p \leq 0.05$ .

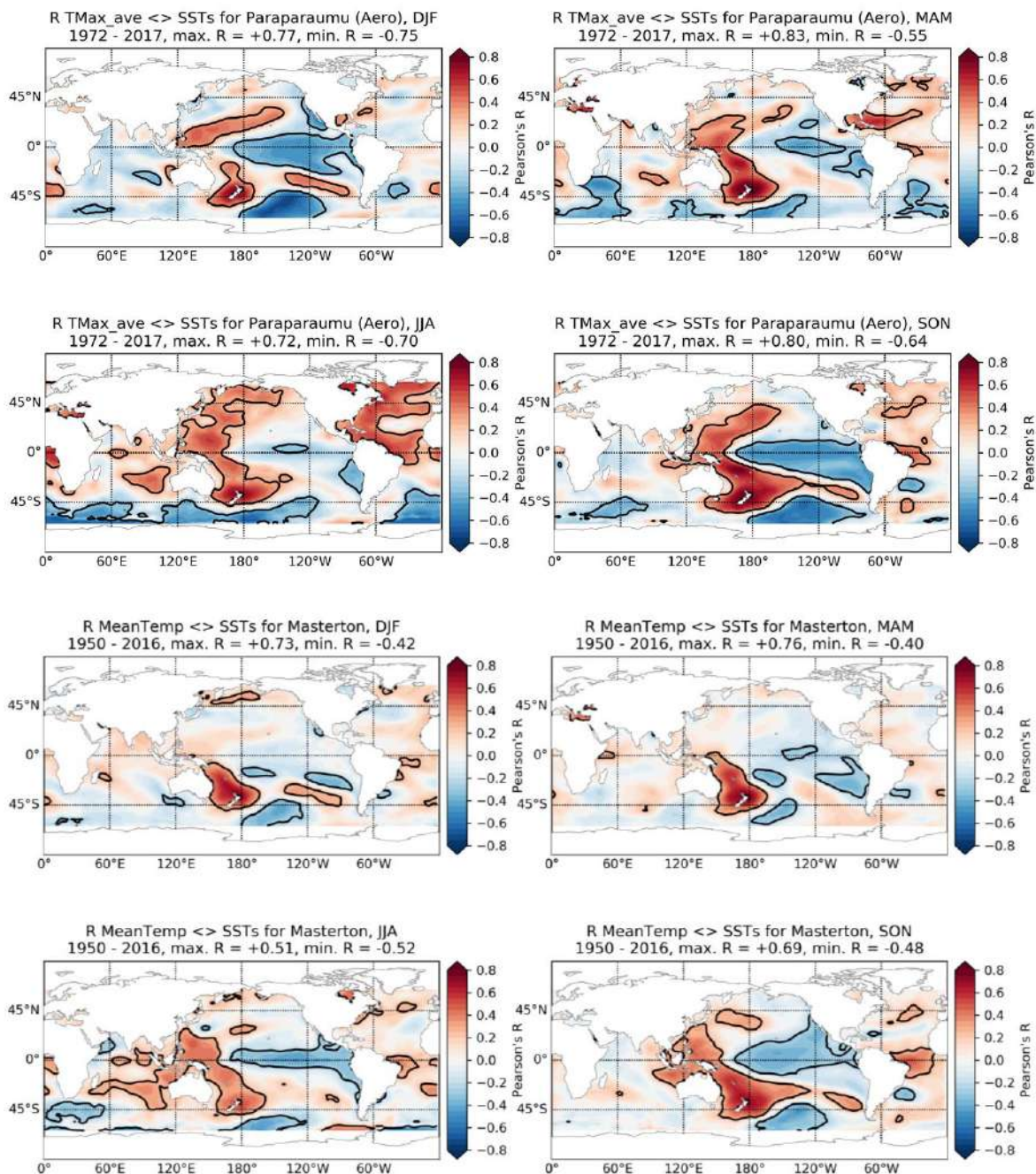


Of interest as well is that generally, the correlations with the central and eastern Pacific are relatively weak, in keeping with an ENSO signal over the Wellington Region which seems to a large



extent non-linear. The only stations which display strong and extent correlations with SSTs in the central and eastern Pacific are Paraparaumu Aero and Masterton (Figure 5-2). In broad accordance with the station level composite anomalies, the correlations are negative: i.e. the positive phase of ENSO (El Niño) tends to be associated with lower mean maximum temperatures, with the reverse being observed during La Niña.

**Figure 5-2: Correlation field between respectively mean maximum temperature at Paraparaumu Aero (top) and mean temperature at Masterton (bottom) and seasonal SST anomalies. The black lines highlight the areas of statistical significance at  $p \leq 0.05$ .**



# Regional climate mode impacts on the Wellington Region

*Part D: Relationship between climate modes and wind*

## Contents

<b>1</b>	<b>Mean Wind .....</b>	<b>132</b>
1.1	ENSO .....	132
1.2	SAM .....	135
1.3	IOD.....	138
1.4	SPSD.....	141
<b>2</b>	<b>Days with wind gusts over 63 km/h and 96 km/h .....</b>	<b>144</b>
2.1	ENSO .....	144
2.2	SAM .....	145
2.3	IOD.....	145
2.4	SPSD.....	146
<b>3</b>	<b>Relationship to Sea Surface Temperature (SST) anomalies .....</b>	<b>147</b>

This is Part D of the 'Regional climate mode impacts on the Wellington Region' report. Refer to Part A: Introduction, Methodology and Background for a thorough introduction to this study.

In this section, the relationships between seasonally (DJF, MAM, JJA, SON) aggregated wind parameters (mean wind speed and number of days with gusts over 63 and 96 km/h) and the inter-annual climate modes (El Niño Southern Oscillation (ENSO), Southern Annular Mode (SAM), Indian Ocean Dipole (IOD) and South Pacific Subtropical Dipole (SPSD)) are presented, first using the Virtual Climate Station Network (VCSN) by means of composite analyses, then using the available station data. Gust data is not available for the VCSN so only station data is used for those analyses.

For the VCSN, composite anomalies are calculated for the extreme phases of each mode: i.e. when standardized seasonal values exceed + 1 standard deviation (referred to as the positive phase of the mode) and are below -1 standard deviation (negative phase of the mode). For consistency, the 1981-2010 climatological normal is used for both the VCSN dataset (to define the 'normal' mean wind speed) and for the climate mode index (to define the mean and standard deviation for the seasonally stratified standardisation).

For the station data, the composite anomalies are expressed in the original unit (e.g. km/h for mean wind speed, days for the number of days with certain wind gusts), and shown for each season and for each phase of the mode (positive, negative, neutral) and displayed as a line plot. This representation thus gives a summary of the distribution of the values included in the three samples, and illustrates the variability in the corresponding rainfall parameter observed during each phase of the mode. For the sake of brevity, we only present the line plots for some of the stations displaying a significant ( $p \leq 0.05$  according to a Student t-test) association for the mode during at least one season. The figures not included are available as supplementary electronic material to this report.

# 1 Mean Wind

Mean wind anomalies (km/h) are presented for the extreme phases of ENSO, bearing in mind that the period available (1998-2017) is extremely short, and therefore the composite samples only include a few events (2 to 3 for each season and phase). The results presented below are therefore only indicative and should be interpreted with caution.

## 1.1 ENSO

### 1.1.1 VCSN

The VCSN composites suggest that mean wind speed tends to increase over the eastern half of the Wellington region during the positive phases of ENSO, notably during MAM and JJA (Figure 1-1). During the negative phases of ENSO, the anomalies tend to be negative (albeit non-significant) over the same area (Figure 1-2).

**Figure 1-1: Mean wind speed anomalies during the positive phase (El Niño) of ENSO (VCSN anomalies).** Red lines outline areas of statistical significance at  $p \leq 0.05$ .

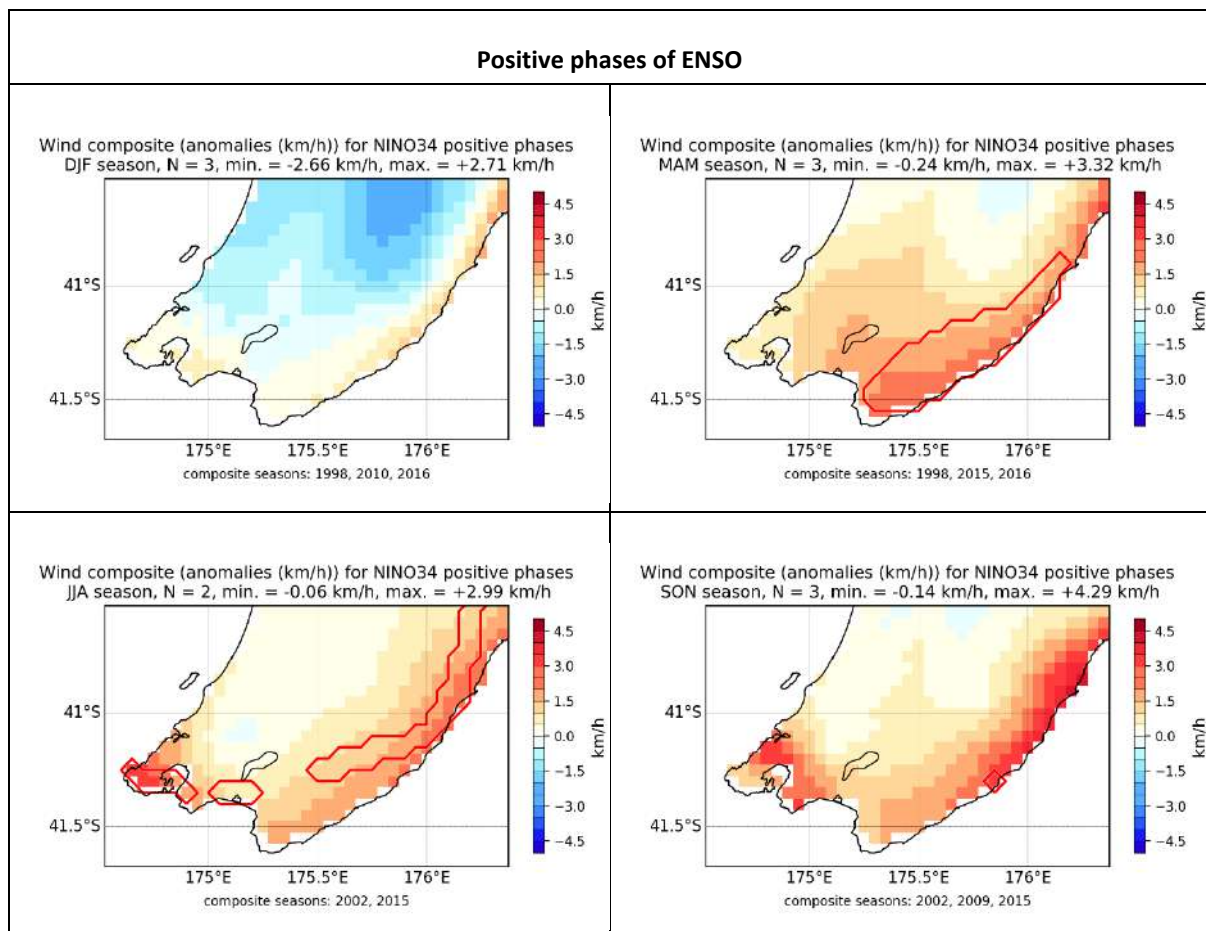
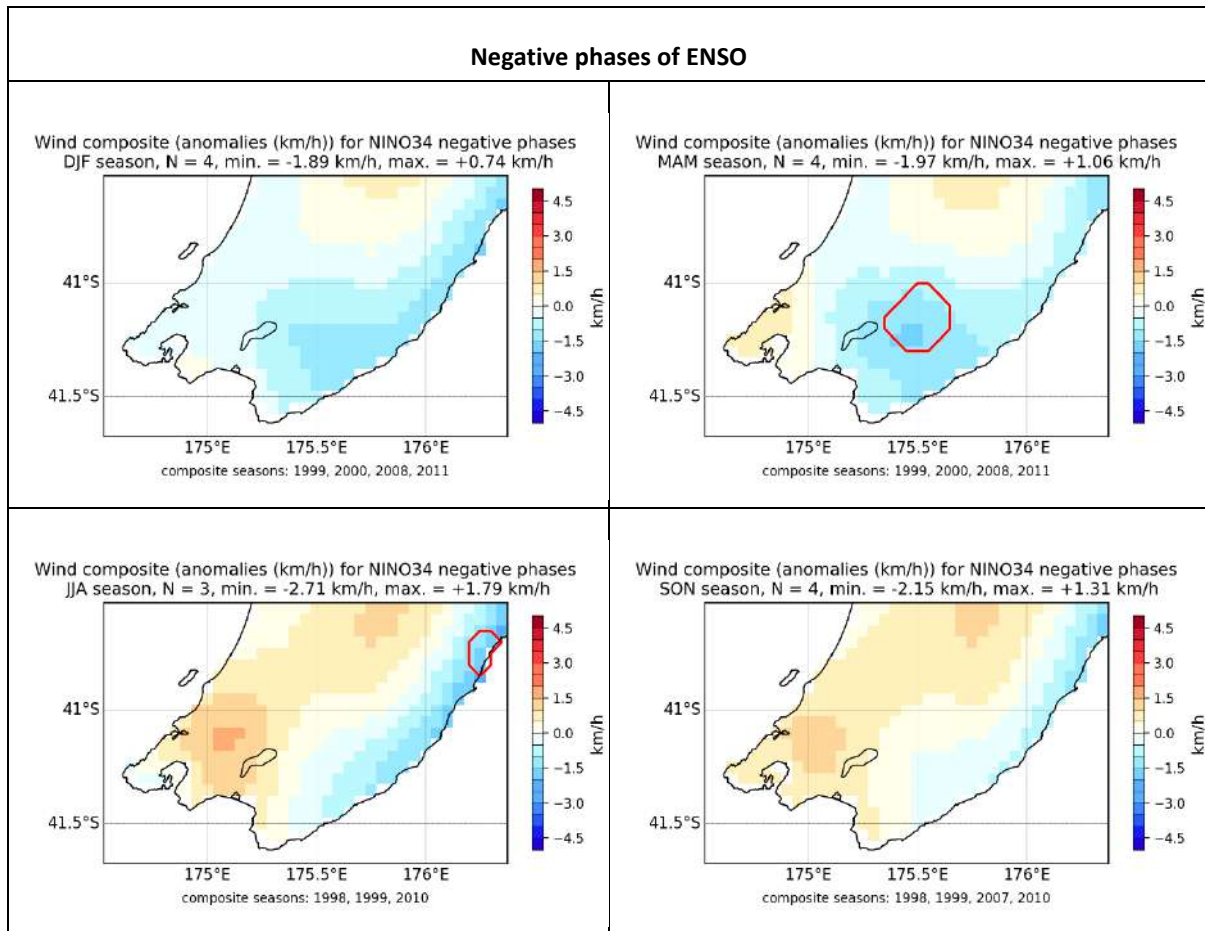


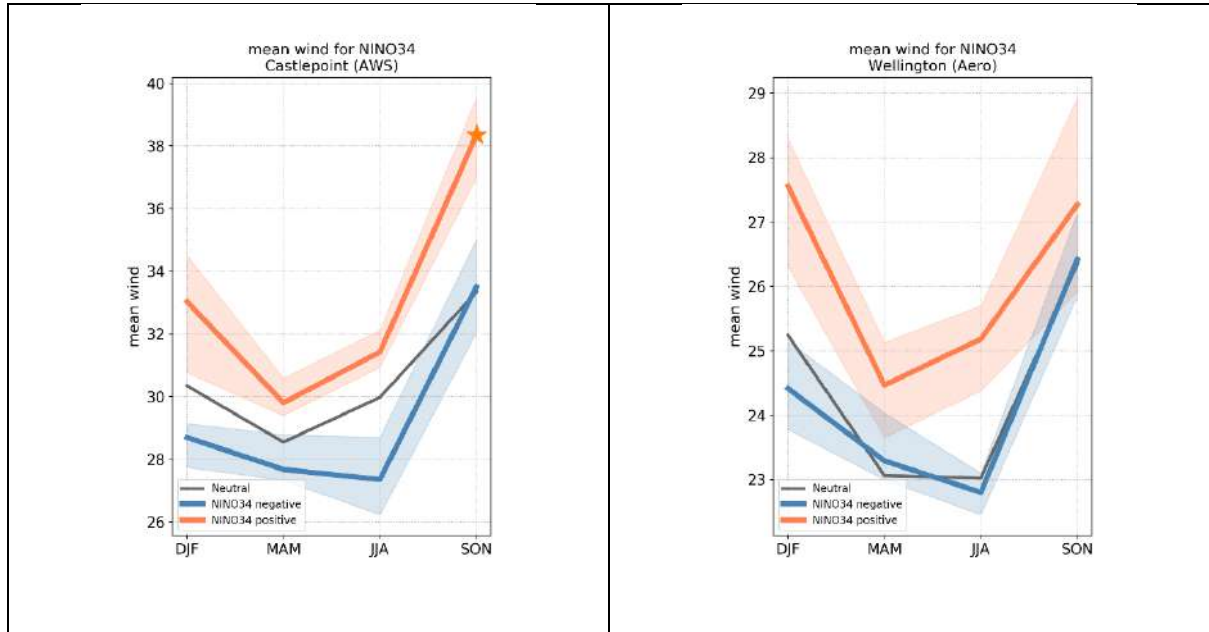
**Figure 1-2: Mean wind anomalies during the negative phase (La Niña) of ENSO (VCSN anomalies).** Red lines outline areas of statistical significance at  $p \leq 0.05$ .



### 1.1.2 Station data

The station level data tends to broadly confirm the patterns indicated by the VCSN composites. For example, at Castlepoint AWS and Wellington Aero stations, the mean wind speed tends to increase during the positive phases of ENSO, and decrease during the negative phases (Figure 1-3).

**Figure 1-3: Mean wind speed and ENSO phase at Castlepoint AWS and Wellington Aero.** The stars indicate statistical significance at  $p \leq 0.05$ , and the shaded area indicates the interquartile range (25<sup>th</sup> to 75<sup>th</sup> percentile) of the corresponding composite sample.



## 1.2 SAM

### 1.2.1 VCSN

Again with the strong caveat of a very short period available and very small sample sizes, the VCSN mean wind speed composite anomalies for the extreme phases of the SAM tend to indicate an increase in wind speed over the eastern seaboard of the Wellington Region in MAM during the positive phases of the SAM (Figure 1-4), and an increase over some parts of the western half of the Wellington Region in the same season during the negative phases of the SAM (Figure 1-5).

**Figure 1-4: Mean wind anomalies during the positive phase of SAM (VCSN anomalies).** Red lines outline areas of statistical significance at  $p \leq 0.05$ .

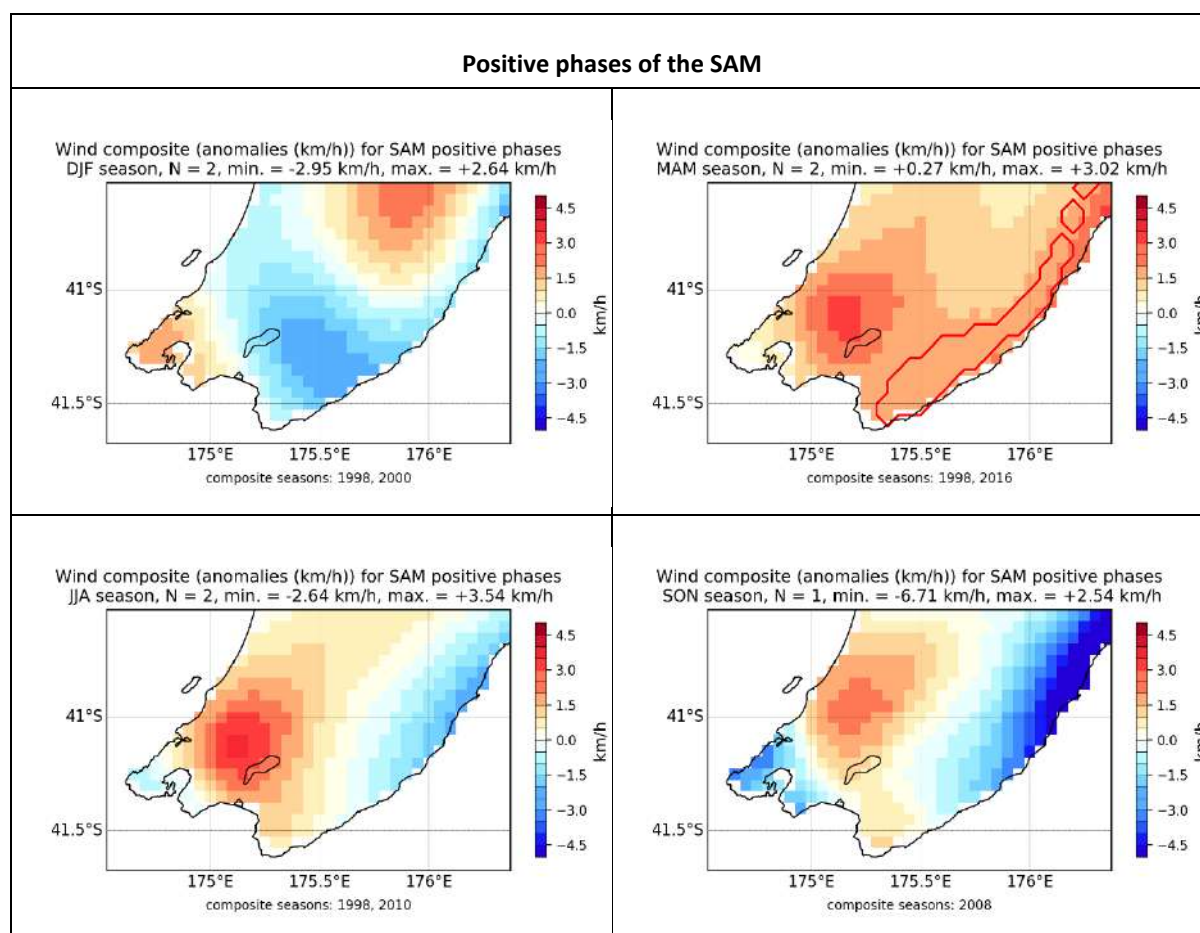
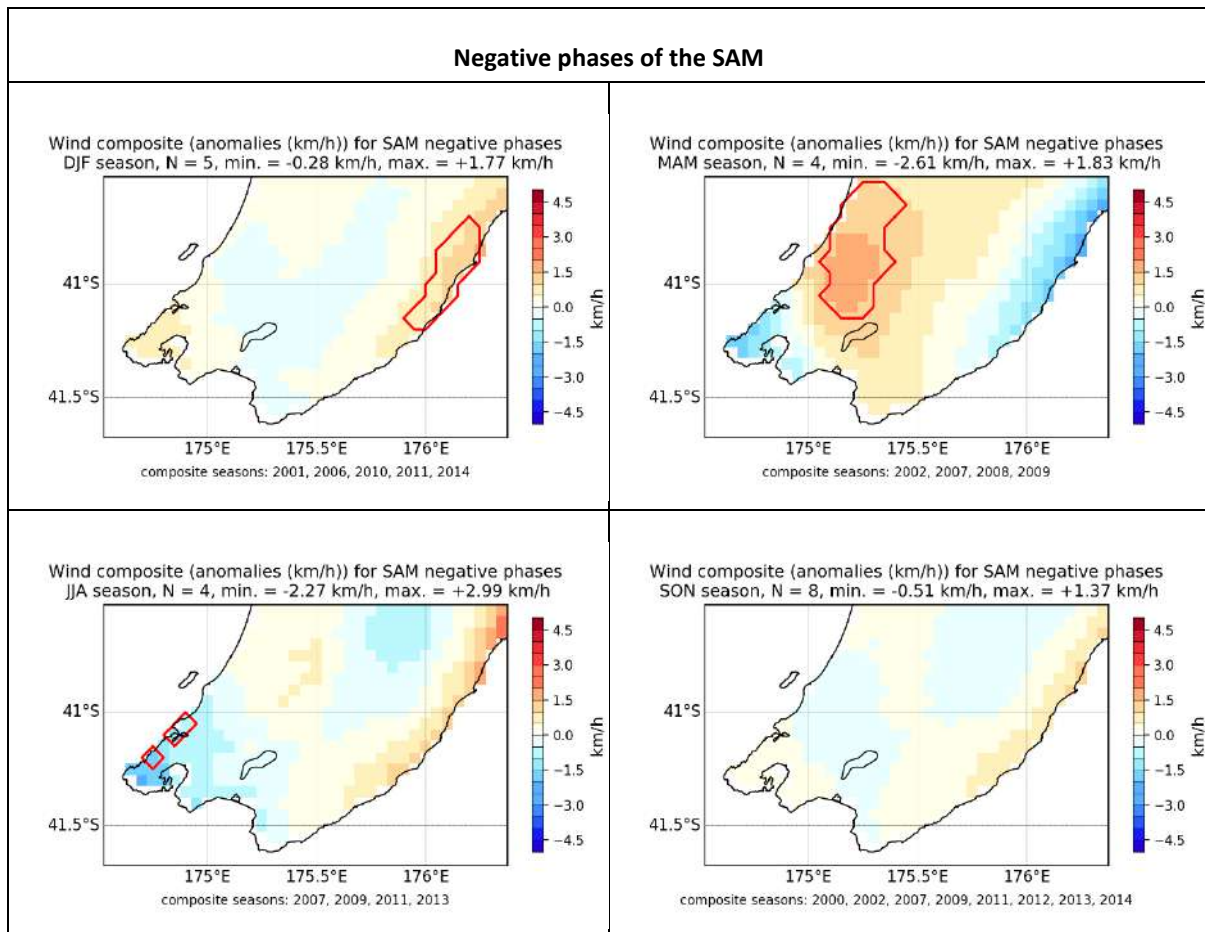




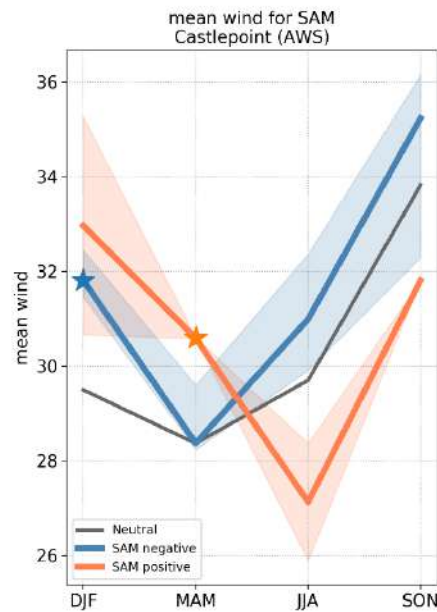
**Figure 1-5: Mean wind speed anomalies during the negative phase of SAM (VCSN anomalies).** Red lines outline areas of statistical significance at  $p \leq 0.05$ .



### 1.2.2 Station data

The station level mean wind speed anomalies indicate an increase in wind speed in MAM during the positive phase of the SAM at the Castlepoint AWS station (Figure 1-6). An increased wind speed is also registered in DJF during the negative phases of the SAM.

**Figure 1-6: Mean wind speed and SAM phase at Castlepoint AWS.** The stars indicate statistical significance at  $p \leq 0.05$ , and the shaded area indicates the interquartile range (25<sup>th</sup> to 75<sup>th</sup> percentile) of the corresponding composite sample.



## 1.3 IOD

### 1.3.1 VCSN

The mean VCSN wind speed anomalies associated with the IOD suggest a weak and inconsistent relationship, statistical significance is reached for parts of the eastern half of the Wellington Region during the positive phase of the IOD in SON, but again the sample size is small (3 seasons) (Figure 1-7).

**Figure 1-7: Mean wind speed anomalies during the positive phase of IOD (VCSN anomalies).** Red lines outline areas of statistical significance at  $p \leq 0.05$ .

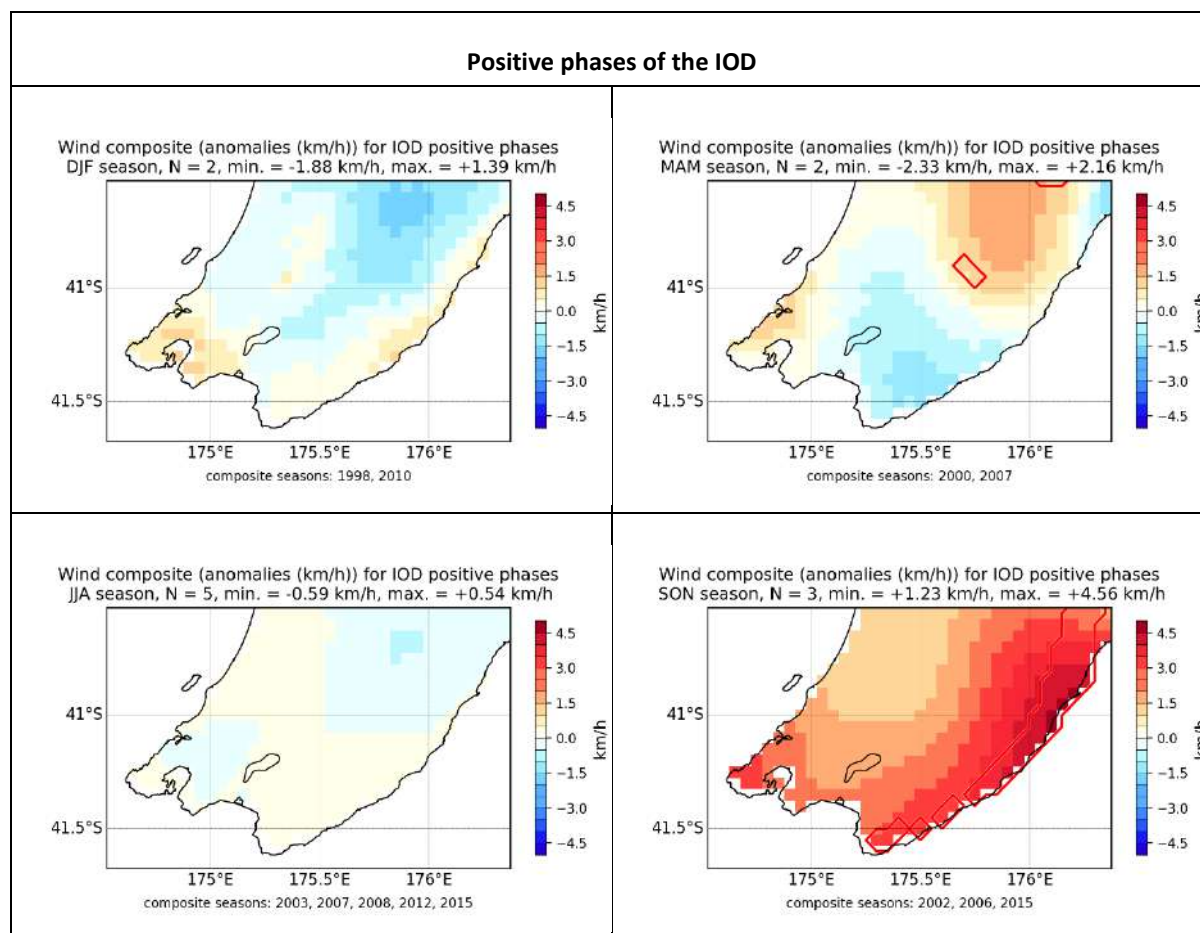
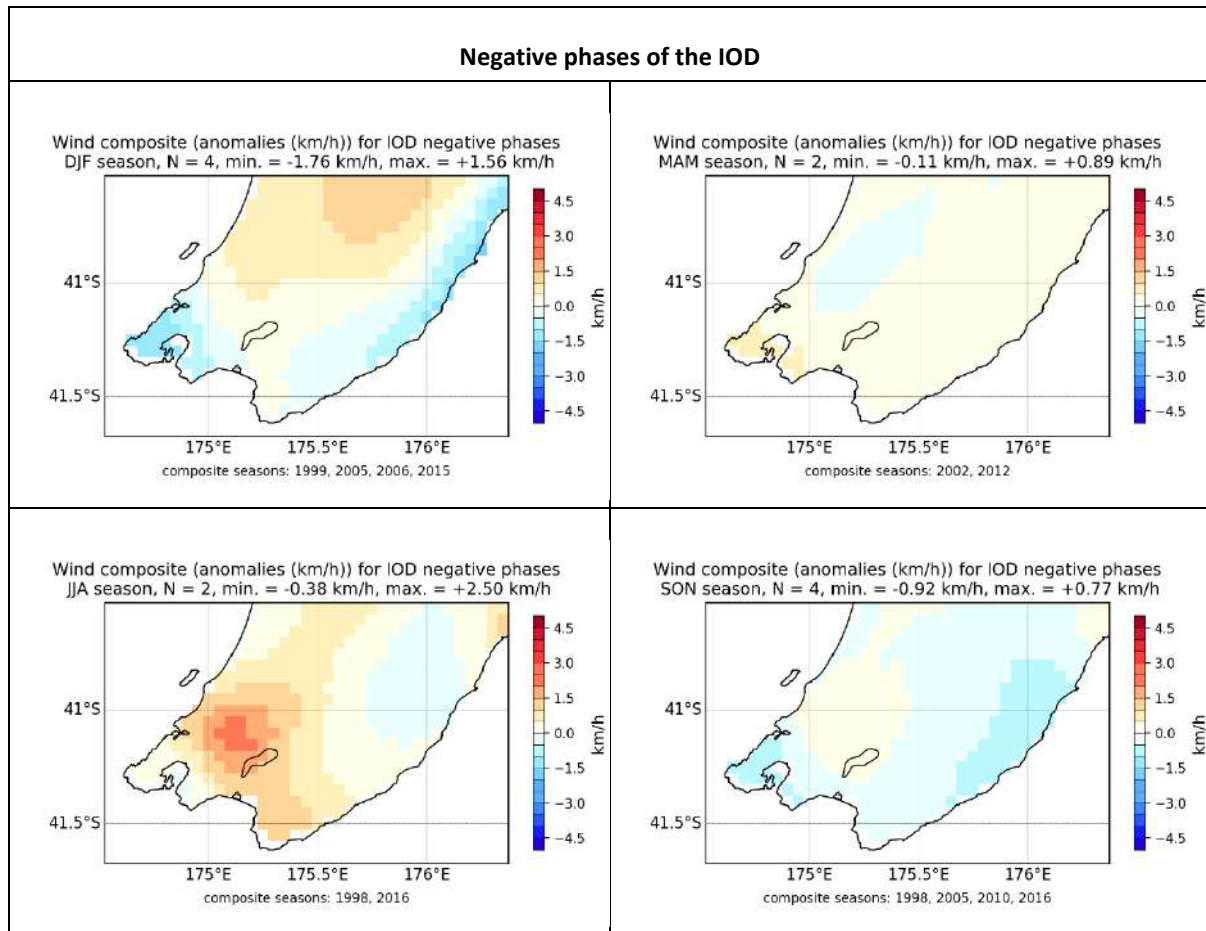


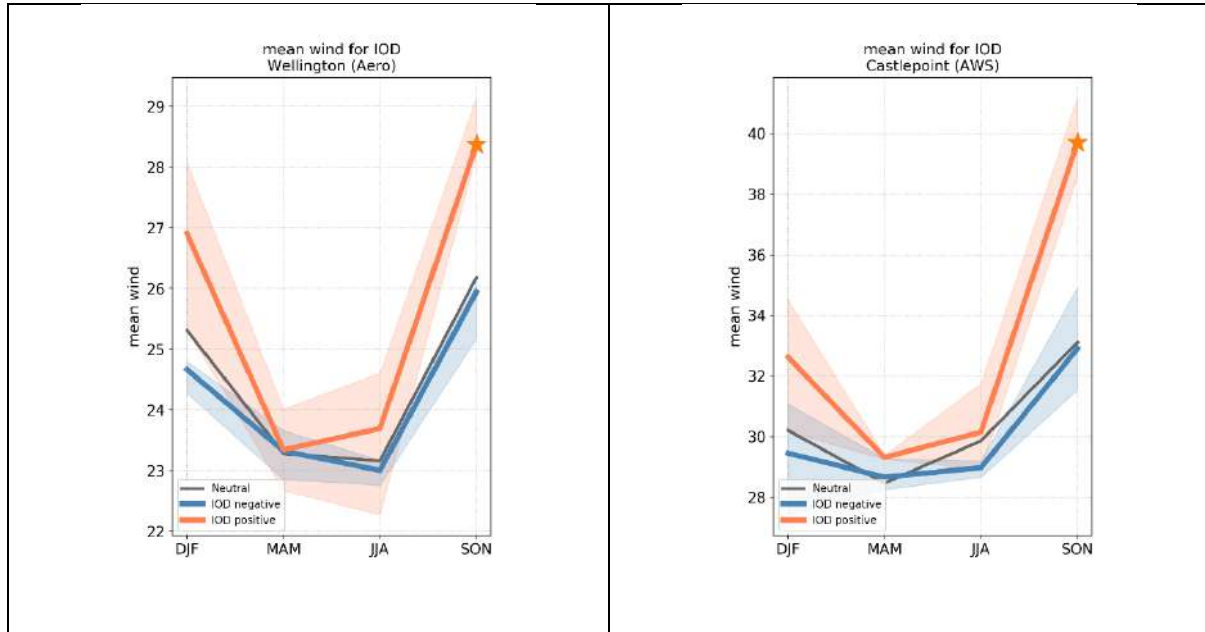
**Figure 1-8: Mean wind speed anomalies during the negative phase of IOD (VCSN anomalies).** Red lines outline areas of statistical significance at  $p \leq 0.05$ .



### 1.3.2 Station data

The station level data tends to confirm the VCSN-derived composite anomalies, with significant increase in mean wind speed at Wellington Aero and Castlepoint AWS stations in SON during the positive phases of the IOD (Figure 1-9).

**Figure 1-9: Mean wind speed and IOD phase at Wellington Aero and Castlepoint AWS.** The stars indicate statistical significance at  $p \leq 0.05$ , and the shaded area indicates the interquartile range (25<sup>th</sup> to 75<sup>th</sup> percentile) of the corresponding composite sample.



## 1.4 SPSD

### 1.4.1 VCSN

The VCSN composite anomalies tend to suggest that the positive phase of the SPSD is associated with a decrease in wind speed over the region, notably in MAM to SON, with the most widespread and the strongest anomalies being registered in SON (Figure 1-10).

**Figure 1-10: Mean wind speed anomalies during the positive phase of SPSD (VCSN anomalies).** Red lines outline areas of statistical significance at  $p \leq 0.05$ .

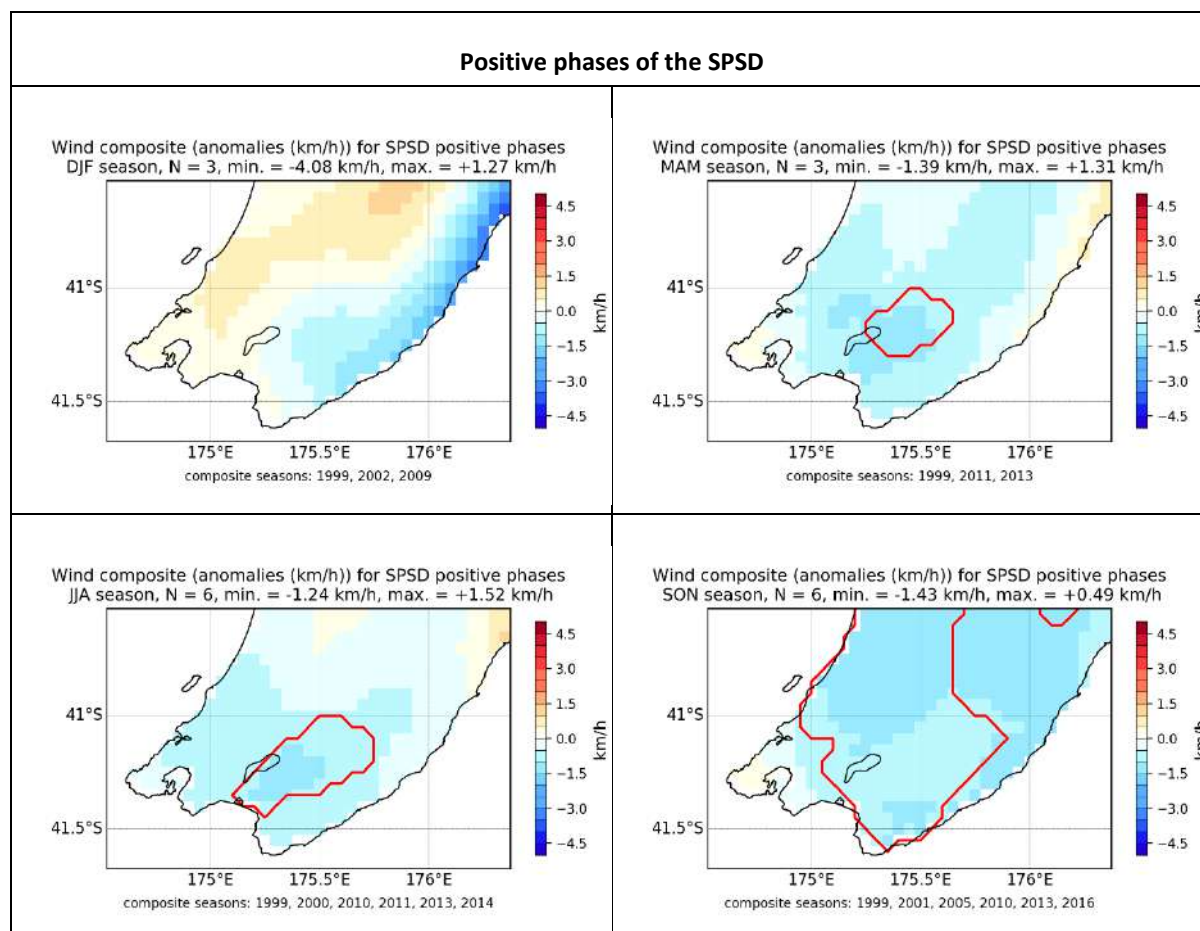
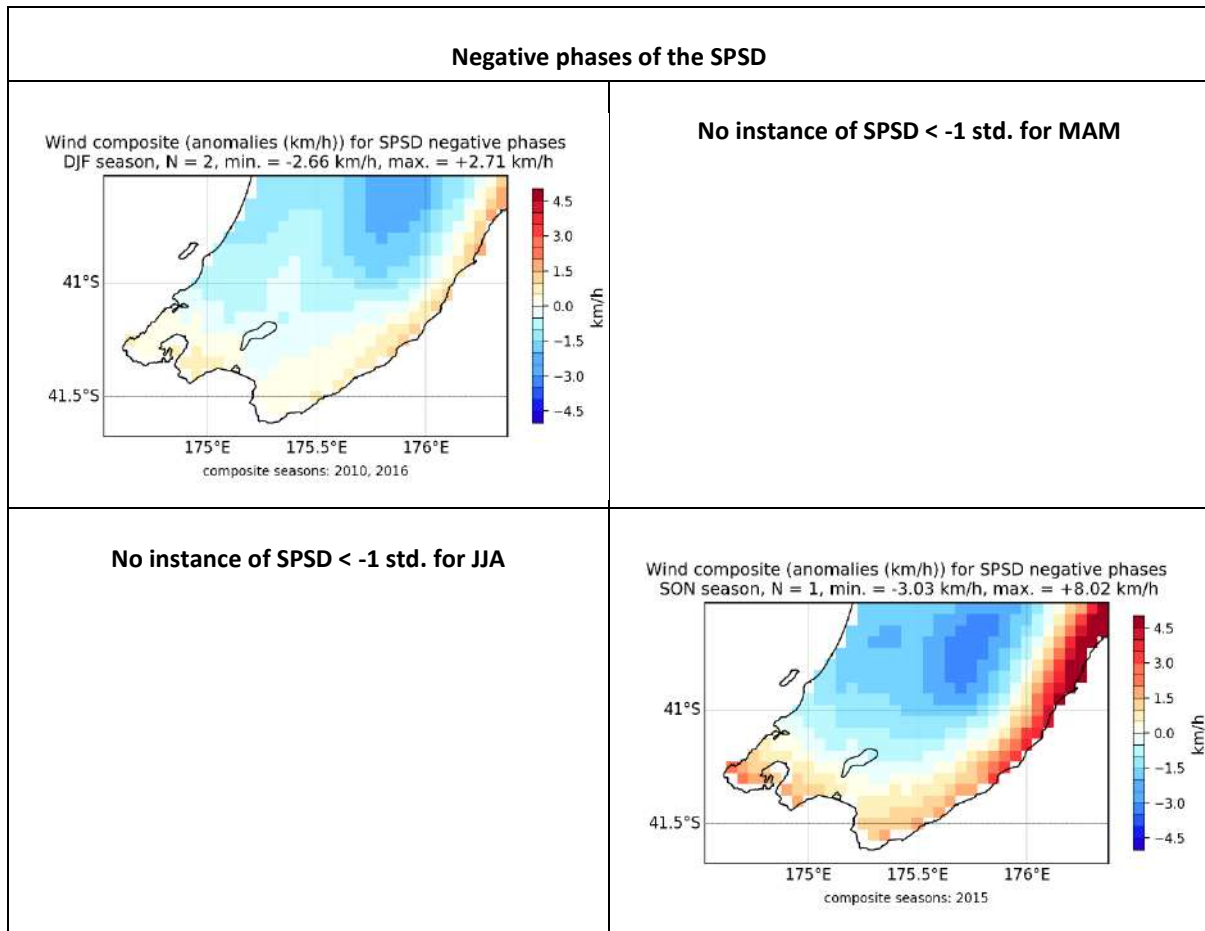


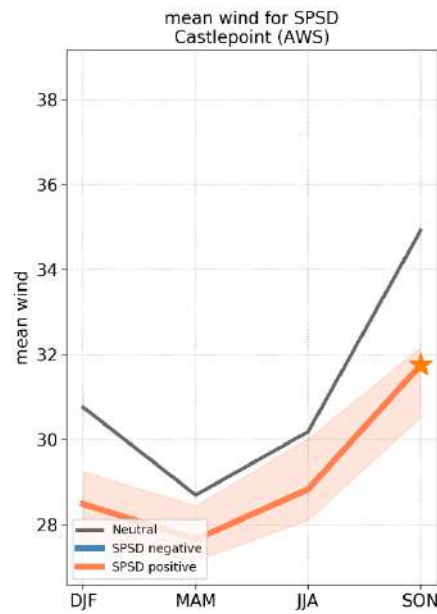
**Figure 1-11: Mean wind speed anomalies during the negative phase of SPSP (VCSN anomalies).** Red lines outline areas of statistical significance at  $p \leq 0.05$ .



### 1.4.2 Station data

Statistical significance is only reached for the Castlepoint AWS station, where mean wind speed is lower than normal in SON during the positive phase of the SPSD (Figure 1-12). Note that this tends to support the interpretation of the VCSN composite anomalies.

**Figure 1-12: Mean wind speed and SPSD phase at Castlepoint AWS.** The stars indicate statistical significance at  $p \leq 0.05$ , and the shaded area indicates the interquartile range (25<sup>th</sup> to 75<sup>th</sup> percentile) of the corresponding composite sample.





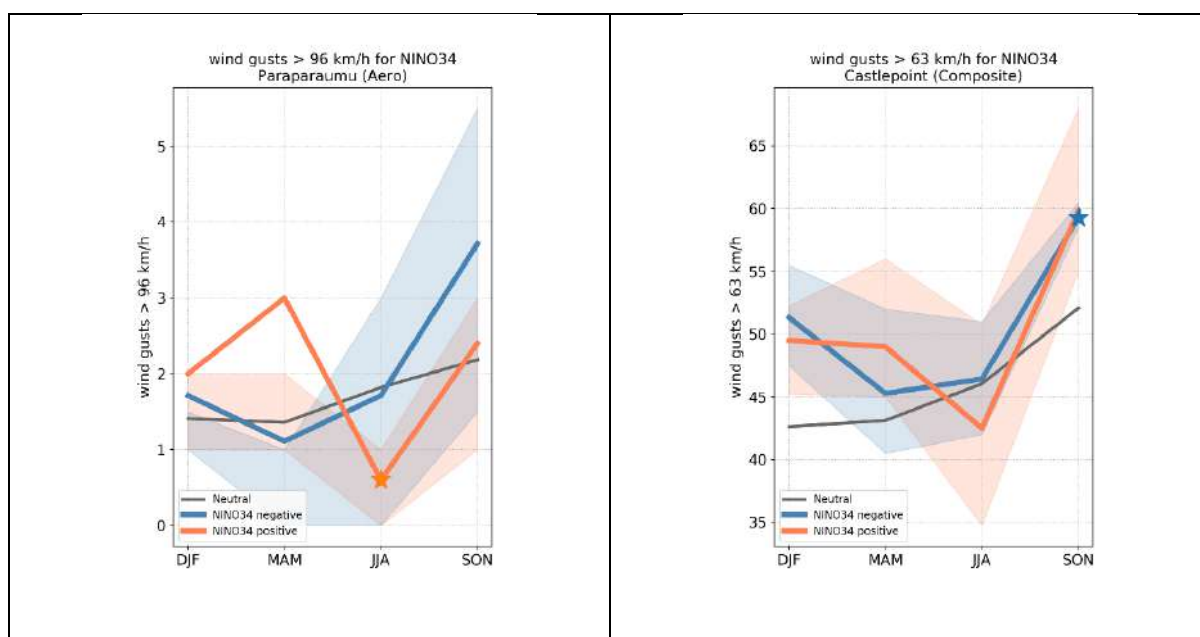
## 2 Days with wind gusts over 63 km/h and 96 km/h

The relationships between the seasonally aggregated number of days with maximum wind gusts exceeding 63 km/h and 96 km/h and the climate modes has been investigated in a similar fashion as for the rainfall and temperature parameters, by calculating the composite means for the positive, negative and neutral phases of each mode for each season. Few anomalies were significant, and were generally lacking a coherent response. Reported here the main results found for each climate mode.

### 2.1 ENSO

The only significant response was found for Paraparaumu Aero in JJA (decrease in the number of days with gusts exceeding 96 km/h during the positive phase of ENSO) and Castlepoint Composite in SON (increase in the number of days with gusts exceeding 63 km/h during the positive phase of ENSO) (Figure 2-1). The lack of a clear seasonally consistent response indicates that these results should be interpreted with extreme caution however.

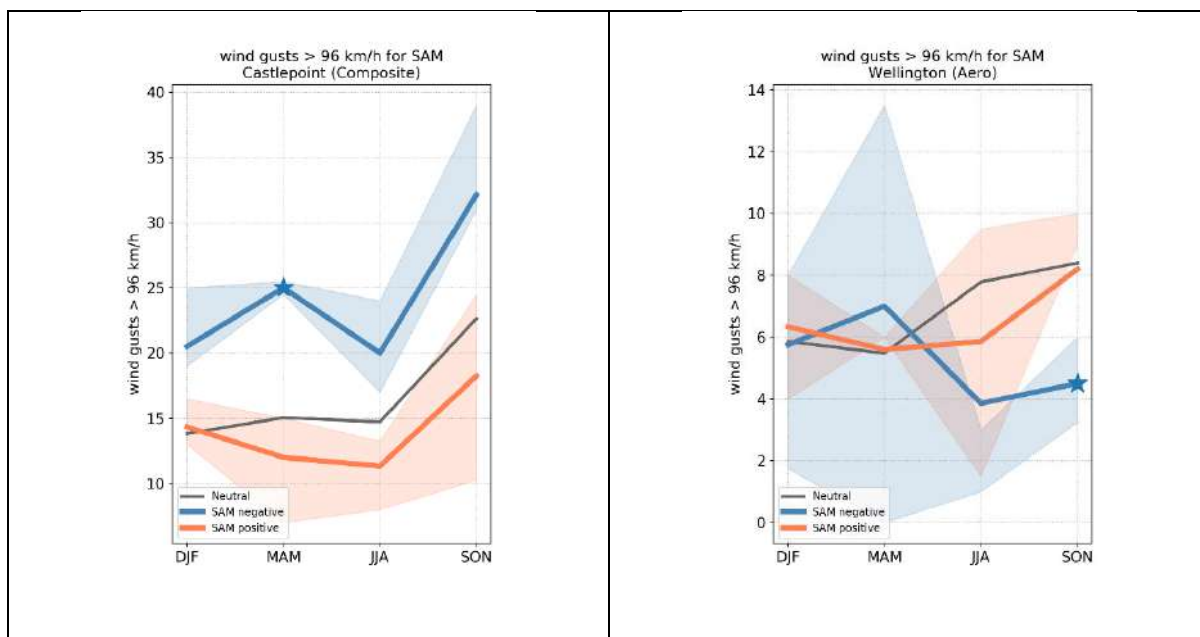
**Figure 2-1: Relationship between ENSO phase and days with wind gusts >96 km/h at Paraparaumu Aero (left) and days with wind gusts >63 km/h at Castlepoint composite (right).** The stars indicate statistical significance at  $p \leq 0.05$ , and the shaded area indicates the interquartile range (25<sup>th</sup> to 75<sup>th</sup> percentile) of the corresponding composite sample.



## 2.2 SAM

For the Castlepoint Composite station, a relatively consistent signal associated with the negative phase of the SAM is observed, where the number of days with wind gusts exceeding 96 km/h increases for all seasons (with MAM only being significant however) (Figure 2-2). For Wellington Aero, the negative phase of the SAM seems to be related to a decrease in the number of days with extreme wind in SON.

**Figure 2-2: Relationship between SAM phase and days with wind gusts >96 km/h at Castlepoint composite (left) and Wellington Aero (right).** The stars indicate statistical significance at  $p \leq 0.05$ , and the shaded area indicates the interquartile range (25<sup>th</sup> to 75<sup>th</sup> percentile) of the corresponding composite sample.



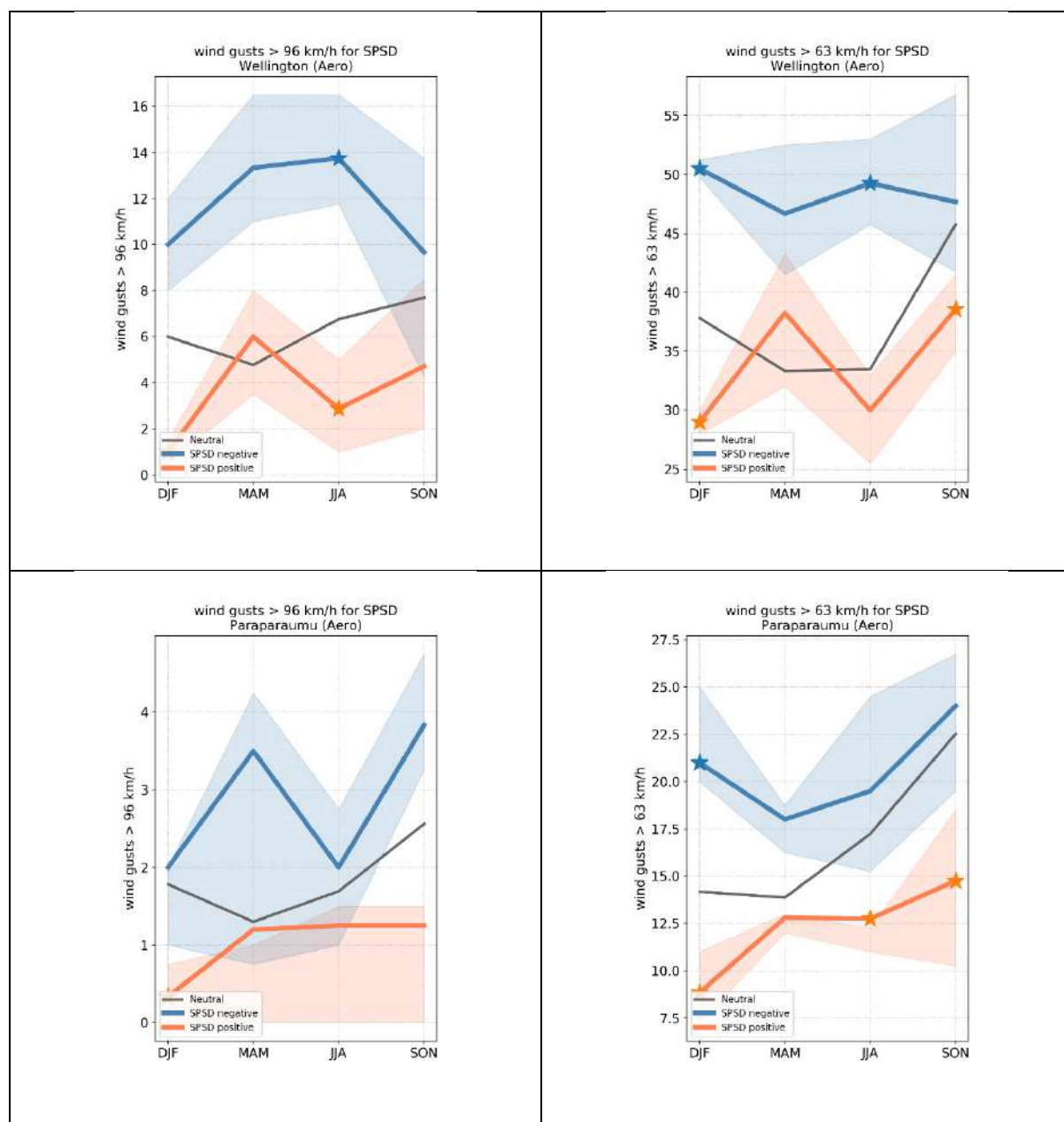
## 2.3 IOD

No significant nor consistent anomalies were found to be associated with the IOD.

## 2.4 SPSD

The SPSD shows the strongest and most consistent response at the station level, with both Wellington Aero and Paraparaumu Aero showing a general increase in the number of days with maximum wind gusts exceeding both thresholds during the negative phase of the SPSD, and a reduction in the number of occurrences of these events during the positive phase of the SPSD (Figure 2-3).

**Figure 2-3: Relationship between SPSD phase and days with wind gusts >96 km/h at Wellington Aero (top left), Paraparaumu Aero (bottom left), and days with wind gusts >63 km/h at Wellington Aero (top right) and Paraparaumu Aero (bottom right).** The stars indicate statistical significance at  $p \leq 0.05$ , and the shaded area indicates the interquartile range (25<sup>th</sup> to 75<sup>th</sup> percentile) of the corresponding composite sample.

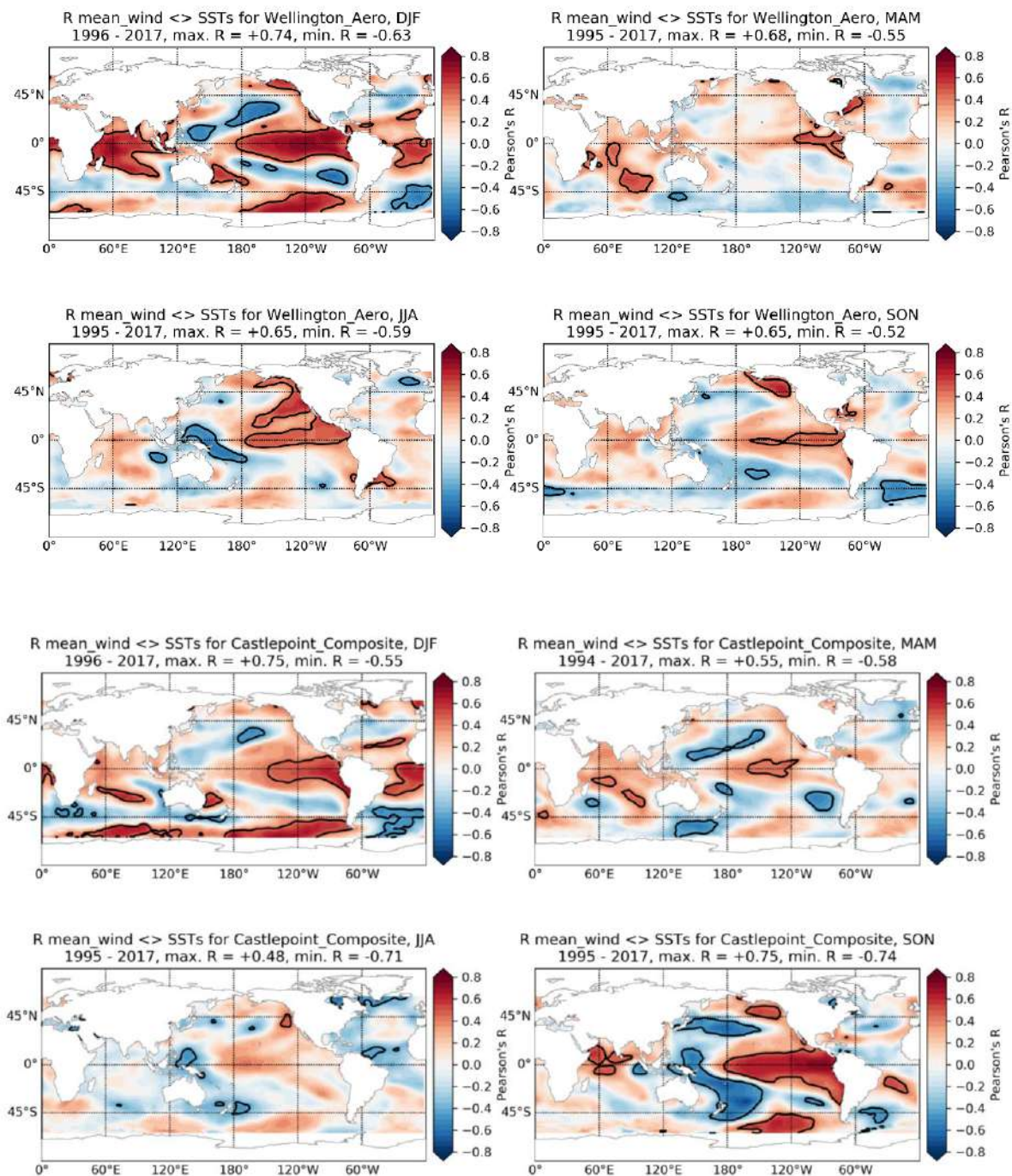


### 3 Relationship to Sea Surface Temperature (SST) anomalies

As with rainfall and temperatures, time series of seasonally aggregated wind parameters for the available stations were correlated to seasonal detrended SST anomalies. Only the most meaningful results are presented in this section, with the remaining figures being available in the electronic supplementary material to this section. Caution must be used in interpreting the results given the usually short periods for which station wind data is available.

Two main results can be highlighted: first, Wellington Aero's mean wind speed is related to a relatively clear ENSO-like signal, notably in DJF, SON and JJA (Figure 3-1). This result is relatively consistent with the station level composites, which indicated a tendency for Wellington Aero's mean wind to increase during the positive phases of the ENSO. The Castlepoint (composite) station is also associated with a strong El Niño-like signal in the eastern Pacific during SON and DJF.

**Figure 3-1: Correlation field between the mean wind speed at Wellington Aero (top) and Castlepoint composite (bottom) and seasonal SST anomalies. Black lines indicate areas of statistical significance at  $p \leq 0.05$ .**

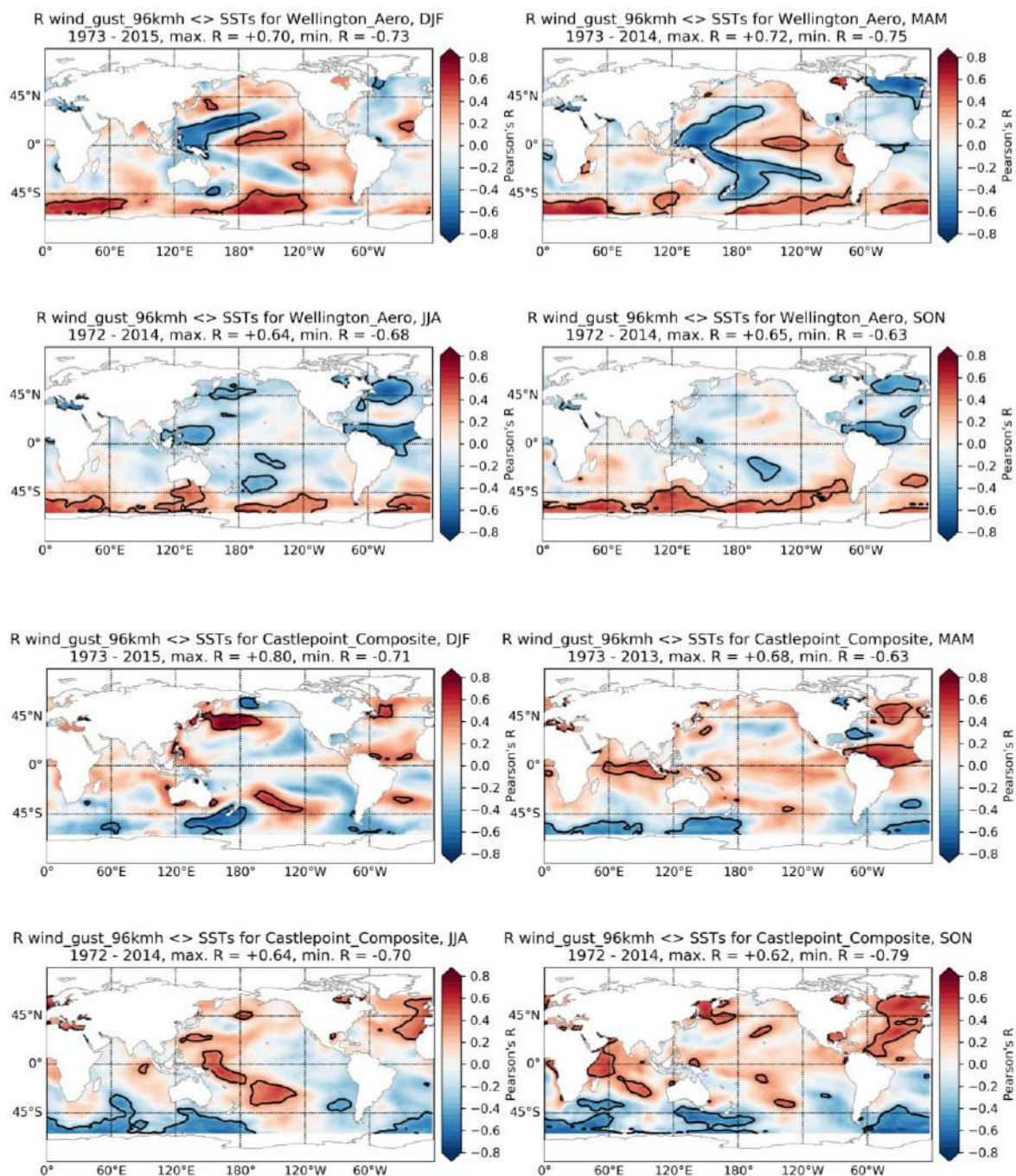


A second result worth highlighting is contrasting patterns emerging between Wellington (Aero) and Castlepoint (composite) for the strong and extreme wind gusts ( $> 63$  and more so  $96$  km/h) (

**Figure 3-2: Correlation field between the number of days with gusts  $>96$  km/h at Wellington Aero (top) and Castlepoint composite (bottom) and seasonal SST anomalies. Black lines indicate areas of statistical significance at  $p \leq 0.05$**

). The number of days with strong wind gusts in Wellington tend to be positively correlated to SSTs at the high latitudes of the Southern Hemisphere ( $> 45^{\circ}\text{S}$ ), while the reverse is true for Castlepoint composite. It is notably the case during JJA and SON. While the signals related to the SAM were not very strong, this would be however consistent with a differential response of extreme wind to the SAM on the western and eastern sides of the Wellington Region, and as illustrated by Figure 3-2, gustiness tends to increase at Castlepoint during the negative phase of the SAM, while it tends to decrease in Wellington.

**Figure 3-2: Correlation field between the number of days with gusts  $>96$  km/h at Wellington Aero (top) and Castlepoint composite (bottom) and seasonal SST anomalies. Black lines indicate areas of statistical significance at  $p \leq 0.05$**



# Regional climate mode impacts on the Wellington Region

*Part E: Relationship between inter-annual climate modes and soil  
moisture*

## Contents

<b>1</b>	<b>Soil Moisture.....</b>	<b>153</b>
1.1	ENSO.....	153
1.2	SAM.....	155
1.3	IOD.....	157
1.4	SPSD.....	159
1.5	Extremes and soil moisture variability in the Wairarapa.....	161



This is Part E of the 'Regional climate mode impacts on the Wellington Region' report. Refer to Part A: Introduction, Methodology and Background for a thorough introduction to this study.

In this section, the relationships between seasonally (DJF, MAM, JJA, SON) aggregated soil moisture and the inter-annual climate modes (El Niño Southern Oscillation (ENSO), Southern Annular Mode (SAM), Indian Ocean Dipole (IOD) and South Pacific Subtropical Dipole (SPSD)) are presented using the Virtual Climate Station Network (VCSN) by means of composite analyses. Soil moisture data is not available for individual climate stations, so only the VCSN data are considered here.

For the VCSN, composite anomalies are calculated for the extreme phases of each mode: i.e. when standardized seasonal values exceed + 1 standard deviation (referred to as the positive phase of the mode) and are below -1 standard deviation (negative phase of the mode). For consistency, the 1981-2010 climatological normal is used for both the VCSN dataset (to define the 'normal' soil moisture) and for the climate mode index (to define the mean and standard deviation for the seasonally stratified standardisation).

# 1 Soil Moisture

Soil moisture integrates information from rainfall, temperature, and heat and radiation fluxes, and can be utilised as an overall indicator of drought conditions over the Wellington Region.

## 1.1 ENSO

The VCSN composites indicate that the largest and most significant soil moisture anomalies tend to occur in SON and DJF over the Wellington Region, particularly in the southwest of the region. As was the case for rainfall, negative soil moisture anomalies (i.e. drier soils) are associated with both the positive and negative phases of ENSO, underlining the non-linear and non-symmetric impact of ENSO on the climate of the Wellington Region (Figure 1-1 and Figure 1-2).

**Figure 1-1: Soil moisture anomalies during the positive phase (El Niño) of ENSO (VCSN anomalies).** Red lines outline areas of statistical significance at  $p \leq 0.05$ .

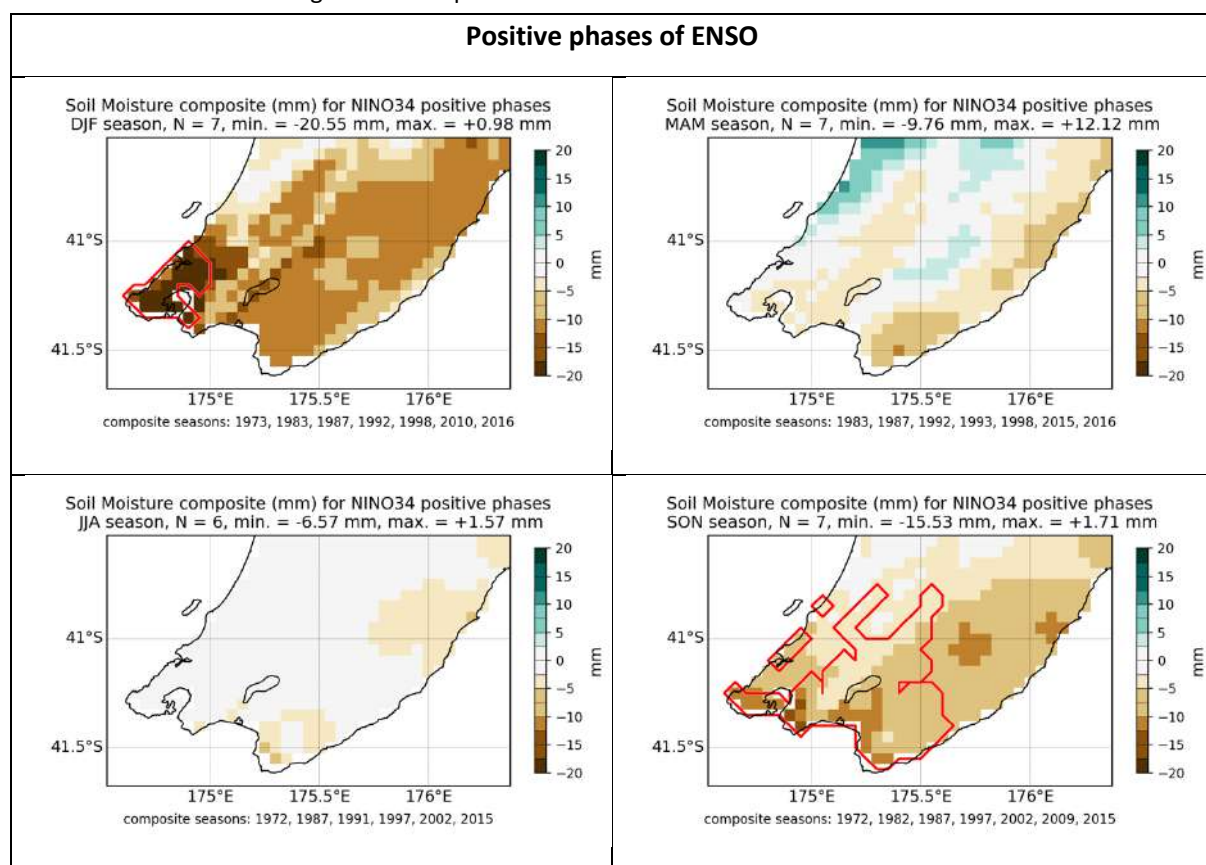
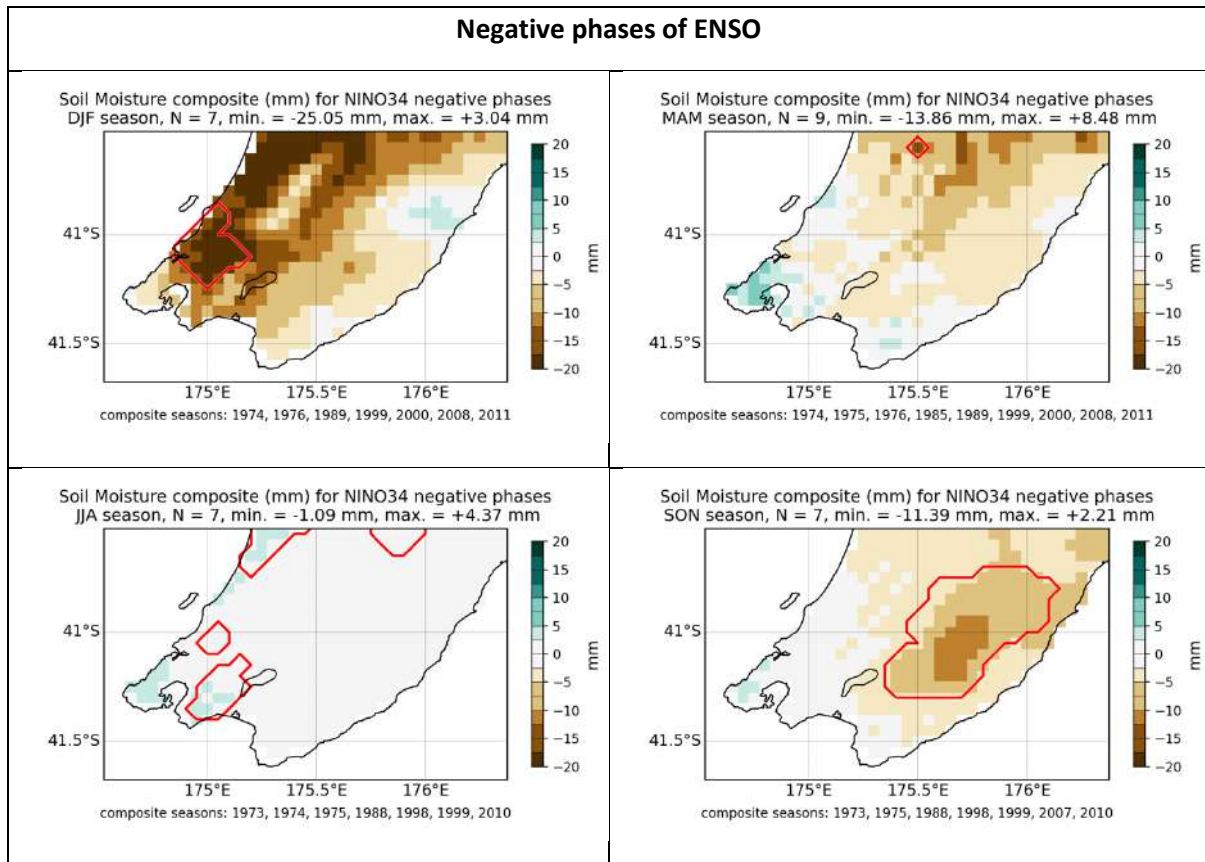


**Figure 1-2: Soil moisture anomalies during the negative phase (La Niña) of ENSO (VCSN anomalies).** Red lines outline areas of statistical significance at  $p \leq 0.05$ .



## 1.2 SAM

While some seemingly relatively large amplitudes soil moisture anomalies are associated with the positive phase of the SAM (Figure 1-3) in DJF and MAM, they are not statistically significant. Statistically significant anomalies are only found over limited areas during the negative phase of the SAM (Figure 1-4), when drier soils than normal occur near the southeast coast of the Wellington Region in MAM, and southwestern parts of the region in SON. The soil moisture anomalies do not show a consistent response to the SAM.

**Figure 1-3: Soil moisture anomalies during the positive phase of SAM (VCSN anomalies).** Red lines outline areas of statistical significance at  $p \leq 0.05$ .

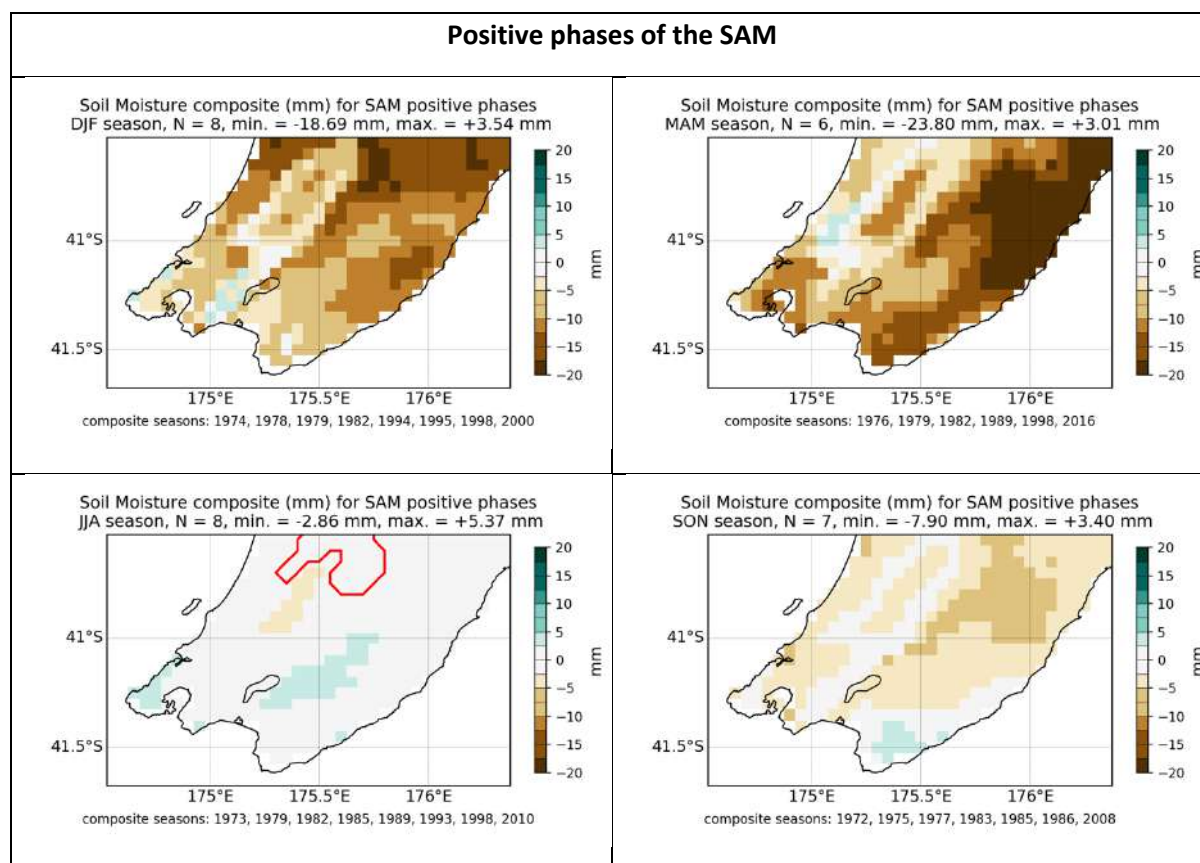
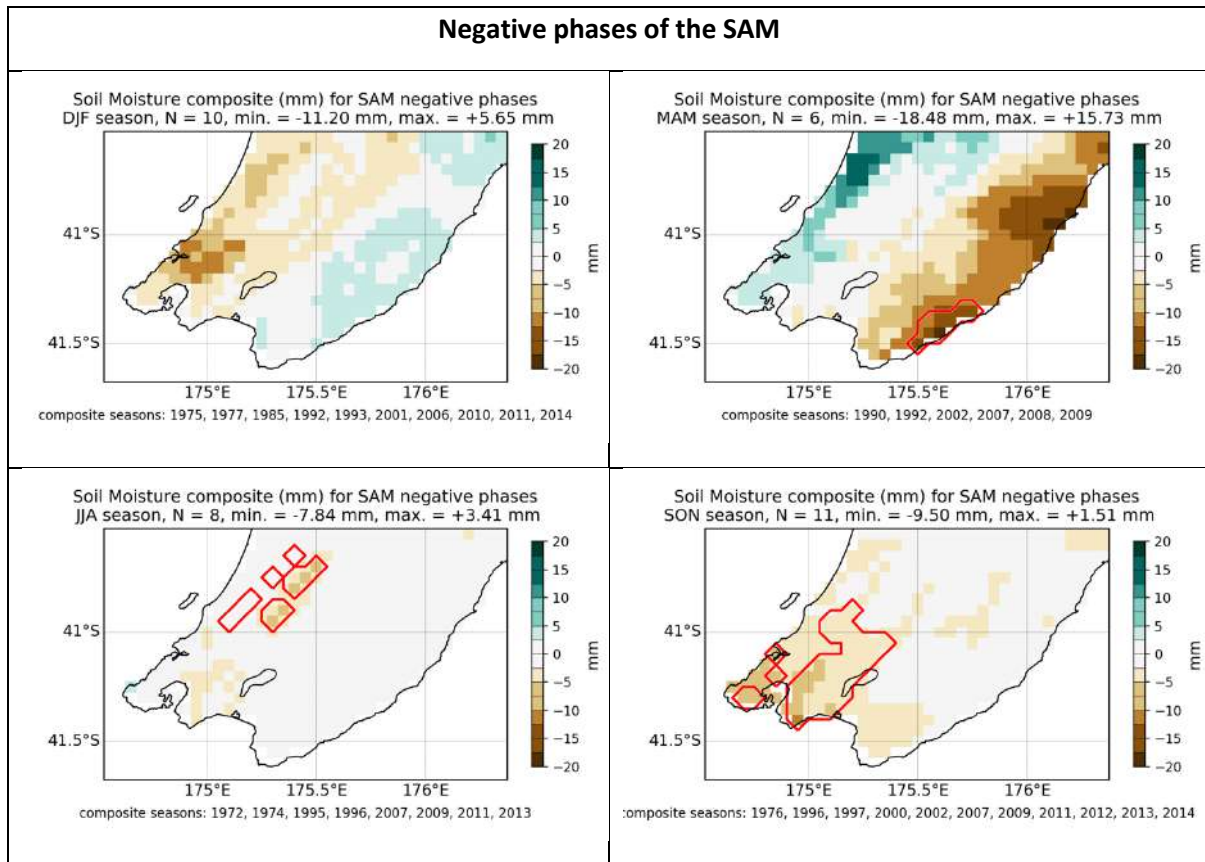


**Figure 1-4: Soil moisture anomalies during the negative phase of SAM (VCSN anomalies).** Red lines outline areas of statistical significance at  $p \leq 0.05$ .



### 1.3 IOD

As was the case for rainfall, the VCSN composite patterns do not show a strong and consistent relationship between the IOD and soil moisture. The only significant anomalies are found during the positive phase of the IOD in DJF, during which limited areas around Wellington city experience lower than normal soil moisture (Figure 1-5), and in MAM during the negative phase of the IOD, during which larger parts of the western half of the Wellington Region experience higher than normal soil moisture (Figure 1-6).

**Figure 1-5: Soil moisture anomalies during the positive phase of IOD (VCSN anomalies).** Red lines outline areas of statistical significance at  $p \leq 0.05$ .

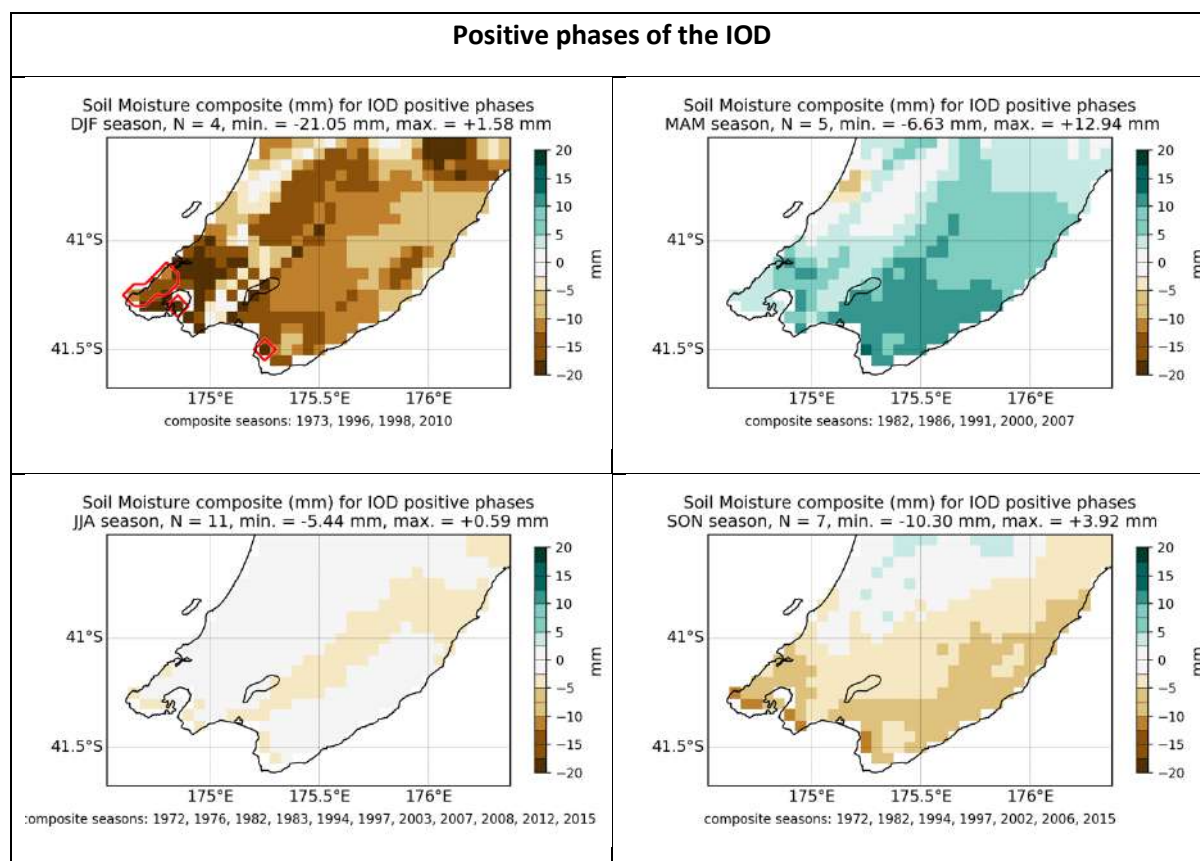
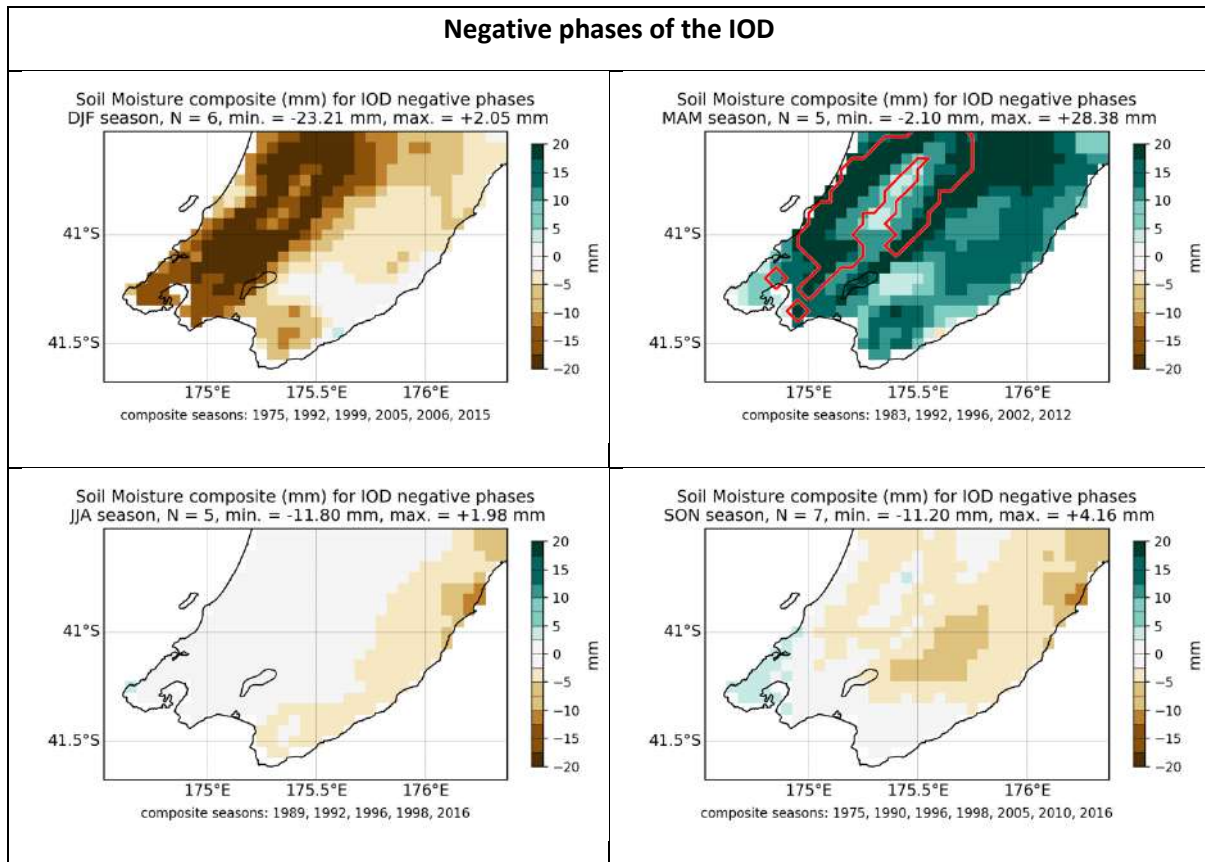


**Figure 1-6: Soil moisture anomalies during the negative phase of IOD (VCSN anomalies).** Red lines outline areas of statistical significance at  $p \leq 0.05$ .



## 1.4 SPSD

The VCSN composites show again (as was the case for rainfall) a relatively inconsistent and weak response of soil moisture to the SPSP. During the positive phase of the SPSP in the JJA season (Figure 1-7), soil moisture tends to be lower than normal around the Tararua Ranges, and higher than normal in the Wairarapa. During the negative phase of the SPSP (Figure 1-8), a similar pattern is found in the same season, indicating non-linear relationships. The negative phase of the SPSP is also associated with limited areas of higher than normal soil moisture in DJF and MAM.

**Figure 1-7: Soil moisture anomalies during the positive phase of SPSP (VCSN anomalies).** Red lines outline areas of statistical significance at  $p \leq 0.05$ .

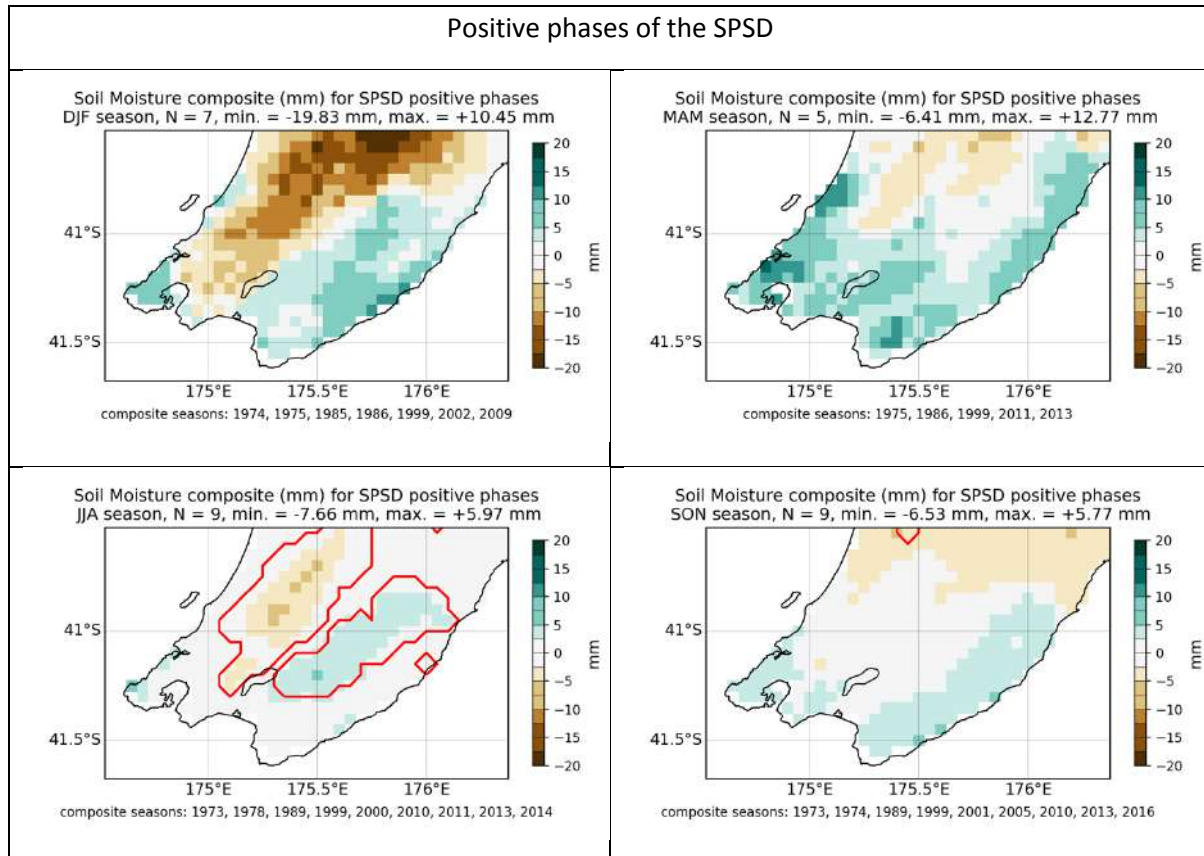
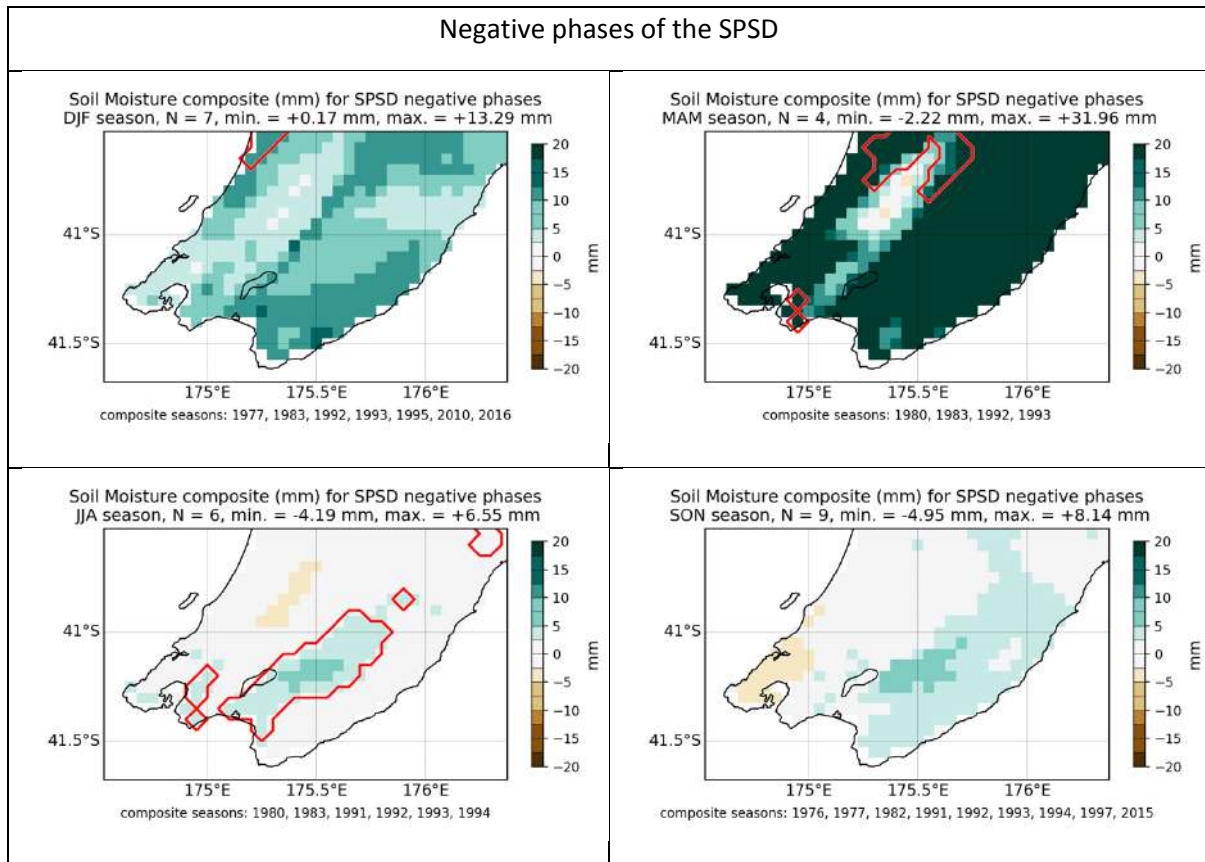




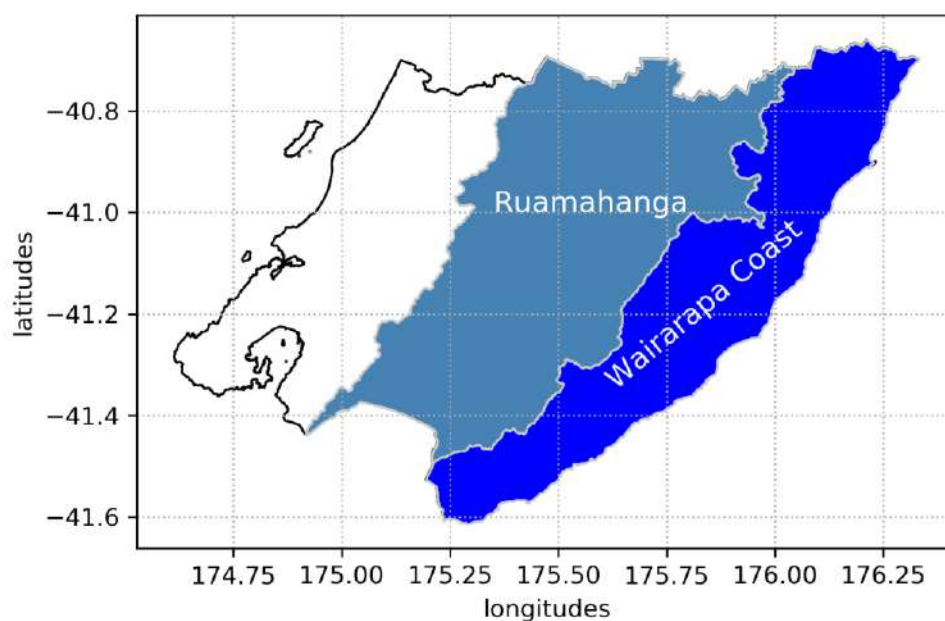
**Figure 1-8: Soil moisture anomalies during the negative phase of SPSP (VCSN anomalies).** Red lines outline areas of statistical significance at  $p \leq 0.05$ .



## 1.5 Extremes and soil moisture variability in the Wairarapa

This section presents additional results focusing on the variability of soil moisture, including extreme conditions, in the Wairarapa area of the Wellington Region. In order to investigate the large-scale background conditions related with soil moisture variability in this region, we derived two regional indices from the VCSN soil moisture dataset, using boundaries provided by GWRC for the Ruamahanga and the Wairarapa Coast areas respectively (See Figure 1-9). We selected the VCSN grid points contained in each of these areas and calculated the spatial average of the seasonal soil moisture anomalies for each year, yielding two time-series. The two time-series are strongly correlated ( $R = 0.96$ ). These time-series are then correlated to the large-scale SSTs independently for each season, and we completed a composite analysis: extreme seasons are defined as seasons where the standardized anomalies exceeded 1 std (wet seasons) and -1 std (dry seasons). The composite SST anomalies are then calculated, as well as the distribution of climate modes values for the extreme seasons and the 'normal' seasons (between -1 and 1 std). The figures not included in this section are available in the electronic material supplementary to the report.

**Figure 1-9: Location of the Ruamahanga and Wairarapa coast areas of the Wellington Region used to define the regional soil moisture seasonal anomalies indices.**



Despite the high correlation of the two regional soil moisture time-series ( $R = 0.96$ ), the background SST anomalies associated notably with the dry seasons are quite different between the two regions. Figure 1-10 presents the SST anomalies associated with the regional extreme wet seasons for Ruamahanga (top) and Wairarapa Coast (bottom) respectively. For Ruamahanga, the main signal is found during the DJF season, when SST anomalies in the central Equatorial Pacific tend to be warmer than normal, and the JJA season, when large-scale cooler than normal SSTs dominate the far western Pacific and Maritime Continent region. Note that the anomalies in the central Pacific are reminiscent of the 'central Pacific' flavour of ENSO (also referred to as El Niño Modoki). Of note as well is the presence of a large region of warmer than normal ocean waters to the east of the country in DJF, albeit not significant. For the Wairarapa coast region, the anomalies found in DJF in the

central Pacific are of a smaller amplitude (and non-significant), and the main signal is associated with warmer than normal SSTs to the east of the country.

**Figure 1-10: SST anomalies associated with anomalously wet soils in the Ruamahanga and Wairarapa Coast regions.**

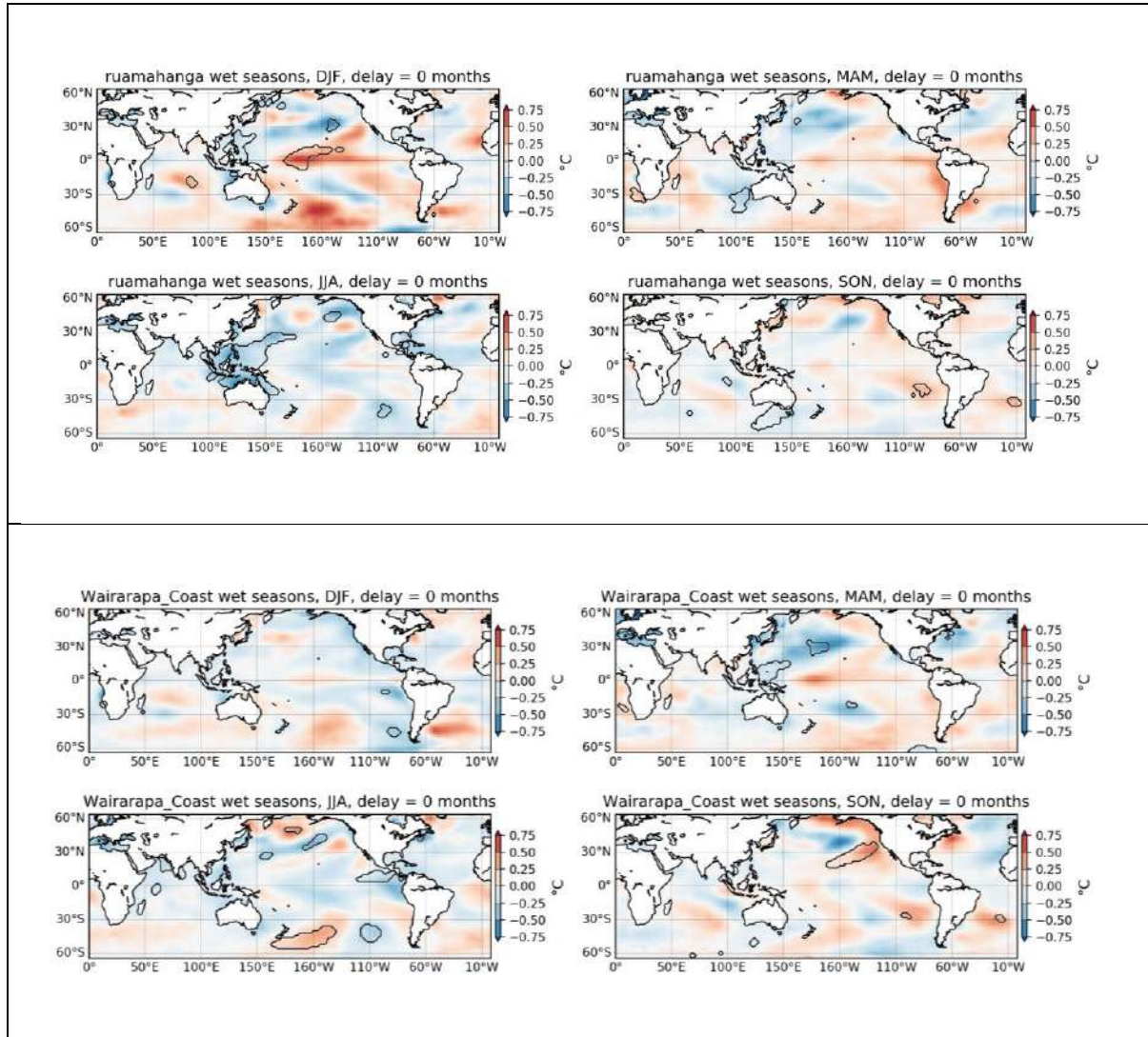
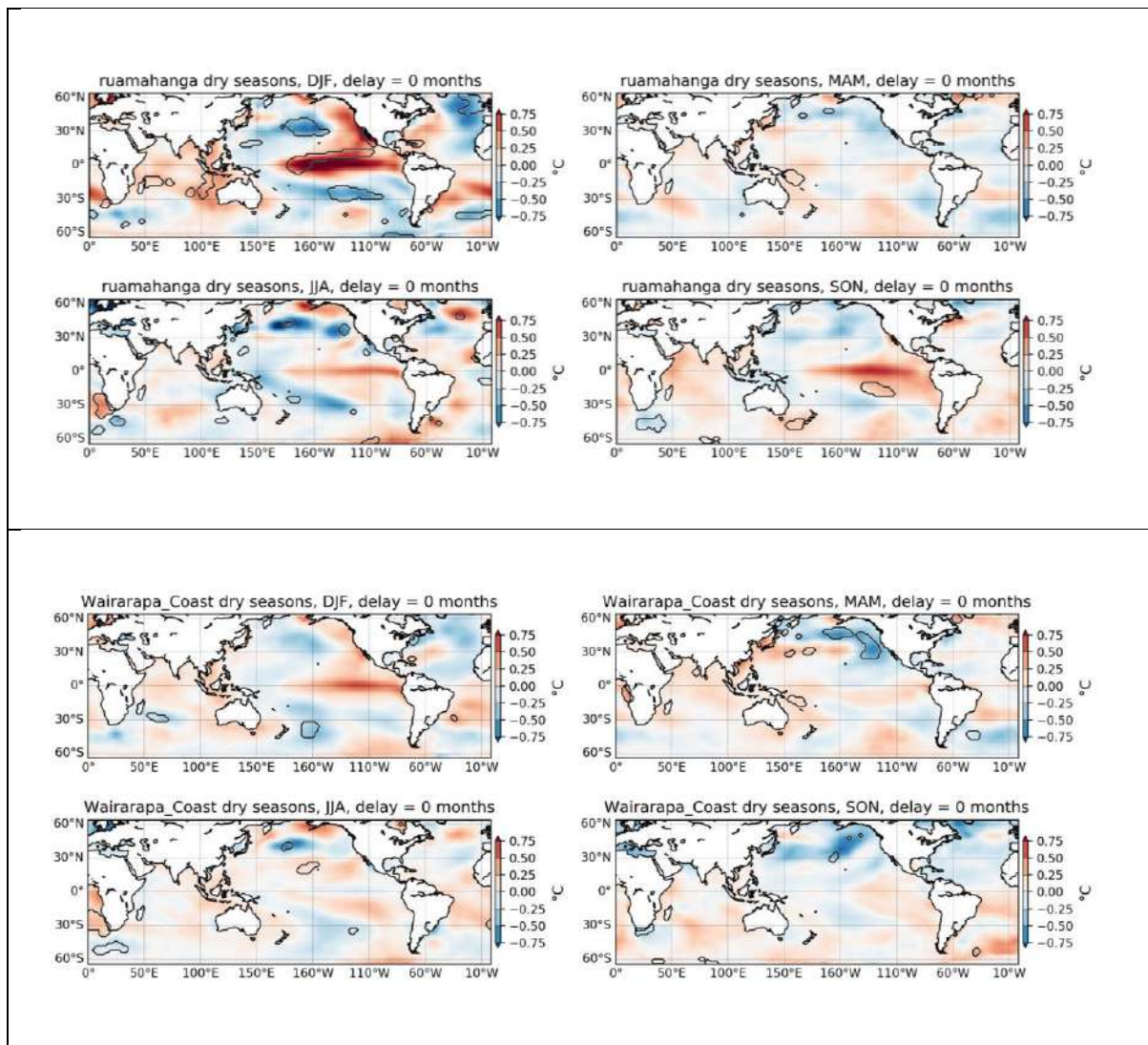


Figure 1-11 presents the SST anomalies associated with the regional extreme dry seasons for Ruamahanga (top) and Wairarapa Coast (bottom) respectively. The most prominent signal is found during DJF for the Ruamahanga region: dry summers are associated with a distinctive El Niño pattern in the Eastern Equatorial Pacific, with SST anomalies exceeding 1°C from the International Dateline to the coast of South America. This pattern is related to the ‘canonical’ flavour of El Niño. Again, this time, while broadly similar patterns are associated with dry seasons in the Wairarapa Coast region, the anomalies are of weak amplitude and are usually non-significant.

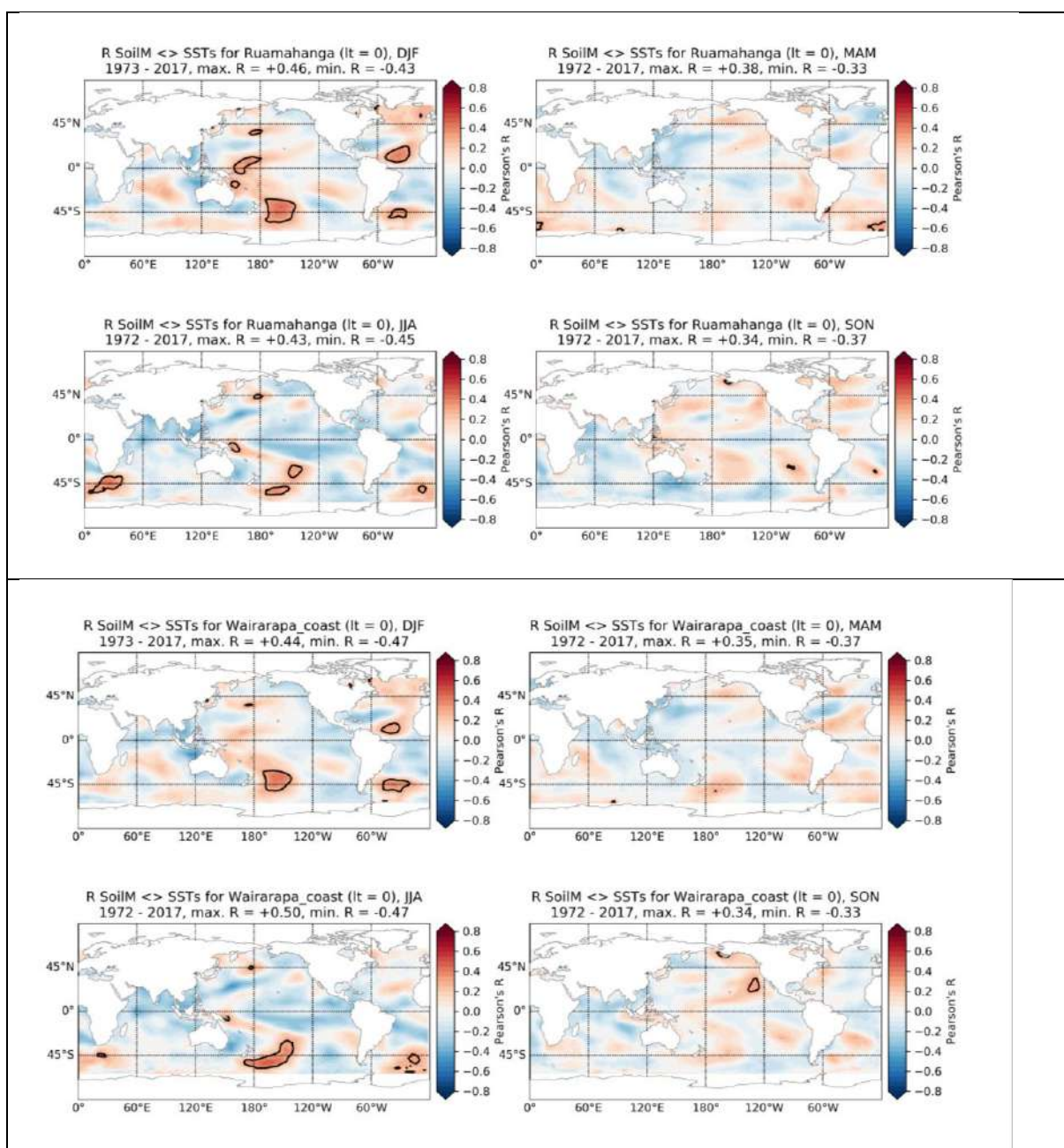
**Figure 1-11: SST anomalies associated with anomalously dry soils in the Ruamahanga and Wairarapa Coast regions.**



In summary, while the two regional soil moisture anomaly time-series are strongly correlated, larger amplitude and more significant SST patterns are found to be associated with anomalous seasons in the Ruamahanga region than with the Wairarapa Coast region. For the Ruamahanga region, the main signals are found during the DJF season: both anomalously wet and dry soils are associated with warmer than normal SSTs in the Equatorial Pacific, but important differences exist in the exact location of the largest SST anomalies: during the anomalously wet seasons, the stronger anomalies are found in the central Pacific (around the International Dateline) in a pattern reminiscent of the ‘Central Pacific’ or ‘Modoki’ flavour of ENSO. On the other hand, during the anomalously dry DJF seasons, the largest SST anomalies are found in the eastern Pacific, with a pattern very clearly corresponding to the ‘canonical’ (or ‘eastern Pacific’) flavour of ENSO. These results therefore confirm the non-linearity noted elsewhere between several climate parameters over the Wellington Region and the ENSO phenomenon, but also suggests that the exact location of the maximum SST anomalies (and therefore the ‘flavour’ of El Niño in particular) may be important in determining the sign and amplitude of the Wellington Region climate’s response to ENSO.

Figure 1-12 presents the correlation field between the seasonal soil moisture anomalies in the Ruamahanga (top) and Wairarapa Coast (bottom) and the large scaled seasonal SST anomalies. The correlation with SSTs in the tropical Pacific are generally weak and inconsistent, a reflection of the apparent non-linearity of the relationship between regional soil moisture conditions and the ENSO phenomenon, discussed above. On the other hand, relatively strong correlations are indicated for regional SSTs, notably to the southeast of NZ in the DJF season: Soil moisture levels tend to be elevated when ocean waters to the southeast of the country are warmer than normal. Again, this analysis tends to suggest that linear relationships between hydrological parameters are mostly found with regional SSTs, with the relationships with near-global patterns (notably ENSO) being non-linear and asymmetric.

**Figure 1-12: Correlation field between SST anomalies and soil moisture anomalies in the Ruamahanga and Wairarapa Coast regions.**



# Regional climate mode impacts on the Wellington Region

*Part F: Relationships between sub-seasonal and decadal climate modes  
and climate variables*

## Contents

<b>1</b>	<b>The Madden Julian Oscillation .....</b>	<b>168</b>
1.1	Rainfall .....	168
1.2	Mean maximum temperature .....	175
1.3	Mean minimum temperature .....	181
<b>2</b>	<b>The impact of the Southern Annular Mode on the Wellington Region’s climate at the sub-seasonal timescale .....</b>	<b>187</b>
2.1	Rainfall .....	187
2.2	Maximum and minimum daily temperatures .....	189
<b>3</b>	<b>Relationship to the Interdecadal Pacific Oscillation (IPO) .....</b>	<b>192</b>
3.1	Total rainfall and number of heavy rainfall days.....	193
3.2	Number of rain days (> 0.5 mm) .....	193
3.3	Number of dry days (0 mm rain) .....	194
3.4	Temperature indices .....	194
<b>4</b>	<b>References .....</b>	<b>195</b>

This is Part F of the ‘Regional climate mode impacts on the Wellington Region’ report. Refer to Part A: Introduction, Methodology and Background for a thorough introduction to this study. This section is devoted to the investigation of how sub-seasonal (1 day to ~60 days) and decadal (~10 years and longer) climate variability in the Wellington Region relates to large scale modes of climate variability operating in the Southern Hemisphere.

For the sub-seasonal timescales, two modes are considered, the Madden-Julian-Oscillation (MJO) and the Southern Annular Mode (SAM).

The MJO is a mode of intra-seasonal variability, with characteristic timescales of 30 to 60 days. The MJO – as characterized by the so-called Real Time MJO Monitoring indices (RMM1 and 2) of Wheeler and Hendon (2004) – is here related to daily rainfall, minimum and maximum temperature and mean daily wind speed from the VCSN, as well as the same parameters derived from the available daily station time-series. The RMM1 and RMM2 indices are available from 1974 onwards, but are of less quality prior to the satellite era (1979). We conducted the analyses for both the whole period available (1974-2017) as well as the high quality post-1979 period, and present here the latter, the results being qualitatively similar.

In the second part, we re-assess the impact of the SAM over some climate variables (rainfall and temperature) over the Wellington Region, but considering now the sub-seasonal timescale. Contrary to, for example, ENSO, which is a coupled Ocean – Atmosphere mode of variability, and has a clear preferred inter-annual timescale (2-7 years), the SAM is an internal mode of atmospheric variability, and appears at all timescales from sub-seasonal to decadal (*e.g.* when using EOF analyses of the pressure field in the Southern Hemisphere). When considering the sub-seasonal timescale, typical e-folding time scales of SAM variability in the observed troposphere are on the order of 10 days (Gerber et al., 2008, Baldwin et al., 2003), i.e. indicating significant sub-seasonal persistence of the SAM.

For the decadal timescale, we consider the Interdecadal Pacific Oscillation (IPO) index, calculated as the Principal Component (PC) associated with the second EOF (Empirical Orthogonal Function) of low-pass filtered (periodicities > 11 years) monthly SST anomalies in the Pacific region (see Part A for methodology details). Given the timescale involved, the analyses can only be conducted using station time-series providing long enough records, and exclude the VCSN, which is only available from 1972.



# 1 The Madden Julian Oscillation

## 1.1 Rainfall

### 1.1.1 VCSN

The daily composite anomalies for the eight phases of the MJO were calculated independently for each season. For all seasons, daily rainfall is significantly modulated by the MJO for at least parts of the Wellington Region. Given the propagative nature of the MJO, these results open the opportunity for the development of guidance products for forecast horizons beyond the ‘weather timescale’ (i.e. 15 days to a month) based on the MJO current state and available dynamical forecasts. Note also that given the preferred life-time of the MJO (30 to 60 days) the MJO tends to persist in each phase between about 4 to 8 days.

The strongest and most significant anomalies are generally found in winter (JJA) (Figure 1-3). During this season, the phases 8 to 2 of the MJO (when the decreased convection envelope associated with the MJO propagates from the maritime continent (MC) to the western Pacific Ocean) are generally associated with decreased rainfall over large parts of the Wellington Region. Phases 5 to 7 of the MJO (increased convective activity associated with the MJO propagating from the MC to the western Pacific Ocean) are on the other hand generally related to increased daily rainfall. In both cases, the anomalies are non-negligible (exceeding +/- 2 mm.day<sup>-1</sup>). Table 1 below attempts to summarize the sign and location of the anomalies as a function of the phase of the MJO and the season, with the symbol ‘-’ indicating that statistical significance was reached for very limited or no areas of the region. Figures 1-1 to 1-4 show the VCSN composites for each season and each phase of the MJO.

**Table 1: MJO sign and location for different seasons in the Wellington Region.**

MJO / season	DJF	MAM	JJA	SON
<b>1</b>	-	-	Dry (E)	-
<b>2</b>	Dry (most regions)	Dry (W)	Dry (W)	Wet (W) / Dry (E)
<b>3</b>	Dry (E)	Dry (NE)	-	Dry (all region)
<b>4</b>	Dry (most areas)	-	Dry (E)	-
<b>5</b>	-	Wet (NE)	Wet (most regions)	Dry (W)
<b>6</b>	-	Wet (NE)	Wet (E)	-
<b>7</b>	-	-	Wet (parts of the S)	Dry (E and NW)
<b>8</b>			Dry (Tararua ranges)	Wet

**Figure 1-1: Daily rainfall anomalies associated with each phase of the MJO for the DJF season (VCSN composite) over the period 1979 – 2017. Red lines outline areas of statistical significance at  $p \leq 0.05$ . Note that the panels succeed each other clockwise, in order to reflect the cyclic nature of the MJO and the fact that e.g. the phase 8 of the MJO is phenomenologically close to the phase 1. This convention is adopted in all the following figures presenting the VCSN composite anomalies associated with the MJO.**

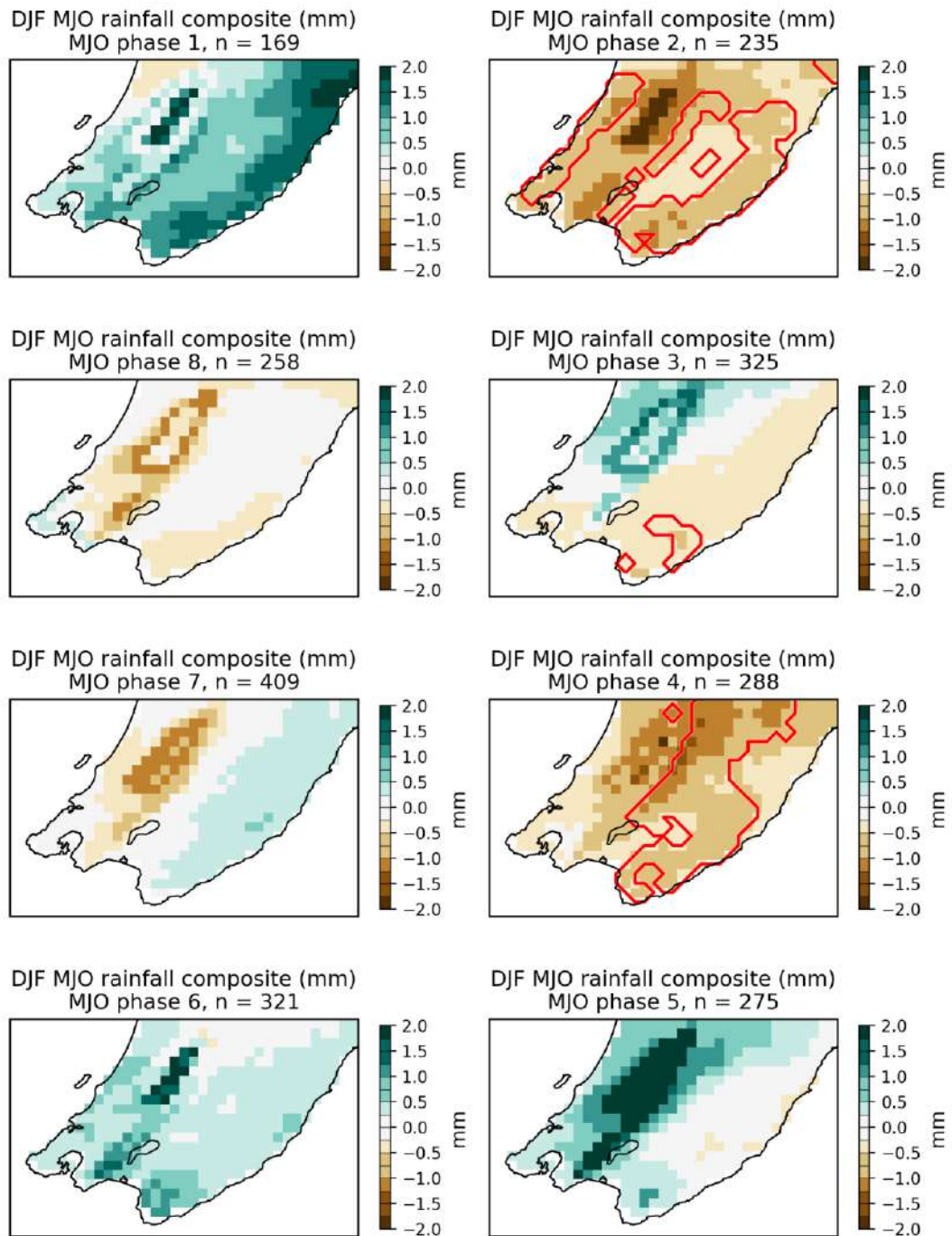


**Figure 1-2: Daily rainfall anomalies associated with each phase of the MJO for the MAM season (VCSN composite) over the period 1979 - 2017. Red lines outline areas of statistical significance at  $p \leq 0.05$ .**

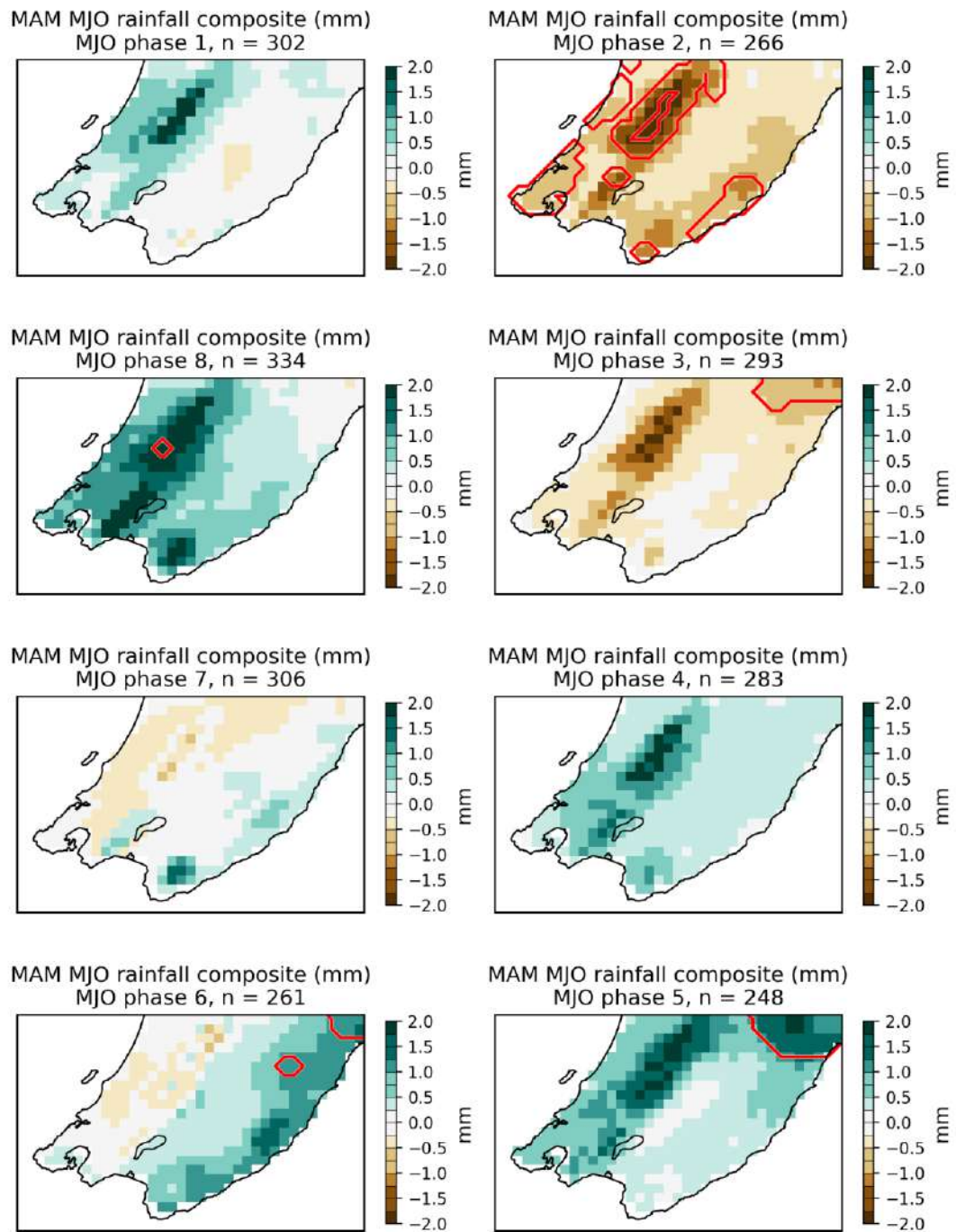


**Figure 1-3: Daily rainfall anomalies associated with each phase of the MJO for the JJA season (VCSN composite) over the period 1979 - 2017. Red lines outline areas of statistical significance at  $p \leq 0.05$ .**

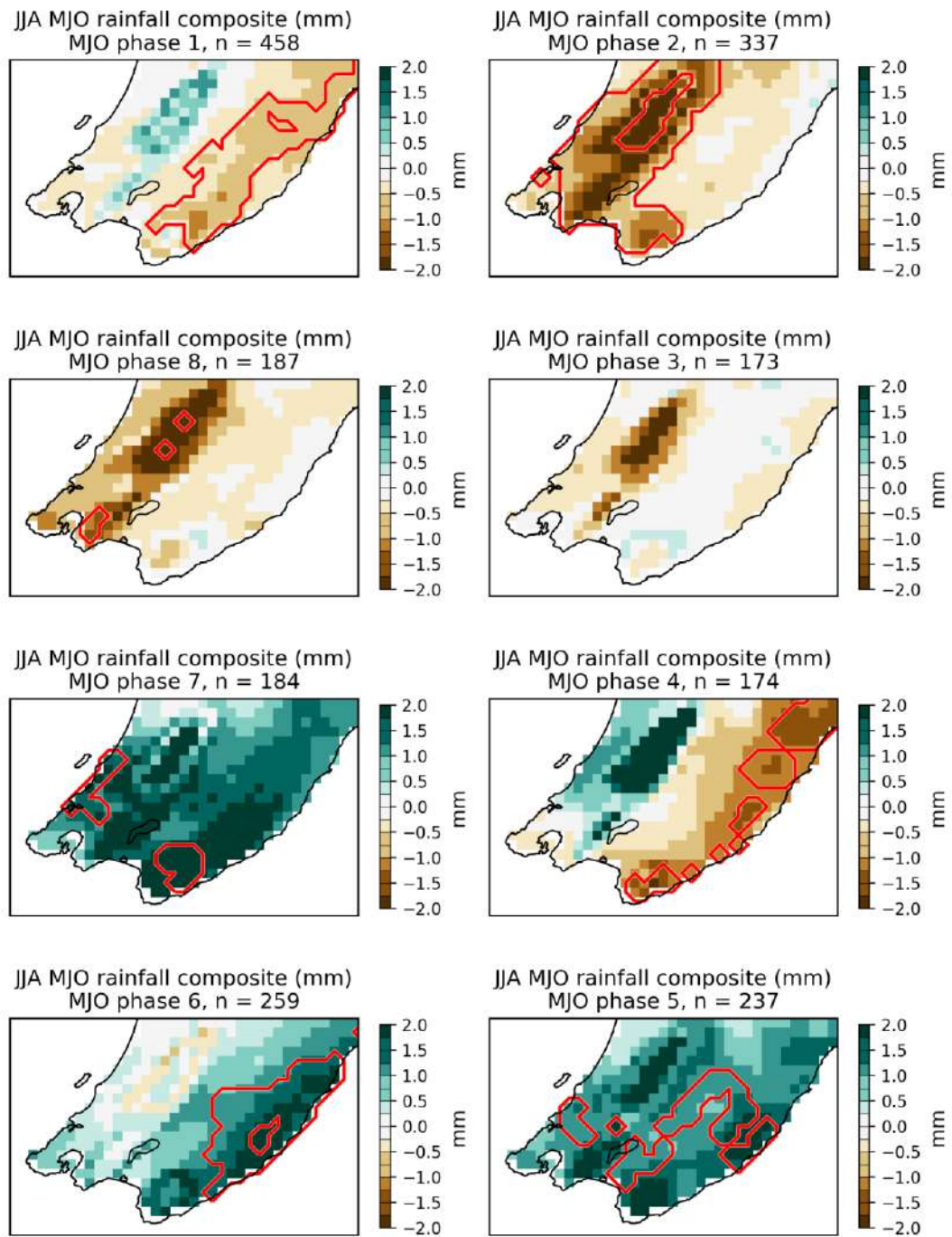
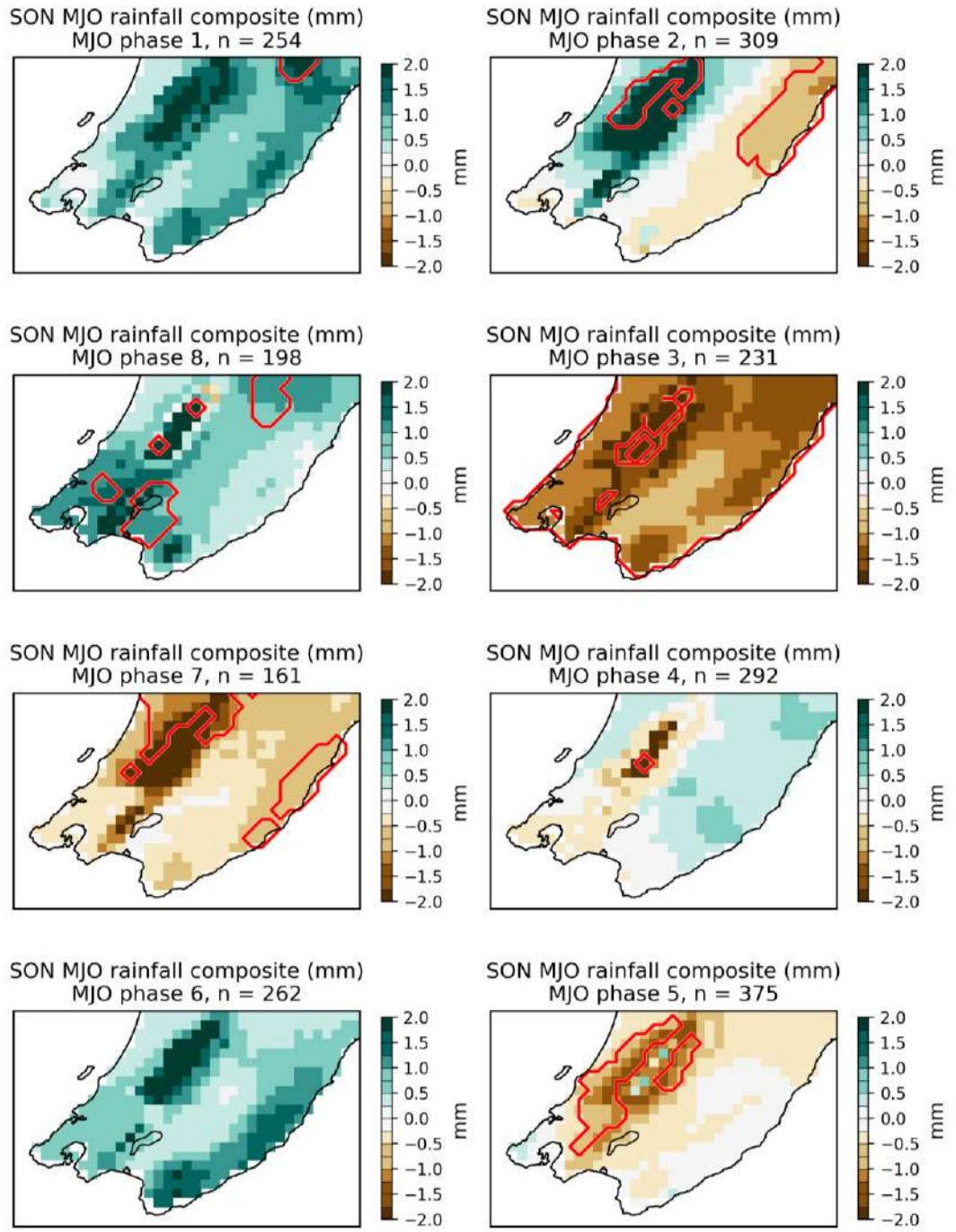


**Figure 1-4: Daily rainfall anomalies associated with each phase of the MJO for the SON season (VCSN composite) over the period 1979 - 2017. Red lines outline areas of statistical significance at  $p \leq 0.05$ .**

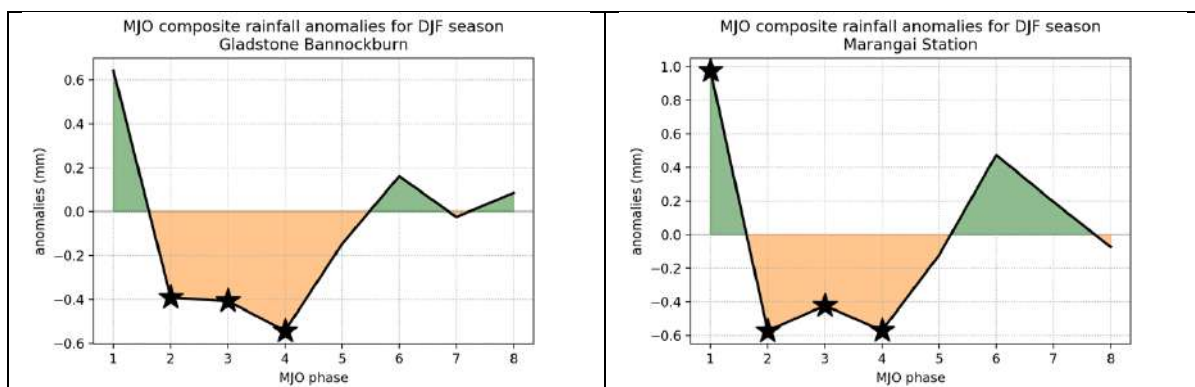


### 1.1.2 Station data

The station level daily rainfall also tends to be significantly modulated by the MJO, with good agreement between the stations within each season, and a sign and amplitude of the anomalies as a function of the season and MJO phase consistent with the VCSN composite anomalies. We here present two representative examples for each season, with the full set of composites conducted for all available stations being available in the electronic supplementary material to this report.

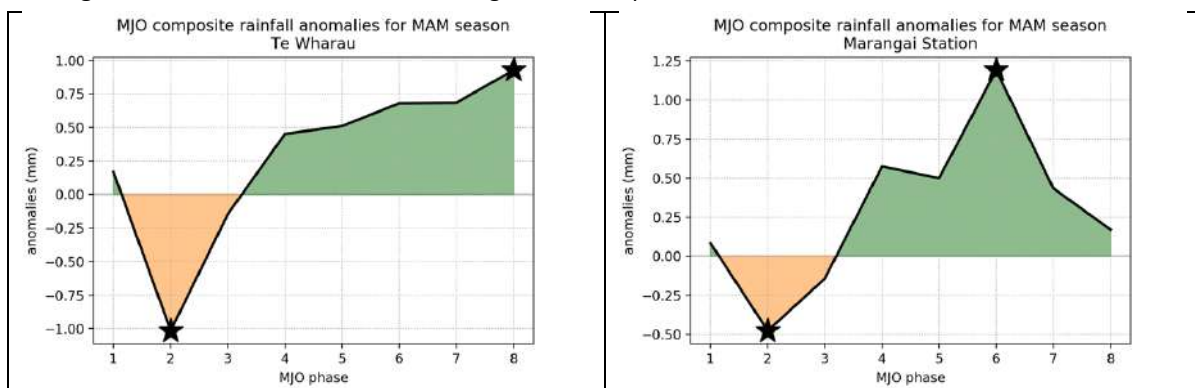
## DJF

**Figure 1-5: Daily rainfall anomalies associated with each phase of the MJO for DJF for Gladstone Bannockburn and Marangai Station.** Stars indicate statistical significance at  $p \leq 0.05$ .



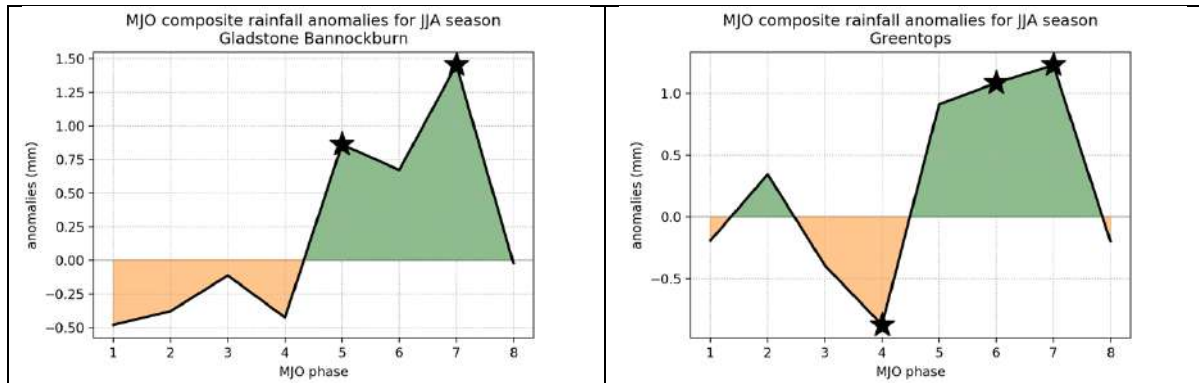
## MAM

**Figure 1-6: Daily rainfall anomalies associated with each phase of the MJO for MAM for Te Wharau and Marangai Station.** Stars indicate statistical significance at  $p \leq 0.05$ .



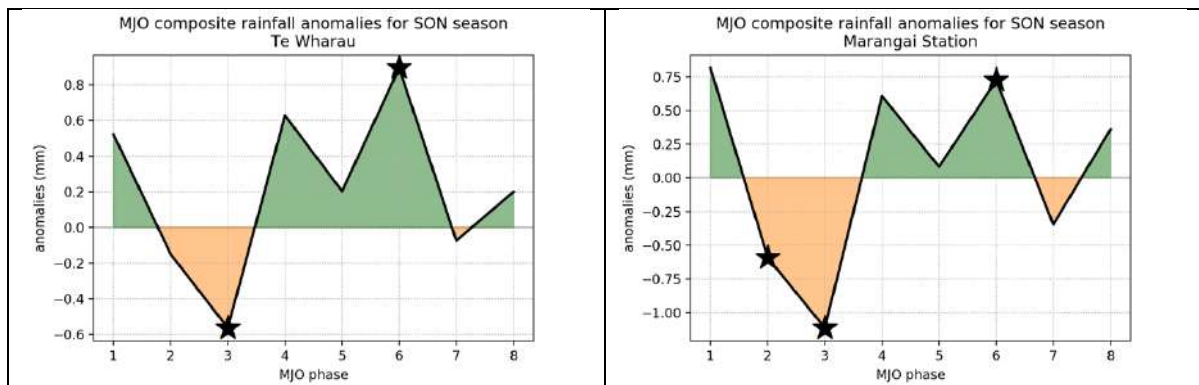
## JJA

**Figure 1-7: Daily rainfall anomalies associated with each phase of the MJO for JJA for Gladstone Bannockburn and Greentops. Stars indicate statistical significance at  $p \leq 0.05$ .**



## SON

**Figure 1-8: Daily rainfall anomalies associated with each phase of the MJO for SON for Te Wharau and Marangai Station. Stars indicate statistical significance at  $p \leq 0.05$ .**



## 1.2 Mean maximum temperature

### 1.2.1 VCSN

As was the case for rainfall, the VCSN composite anomalies associated with each phase of the MJO indicate a significant modulation of daytime daily temperatures over the Wellington Region by the MJO signal. However, with a few exceptions, the anomalies are relatively modest. A summary of the main results of interest is given below:

In DJF (Figure 1-9), daily maximum temperatures are higher than normal over large parts of the Wellington Region during phase 5 and moreover 6 of the MJO.

In MAM (Figure 1-10), phases 2 and to some extent phase 3 of the MJO are related to increased daytime temperatures over the region.

In JJA (Figure 1-11), the main signal is found for phase 3 of the MJO (increased daytime temperatures).

In SON (Figure 1-12), phases 4, 5 and 6 are associated with higher daily maximum temperatures, during phase 2, higher temperatures are found in the eastern half of the Wellington Region, and during phase 1 the western part of the Wellington Region tends to register lower than normal daytime temperatures.



**Figure 1-9: Daily mean maximum temperature anomalies associated with each phase of the MJO for the DJF season (VCSN composite) in the Wellington Region.** Red lines outline areas of statistical significance at  $p \leq 0.05$ .

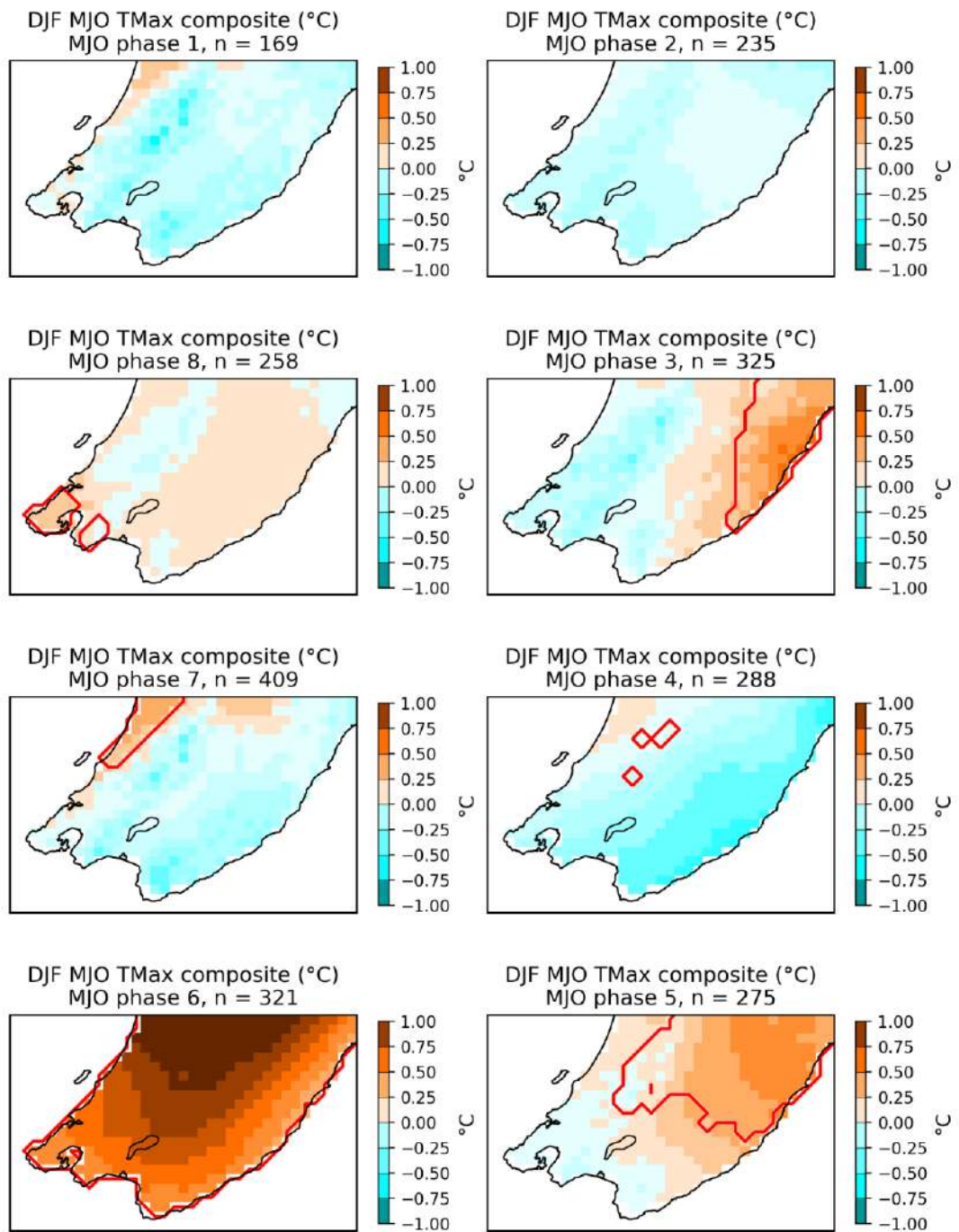


**Figure 1-10: Daily mean maximum temperature anomalies associated with each phase of the MJO for the MAM season (VCSN composite) in the Wellington Region. Red lines outline areas of statistical significance at  $p \leq 0.05$ .**

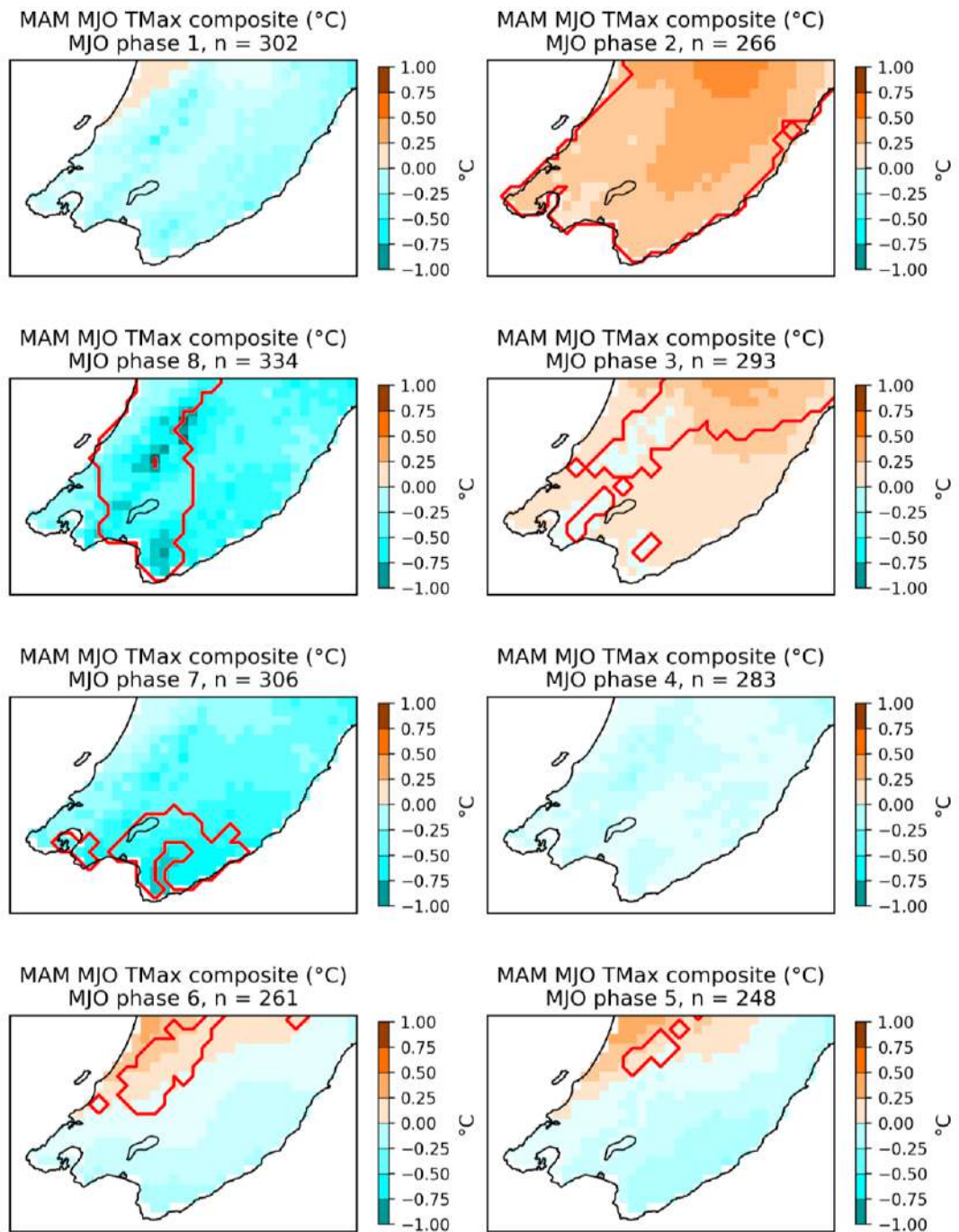


**Figure 1-11: Daily mean maximum temperature anomalies associated with each phase of the MJO for the JJA season (VCSN composite) in the Wellington Region.** Red lines outline areas of statistical significance at  $p < 0.05$ .

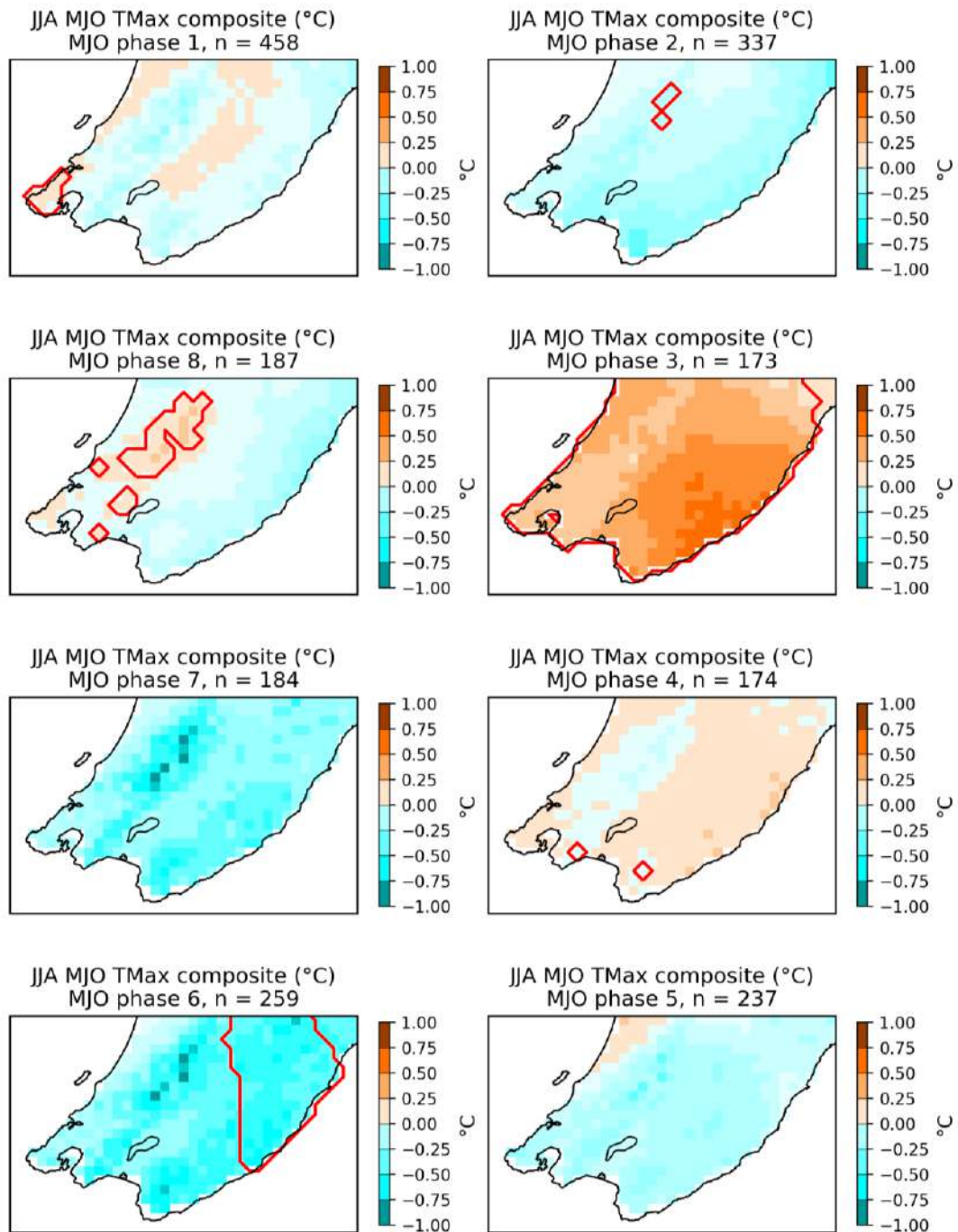
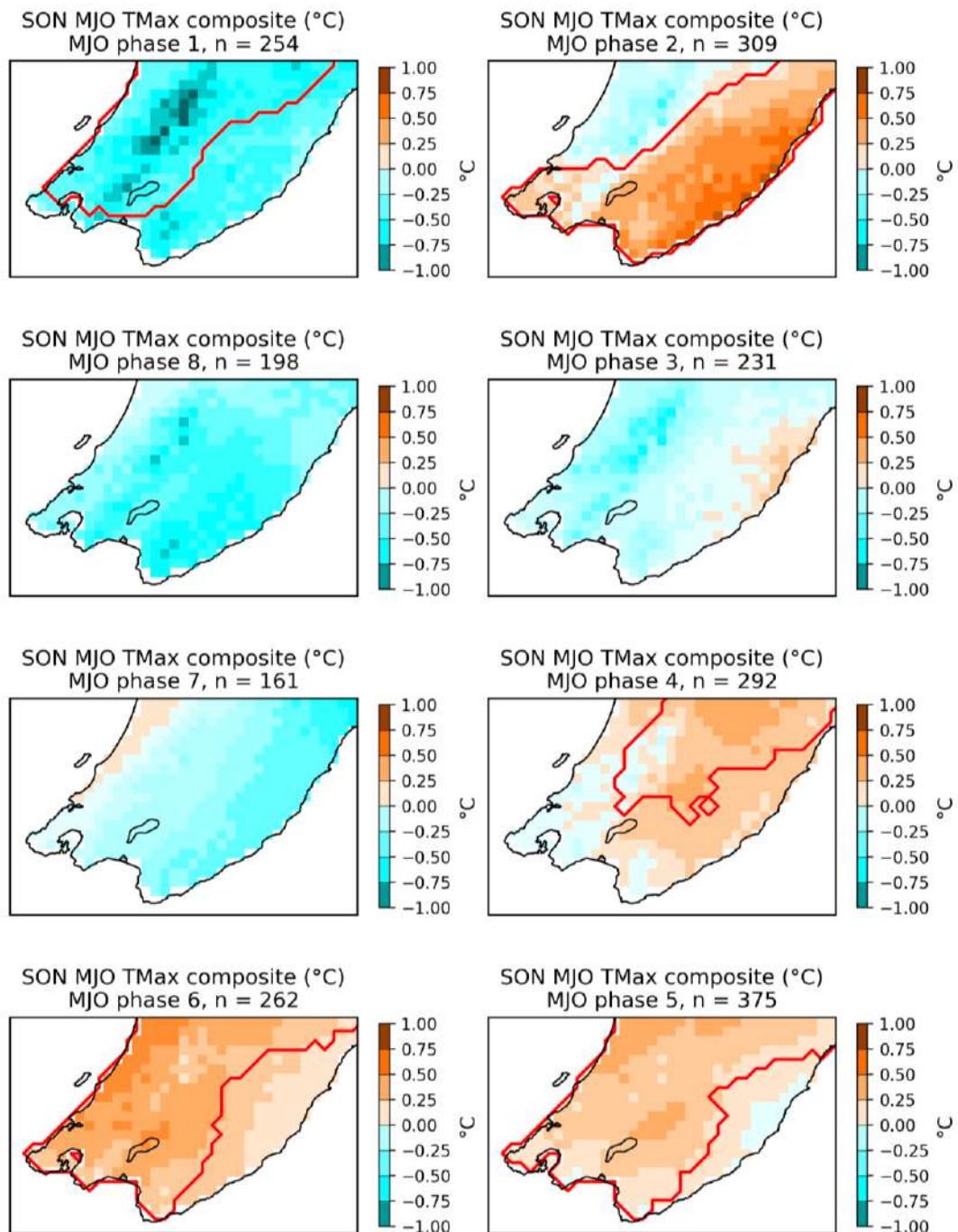


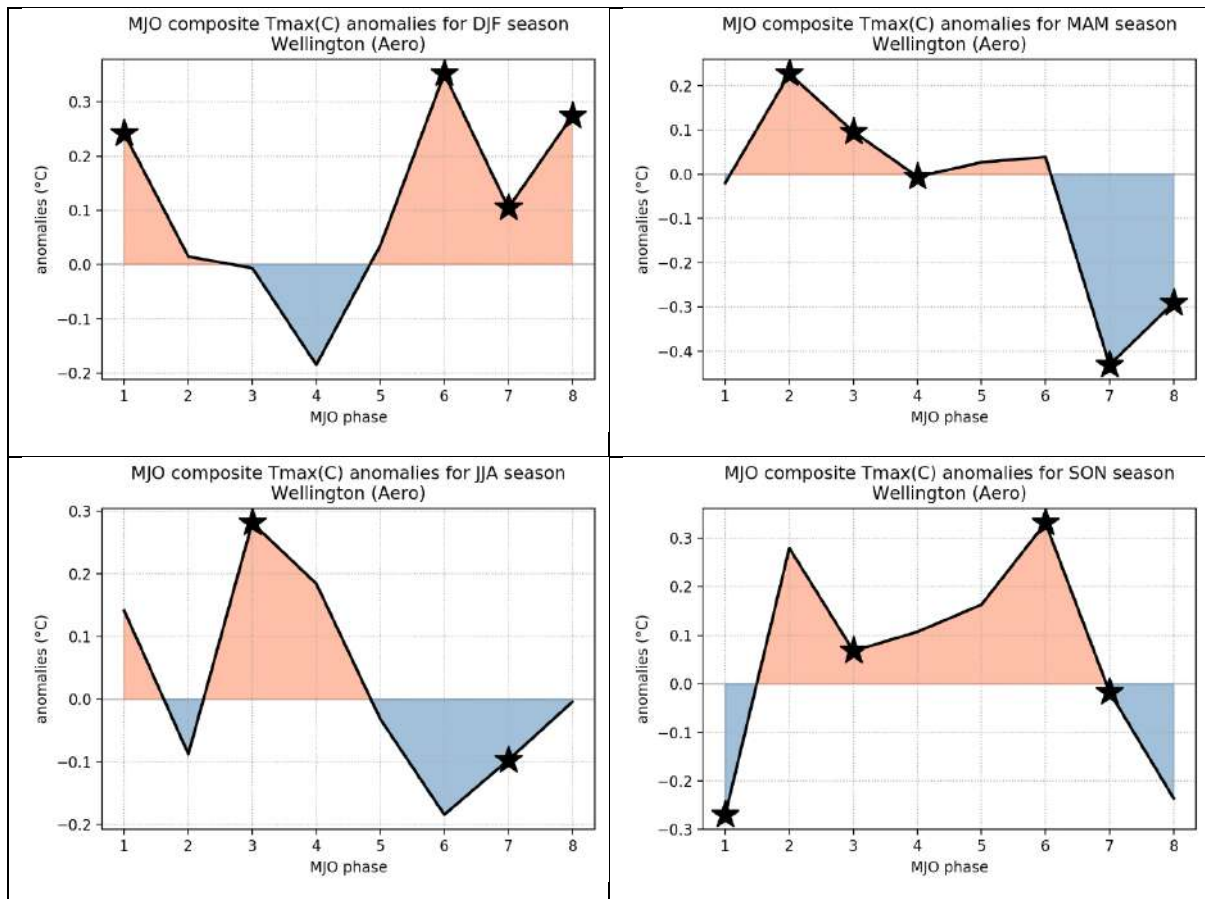
**Figure 1-12: Daily mean maximum temperature anomalies associated with each phase of the MJO for the SON season (VCSN composite) in the Wellington Region. Red lines outline areas of statistical significance at  $p \leq 0.05$ .**



### 1.2.2 Station data

The station level data broadly confirms the patterns displayed by the VCSN. For the sake of brevity, we present here the results for the Wellington Aero station (Figure 1-13), with the results for the stations of Castlepoint (Composite), Kelburn and Paraparaumu Aero being available in the electronic supplementary material for this report.

**Figure 1-13: Seasonal mean maximum temperature anomalies associated with each phase of the MJO for Wellington Aero.** Stars indicate statistical significance at  $p \leq 0.05$ .



## 1.3 Mean minimum temperature

### 1.3.1 VCSN

While significant anomalies in daily minimum temperatures are observed as a function of the MJO phase (Figures 1-14 to 1-17), it is important to note that in some cases, they are opposite to the sign of the anomalies recorded for the daily maximum temperature. In other words, daytime and night-time temperatures seem to be affected differently by the MJO life-cycle, therefore likely implicating cloud cover and its differential effect on long-wave and short-wave radiation fluxes. For example, increased cloud cover would tend to decrease daytime temperature (decreased short-wave downward radiation flux) and increase night-time temperatures (decreased long-wave outgoing radiation flux). An illustration can be given for the phase 5 of the MJO in the JJA season: this phase of the MJO is associated with warmer than normal night-time temperatures (positive minimum temperature anomalies), cooler than normal daytime temperatures (negative maximum temperature anomalies) and corresponds to increased rainfall (and therefore presumably cloud cover). In many instances however the relationships between the rainfall, daytime and night-time temperatures anomalies indicate more complex processes, probably mediated by the circulation anomalies associated with the MJO (see Fauchereau et al. (2016)), via airmass origins and the interactions with the topography of the Wellington Region. A detailed investigation of these processes is outside the scope of this report, but certainly would need attention in the context of a follow-up study.

**Figure 1-14: Daily mean maximum temperature anomalies associated with each phase of the MJO for the DJF season (VCSN composite) in the Wellington Region. Red lines outline areas of statistical significance at  $p \leq 0.05$ .**

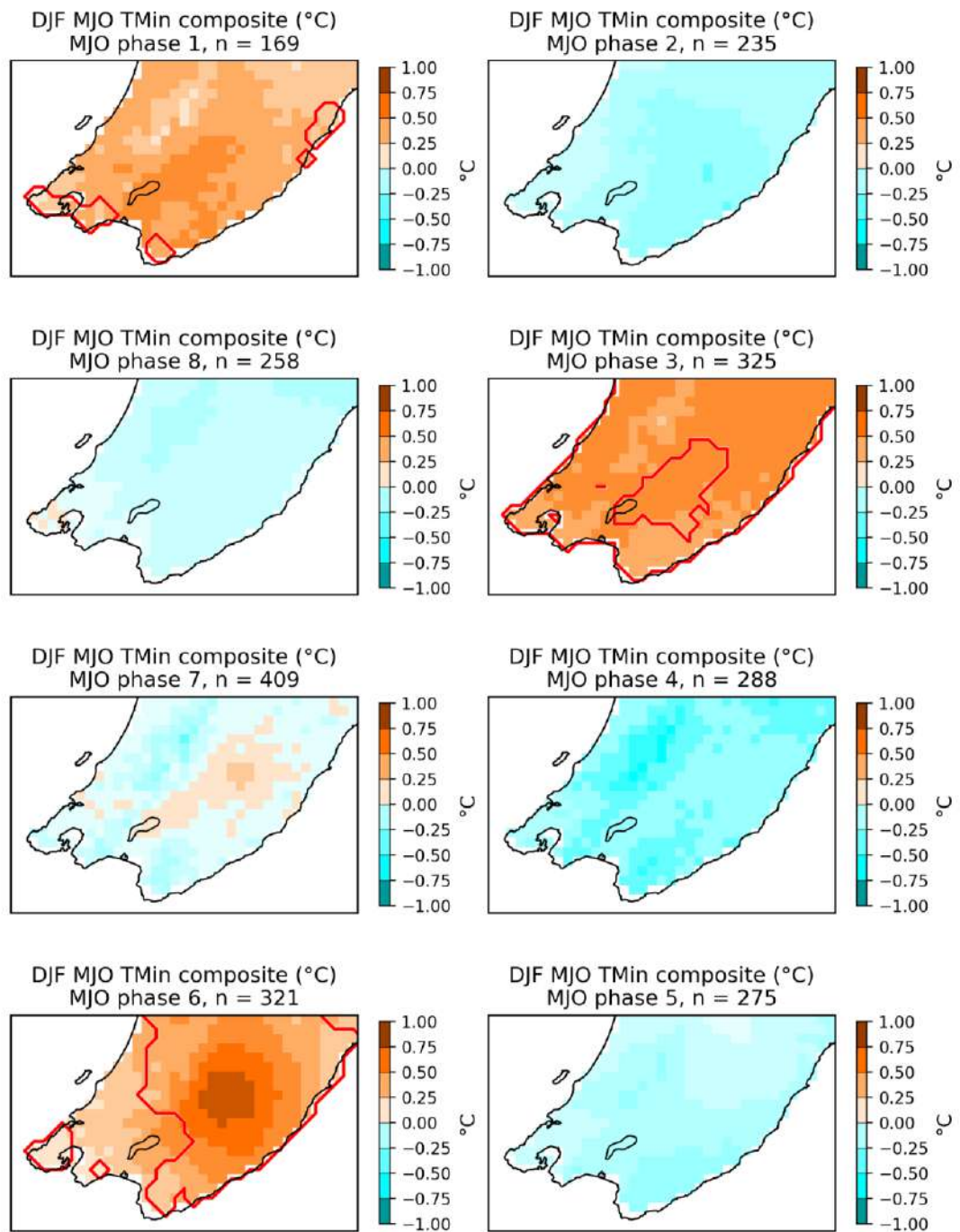


**Figure 1-15: Daily mean maximum temperature anomalies associated with each phase of the MJO for the MAM season (VCSN composite) in the Wellington Region. Red lines outline areas of statistical significance at  $p \leq 0.05$ .**

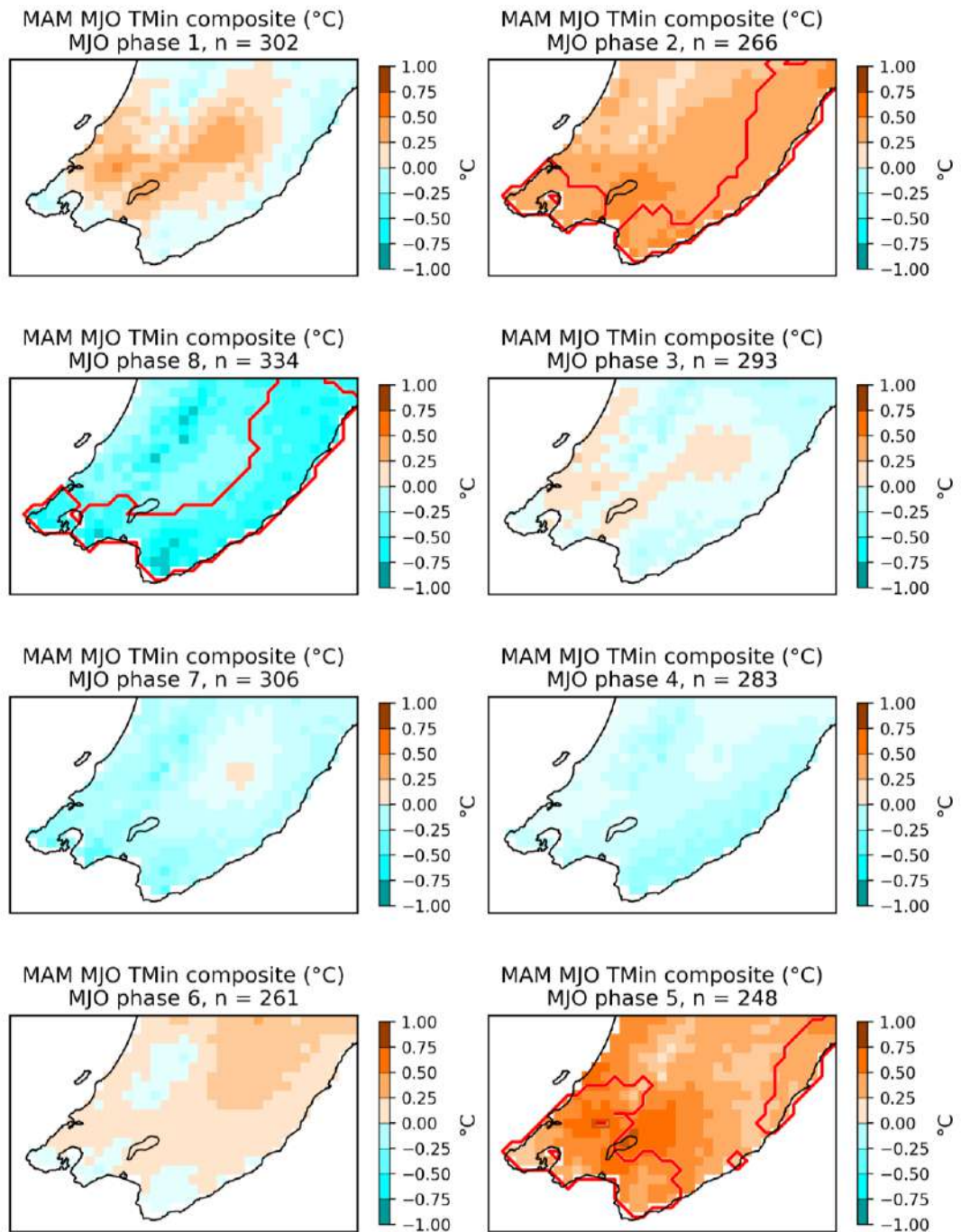




**Figure 1-16: Daily mean maximum temperature anomalies associated with each phase of the MJO for the JJA season (VCSN composite) in the Wellington Region.** Red lines outline areas of statistical significance at  $p \leq 0.05$ .

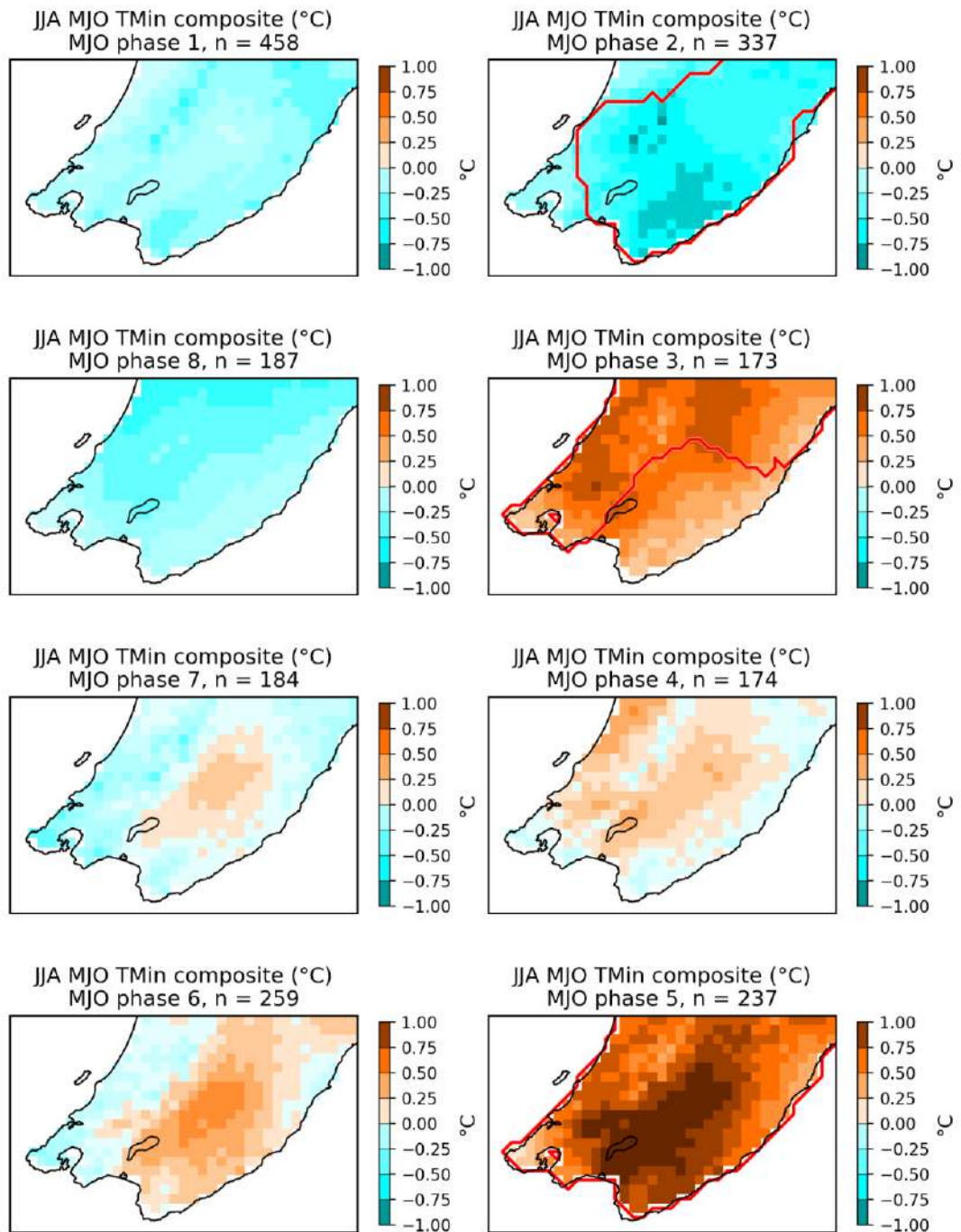
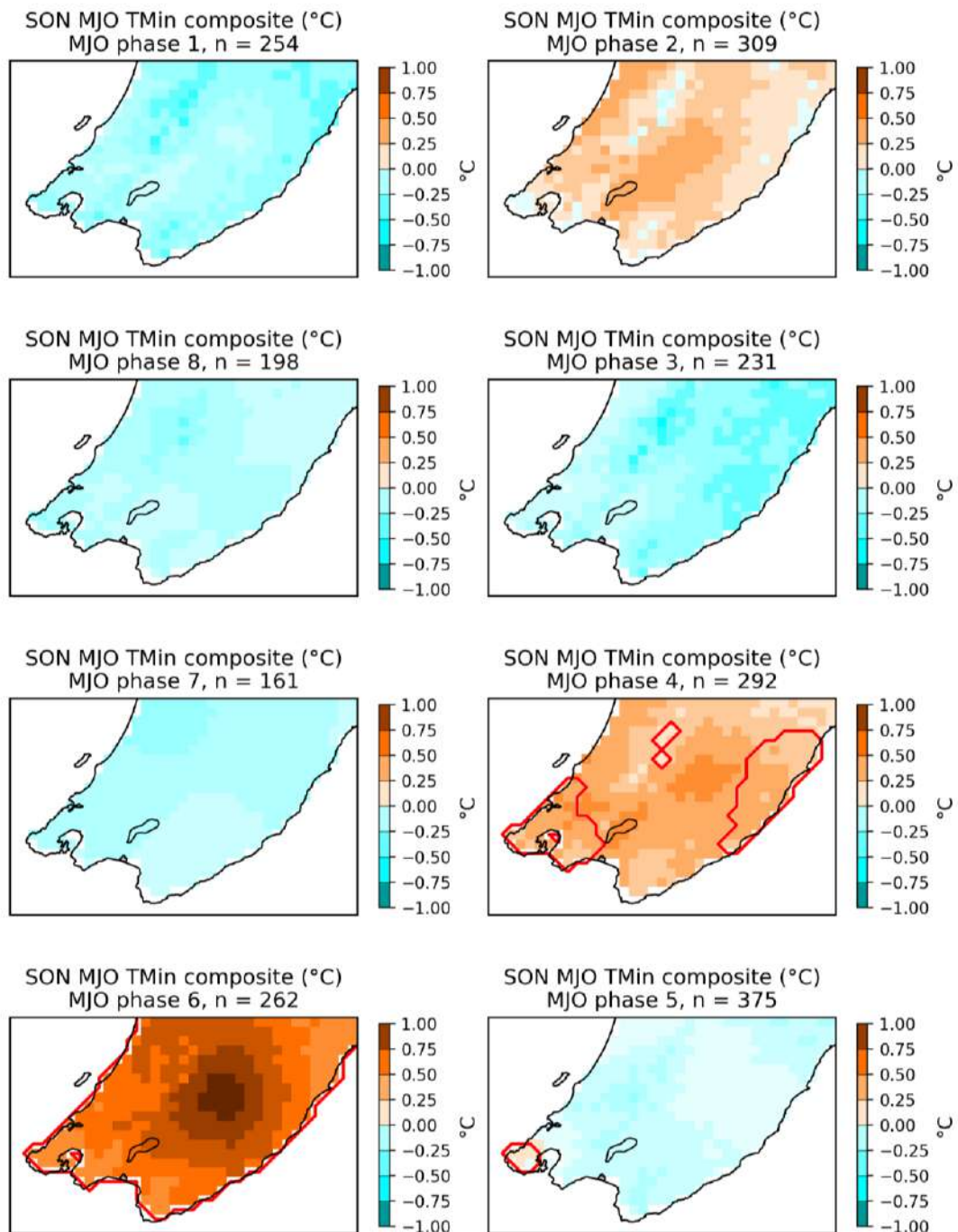


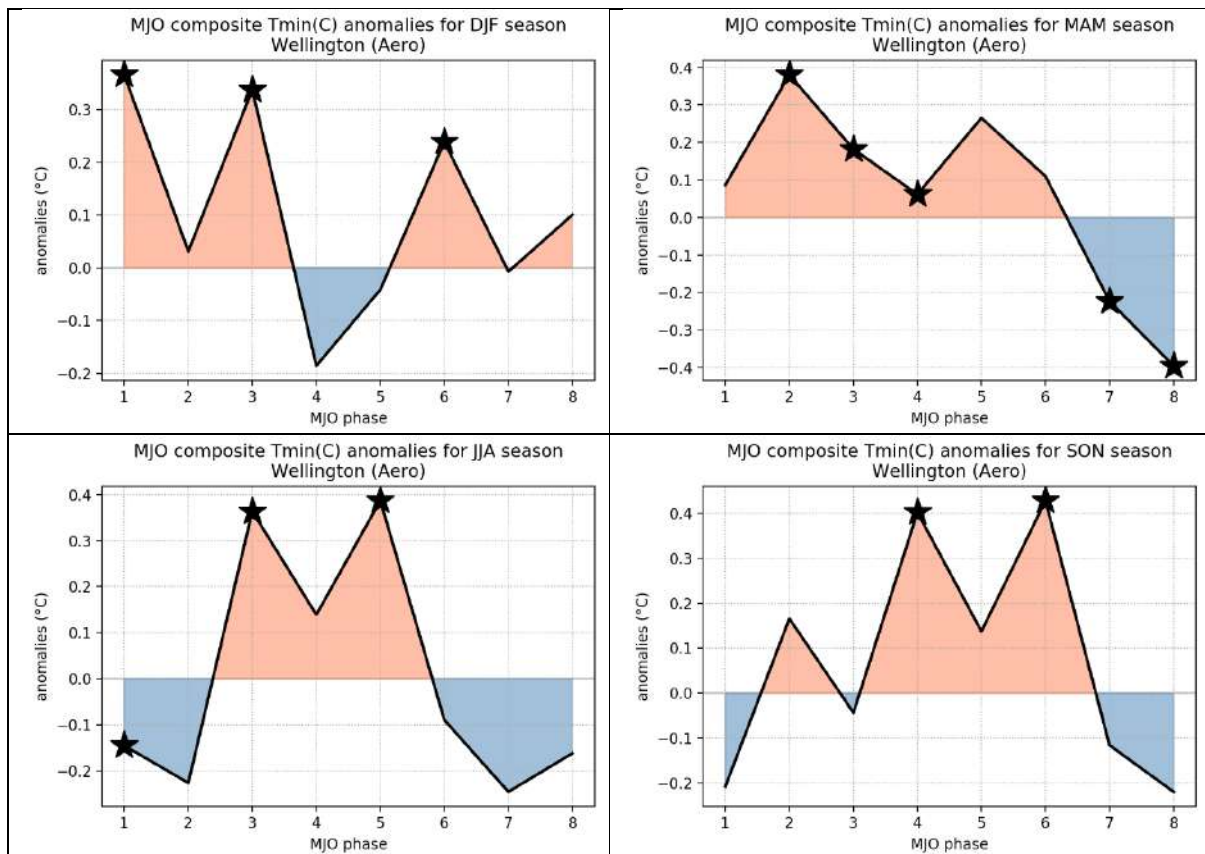
**Figure 1-17: Daily mean maximum temperature anomalies associated with each phase of the MJO for the SON season (VCSN composite) in the Wellington Region. Red lines outline areas of statistical significance at  $p \leq 0.05$ .**



### 1.3.2 Station data

As for Section 1.2.2 on the mean maximum temperature anomalies, we only present here the results for the Wellington Aero station (Figure 1-18), with the results for the stations of Castlepoint (Composite), Kelburn and Paraparaumu being available in the electronic supplementary material for this report.

**Figure 1-18: Seasonal mean minimum temperature anomalies associated with each phase of the MJO for Wellington Aero.** Stars indicate statistical significance at  $p \leq 0.05$ .



## 2 The impact of the Southern Annular Mode on the Wellington Region's climate at the sub-seasonal timescale

In this section, instead of considering the seasonal SAM index derived from the **monthly** mean anomalies of geopotential height in the Southern Hemisphere (see Part A - Methodology section), we use the so-called daily AAO (Antarctic Oscillation) index, available from the CPC from 1979 to present, at URL: <ftp://ftp.cpc.ncep.noaa.gov/cwlinks/norm.daily.aao.index.b790101.current.ascii>

We use the same compositing approach to derive the daily rainfall, maximum and minimum temperature anomalies (in the VCSN) associated with the positive (daily AAO index > 1 std.) and negative (daily AAO index < -1 std.) phases of the SAM, independently for each season.

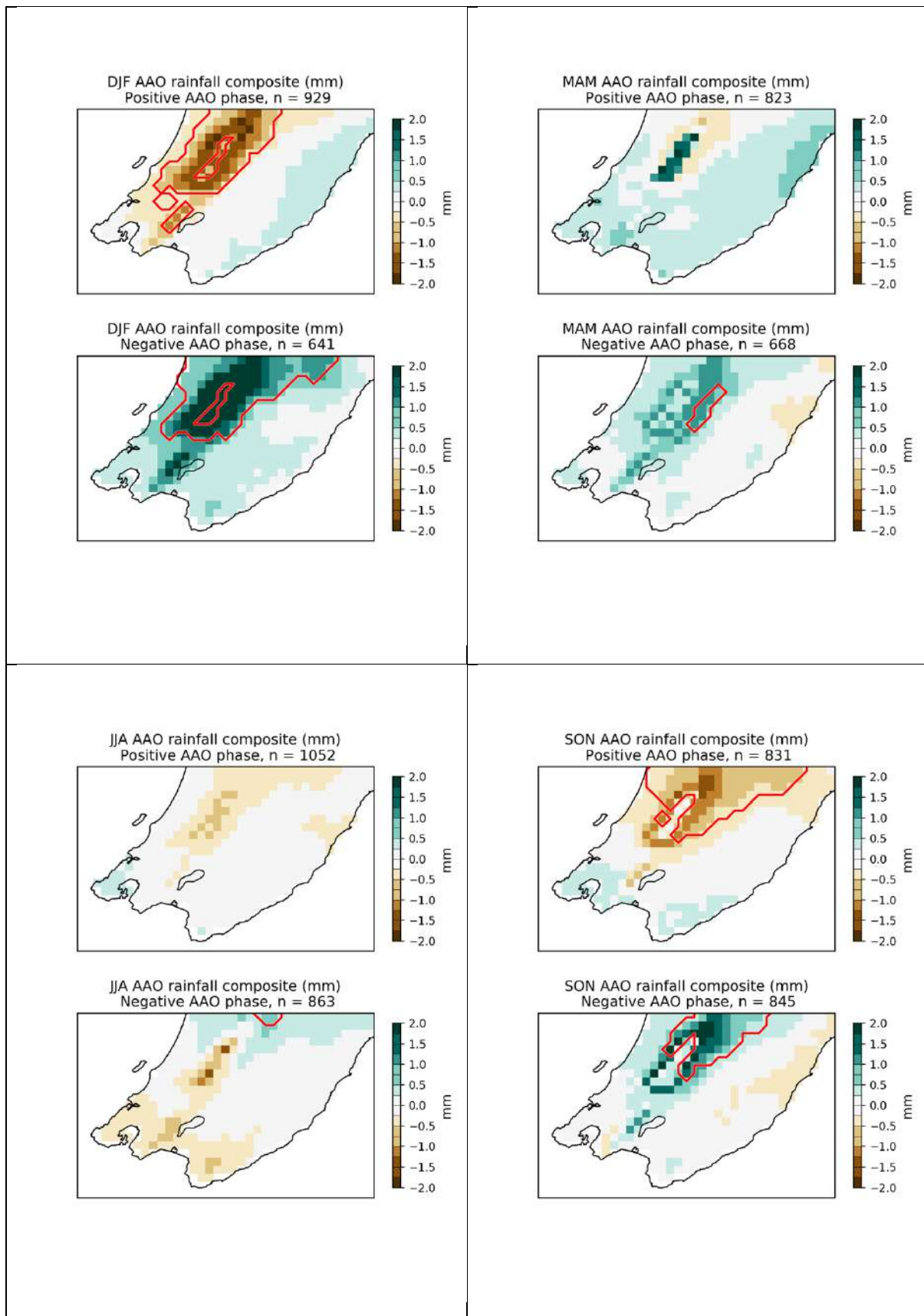
### 2.1 Rainfall

The results indicate that at the sub-seasonal timescale, the SAM is associated with significant rainfall anomalies, notably over the western part of the Wellington Region (Figure 2-1). In SON and moreover in DJF, a positive SAM is associated with decreased rainfall in this area, while a negative SAM is associated with increased rainfall.

It is therefore important to note that the rainfall's response to the SAM signal is therefore stronger and more consistent (*i.e.* symmetric, and spatially coherent) at the sub-seasonal (*i.e.* when the daily SAM index and daily rainfall anomalies are considered) than at the inter-annual timescale (when seasonally aggregated variables are considered).

This is an important result and has implications in terms of predictability at the sub-seasonal timescale: As Fauchereau et al (2016) indicated that the MJO signals over the NZ region appears mostly to be independent from the SAM, the combined impact of the MJO and the SAM at the sub-seasonal timescale therefore could provide enhanced potential predictability of some aspects of the Wellington Region's climate at timescales beyond the weather timescale (~ 10 days to ~ a month).

**Figure 2-1: Daily rainfall anomalies and AAO phase for the Wellington Region (VCSN composite) for each of the four seasons. Red lines outline areas of statistical significance at  $p \leq 0.05$ .**



## 2.2 Maximum and minimum daily temperatures

Similar to rainfall, significant and consistent anomalies are obtained for the positive and negative phase of the SAM for the maximum daily temperatures from the VCSN (Figure 2-2). In all seasons, but with larger amplitudes and extent in SON and DJF, the positive phase of the SAM is related to increased daily maximum temperatures while the negative phase of the SAM is associated with cooler than normal daytime temperatures. This signal is stronger and more coherent in the northwest part of the Wellington Region, a characteristic also present for the rainfall anomalies.

Daily minimum (*i.e.* night-time) temperatures anomalies associated with the SAM (Figure 2-3) are however much less strong and less consistent than for daily maximum temperatures, indicating possibly that the response of daily temperatures to the SAM involves a complex interplay of radiative effects and modulation by changes in the atmospheric circulation (airmass origins). As for the MJO, an examination of the physical mechanisms leading to changes in rainfall, daytime and night-time temperatures could be conducted in a follow-on study.

**Figure 2-2: Daily mean maximum temperature anomalies and AAO phase for the Wellington Region (VCSN composite) for each of the four seasons. Red lines outline areas of statistical significance at  $p \leq 0.05$ .**

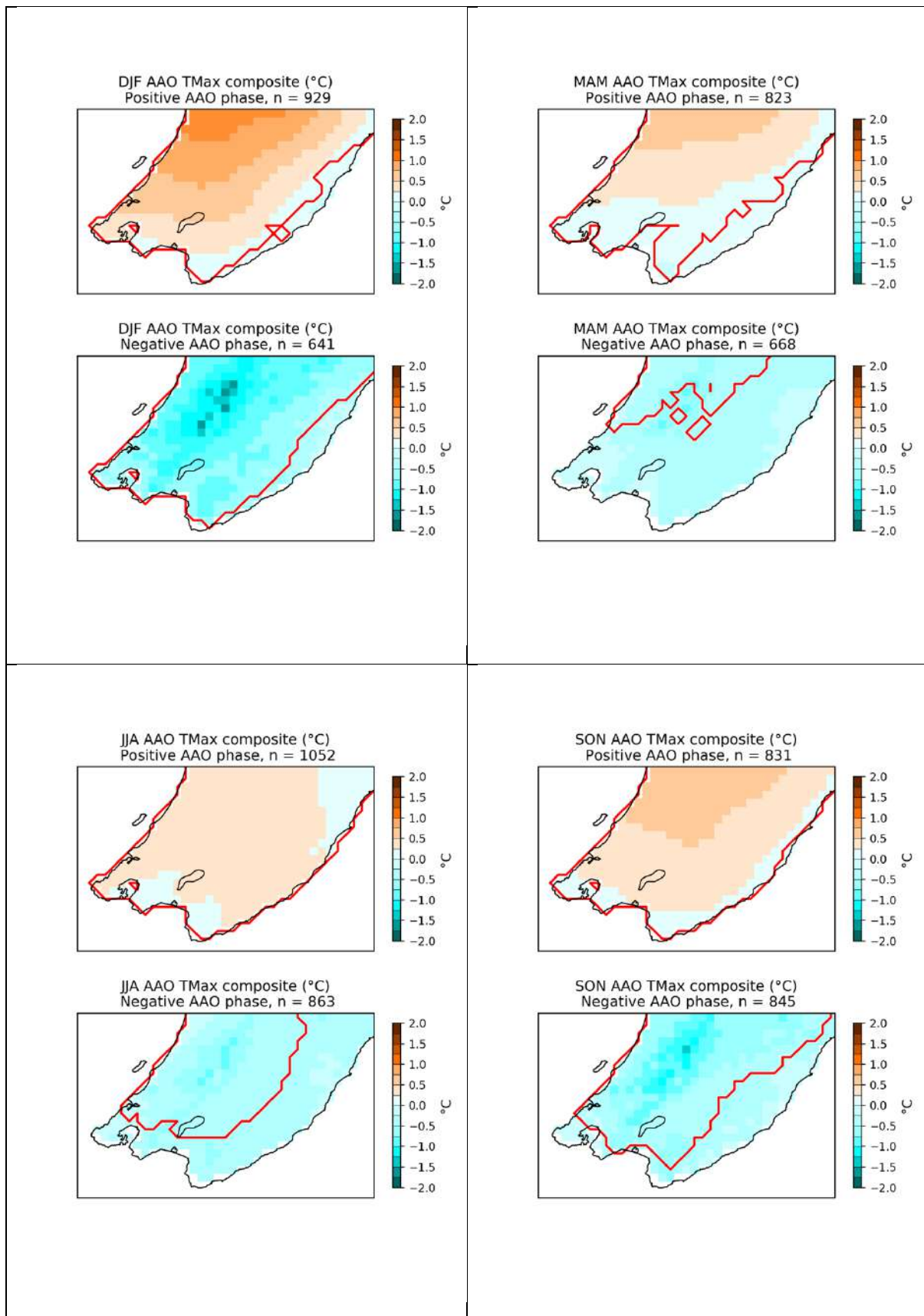
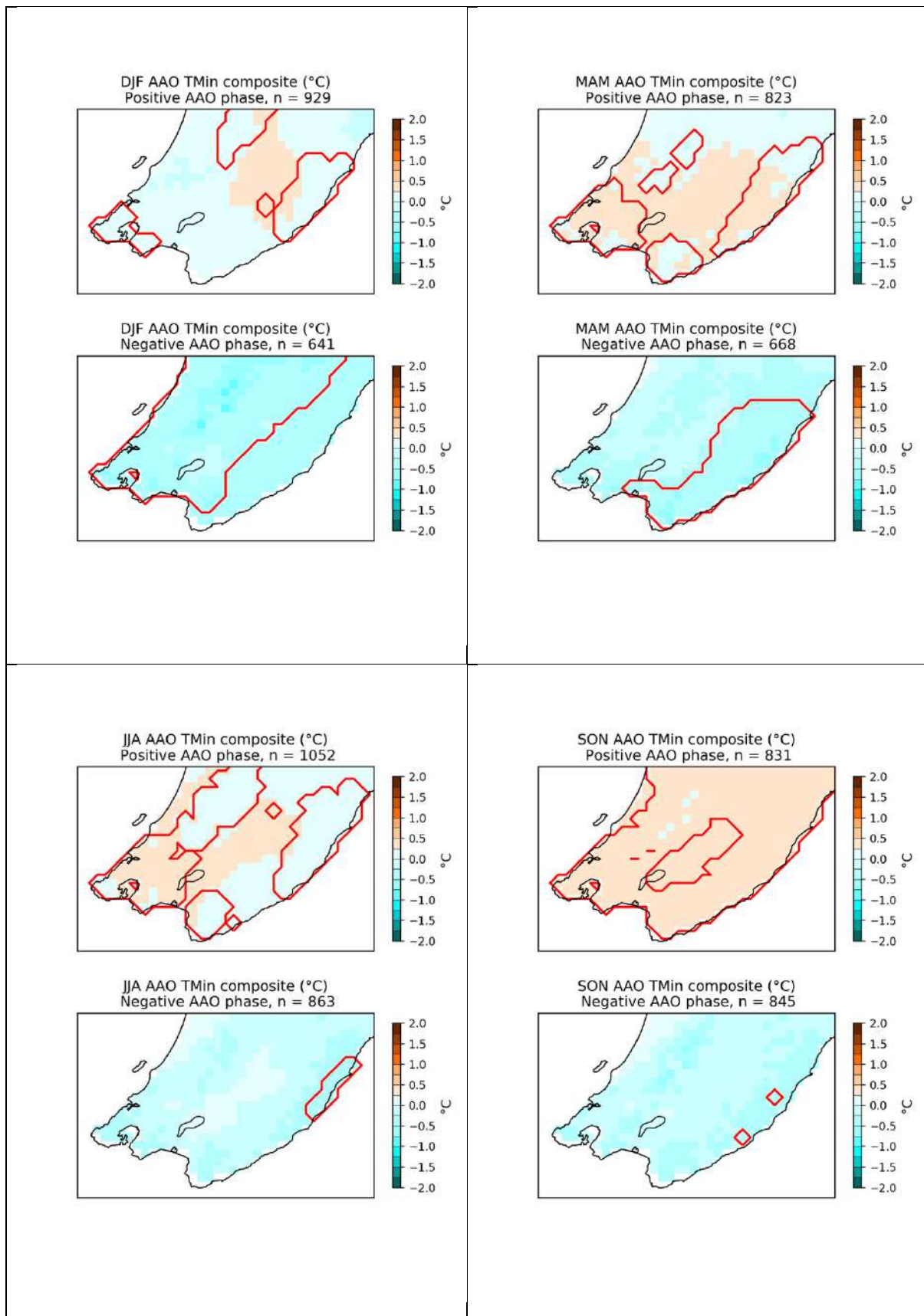


**Figure 2-3: Daily mean minimum temperature anomalies and AAO phase for the Wellington Region (VCSN composite) for each of the four seasons. Red lines outline areas of statistical significance at  $p \leq 0.05$ .**

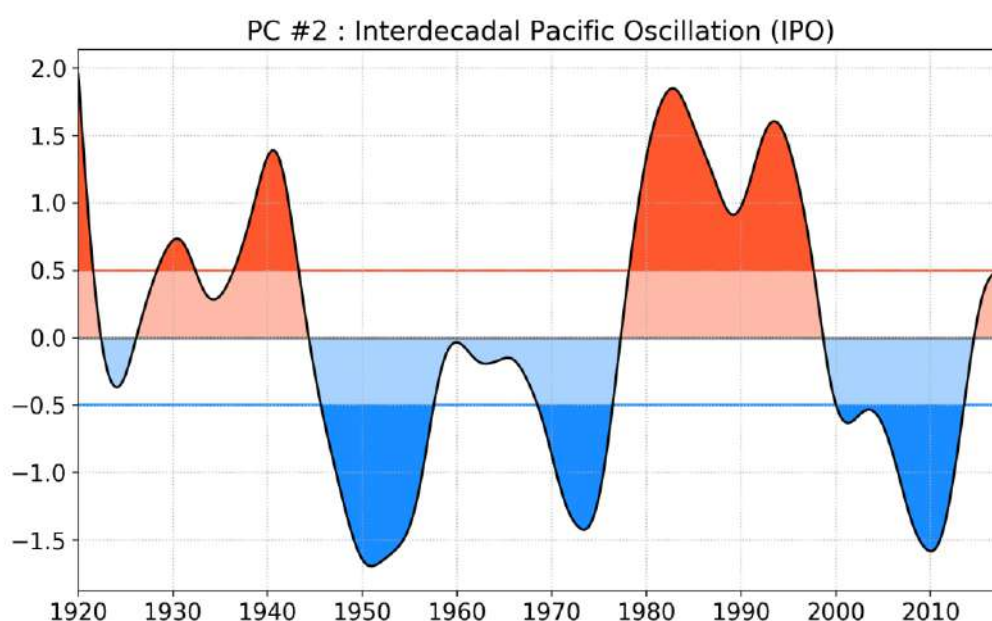




### 3 Relationship to the Interdecadal Pacific Oscillation (IPO)

As indicated in Part A - Introduction and methodology section and in the introductory part of this section, to characterise the variability of the IPO we use the second PC derived from an EOF (Empirical Orthogonal Function) analysis of low-pass (periodicities > 11 years) filtered monthly SST anomalies in the Pacific region (see Part A - introduction and methodology section for more information). We here again use a compositing approach, selecting samples corresponding to when the normalized IPO index exceeds 0.5 std. (positive IPO) or is less than -0.5 std. (negative IPO). Figure 3-1 illustrates the IPO with the periods corresponding to the thresholds above highlighted.

**Figure 3-1: Phases of the IPO. Positive >0.5 std (red), negative <-0.5 std (blue).**



Over the period 1920-2017, the IPO was positive mostly from the mid-1920s to the mid-1940s, negative from the mid-1940s to the 1970s, then positive again from the late 1970s to the late 1990s. Over the most recent period (2000 onwards) a negative IPO dominated until the past 2 years, where it became positive again.

We performed the composite analyses for the positive and negative IPO periods (for each of the DJF, MAM, JJA and SON seasons independently), and investigated whether the different station level climate variables were significantly different between the positive and negative phases: i.e. we seek to see whether the positive and negative phase of the IPO are related to different climate parameter distributions. To illustrate the full distribution of the different climate variables, we use a 'violin plot' representation. A violin plot is similar to box plot with a rotated kernel density plot on each side - it includes a white marker for the median of the data and a box indicating the interquartile range, as in standard box plots. Overlaid on this box plot is a kernel density estimation, which then provides a convenient summary of the full distribution.

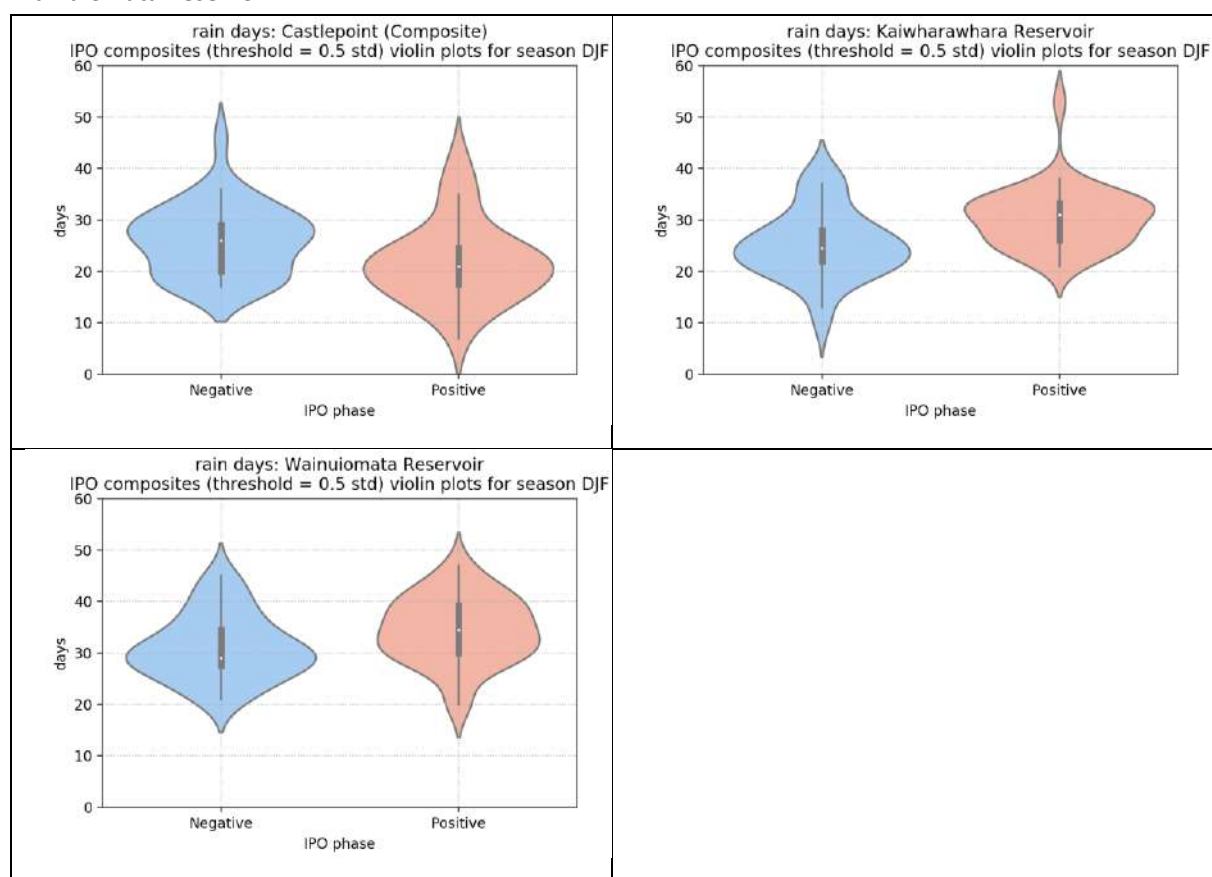
### 3.1 Total rainfall and number of heavy rainfall days

For all stations, we found no significant differences in either the average cumulative rainfall, or the number of heavy rainfall days, between the positive and negative phases of the IPO.

### 3.2 Number of rain days (> 0.5 mm)

In contrast to cumulative rainfall, a number of stations record a significant difference in the number of rain days between the positive and negative phase of the IPO, mostly during SON and DJF (Figure 3-2). This is the case notably for Castlepoint (Composite), which tends to record fewer rain days during the positive than the negative phase of the IPO in DJF. In contrast, Kaiwharawhara Reservoir, and Wainuiomata Reservoir show the reverse relationship (more rain days during the positive IPO phase). (Figure 3-2).

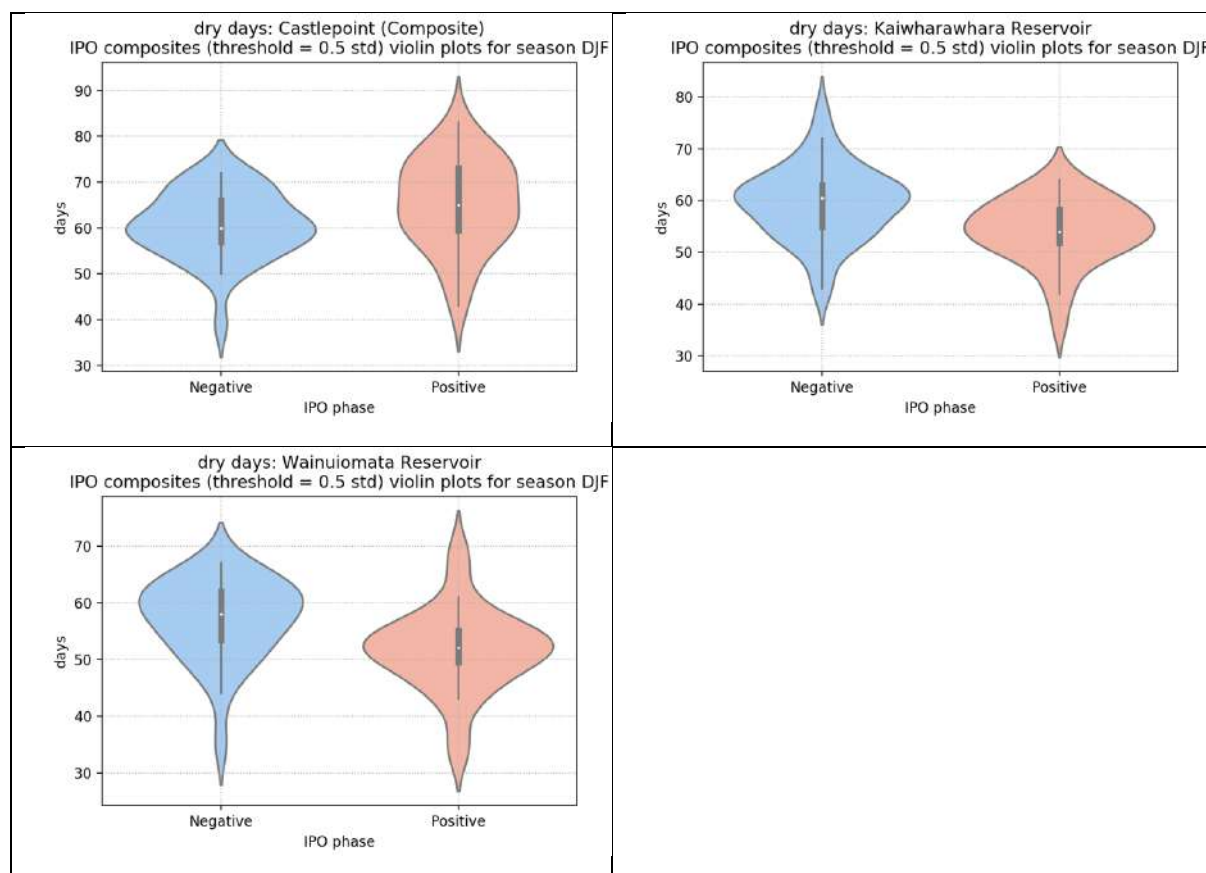
**Figure 3-2: Rain days (> 0.5 mm) and IPO phase for Castlepoint (composite), Kaiwharawhara Reservoir, and Wainuiomata Reservoir.**



### 3.3 Number of dry days (0 mm rain)

Consistent with the relationships shown for the number of rain days, the number of dry days for the above-mentioned stations is significantly different between the positive and the negative IPO phase. Castlepoint (Composite) tends to experience fewer rain days during the negative phase of the IPO compared to the positive phase (Figure 3-3). For Kaiwharawhara Reservoir and Wainuiomata Reservoir conversely, the number of dry days tend to be higher during negative than the positive phase of the IPO.

**Figure 3-3: Dry days (0 mm rain) and IPO phase for Castlepoint (composite), Kaiwharawhara Reservoir, and Wainuiomata Reservoir.**



### 3.4 Temperature indices

No significant relationships with the IPO were found for the mean seasonal temperatures or for the indices derived from the daily station time-series (mean maximum and minimum temperature, number of hot days and number of frost days).

## 4 References

- BALDWIN, M. P., STEPHENSON, D. B., THOMPSON, D. W. J., DUNKERTON, T. J., CHARLTON, A. J. & O'NEILL, A. 2003. Stratospheric memory and extended-range weather forecasts. *Science*, 301, 636-640.
- FAUCHEREAU, N., POHL, B. & LORREY, A. 2016. Extratropical Impacts of the Madden–Julian Oscillation over New Zealand from a Weather Regime Perspective. *Journal of Climate*, 29, 2161-2175.
- GERBER, E. P., VORONIN, S. & POLVANI, L. 2008. Testing the Annular Mode Autocorrelation Time Scale in Simple Atmospheric General Circulation Models. *Monthly Weather Review*, 136, 1523-1536, <http://journals.ametsoc.org/doi/abs/10.1175/2007MWR2211.1>.
- WHEELER, M. C. & HENDON, H. H. 2004. An All-Season Real-Time Multivariate MJO Index: Development of an Index for Monitoring and Prediction. *Monthly Weather Review*, 132, 1917-1932.

# Regional climate mode impacts on the Wellington Region

*Part G: Conclusions, implications for seasonal predictability, and  
limitations*

## 1 Conclusions

This study investigated the relationship between climate variables (rain, temperature, wind, and soil moisture) and climate modes in the Wellington Region. The climate modes considered were El Niño-Southern Oscillation (ENSO), the Southern Annular Mode (SAM), the Indian Ocean Dipole (IOD), the South Pacific Subtropical Dipole (SPSD), the Madden Julian Oscillation (MJO), and the Interdecadal Pacific Oscillation (IPO).

At the inter-annual timescale, composite analyses revealed that there is often a non-linear relationship between climate modes and climate variables. For example, both the positive and negative phases of ENSO (El Niño and La Niña respectively) are associated with decreased rainfall, an increase in the number of dry days, and a decrease in the number of wet days over parts of the Wellington Region. Generally speaking, the VCSN-derived composites suggest that for all seasons, there are no areas of statistically significant positive rainfall anomalies. This suggests that all climate modes tend to imply drying over the Wellington region, no matter what mode, season or phase. The station data tends to confirm this interpretation, except for Marangai and Lagoon Hill which indicate a significant positive rainfall anomaly during spring for both phases of the PSD. Often there are no statistically significant relationships between seasonally-aggregated climate modes and climate variables. However, temperature-derived indices (e.g. mean seasonal minimum and maximum temperatures, number of hot days and frost days) are most significantly associated with the PSD, a climate mode which is associated with regional sea surface temperatures (SSTs) in the South Pacific. In addition, temperatures in the Wellington Region are strongly correlated with SSTs around New Zealand, i.e. SSTs are an important driver of surface air temperature in the region.

Investigations of lagged composite and correlations between the climate modes and climate variables in the Wellington region indicated that the maximum impacts tend to be synchronous rather than delayed.

At the sub-seasonal timescale (1 to ~60 days), there are strong, statistically significant relationships between the Madden-Julian Oscillation and rainfall and temperature indices. There is a particularly strong signal with regards to rainfall in winter (JJA). Given the propagative nature and relative predictability of the MJO at the horizon of 2-4 weeks, this finding opens the possibility for developing forecast products for timescales beyond the weather forecasting horizon (i.e. ~10 days to ~1 month).

This potential is further enhanced by relationships evidenced with the SAM. While limited significant relationships between the Southern Annular Mode and climate variables were found the inter-annual timescale, the impacts of the SAM on rainfall and temperature at the sub-seasonal timescale are generally strong, statistically significant, and symmetric between the positive and negative phase of the SAM. The positive phase of the SAM is related to decreased rainfall over the western part of the Wellington Region in spring and summer, while the reverse is true during the negative phase. Mean maximum temperatures tend to increase during the positive phase of the SAM and decrease during the negative phase.

At the decadal timescale, there were limited relationships identified between the climate variables and the Interdecadal Pacific Oscillation for the Wellington Region. The only consistent relationships identified were regarding the number of rain days and dry days for some stations during the different phases of the IPO.

Overall, this study has revealed a number of interesting findings regarding the regional climate mode impacts on the climate of the Wellington Region. One of the most surprising findings was the non-

linearity of the relationships between climate variables and ENSO. This report and associated image dataset provides Greater Wellington Regional Council with a significant resource to understand climate variability in the Wellington Region, and there is the potential to develop forecasting guidance in the future, particularly using the results from the analyses focusing on the sub-seasonal timescale, showing strong and consistent relationships with the MJO and the SAM.

## 2 A summary of the relationships for seasonal prediction

While the relationships between the climate modes (ENSO, SAM, IOD and SPSP) and the climate of the Wellington Region are often weak and non-significant, and in some cases non-linear, some guidance can nevertheless be gained for the purpose of deriving a tailored seasonal climate outlook for the Wellington Region. A proposed approach would be to complement the guidance material and outlook that NIWA produces each month as part of its seasonal climate outlook (SCO, <https://www.niwa.co.nz/climate/seasonal-climate-outlook>) by monitoring of the current phase and amplitude of the main inter-annual climate modes presented in this report, most of them being updated in near-real-time (and in some case as for the NINO3.4 index explicitly forecast by international institutions). For this purpose, this section attempts to provide a brief summary of the main regional climate anomalies associated with the extreme (positive and negative) phases of each mode for each season. The goal is to provide a relatively easily searchable ‘quick reference’ for a climate researcher at the GWRC to complement the information provided by NIWA as part of its SCO.

The tables below are organised by season (DJF, MAM, JJA and SON) and for each mode in its opposite phases (positive and negative) provides a simple graphic summary of the anomalies over the Wellington Region. This graphic summary is organised according to the five Whaitua catchments of the Wellington Region and is mapped as follows in Figure 2-1: The colour of Whaitua reflects the sign of the anomalies: for hydrological conditions, brown means drier conditions (e.g. decreased rainfall and soil moisture) while blue means wetter conditions. For temperatures, the blue shade indicates negative anomalies, and the yellow shade positive anomalies. For wind, blue means windier than normal conditions, and orange less windy than normal. Note that in addition to the statistical significance, we also considered the magnitude of the anomalies, and Whaitua catchment is coloured if at least some VCSN grid-points are considered significant. We stress again that this simple graphical summary is a broad guidance tool, and the reader is referred to the actual composite anomaly maps in the relevant sections of this report for more details.

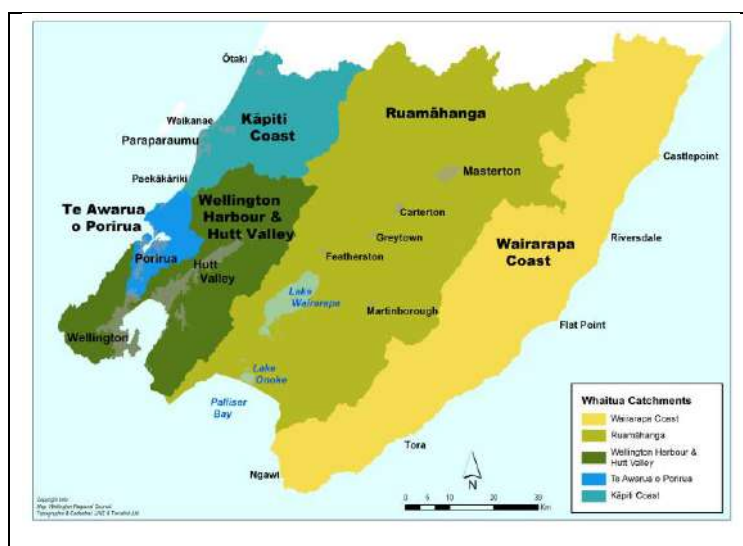


Figure 2-1: The five GWRC Whaitua catchments in summary tables, map from the Wellington Regional Council, URL <http://www.gw.govt.nz/assets/Environment-Management/Whaitua/whaituamap3.JPG>



## 2.1 Hydrological conditions summary

Table 2-1 presents a broad summary of the hydrological conditions in the Wellington Region (five Whaituas) associated with each of the four modes in their positive and negative phases, for each season (DJF, MAM, JJA, SON). Brown indicates drier conditions.

Table 2-1: Summary of hydrological conditions in the Wellington Region

		DJF	MAM	JJA	SON
NINO3.4	+				
	-				
		DJF	MAM	JJA	SON
SAM	+				
	-				
		DJF	MAM	JJA	SON
IOD	+				
	-				
		DJF	MAM	JJA	SON
SPSD	+				
	-				

## 2.2 Temperatures summary

Table 2-2 presents a broad summary of the temperature anomalies in the Wellington Region (five Whaituas) associated with each of the four modes in their positive and negative phases, for each season (DJF, MAM, JJA, SON). Blue means cooler than normal conditions, and yellow warmer than normal.

**Table 2-2: Summary of temperature anomalies in the Wellington Region**

		DJF	MAM	JJA	SON
NINO3.4	+				
	-				
		DJF	MAM	JJA	SON
SAM	+				
	-				
		DJF	MAM	JJA	SON
IOD	+				
	-				
		DJF	MAM	JJA	SON
SPSD	+				
	-				

## 2.3 Wind conditions summary

Table 2-3 presents a broad summary of the wind speed anomalies in the GWRC region (five Whaituas) associated with each of the four modes in their positive and negative phases, for each season (DJF, MAM, JJA, SON). Blue means windier than normal conditions, and orange means less windy than normal conditions.

**Table 2-3: Summary of wind conditions in the Wellington Region**

		DJF	MAM	JJA	SON
NINO3.4	+				
	-				
		DJF	MAM	JJA	SON
SAM	+				
	-				
		DJF	MAM	JJA	SON
IOD	+				
	-				
		DJF	MAM	JJA	SON
SPSD	+				
	-				

## 3 Limitations

### 3.1 Data limitations

- The VCSN data used in this study starts in 1972, which is a relatively short timescale for analysing inter-annual climate modes of variability, as there are small numbers of each phase during this time (note that VCSN rainfall data starts in 1960, but this earlier period was not used here). Also, this length of record is too short to analyse the Interdecadal Pacific Oscillation, which varies between positive and negative phases every 20-30 years. There are limited numbers of stations with records back to the early 20<sup>th</sup> century, so analysis of the relationship between climate variables and the IPO was difficult and showed only weak relationships.
- Wind data in the VCSN only goes back to 1998. Using only 20 years of data to analyse the relationship between wind and inter-annual climate modes is not ideal and the results should be used with caution.
- The VCSN rainfall estimates at higher elevations may have larger errors than estimates at lower elevations, due to the interpolation procedure (stations are mainly at low elevations) (Tait et al., 2012). Therefore, the relationships between rainfall parameters and climate modes at high elevations (particularly over the Tararua Ranges) should be interpreted with caution.
- All reasonable skill and care has been applied so that the data in NIWA's National Climate Database (CliDB) are as reliable as possible. However, we do not know the quality assurance and control procedures that were undertaken with GWRC's rainfall data that was supplied for this study. We have assumed that the GWRC data is of the same quality as the CliDB data and no additional quality control was undertaken.

### 3.2 Analysis limitations

- There are some disparities between the VCSN composite results and the station results, for the same climate mode phase and climate variable. This could be due to the different time periods of analysis (post-1972 for VCSN and up to a few decades longer for stations). A future step could be to analyse the station data post-1972 only and compare the station data with VCSN results.
- Local-scale atmospheric processes were not considered in this study. It was outside the scope of this study to consider these local processes which might have an effect on the relationships between the climate modes and climate variables (e.g. rainfall). For example, the relationships between temperature and rainfall and the MJO are complex, and these may relate to changes in short wave and long wave radiation fluxes modulated by the MJO and airmass interactions with the topography of the Wellington Region.

## 4 References

TAIT, A., STURMAN, J. & CLARK, M. 2012. An assessment of the accuracy of interpolated daily rainfall for New Zealand. *Journal of Hydrology (NZ)*, 51, 25-44.